THERMOMECHANICAL RESPONSES OF TEXTURED YARNS

by

STEVEN CRAIG SMITH

S.B./S.M.M.E., Massachusetts Institute of Technology
(1972)

S.M., Massachusetts Institute of Technology
(1975)

SUBMITTED IN PARTIAL FULFILLMENT
OF THE REQUIREMENTS FOR THE
DEGREE OF

DOCTOR OF SCIENCE

at the

MASSACHUSETTS INSTITUTE OF TECHNOLOGY

JUNE 1978

Signature of Author.....
Department of Mechanical Engineering, 3/30/78

Certified by.....
Thesis Supervisor

Accepted by.....
Chairman, Department Committee

THERMOMECHANICAL RESPONSES OF TEXTURED YARNS

by

STEVEN CRAIG SMITH

Submitted to the Department of Mechanical Engineering on May 1, 1978 in partial fulfillment of the requirements for the Degree of Doctor of Science

ABSTRACT

Dyed fabrics made from textured yarns often show objectionable stripes, or barré. The loss of production due to barré rejects has been a problem in the textile industry for many years. Barré can be caused by small (1-2%) differences in the geometry or dye shade of adjacent yarns in the dyed fabric. The properties of the feed yarn and the value of process parameters during texturing are most influential in determining the appearance of a textured yarn in a dyed fabric.

Control limits which should prevent barré have been established for these key texturing process parameters and the open loop control of texturing machine actions which dictate the process parameters has been found to be adequate. However, inherent instabilities in the texturing process itself or changes in the transmission of machine actions to yarn process parameters undermine the success of the open loop approach. Control of textured yarn quality through on-line closed loop control of process parameters has been

considered and found to be infeasible for technical and economic reasons. Current off-line methods of quality control have been reviewed and found to be inadequate.

In the current study, an instrument has been developed to measure (off-line) those thermomechanical responses of textured yarns which correlate with the appearance of the yarns in a dyed fabric. The ability of the instrument to predict the appearance of a textured yarn in a dyed fabric has been confirmed by tests on laboratory knitted, and on commercial fabrics.

The thermomechanical test used in this instrument is similar to the commercially important setting operation on a texturing machine. A detailed investigation of the behavior of a textured yarn during the continuous setting process has led to the discovery of twist and contraction distributions within this setting operation. The twist distribution is consistent with the existence of a "pseudo-spindle". A qualitative model has been developed to explain the observed twist and contraction distributions.

DEDICATION

This thesis is dedicated with love to my wife, Ann, and to our sons, Craig and Geoffrey.

MASSACHUSETTS INSTITUTE OF TECHNOLOGY
DEPARTMENT OF MECHANICAL ENGINEERING

Doctoral Thesis Presentation

THERMOMECHANICAL RESPONSES OF TEXTURED YARNS

by

Steven C. Smith

Monday, May 1, 1978

Room 16-310 2 P.M.

Thesis Supervisor: Professor Stanley Backer

Thesis Committee: Professor I. V. Yannas
Dr. Frans Van Dyck
Professor J. H. Williams

ACKNOWLEDGEMENTS

During the course of my graduate studies at M.I.T., I have received various components of support from the Celanese Corporation, from the Allied Chemical Corporation, the National Science Foundation, J. P. Stevens Company, Chicopee Manufacturing Company, and the Emery I. Valko Fellowship Fund. This support is gratefully acknowledged. Primary sponsorship of my dissertation research was provided by UNIFI, Inc., and by WESTVACO Corporation. In addition, one segment of the thesis reflects a separate investigation conducted with support of the du Pont Company. The encouragement and assistance of these firms are very much appreciated.

Many people have been especially helpful to me in both technical and personal matters. At M.I.T. Dr. Subhash Batra, Fred Silver, Chris Brogna, Charles Bell, and Wayne Hawkins were stimulating friends and I will surely miss them. My thesis committee members were most generous in extending their time to help me, and I thank them. Jan Krizik at I.D.R., Inc. deserves special thanks for his talented help in the design and construction of the instruments which were developed as part of this thesis. The entire staff of UNIFI, Inc. has shown me great friendliness and cooperation. Virgil Dodson, Dick Hardin, and Allan Mebane were guiding forces in the industrial trials section of this work. Dana Shore, Mike Mebane, and Joe Hutchins conducted the in-plant testing

of the instrument. Many fruitful discussions were held with Rony Conkle. My thanks are extended to all of them, especially to Virgil Dodson.

I wish to thank Miss Dorothy Eastman for typing the manuscript and attending to the many details during preparation of the final document. The acknowledgement here can not repay the kindness and generosity she has shown me and my family.

It is difficult to express the depth of my gratitude to Professor Stanley Backer. He has been a teacher, a thesis supervisor, and also a true advisor. I feel that I have grown a great deal from my association with him in the last four years. In his professional life he has established a high standard of achievement to which I can continue to aspire, and for this I thank him most of all.

TABLE OF CONTENTS

CHAPTER I

THE CONTROL OF BARRÉ IN TEXTURED YARN PRODUCTS

False-twist draw-texturing is a process wherein bulk, cover, and stretch are imparted to continuous multifilament yarns. Figure 1 shows the essential features of the false twist process. In passage through the texturing process, the filaments in the feed yarn are twisted, drawn, twisted further, heat set, untwisted, and wound onto a package. Texturing leaves the yarn with a process-dependent thermo-mechanical history and a molecular morphology which will determine the response and properties of the yarn during future thermal, chemical, and mechanical treatments.

The most important treatments given to textured yarns are those encountered in the fabric formation, dyeing, and finishing operations. The desired response is a fabric with uniform appearance, with acceptable mechanical properties, and one meeting the cutting room requirements for weight and width. From the beginning, fabrics produced from textured yarns manifested considerable streakiness, or barré, which lead to fabric rejection, and loss of production. Pratt has defined barré as a "continuous visual barred pattern, or stripiness parallel to the yarn direction in a knit or woven fabric that is caused by physical, optical, or dye differences in the yarns, or geometrical differences in the fabric structure acting either singly or

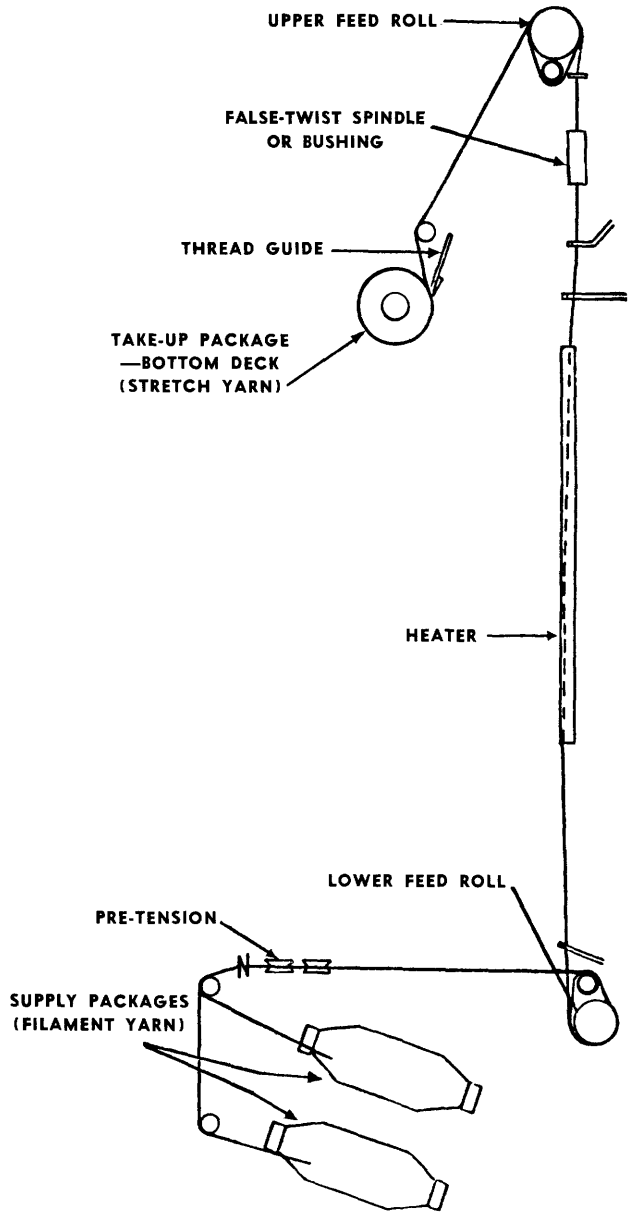

FIGURE 1. SCHEMATIC DIAGRAM OF FALSE-TWIST TEXTURING OPERATION [138]

in combination to produce the barred pattern" [1]. Pratt summarized the extent of the barré problem as follows: "Without a doubt, barré in textured polyester knits has caused more finger pointing and more side stepping of responsibility than any problem in the annals of the textile industry. It has been written about, lectured about, and argued about. It has cost the industry untold millions of dollars and, undoubtedly, will continue to do so in the foreseeable future" [2]. Examples of barré are shown in Fig. 2.

The severity of barré, like beauty, is quite literally in the eye of the beholder. Current industrial assessment of barré in fabric is by eye. A set of ruled lines of variable contrast with a fixed gray background forms the standard in the HATRA Barriness scale described by Brown [19]. An alternate system employs photographs of a barred fabric as standards [6]. Brown emphasizes that the ratings are a function of angle of illumination, and angle of viewing, and that acceptable rating limits will vary with end-use reguirements, color, and fabric construction. The reproducibility is improved by comparing similarly rated fabrics and by limiting operator grading time to 15 minutes per session.

Recently, Kok et al. [20] have described an instrument for assessing the severity of barré using green (dye sensitive) and infrared (dye insensitive) photodetectors for reflected light and a phototransistor for transmitted light. By subtracting the infrared signal from the green signal, they

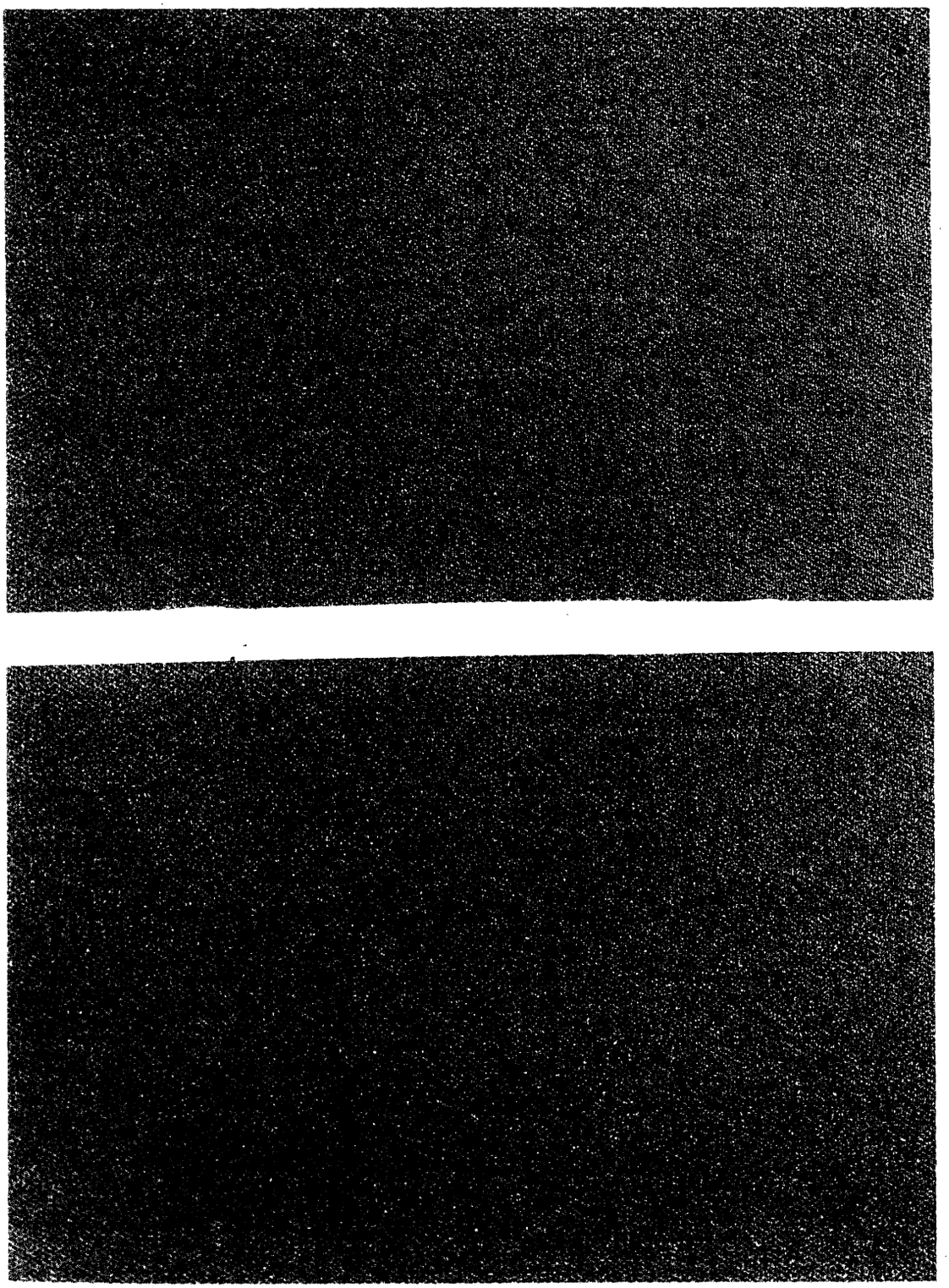

FIGURE 2 EXAMPLES OF BARRÉ

obtain an output corresponding to the dye depth of the fabric sample. The output of the transmitted light detector is inversely related to the output of the infrared (reflected) light sensor. This means more yarn bulk in the course will reflect more light and allow less light to be transmitted through the fabric. Higher bulk courses should appear lighter in reflected and darker in transmitted light, and vice versa. The absolute value of the difference between green and infrared reflected light is integrated over the fabric length to arrive at a barré rating. Good correlation with visual ratings is claimed as well as reproducibility of about 5%.

As useful as these barré level measurements may be, most analysis of barré is not undertaken to quantify the level of barré, but rather to assign the blame to one of the sources--thus addressing the question of financial responsibility for the fabric fallouts.

Barré is a problem relating to dyed and finished fabric. To eliminate the problem we must <u>first</u> identify the non-uniformities within the fabric that are the <u>causes</u> of barré. <u>Second</u>, these non-uniformities must be linked in a causal sense to specific manufacturing processes, thus identifying the <u>sources</u> of barré. <u>Third</u>, the <u>governing parameters</u> in such processes must be identified. <u>Fourth</u>, the <u>control</u> of these governing parameters must be tightened.

It is the purpose of this chapter to summarize progress along these four avenues and to indicate why the measurement

of thermomechanical responses of textured yarns is so important in dealing with the barré problem.

1. Causes of Barré in Fabrics.

Barré in filling knit fabrics is caused by differences in geometry and/or dye shade of successive yarn courses [3]. For this reason, inter-course differences and not intra-course variations will be considered here. The geometric differences between knit courses can exist at the knit loop, yarn, or filament level. Dye shade variations due to actual dye uptake differences are easily observed at the yarn or fabric level, although differences between filaments and within filaments at a given yarn cross section exist as well. These filament differences have been the subject of studies by Morizane et al. [5].

Before identifying the sources of the variations in geometry and dye shade, one should quantify the variations that can cause barré. The magnitude of the variation in geometry or dye required to produce barré has been assessed by many workers. As summarized in Tables 1 and 2, we note that the variation in yarn or fabric geometry required to produce barré is quite low. Similarly, the magnitude of relative dye variations which cause barré is quite small as indicated in Table 2. One reason for this extreme sensitivity to inter-yarn variation can be traced to the low intra-yarn variation in continuous filament yarns. Munden in [6] claims that continuous filament yarns with 3% inter-yarn variation produce the same severity of barré as

Table 1

MAGNITUDE OF RELATIVE GEOMETRIC DIFFERENCES WHICH CAUSE BARRÉ

Geometric Level	Measured Defect	Single Courses	Banded Courses	References
Fabric	Shadow Barré (Moire)	2°*		Holfeld and Pratt (1972) [7]
Course	Stitch Length variation	3% synthetic continuous filament		Vaidya and Nigam (1977) [6]
		7% natural fiber		
	Runner Length variation	3%		Grant (1972) [8]
	Course Length	3%		Blore (1972) [9]
	Knit Extension		1%	Holfeld and Nash (1976) [10]
	Relative Course length	>2%	>0.75% average of 3 ends	Coryell and Phillips (1977) [11]
Yarn	Yarn Bulk in fabric (6-10% typical crimp values)	18-20%	4-6% on 1/4-1/2 of face feeds	Coryell and Phillips (1977) [11]
Filament	Flat Sides	60% differences in flat sides, (1.5-2.5)		Pratt (1977) [2]

*Angle Difference from face to back loops.

Table 2

MAGNITUDE OF RELATIVE DYE DIFFERENCES

WHICH CAUSE BARRÉ

Measured Defect	Single Course	Banded Courses	Reference
Dye uptake	20%	8% for a pair	Clements (1972)[12]
		1% for large bands	
		2%	Pratt (1972)[1]
	<4-6%	<2%	Goldin (1977)[13]
Dye Rate		>.75%	Willingham (1972) [106]

staple yarns with 7% inter-yarn variation. Thwaites [15] observes that draw-textured yarns with more intra-yarn variation in linear density than conventionally textured yarns are less prone to barré. Unfortunately, this effect is not large enough to mask the inter-yarn variations that produce barré. Pratt [2] suggests that it is theoretically possible to have so many variations in fiber, yarn, and fabric that the effects cancel each other and the fabric appears uniform. This idea has considerable merit and should be considered as a viable alternative to current methods of reducing barré by reducing inter-yarn differences.

The magnitudes of geometric or dye variation that cause barré depend on the details of fabric structure, formation and end-uses. In the case of plain knits, the fabric is characterized by parallel, horizontal courses of loops. In modern multifeed knitting machines, each course is knit from yarn drawn off a different package. The number of packages determines the repeat period. Clearly, this is the ideal fabric structure to highlight inter-course and therefore inter-yarn differences. Thus, plain knits are "critical" fabrics with respect to barré. As yarn paths become less linear, fabric criticality to barré decreases (e.g. Swiss pique > ponte-di-roma > 2 x 2 twill > crèpe) [16]. Figure 3 shows knit structures with varying degrees of yarn path linearity.

Increasing the number of feed packages going into a

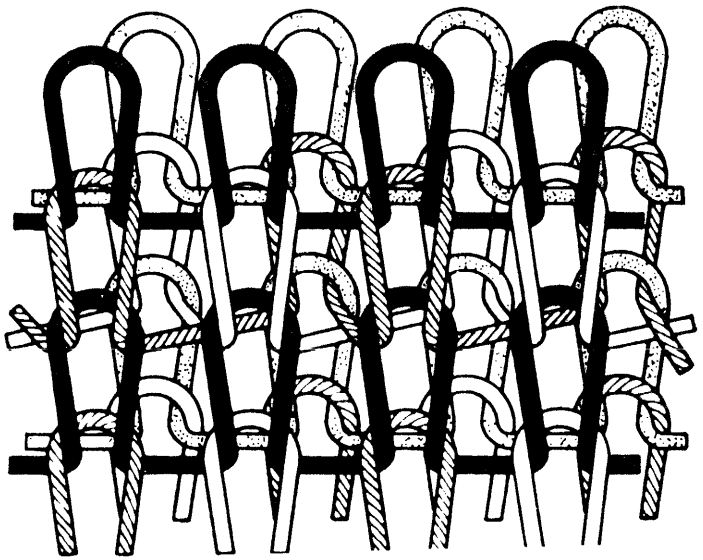

Ponte di Roma

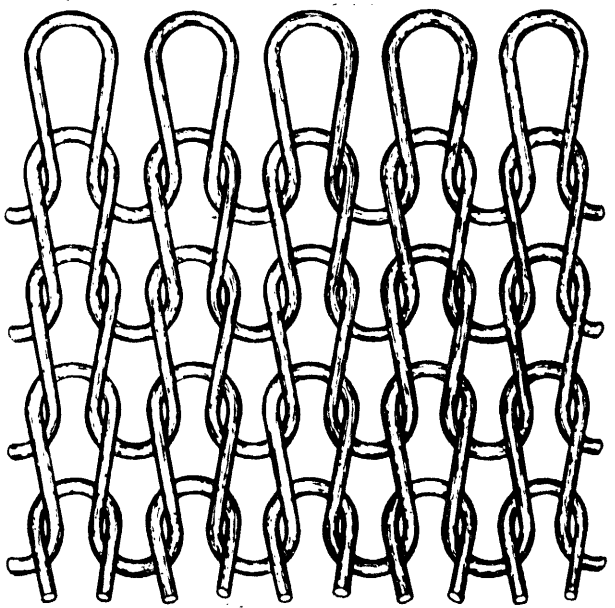

SINGLE KNIT FABRIC

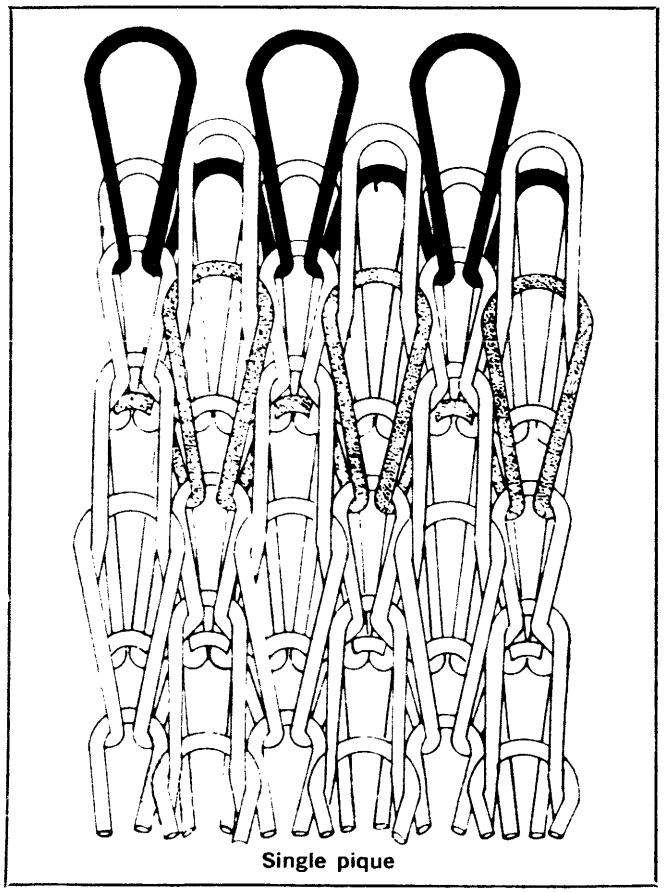

Single pique

FIGURE 3. KNIT STRUCTURES WITH VARYING DEGREES OF YARN LINEARITY.

fabric by using larger circular knitting machines or warp knitting allows a small difference in geometry or dye to be more easily perceived as barré. For, with more feeds in the larger diameter machine, the offending courses are spread farther apart and are therefore easier to observe. This feature is carried to the extreme in warp knitting which has thousands of individual feeds. Also, with more feeds, the chance is heightened for two or more ends with small variations in geometry or dye to combine and produce barré. This is shown in Fig. 4a, 4b from Hale [17]. The ordinate in both figures is the number of feed packages going into the fabric and the abscissa corresponds to the percentage of "rogue" yarns (i.e. yarns having variations in dye or geometry large enough to produce barré). In Fig. 4a the calculation of the rate of fabric rejection is based on the assumption that a rogue doublet will produce barré, while in Fig. 4b a rogue triplet is required for fabric fallout. The labelled lines in these figures define the loci of equal probability of fabric barré. We can assess the allowable percentage of rogue yarns in a feed yarn lot needed to limit fabric fallout to an acceptable level (2%), an unacceptable level (4-5%), or a very serious (20% level)[18]. The results are shown in Table 3. The figures and the table show that tighter controls on rogue yarns are needed as the number of feeds increases or as the rogues become more apparent, i.e. fewer adjacent rogues are discernible as barré. The increase in barré due to increasing the number of feeds is

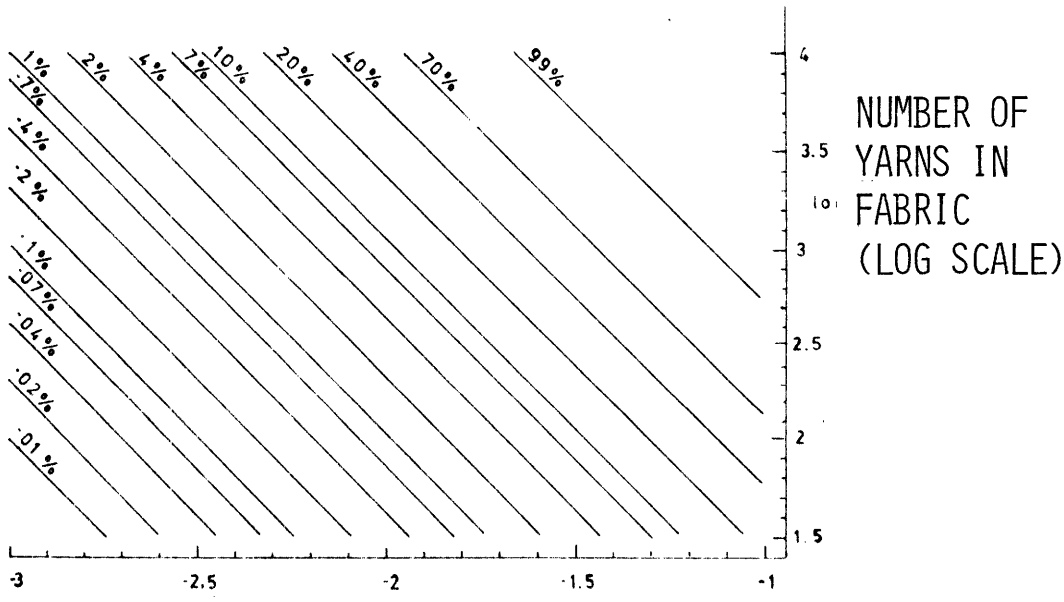

A. PERCENTAGE OF ROGUE DOUBLETS IN YARN LOT (LOG SCALE)

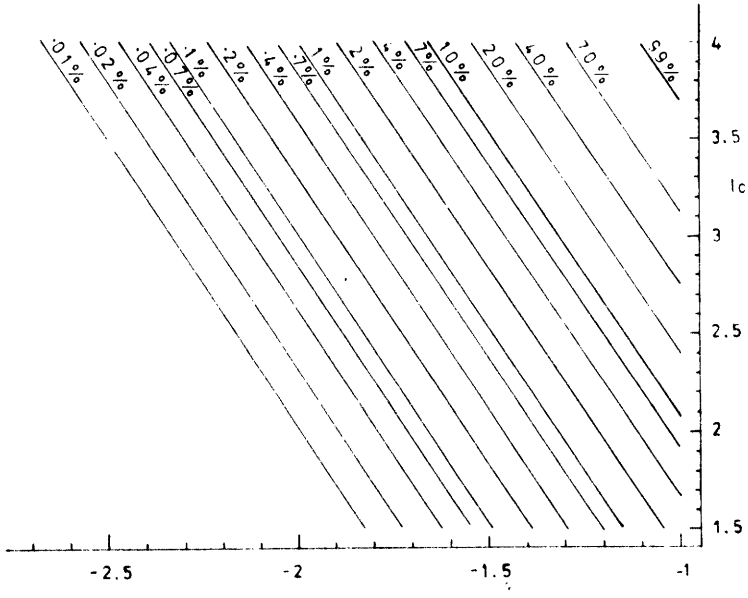

B. PERCENTAGE OF ROGUE TRIPLETS IN YARN LOT (LOG SCALE)

FIGURE 4. PREDICTED LEVEL OF FABRIC FALLOUT DUE TO BARRÉ [4]

Table 3

PREDICTED FABRIC REJECTS AS

FUNCTION OF ROGUE YARNS

Fabric Fallout	Number of Feeds	Allowable % of "Rogue" Yarns in Lot Rogue Doublets	Rogue Triplets
2%	50	2.0	7.8
Acceptable	100	1.5	6.2
	1000	.5	2.9
5%	50	3.0	10.5
Unacceptable	100	2.2	8.0
	1000	.7	3.7
20%	50	6.9	17.4
Serious	100	4.8	13.4
Problem	1000	1.5	6.2

noticeably reduced as the severity of rogue ends is reduced, that is, when Fig. 4b is used as compared to Fig. 4a.

Hale [4] also has considered the more practical problem of barré due to adjacent groups of p yarns and q yarns, each group having a different average value of the barré-producing characteristic. In this case, a yarn may appear either light or dark, and its appearance is affected by local, much less apparent, variation of adjacent yarns. This "local reference", or "Monte Carlo" effect, has led to the common practice of moving barré-producing packages around the knitting creel or beam after knitting and observing short fabric lengths. Yarns and knitting feeds can interact to reduce or enhance barré in this "shuffling" of the creel [12].

In Hale's treatment, the two groups of p yarns and q yarns are assumed to come from a normally distributed population with a mean μ and standard deviation σ with respect to the single barré-producing characteristic. It follows that, $|d_{pq}|$, the difference in average value of yarn characteristic between the p and q groups will be normally distributed with zero mean and variance given by $[(p + q)/pq]\sigma^2$. He proposed two forms of stripe criterion,

$$(1)\quad |d_{pq}| > t\sigma$$

$$(2)\quad |d_{pq}| > t\sigma\sqrt{\frac{p + q}{pq}}$$

where t equals the barré tolerance parameter. The second form recognizes that the severity of barré increases with increasing band size. Simulations of stripiness in fabrics produced from

increasing numbers of feeds were run on a computer using the two criteria. Values from 2 to 5 were used for p and q; t was varied in the range 2 to 6. The results are shown in Fig. 5a,b.

As expected, fabrics with more feeds have more stripes at a given value of the tolerance parameter. When $|d_{pq}|$ is weighted by $\sqrt{(p + q)/pq}$, as in Fig. 5b, compared to Fig. 5a, the number of stripes increases since these wider stripes are more apparent.

This band width weighting factor was used to correlate successfully the results of a fabric trial run by Hale. Fabrics were knitted, dyed, and numerically graded on the basis of the HATRA Barriness scale. Blocks of progressively larger differences in yarn characteristic were then knitted into the fabrics. When the differences in yarn characteristic were divided by $(p + q)/pq$, the HATRA Barriness rating decreased linearly with yarn differences as shown in Fig. 5c. The barré ratings were consistent with the second stripe criterion, namely:

$$\left|\frac{d_{pq}}{\frac{p+q}{pq}}\right| > T, \quad \text{where } T = t\sigma.$$

If the level of barriness that can be accepted in the fabric is known, (a value of 3 on the HATRA scale is reasonable for critical end uses) then T is the corresponding value on the yarn characteristic axis. Once T, the tolerance level, has been found, predictions can be made for fabric rejections if yarn lot σ is known using Fig. 5b. The value of $t = T/\sigma$ and the number of feeds in the fabric are used to find the percentage of

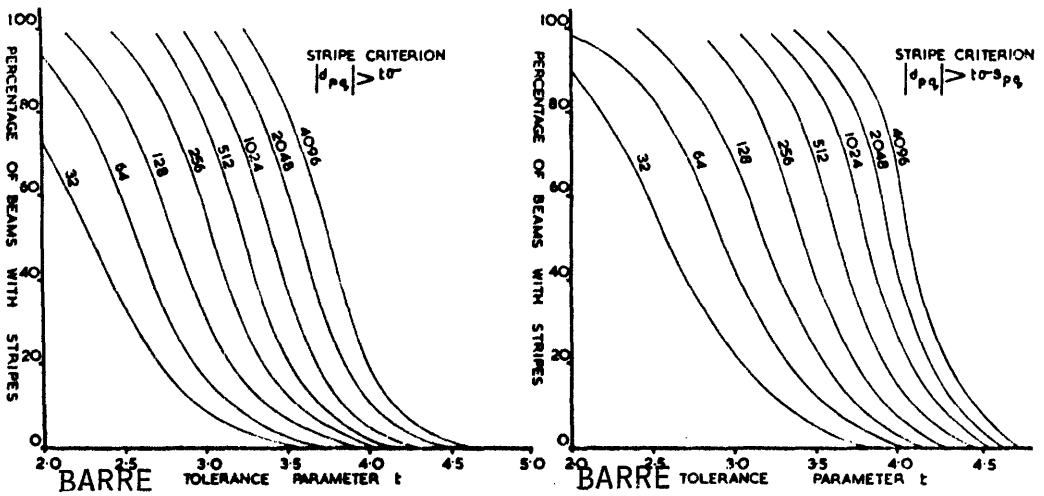

FIGURES 5A,B. PREDICTION OF PER CENT BARRED FABRIC FOR VARYING NUMBERS OF FEED YARNS AS A FUNCTION OF ALLOWABLE LEVEL OF BARRÉ. A AND B DIFFER IN SCALING OF STRIPE CRITERION [17]

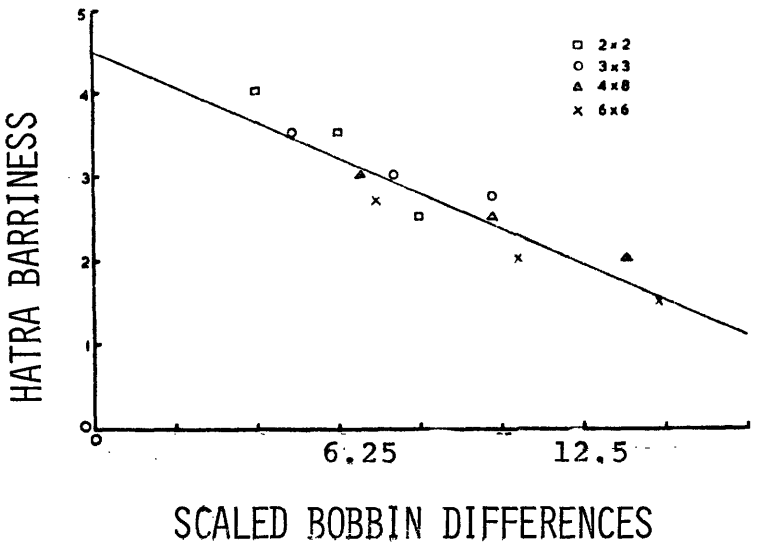

FIGURE 5c. CORRELATION BETWEEN SEVERITY OF FABRIC STRIPES AND SCALED YARN DIFFERENCES IN THE FABRIC [17]

rejected fabrics*.

On the basis of Hale's theory and experiment, textured yarn lots having C.V.'s of 1.7% of the mean for the critical barré-producing property will result in no fabric rejects in 96-feed doubleknits, if a HATRA Barriness rating of 3 is acceptable. This presupposes, as did Hale, that no single end barré will occur. The selection process will have to remove all packages which manifest sufficient variation to produce single end barré. The textured yarn lot C.V. required for zero fabric rejects will depend on fabric construction and dye selection, so the value of 1.7% derived here cannot be expected to have universal application.

Clements [12] has calculated fabric fallout based on the variance (σ^2) of dye shade in the feed yarns for a various

---

*An example calculation could be for the case of a 96-feed knitting machine producing the same fabric from the same yarns used in Hale's fabric trials. We want to know what yarn lot σ is required to give no barré worse than 3 on the HATRA scale. The steps in the calculation are as follows:

(1) Given HATRA Barriness 3, find T on Fig. 5c.
T = 7.2% variation.

(2) On Fig. 5b, find the value of t required to give no stripes at 96 feeds. t = 4.2.

(3) $\sigma = T/t = 1.7$

number of feeds in the fabric. Table 4 shows the results assuming two yarns with 8% dye variation from the mean will produce barré when adjacently creeled. Clements' results are in substantial agreement with Hale's, but are less conservative. It is recommended that Hale's approach be used to the extent that it is economically feasible to have the tighter controls.

Thus far we have indicated that fabric barré is caused by a repeating difference in the visual appearance of adjacent yarns or courses (or of groups thereof). The visual difference between given yarns will depend to some extent on the geometry of the fabric structure. For a given variance of appearance in a population of yarns, it has been noted that the probability of occurrence of barré will increase with the number of feed packages used in the knitting process. For a given dye, there is generally a critical value of difference in dye uptake (or optical effect) which is detectable by the observer. Thus, if the variance of dye uptake in a population of yarn packages increases, it may be expected that the probability of fabric barré will increase for a given number of feed yarns. The same can be said about geometric differences from yarn to yarn. If geometric variance increases, so should the probability of barré. Examples of combined effects on barré are given in tabular and graphical form. Now it remains to identify the sources of troublesome differences between yarns used in a fabric.

2. Sources of Differences in Geometry and Dye Shade.

Table 4

ESTIMATE OF FABRIC REJECTS [12]

Yarn Dye Variance (%)	48 Feed	96 Feed	Tricot Beam
<10	0%	0%	0%
10-12	0-1%	0-3%	≤25%
12-14	1-3%	3-15%	≤75%
14-16	3-10%	15-30%	≤100%
16-18	10-18%	30-50%	100%

The differences in yarn geometry and/or dye shade which appear in a given fabric as barré can be attributed to variations in one or more of the four main processes leading to the finished fabric, namely:

(1) spinning (yarn extrusion, including drawing),

(2) texturing,

(3) knitting or weaving (including preparatory processes),

(4) dyeing and finishing.

Spinning, in the case of polyester, involves extrusion of a high-temperature melt under pressure through parallel orifices to form a multi-filament yarn. Polymer (molecular) properties and the manner in which the filaments are drawn and quenched determine the properties of the resulting yarn. After the parallel filaments have been gathered together in a yarn bundle, they are given a coating of spin finish with a lubricant and generally given a slight degree of entanglement to enhance yarn integrity. Denier (a measure of linear mass density), denier/filament, cross sectional geometry, molecular orientation, molecular weight, crystallinity, percentage of spin finish, amount of delustrant, and entanglement level are the important qualities of the melt spun yarn as related to subsequent texturing processes [21]. Further, the level and uniformity of its subsequent hot draw force plays an important role in the texturing process and in determining the properties of the textured yarn.

Draw texturing combines in a single process the two

operations of (residual) drawing and texturing, thereby saving time, money, and energy. Gross changes in filament structure are brought about during false-twist draw texturing by the combined action of drawing, twisting, and heat setting. After heat setting, the cooling yarn is continuously untwisted in the presence of tension. The yarn is then oiled and wound onto a package. Details of the single heater process will be examined later.

Fabric formation follows the texturing. In the case of knitting, the yarn is textured and pulled off its package under tension and fed into a circular knitting machine. A constant length of yarn from each feed package is generally supplied (by means of a positive feed) to the needles to form a single course during every revolution of the machine cylinder. The number of courses knitted per revolution of the machine is determined by the number of feeds. The tension history of the yarn depends on the package-to-feed tension, details of the stitch pattern, yarn friction on the needle and sinker, yarn-on-yarn friction, and fabric "take down" tension. A properly operating knitting machine has equal package-to-feed tensions, equal feed-to-needle tensions, uniform needle geometry and friction characteristics, and regular, uniform fabric windup action [2,3,10].

Once in the fabric the yarns are subjected to dyeing and finishing operations. These comprise scouring, bulk development, dyeing, tenter setting and drying operations. The

thermomechanical memory of the yarn interacts with the operating parameters of dyeing and finishing to determine the average level of bulk (or crimp) in each course. Thus, in the presence of inter-yarn differences, there will be bulk variation between courses, which can lead to barré.

Since barré is associated with dye shade or geometric difference between courses within a fabric, we cannot consider those processes that deal with the fabric as a unit to be the sole source of barré. In short, dyeing and finishing operations cannot be blamed entirely for the inter-course differences within a fabric that appear after fabric processing. However, it is well known that dyeing and finishing operations can be carried out under conditions which accentuate course or yarn differences; obviously, these must be avoided. From this point on, we shall assume that dyeing and finishing practices will partially mask inter-course or inter-yarn differences, rather than accentuate them, and we shall concentrate on earlier processes wherein yarn differences originate.

Before indicting any of the remaining operations (spinning, texturing, knitting), we will briefly consider the physics of dyeing as related to dye shade, and of setting and shrinkage, as they relate to yarn geometry in the knitted fabric.

Dyeing of polyester with disperse dyes is essentially a diffusion process limited by a maximum dye absorption at infinite time. The diffusion process is controlled by the size of the dye molecule, the absorption forces between the dye

molecule and the polymer chains, and the mobility of the polymer chain segments [24]. The mobility of the polymer chains is limited below the glass temperature, but increases rapidly as the glass temperature is exceeded. Both dye diffusion and dye capacity depend on the fine structure of the fiber, i.e. arrangement of molecular chains in the fiber. Simplifying concepts for dealing with various arrangements of molecular chains in a fiber are: amorphous regions, crystalline regions, and orientation of the chains within these regions. These simple concepts are not sufficient to explain all aspects of fiber behavior, but do provide convenient starting points for interpretation of essential phenomena. The orientation and volume fraction of amorphous regions play a predominant role in most fiber properties, such as strength, creep, and strain-to-fail, while the crystallites add thermal stability to the structure by forming a kind of crosslinked network [25].

Dye molecules can only easily enter regions of high chain segment mobility, but are virtually excluded from crystallites and the immediately adjacent non-crystalline regions. Dye diffusion is slower through oriented amorphous regions due to their reduced segmental mobility. Distributed small crystallites more effectively restrict neighboring non-crystalline chains than do a few large crystals.

The amorphous volume fraction of a polymer decreases monotonically with increasing temperature and time of heat treatment; at the same time, crystalline volume fraction increases [26,27]. At heat setting temperatures of 150-200°C

the size and number of crystallites undergo a dramatic change, as shown in Fig. 6 from Dumbleton et al. [28]. These structural changes are reflected in the dyeing behavior of the same fibers shown in Fig. 7. Both the diffusion constant (Fig. 7b) and the equilibrium dye capacity, C_∞, (Fig. 7c) exhibit minima in the region of maximum number of crystallites. Processes that operate in the range of 150 to 200°C will clearly have large effects on the structure and dyeability of polyester fibers. Draw ratio and quench rate during spinning determine the amorphous orientation. Higher draw ratios clearly reduce both the dye diffusion coefficient and the dye capacity.

Simplified models of the effect of fiber orientation and crystal volume fraction variation were developed by Klein in summarizing extensive experiments in dyeing of polyester fibers [29]. The predicted dye response for fibers varying in orientation and/or crystal volume fraction are shown in Fig. 8. Figure 8a shows the dye uptake in fibers of equal dye capacity (per cent amorphous), but different dyeing rate (amorphous orientation). The fiber with less orientation in the amorphous regions (more polymer chain mobility) dyes faster, but after sufficient time has elapsed, both fibers are equally dyed. Figure 8b shows fibers with different dye capacities, but similar dyeing rates. The two fibers absorb similar amounts of dye during the initial dye strike and for short periods of dyeing will show no dye difference, but at longer times, the fiber with more amorphous volume dyes darker. Figure 8d shows that fibers

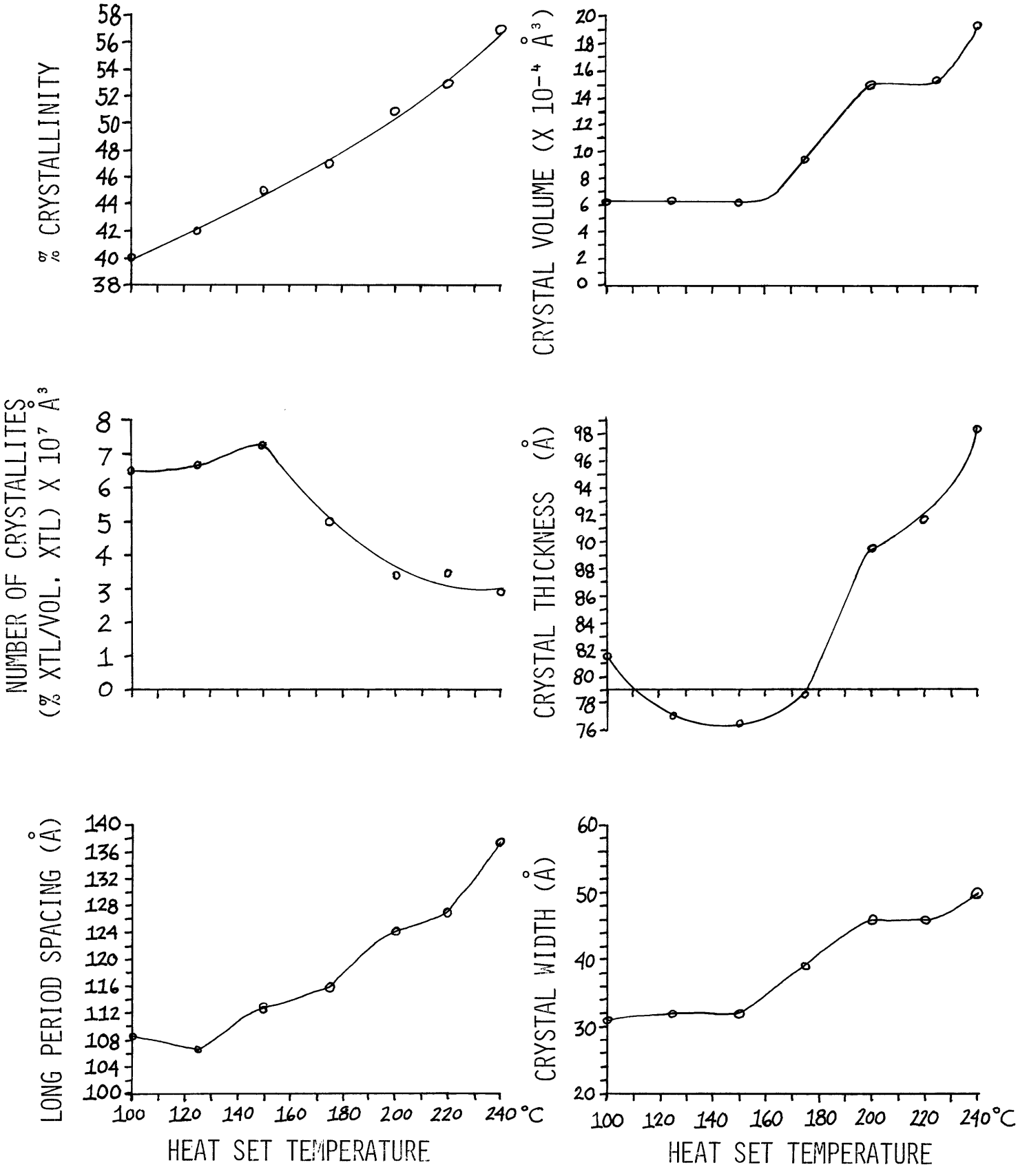

FIGURE 6. STRUCTURAL CHANGES DURING HEAT SETTING OF PET YARN DRAWN 4.25X ON 80°C.

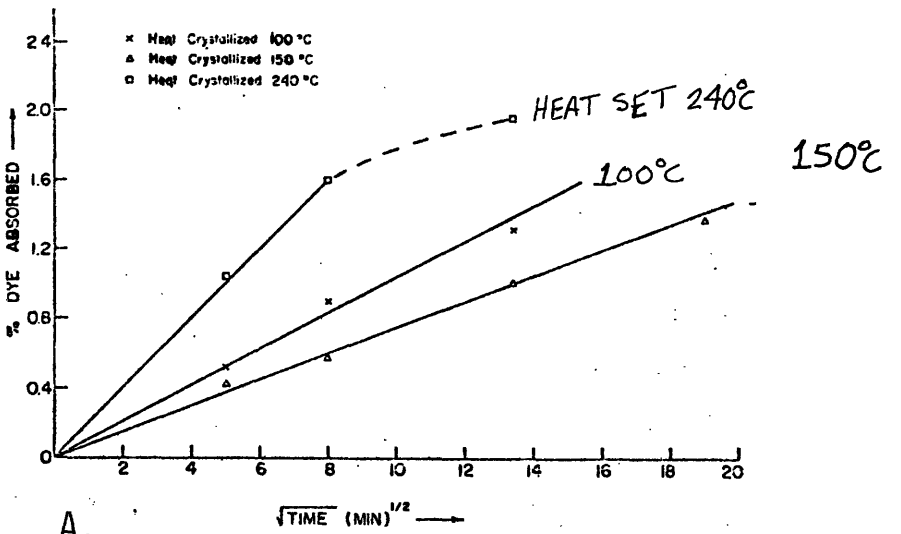

A. Per cent dye on fiber versus $(\text{time})^{1/2}$ for fiber drawn 4.25×.

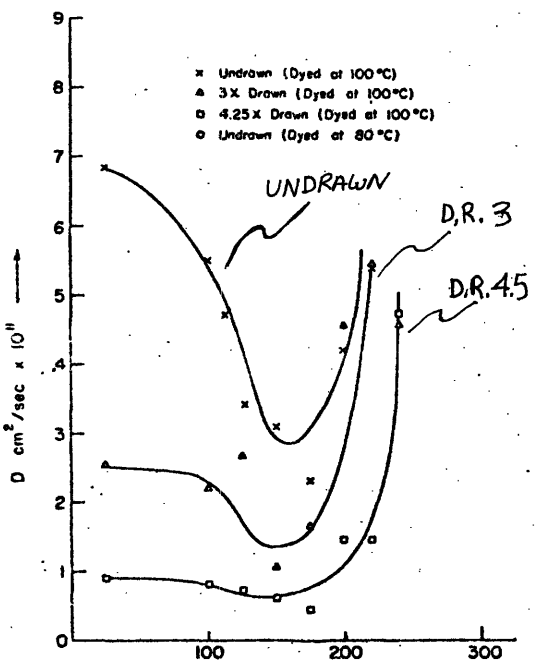

B. D versus annealing temperature.

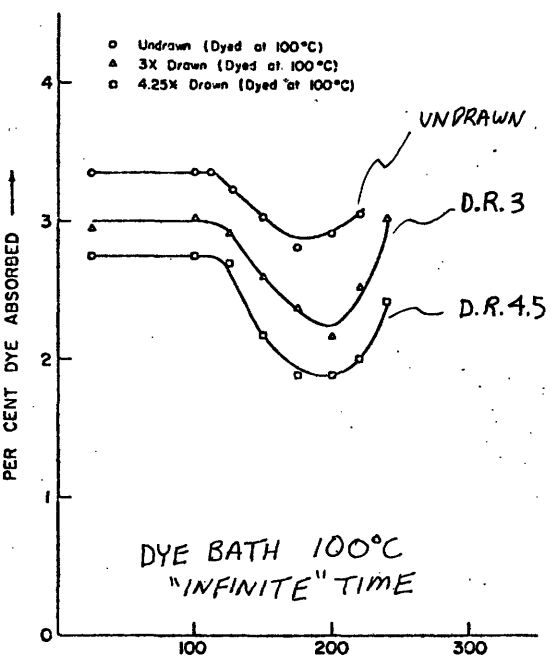

C. C_∞ vs. annealing temperature.

FIGURE 7. DYEING BEHAVIOR OF PET YARN DRAWN AT 80°C AND HEAT SET FOR SIX HOURS AT THE INDICATED TEMPERATURE.

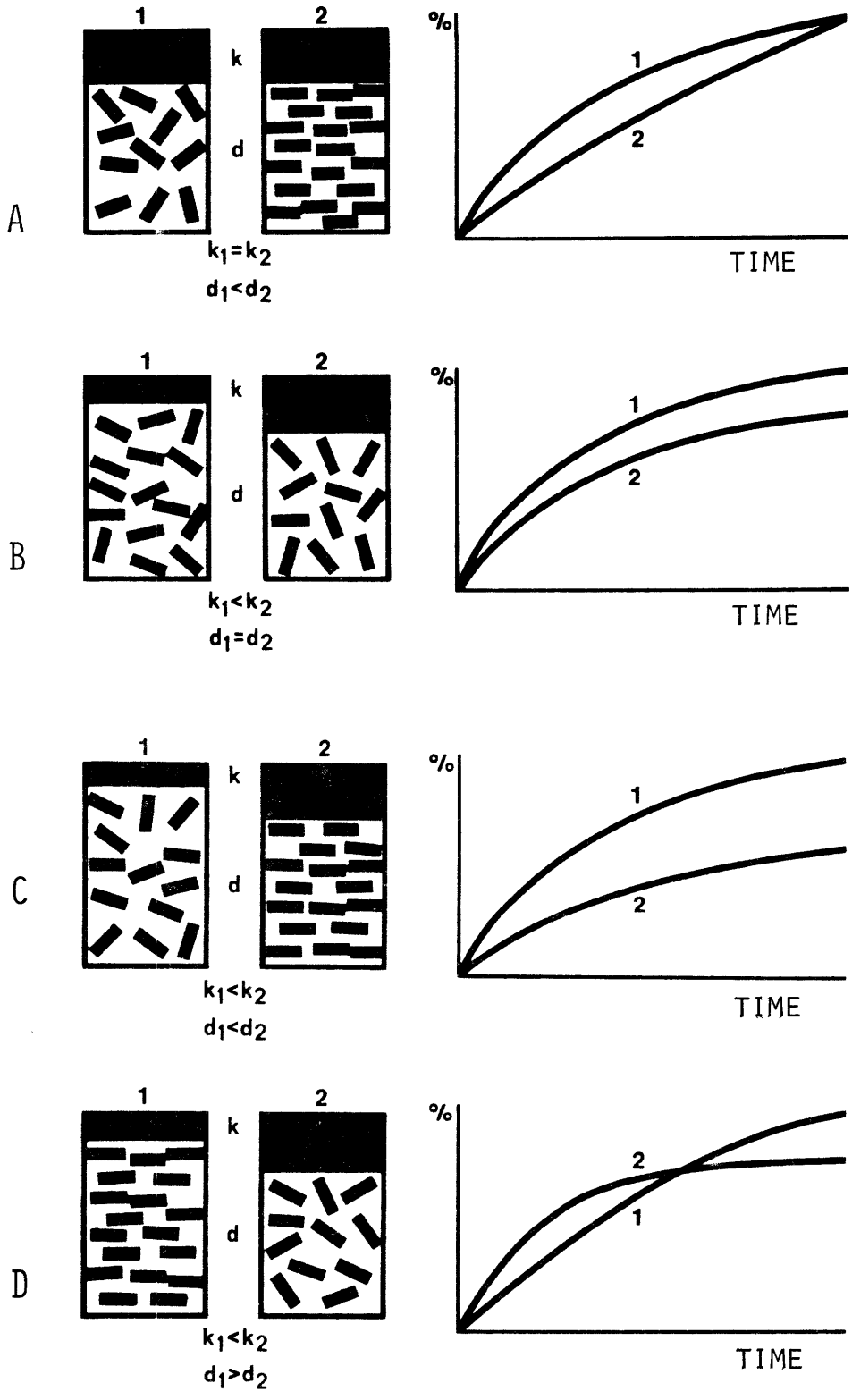

FIGURE 8. PREDICTED DYE UPTAKE FOR FIBERS WITH DIFFERENT FINE STRUCTURES. (K = % CRYSTALLINE; D = ORIENTATION OF AMORPHOUS REGIONS) [29]

with both dye capacity (amorphous fraction) and dye rate (orientation) differences show similar shade depth at one point in time, but are reversed in their relative darkness on either side of this point in the dyeing cycle. As shown in Fig. 8c, fibers with both orientation and crystalline difference show gross dye differences at all times. The sensitivity of dye or solvent diffusivity to structural differences is so great that several workers have used diffusion rates as an indicator of structural changes [30,31]. Some of these structural changes cannot be detected by any other method [32].

Dye selection and dye bath composition can have large effects on the amount of dye-related barré visible in a finished fabric. Dyes having high ratios of S, the dye saturation concentration, over D, the dye diffusivity, have the greatest tendency to show barré. These dyes are also known as high energy dyes, since they require higher temperatures (130°C), longer times, or more dye carrier (swelling agents) to penetrate the fibers [13]. Figure 9 shows the difference in dye uptake of two fibers with different heat histories plotted against the S/D ratio of various dyes. Figure 10 shows an example of the time-temperature cycle used during dyeing and finishing of fabrics of textured polyester yarns.

Setting involves changing the stress-free geometry of a filament, yarn, or fabric by the application of force, temperature, or chemical treatments [33]. Shrinkage is a de-setting operation, wherein the previous mechanisms of setting within a fiber (yarn, fabric) are, in effect, reversed. After the rapid

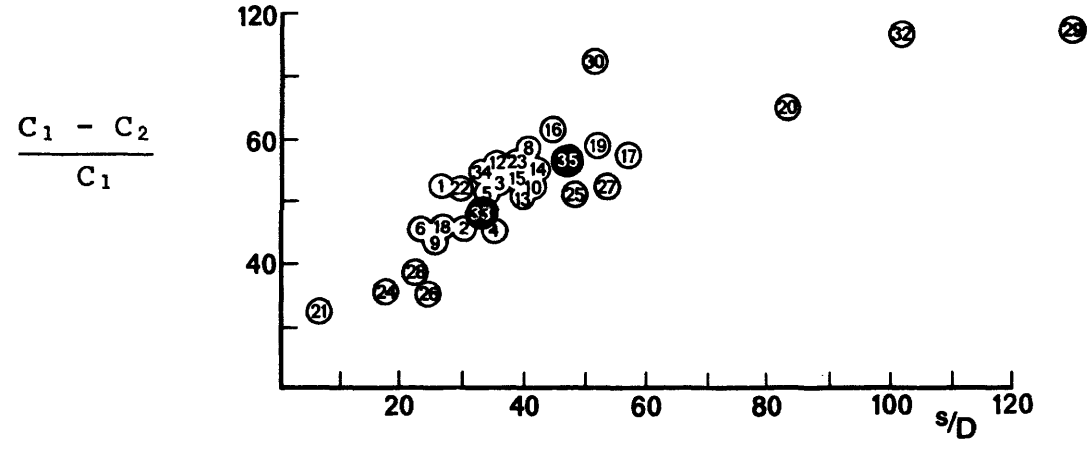

FIGURE 9. DIFFERENCE IN DYE UPTAKE FOR TWO FIBERS WITH DIFFERENT HEAT HISTORY AS A FUNCTION OF THE S/D RATIO OF THE DYE [29]

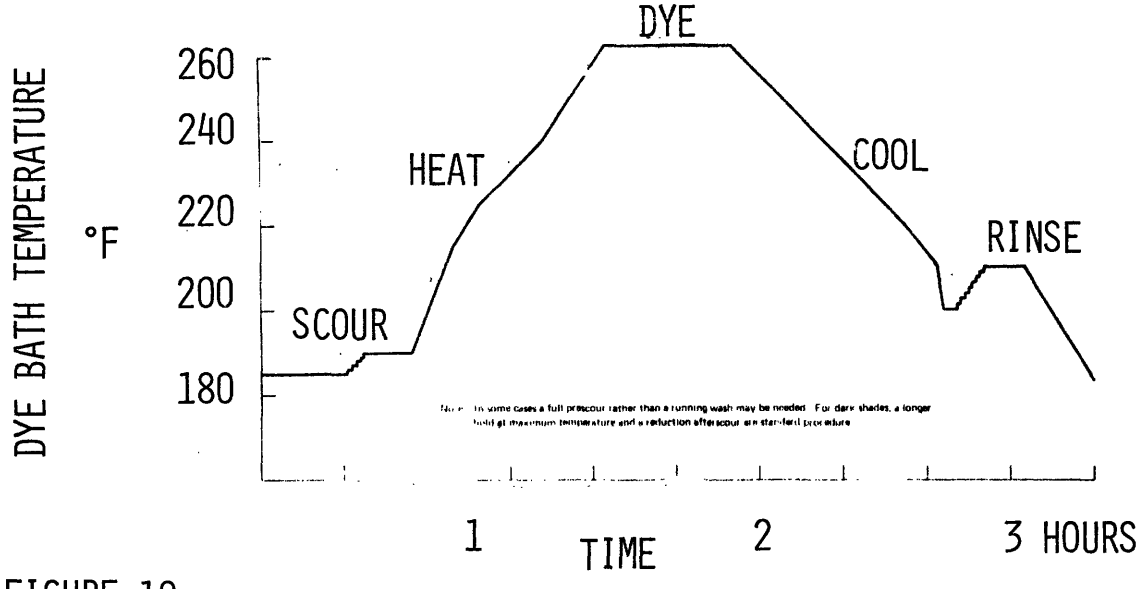

FIGURE 10. TEMPERATURE CYCLE DURING JET DYEING OF POLYESTER [105]

initial de-setting process, a much slower secondary re-setting (crystallization) process may occur as part of the overall shrinkage [34].

In general, neither setting nor shrinkage (de-setting) are ever 100% effective or permanent. The setting efficiency, defined as the ratio of set deformation to the imposed deformation [35,36], increases with lower tension, higher temperature, and longer setting times. A set obtained under these conditions is more permanent than one obtained under other conditions and will generally be more difficult to reverse. The geometry of the textured filaments in the fabric course will depend on their textured set geometry, on post-setting mechanical or thermal treatments, and on the extent of shrinkage, or de-setting, generated by the thermal, mechanical, or chemical actions during dyeing and finishing. The combination of temperature, twist, and tension reached during texturing determines both filament cross sectional shape changes and filament crimp geometry in the yarn.

In summary, the dye uptake and geometry of the as-spun filaments depend on their molecular composition and the fine structure, or arrangement, of their molecules in the fiber. Furthermore, this fine structure of the spun fiber changes drastically by the combined action of drawing and heating during texturing. The conclusion is that spinning and texturing will have the predominant effect on dye behavior, and filament geometry in the yarn.

Course geometry will depend on both the behavior of the yarn in the course during dyeing and finishing, and on the original geometry of the course as determined during knitting. Blore [9] has estimated that about 10% of the barré is due to faults during the knitting operation. Other authors have recently stressed knitting machine faults as the cause of barré [3,7,9,10,11]. However, it is conceded that most barré is yarn related and thus is determined by the variations in yarns occurring during the spinning and/or texturing processes [2,6,8,12].

The two properties of textured yarns that correlate best with the occurrence of barré are crimp development and dye uptake [37,38,39,40]. The important differences in filament flattening and associated light scattering differences occur mainly with pin-twisted, conventionally textured yarns whose filaments have round cross sections. The use of multi-lobal cross sections and draw-texturing with friction twisters has minimized the variations in filament flattening [41]. Part of the reason for the reduction in barré due to variations in filament flattening with draw-textured yarns is due to the intra-yarn variation in filament flattening which helps to cover the inter-yarn differences [42,69].

We now proceed to identify the key process parameters of the texturing operation that correlate with the occurrence of fabric barré. Since spinning and texturing were established as the major sources of barré, many workers have investigated

these two processes to uncover their fundamental physics and to study the effects that variations in their processing conditions and material differences have on the quality of yarn produced. Most of the spinning research has been conducted by the fiber producers and is not in the open literature. The texturing literature has been conducted in camera and ex camera. We will base our discussion on the available texturing literature.

3. Key Process Parameters of the False-Twist Draw-Texturing Operation.

The basic false-twist, draw-texturing machine (Fig. 1) consists of yarn feeding and withdrawal mechanisms, a device to impart rotation to the yarn, and a heater capable of increasing the yarn temperature to a level at which drawing and setting can occur. The principal texturing process parameters related to yarn quality are yarn twist, yarn temperature, and yarn orientation [43]. These parameters directly influence textured yarn crimp and dyeability. The process parameters are, in turn, dictated by machine dimensions (cold, hot, cooled, exit zones), machine settings (feed speeds, heater temperature, twister speed), the feed yarn properties (residual draw ratio, friction, hot draw force), and their interactions [44].

A. Yarn Twist. The first parameter of interest is the yarn twist. False-twist texturing depends on the dual role of the twister as an uptwister for the entering yarn and detwister for the exiting yarn. In the absence of heating, this leads to a steady-state twist distribution, as shown in

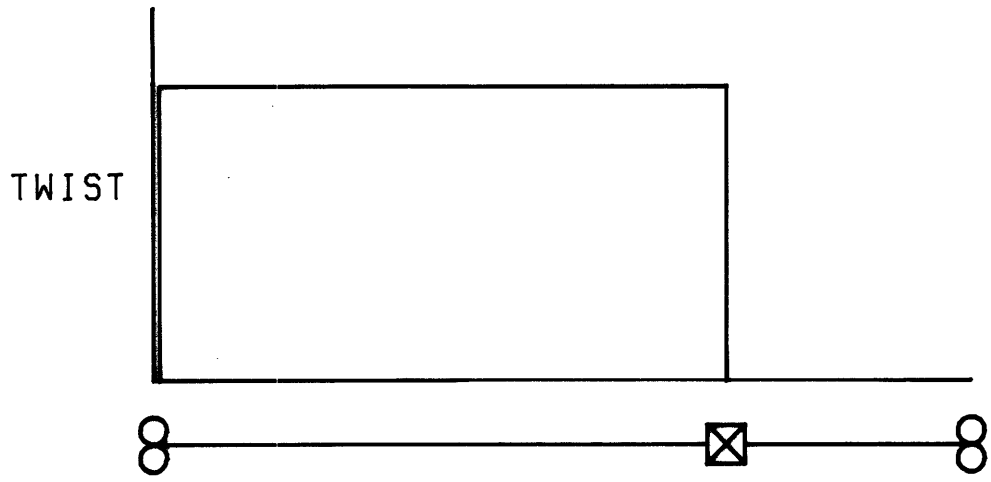

FIGURE 11A.
STEADY-STATE TWIST DISTRIBUTION DURING
FALSE-TWISTING

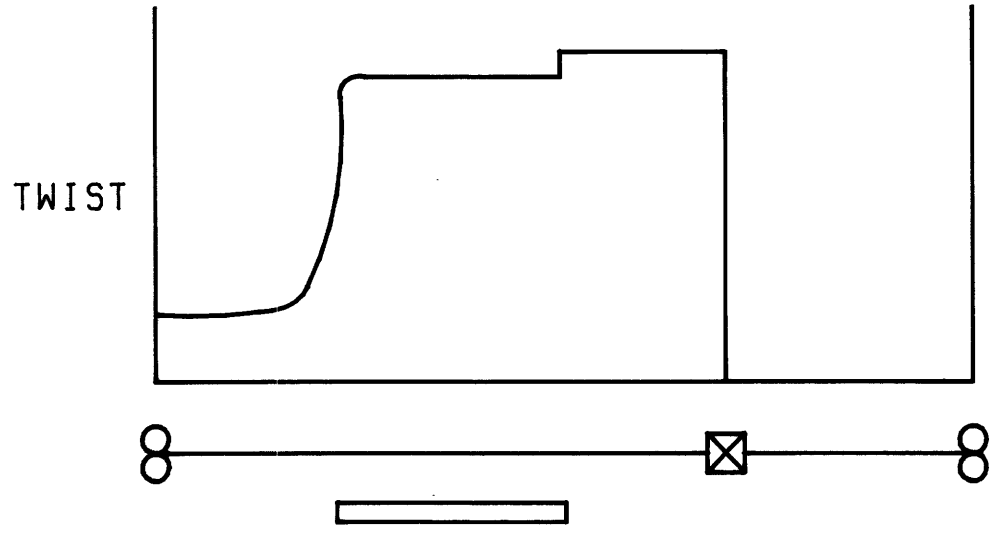

FIGURE 11B.
STEADY-STATE TWIST DISTRIBUTION DURING
FALSE-TWIST TEXTURING

Fig. 11a. When the ratio of local yarn rotational velocity to yarn linear velocity through the twister equals the local twist at the entry to the twister, the yarn will be exactly untwisted as it passes through the twister. In essence, the yarn has been twisted temporarily, hence the name "false-twist". At this steady-state condition of operation, one turn of twist is removed for each pitch length of yarn pulled through the twister. During startup and transient operations, this balance is disturbed and the exiting yarn has real local twist.

To achieve a more permanent setting of this temporary twist, the yarn is heated in the twisted state. The simple case of twisting a uniform rod at room temperature now changes to the case of torsional springs, possessing different torsional rigidities, being twisted in series as shown in Fig. 11b. Since the threadline torque is constant along the threadline, we may expect the cold spring with higher torsional rigidity to uptwist less than the hot spring with lower torsional rigidity. In passing through the heater, the twisted geometry becomes "set" in the yarn, in effect establishing the highly twisted configuration as the new stress-free state of the yarn. When the yarn subsequently cools on exit from the heater, this geometry changes only very slightly because of the high torsional rigidity of the cooled yarn. The level of twist in the cold zone will depend on the level of local twist at the twister unit, on the heater temperature and residence time, and on the feed yarn properties. The level of cold zone twist can be calculated for a given set of machine parameters

and yarn properties [51,52]. Actually, the cold twist level plays a less dominant role in determining textured yarn properties than does the level of hot twist, but it must be considered.

Yarn twist in the hot and cooling zones depends on the machine feeds and twister speed. There are two kinds of texturing twisters (e.g. pin spindles and friction twisters). Pin-spindle twisters operate by wrapping the yarn around a pin mounted perpendicularly to the threadline and rotating the pin on an axis parallel to the threadline. The pin twister has very high torque transmission capability. At normal threadline tension it always inserts one threadline rotation into the pre-spindle zone and one rotation (of the opposite direction) into the post-spindle zone during each pin rotation. Thus, steady-state yarn twist levels can be calculated on the basis of velocity and pin rotational speed. And cooled yarn geometry during steady-state texturing is essentially kinematically determined for a pin twister [54].

Another method of rotating the yarn is by pulling the yarn over the rounded edges of several rotating discs as comprising a friction twister. The disc diameter is hundreds of times larger than the yarn diameter, thus higher yarn rotational velocities (over a million RPM) can be achieved with friction twisters. This is far in excess of that obtainable with pin twisters. Further, with friction twisters, significant noise abatement and energy reduction are possible, as well as much

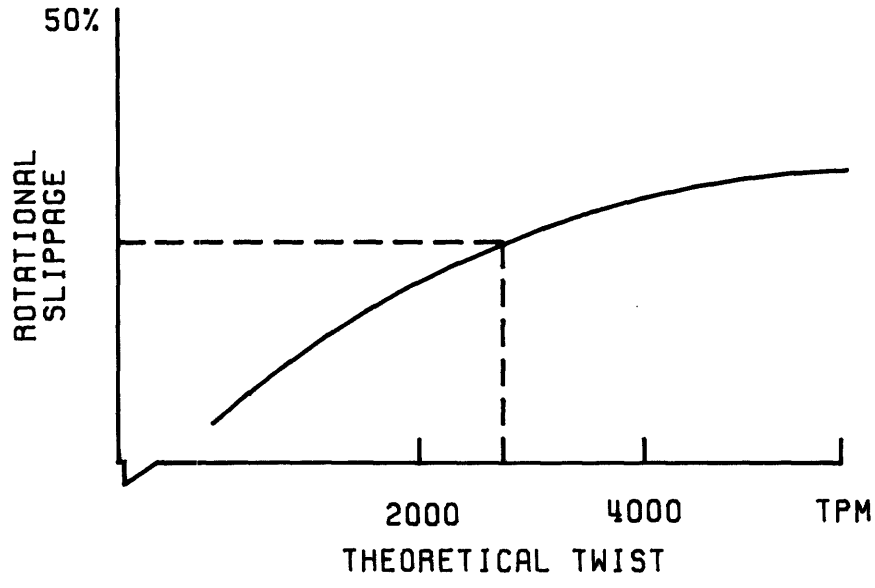

FIGURE 12A: ROTATIONAL SLIPPAGE
AT FRICTION DISCS VERSUS THEORETICAL TWIST
[64]

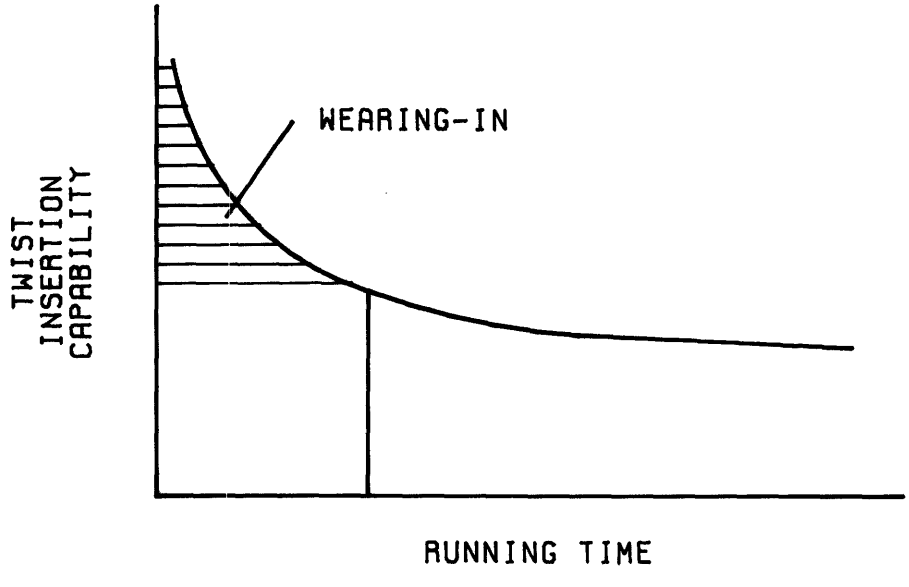

FIGURE 12B: WEARING-IN OF FRICTION
(DISC) TWISTERS
[64]

higher speeds throughout (e.g. >600 m/min) [61].

Unfortunately, friction disc twisters are less exact in their control of yarn (twist) rotation. The amount of rotation imparted to the yarn depends on torque/slip characteristics of the twister/yarn combination, threadline tension, the torque required to twist the yarn, ratio of yarn diameter to friction disc diameter, disc speed, and yarn friction on the discs. The ratio of disc speed to yarn speed through the twister will not be equal to the local yarn twist just before the twister, due to the occurrence of rotational slippage. Figure 12a shows the extent of rotational slippage during friction texturing of the typical 150-denier yarn. The commercial twist range of interest is from 2165 to 2755 turns per meter (55 to 70 turns per inch). The slip, or difference between twist calculated on the basis of yarn takeup speed, disc speed, and yarn/disc diameter ratio, is seen to be in the range of 20 to 30% [61]. The fact that there is rotational slippage presents no problem as long as the yarn diameter, yarn draw and uptwist characteristics, and yarn-on-disc friction are constant with time and the same from position-to-position on the texturing machine. Friction texturing places much greater requirements on the uniformity of feed yarn properties and the constancy of disc friction surfaces with running time. Figure 12b shows that the twist insertion capabilities of friction twisters undergo rapid initial decreases associated with "wearing in" [61]. Pre-buffed discs or discs with profiled

(pre-worn) edges reduce this tendency.

Friction discs with improved twist insertion capability have abrasive contact surfaces. The most commonly used discs are either solid ceramic, or diamond dust coated. The abrasive cutting effect of the disc on the yarn leads to the formation of "snow" on the friction twister and surrounding area. The composition of the snow was examined by electron microscopy and solvent extraction, for yarns with different filament cross sections textured using ceramic or diamond friction discs. In Table 5 we assume that all the material extracted after 10 minutes of boiling in 1,1,1,2 tetrachloroethane was fiber finish and oligomers. This solvent was found to have maximum solubility in PET by Knox et al. [84]. All the residual material was composed of fiber torn off by the action of the friction discs, as shown in Fig. 13. The major difference in snow appearance is between snow from diamond vs. ceramic discs. Diamond discs generate more snow during operation [82] and this snow consists of smaller fiber particles.

The snow from the octolobal yarn run on a ceramic disc (13a) has smaller fragments. The particle size is consistent with the filament lobe size (≈1-2 microns). Octolobal yarns also generate more snow during texturing than do round cross section yarns. The torque needed to twist and untwist the yarn is supplied by the discs acting on the outer filaments in the yarn. When these filaments have protruding lobes on their surfaces (e.g. octolobal yarns), the area of contact between the

Table 5

ANALYSIS OF TEXTURING SNOW

Twister	Fiber Type	% Fiber Fragments	% Finish and Oligomers	% Volatile
Diamond Disc	Round 1	45.9	53.6	0.5
	Round 2	44.2	50.6	5.2
	Round 3	48.7	50.8	0.5
Ceramic Disc	Round 3	41.9	58.2	-.1
	Round 4	43.2	52.6	4.1
	Octolobal 1	55.5	33.5	11

Procedure:

1. Weigh snow sample at standard conditions.
2. Extract sample in 1,1,1,2 tetrachloroethane for 10 minutes at the boil. Filter out fiber fragments.
3. Boil off solvent from extracted finish.
4. Vacuum dry fiber fragments and extracted finish (12 hours).
5. Weigh after reconditioning to laboratory atmosphere.

FIGURE 13. FIBER FRAGMENTS IN TEXTURING SNOW (1000X)

A. OCTOLOBAL FIBER (TYPE 1), CERAMIC DISCS
B. ROUND FIBER (TYPE 3), CERAMIC DISCS
C. ROUND FIBER (TYPE 1), DIAMOND DISCS
D. ROUND FIBER (AS IN B), DIAMOND DISCS

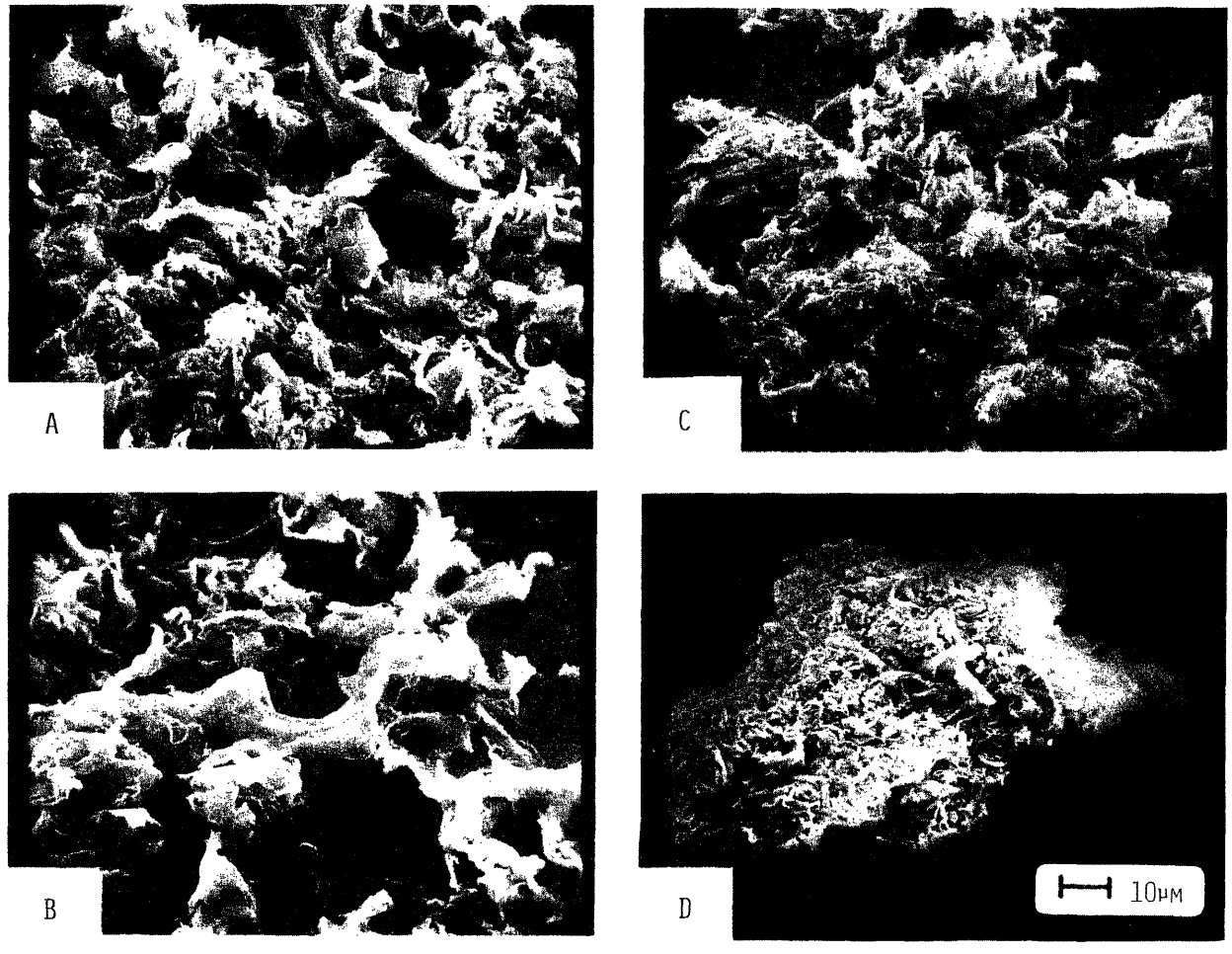

outer filaments and discs is primarily these lobes. Shear failure of these lobes is expected and supported by the data in Table 5. More of the snow from octolobal yarns is fiber as compared with round yarns.

During the course of this study an experiment was undertaken on a running texturing machine (diamond-impregnated discs) to determine the effect of snow buildup on the coefficient of friction and therefore the twist imparted to the yarn. A rag saturated with coning oil was brought into contact with the disc surfaces and sufficient hand pressure applied to remove all visible traces of snow on the discs. The yarn textured before, during, and after the snow removal was knitted and dyed. No visible changes in bulk or dyeability were observed due to cleaning and lubricating the discs. The same experiment was repeated with trichloroethane cleaning fluid with similar results.

The mechanism of friction between abrasive discs and yarns appears to be based on machining forces generated by the cutting action of the asperity particles. This friction mechanism is consistent with greater snow generation, smaller fiber fragments in the snow, and no observed change in fiber/disc friction in the presence of coning oil or finish buildup.

Dupeuble [82] measured the rate of snow generation during texturing and found that diamond discs generate 3.41 grams per threadline in 24 hours of running 150 denier yarn at 600 meters/min. During this period, 14.4 Kg of yarn is processed. This

snow production represents only 0.024% of the yarn mass. But a clearer picture of the snow generation is obtained when one considers what fraction of the 1μm thick outer layer of the 142μm yarn is removed. This layer represents 1.4% of the yarn volume and about 2% of this layer is removed by the abrasive action of the diamond discs. Although the rate of buildup of snow is only a minute fraction of the textured yarn throughput, it can be an important process variable when it accumulates to the point of affecting the frictional properties of drive surfaces. Furthermore, it may turn out to be an undesirable environmental contaminant. For the time, we shall disregard the snow effect and deal with other process variables that influence twist.

Most analyses of twist formation consider that free filament radial migration occurs at the entry (uptwist) point to the cold zone. This migration allows for equalization of tensions amongst filaments as they enter different layers of the twisted yarn. Outer layers require a longer filament length for a given yarn length and vice versa. At the draw point over the heater, the filaments draw and the yarn uptwists further in response to the common threadline torque and tension and lower (hot) extensional and torsional rigidities. Some additional radial migration occurs during this uptwisting operation [44]. The general assumption of the models is that the filaments in the yarn follow uniform right circular helices defined by a radius and an angle. This is not the case during

texturing at some commercial twist levels due to yarn buckling as shown in Fig. 14. As the twist is increased in the range of commercial interest, the amount and severity of torsional buckling increases [44,52]. Buckling is clearly a large deviation from assumed threadline geometry and can cause recurring transients in the texturing zone due to interactions of the buckled yarn with the twister [45]. There is very little in the literature outside of [45,52] referring to the torsional buckling of the texturing threadline; although a similar phenomenon, known as hockling, has been studied for cables [67]. Greenhill's formula has been found to apply, but the severity of buckling in cables was much increased as compared to that in solid rods. A brief investigation on the occurrence of buckling under controlled twisting and heating conditions was carried out as part of this study. The results are presented in Appendix 1.

Yarn twist geometry can also be dramatically affected by the texturing machine phenomenon of "surging". The surging phenomenon represents a limit cycle operation of the texturing process. During surging, all threadline variables (tension, torque, twist, local velocities, temperature) exhibit recurring cycles around their steady-state values [52,54,64]. Severe surging will produce yarns variable along their length in

FIGURE 14 (FROM [52])

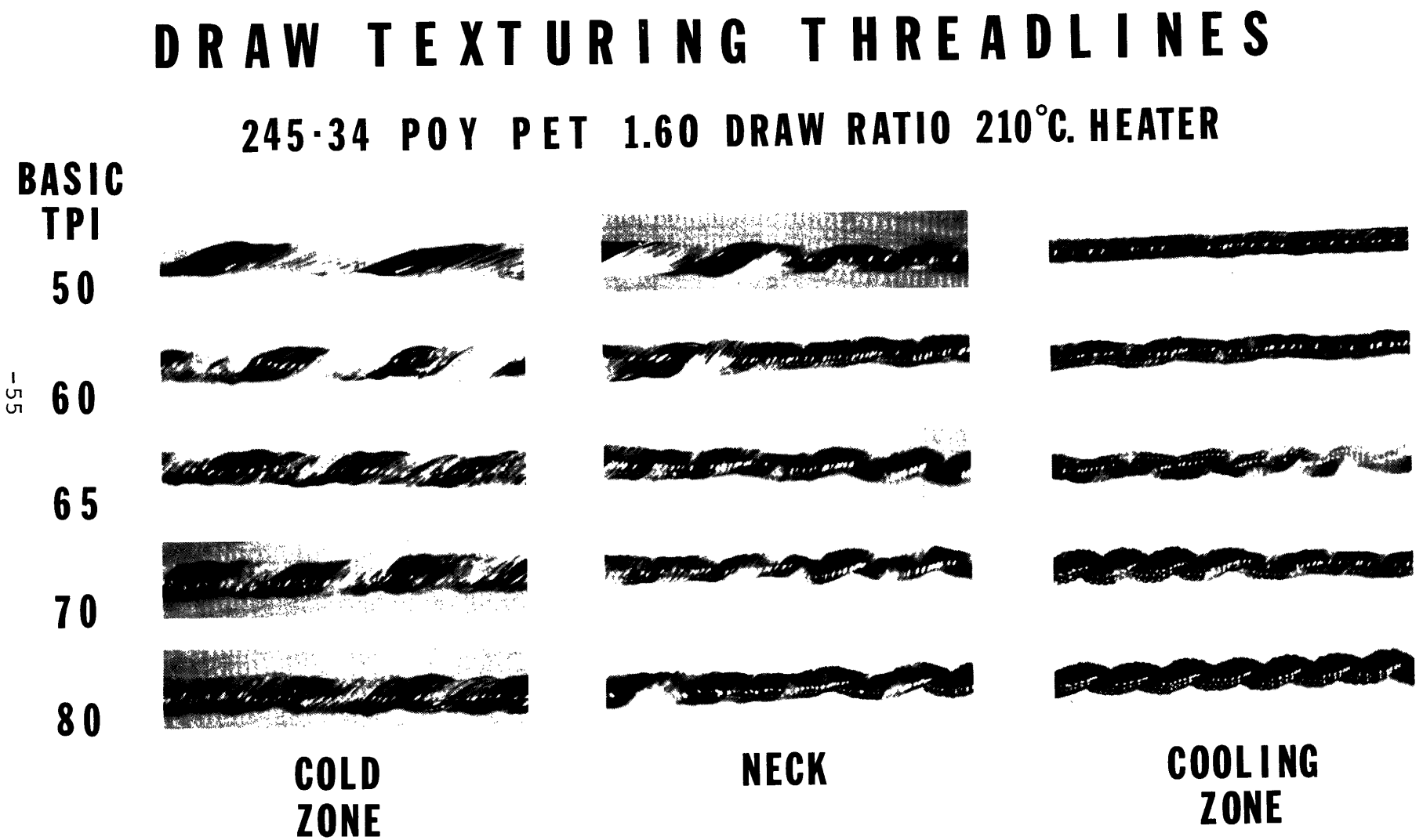

crimp and dye behavior. But the average value of crimp and dyeability need not vary in the presence of mild surging. Surging can be triggered by a single or recurring threadline perturbation, such as a worn feed belt, speed change of the twister, a bad feed yarn package, feed yarn variability, or a knot passing through the machine.

The system dynamics of texturing have been investigated by Thwaites [55]. He has predicted changes in twist, tension, torque for periodic changes in spindle speed of 10% based only on slopes of steady-state characteristics of the process. The predicted responses agree well, in both amplitude and phase, with the observations. According to his model, threadline disturbances occurring at less than 2Hz, or at lengths greater than 2 meters in the feed yarn will have the largest effect on threadline variables during commercial texturing. Maximum threadline disturbances will occur for feed yarn disturbances corresponding to 4.5 times the transit time through the cold, hot, and cooling zones of the texturing machine.

Bell and Backer [50] have recently examined the surging phenomenon. They found the occurrence of surging and its frequency to depend on stored elastic energy in the cooling, twisted yarn. As the texturing temperature was raised, the elastic energy in the twisted yarn was reduced due to increased setting of the deformed geometry and the cycling frequency was reduced and ultimately eliminated. They also found that threadline disturbances were maximum for feed yarn distur-

bances of about 5X the texturing machine length.

In summary, we have seen that the twisted yarn geometry is determined by machine settings, twister-yarn interactions, and yarn torque/tension levels in a complex manner.

B. Yarn Temperature. The yarn temperature appears to be the easiest of the key parameters to dictate by machine settings (i.e. heater temperature, speed). However, the actual temperature-time history of the filaments is important in determining the crimp potential of the textured yarn. The twisted geometry and the temperature of the yarn during texturing will both contribute to the subsequent crimp development. Backer and Yang [44] found that 3/4 second heating and 1/2 second cooling times were required for maximum crimp development during conventional texturing with fully oriented feed yarns. Morris [62] found that a 1/5 second heating time was sufficient during draw-texturing of partially-oriented feed yarns. He further proposed an exponential rise in crimp development with residence time at constant heater temperature. This was based on the similarity of measured yarn temperature at the heater exit and yarn crimp development. Crimp stability, the ratio of yarn crimp after to yarn crimp before the application of a simulated knitting load, was seen to reach a maximum level after 0.2 seconds. Higher heater temperatures lead to higher crimp stability through additional crystallization.

As texturing speeds increase, a longer heater length is

required to avoid an excessive temperature gap between heater and yarn [65]. Threadline tension increases with increased machine draw ratio, lower heater temperature, or reduced feed yarn residual draw ratio. A change in machine draw ratio from 3.6 to 3.8 can produce 4°C exit temperature differences due to differences in heater contact pressure for the slightly curved heater [64]. Changes in twist can result in changes in local velocity over the heater. More highly twisted yarns (i.e. for constancy of mass throughput) move more slowly over the heater due to higher linear density (twist contraction). To first order, this increase in residence time should equal the additional time required for the heat to penetrate the thicker yarn. This equality is based on the fact that residence time is proportional to yarn diameter squared, as is the time to heat up the yarn interior to the specified temperature. So, no changes in yarn temperature with changes in twist are expected for conditions of constant throughput. However, higher yarn rotational speeds, consistent with higher twist, could provide a better heat transfer coefficient.

Of course, differences in per cent finish, or its volatile fraction, or in moisture content of yarns, result in lower yarn temperatures. Again, the critical nature of yarn finish uniformity is emphasized.

In summary, yarn temperature was found to depend primarily on heater temperature, residence time over the heater, and the heat transfer coefficient between yarn and heater as influenced

by threadline tension and fiber finish.

C. Yarn Orientation. Hot yarn molecular orientation within fibers is determined primarily by the imposed strains of drawing and twisting. This hot strain can be permanently locked in by crystallization or temporarily frozen in by cooling the yarn below T_g [85]. Untwisting at the pin leads to a reversed torque and higher tensions on the yarn. Some cold drawing or stress setting will occur under this action. Unless the post-twister stresses are very large (c. 0.5 gpd), or the yarn has not cooled to below T_g, no permanent setting of the yarn in the straightened geometry will occur [63,66].

Significant intra-yarn variations in draw ratio occur in the presence of draw point motion. These can occur when threadline tension, yarn "T_g", or heater contact vary [54]. Inter-yarn differences in orientation can be caused by differences in machine draw, feed yarn, yarn cooling, or guide friction.

D. Magnitudes of Crimp and Dyeability Changes due to Texturing Parameter Changes. Table 6 summarizes some of the changes in feed yarn or in the texturing process that can lead to changes in textured yarn quality [68]. Table 7 lists the percentages of relative changes in textured yarn properties produced by known changes in texturing machine settings and feed yarn properties. It must be noted that crimp and dyeability were measured by different methods in the tests. The data were gathered for both conventional and draw-texturing,

TABLE 6

SOME PARAMETERS INFLUENCING TEXTURED YARN QUALITY

IN SINGLE HEATER FALSE TWIST TEXTURING

Steady State	Non-Steady State Cause of Non-Uniformity
Physical Properties of Entering Yarn	
Fine Structure	Package Relaxation Variations
Cold Stress-Strain Properties	Package Relaxation Variations
Hot Stress-Strain Properties	Package Relaxation Variations
Coefficient of Yarn-Metal Friction	Finish Variation
Coefficient of Fiber-Fiber Friction	Finish Variation
Geometry of Entering Yarn	Interlace Nodes; Twist Accumulation
Pretension of Entering Feed Yarn	Snagging, Package Shape and Size, Balloon Size
Speed of Feed Yarn Entering	Worn Rolls; Traverse
Residence Time in Cold Zone	Linear Speed Variation
Heater Temperature	Temperature Variation
Heat Transfer Coefficient	Finish Variation
Residence Time over Heater	Linear Speed Variation
Twister Parameters	
Rotational Speed	Speed Variation
Geometry and Roughness	Buildup of Finish, Surface Wear
Friction vs. Translational Slippage	Finish Variation
Friction vs. Rotational Slippage	Finish Variation

TABLE 6, (continued)

Steady State	Non-Steady State Cause of Non-Uniformity
Speed of Textured Yarn Through Twister	Tension Variations; Finish Variation
Residence Time in Post-Spindle Zone	Linear Speed Variation
Speed of Textured Yarn at Exiting Rolls	Roll Slippage, Traverse

TABLE 7

DEPENDENCE OF CRIMP AND DYE ON TEXTURING AND SPINNING PROCESS VARIABLES

Textured Yarn Property	Process Variable or Setting	Change in Process Variable	% Relative Change in Textured Yarn Property	Reference
Crimp				
	Primary	+1°C	0.8	[44]
	Heater		1	[65]
	Temperature		1.7	[61]
			2.2	[58]
	Twist	+1 TPI	1.2	[58]
		-1 TPI	1.2	
	Machine Draw Ratio	+1%	-7	[58]
	Feed Yarn Birefringence	.148-.152	-10	[58]
	Yarn Balloon (Pretwister)	None-Small	-6	[65]
		None-Large	-12	
Dye Uptake				
	Primary	+1°C	0.3-1.6	[57]
	Heater		0.5-1	[26]
	Temperature		1 -2	[100]
			1	[90]
	Twist	+1 TPI	-0.8-0.2	[57]
	Tension	1%	-0.3	[90]
	Machine Draw	+1%	-1	[28]
		+1%	-5	[66]
	Feed Yarn Birefringence	.148-.152	-6-12	[57]

using pin or friction-disc twisters. Therefore, absolute values of the effects will be expected to vary.

Primary heater changes of +1°C produce no more than about 2% relative change in crimp or dyeability. McGregor and Adeimy [57] claim that a dye shade variation of this magnitude is about one-half a McAdam unit, or one-half that required to be "just perceptible". The effect of twist variations of 1 TPI on relative dyeability is less than 1% and depends on the feed yarn structure [57]. Twist level changes of 1 TPI up or down increase relative crimp development by 1.2%. These data were taken on a fixed spindle speed machine. Twist changes therefore involved changes of threadline throughput speed. Thus, greater twist would correspond to longer heater times (greater crimp development) and vice versa. The lower twist yarn should then have experienced both lower twist and lower heater residence time. The reported increase in crimp development for lower twists certainly cannot be simply explained. The only hypothesis that can be offered in support of this observation relates to the mechanics of crimp development in a textured yarn.

Crimp development is generally measured by subjecting the textured yarn to a very small axial tension while it is exposed to conditions that promote crimp development. The driving force in crimp development relates to the strain energy in the textured yarn when held in a partially straightened condition. The strain energy is related to the deformational difference

between the set geometry and the lightly loaded configuration, but also to the bending and torsional rigidity of the component fibers. There is no question but that higher twists result in a more extreme set geometry. However, it is well known that higher twists also result in greater lateral distortion of the component filaments and accompanying reductions in bending and torsional rigidity. Obviously, these two effects work against each other as they influence the strain energy of the partially straightened yarn.

Major changes in both crimp and dyeability are associated with changes in yarn orientation produced by variations in texturing machine draw ratio. It is reported in Table 7 that a 1% increase in texturing machine draw ratio effects a reduction in relative crimp of 7% and a reduction in relative dye uptake of 5%. Similar effects are shown for changes in feed yarn birefringence from 0.148 to 0.152. This increase reduces relative crimp by 10% and the relative dye uptake by 6-12% depending on the dye and its application.

In high speed draw-texturing (≈600m/min or higher), the size of the threadline balloon from the heater exit to the twister can have extremely large effects on yarn crimp. Less twist is inserted in the yarn operating with a larger balloon, hot setting time is reduced by faster cooling, and higher tensions reduce the setting efficiency [65]. This combination leads to a marked reduction in crimp.

Based on these average changes in yarn properties pro-

duced by texturing process variations and feed yarn changes, the required control of texturing machine settings and feed yarn birefringence can be estimated using data in Tables 1 and 2. We would like to minimize barré in any fabric, therefore we should use restrictive limits consistent with Tables 1 and 2. The "worst case" relative crimp difference required to produce barré is seen in Table 1 to be about 1%. The worst case relative dye shade difference is also about 1% from Table 2. Using these as design limits, the values of control limits are calculated and shown in Table 8. Additional values have been calculated for POY polyester feed yarns. The birefringence of a PET fiber is directly related to the fiber orientation. Using Ward's [70] data on birefringence vs. draw ratio and assuming a desired residual draw ratio of 1.65 for a POY polyester texturing feed yarn, we can calculate the control limits shown in Table 8. Various techniques are used by fiber manufacturers for monitoring texturing feed yarn quality and are summarized by Dumbleton [98].

4. Control of Key Parameters.

The key parameters of the texturing process that require careful control to avoid barré have been shown to be yarn temperature, yarn twist, and yarn orientation [43]. A first sensible approach to control such yarn parameters is to control those machine actions which dictate the critical threadline parameters. The related machine actions are heater temperature, twister speed, and input/output speeds.

TABLE 8

WORST CASE CONTROL LIMITS TO PREVENT BARRÉ

Machine Setting or Process Parameter	Control Level to Prevent Barré Due to Relative Differences in Dye of 1%	in Crimp of 1%
Primary Heater Temperature	$\pm$ 0.5°C	$\pm$ 0.5°C
Yarn Twist	$\pm$ 2 TPI	$\pm$ 1 TPI
Machine Draw Ratio	$\pm$ 0.1%	$\pm$ 0.1 %
POY Feed Yarn Birefringence	$\pm 4 \times 10^{-3}$	$\pm 1 \times 10^{-3}$
Conventional Feed Yarn Birefringence	$\pm 0.3 \times 10^{-3}$	$\pm 0.5 \times 10^{-3}$

Modern texturing machines have excellent temperature control systems. Their temperature uniformity, both along the heater length and between positions, is theoretically adequate ($\simeq \pm 0.2°C$), if the control system lives up to its design potential. The control of heater temperature does not, however, control yarn temperature. The speed of the twister in the case of friction discs is also well controlled ($\simeq$1%). Again, this does not guarantee a uniform twist level. The variation in speed of a machine ($\simeq$5%) due to voltage changes will not affect the machine draw ratio, since the shafts are geared together. The machining tolerances of the feed rolls should provide for no more than 0.1% variation of local yarn speeds from position to position.

The machine tolerances and closed-loop control (in the case of temperature of the primary heater) appear to be adequate to provide the necessary "open-loop" machine actions on the yarn. However, if this open-loop control were all that was necessary, the barré problem would have vanished 5-10 years ago. It is likely that either variations in machine settings or feed yarn within the acceptable limits for each variable or variations in the manner in which machine settings act on the yarn, combine to cause 10-30% of all texturing production to have unacceptable variations in crimp and dyeability [18].

The situation calls for consideration of on-line, closed-loop control or monitoring. To control the critical yarn parameters on-line requires:

(1) measurement of parameters on-line,

(2) suitable control elements,

(3) formulation of a control law.

A. Yarn Temperature. What methods are available for measuring yarn temperature on-line? The best available method uses the convective null-heat-balance principle. A device using this principle is the Fibretemp available from Transmet Corporation. Its sensing head contains a temperature sensing plate exposed to convection from an enclosed heater (at a known temperature) and the moving yarn. When operated at the null balance conditions, the instrument does not change the temperature of the yarn and imparts negligible rotational or linear friction forces to the yarn. A more complex method involves the use of an infrared microscope such as one offered by Barnes Corp. and utilized by Lunenschloss and coworkers [71].

Both of these methods might work with sufficient accuracy (0.5°C) to provide threadline surface temperature measurements at the heater exit. The Fibretemp clearly has price and convenience advantages. Moussa [72] has calculated that substantial temperature differences (≃50°C) can exist between the yarn surface and its center. He also calculated that yarn surface temperatures for a given heater temperature do not significantly change due to large changes in physical or thermal properties of the threadline. On the other hand, average or centerline temperatures vary considerably under these conditions. In light of Moussa's calculations and the likelihood

that finish or geometric variations lower the true average yarn temperature, the measurement of surface temperature may not correlate well with yarn dye uptake and crimp values. The slightly more "penetrating" measurement of yarn temperature given by the Fibretemp should correlate better with yarn properties.

The next aspect of on-line control of yarn temperature involves choosing a suitable control element for rapidly compensating yarn temperature variations on a continuous basis. The temperature change required to negate variations in yarn thermal properties, primary heater temperature, or heat transfer to the yarn should be on the order of 5-10°C. A simple method might involve changing the length of yarn contact with the existing heater. The geometry of such an arrangement must minimize threadline length changes (tension changes) that could trigger surging [96]. Alternately, a small additional heater with rapid heating capability could be used. Bauer [73] lists potential heating elements for high speed texturing as either radio frequency, laser, ultrasonics, or flame. Of these, radio-frequency heating is the most attractive for a number of reasons:

(1) heat generation throughout the yarn,

(2) efficient heat generation,

(3) instant on-off capability with no yarn path change,

(4) no dangerous radiation hazards to personnel.

The use of radio frequency heaters for texturing yarns is discussed in [108]. The r.f. current drawn would also refelct the temperature of the yarn and could be used as a temperature sensing device.

The control law, under the assumption that only the temperature of the yarn controls both yarn crimp and dyeability, would be to keep the yarn temperature constant as it exits the heater. A temperature of at least 190°C is desired to achieve good yarn setting and to have low sensitivity of dyeability to heater drift [13,65].

B. Yarn Twist. The control of yarn twist is the most obvious route to yarn crimp uniformity. The on-line measurement of twist and twist-related quantities has been summarized by Lunenschloss and Fischer [74], Greenwood [43], Mutschler [75]. Twist measurement is fundamentally a matter of measuring helix angle, α, and diameter, D_y, on the twisted yarn. Twist = $\tan\alpha/\pi D_y$. Most twist measurement schemes assume uniform filament denier so that either a helix angle or a yarn diameter measurement will correspond to the twist. Carruthers [76] and Lunenschloss and Coll-Tortosa [77] have systems based on a pivoting knife-edge lining up with the groove between the outer filaments in the yarn. The angle of the blade is measured photoelectrically and is equated to the helix angle of the yarn. Variations on the order of 1 TPI or 40 turns per meter (basic) twist are important. The required sensitivity of the twist angle measurement is

therefore about 1/2°. The device described in [77] has quick enough response to follow transients during texturing.

Devices based on mechanically measuring the diameter of the twisted yarn as an indication of the twist level have been developed, but meet with considerable difficulty due to the small diameter differences involved. For a 1.5 TPI or 60 TPM change in basic twist at commercial twist levels, a diametral expansion of 1.5-2 μm occurs on a diameter of about 140 μm. Alternately, the change in denier, or yarn mass per unit length, as a function of twist can be monitored using capacitive sensors, but the variation in spin finish, which shows up clearly in capacitance measurements, can be much larger than the variation in yarn denier [74].

Since the twisted yarn screws itself through space during steady-state texturing, measurement of the rotational velocity and translational velocity [78,79], or the velocity along the helix angle [80] will yield the yarn twist. The direction of maximum velocity obtained by vector addition corresponds to the helix angle. The yarn twist can then be calculated as described earlier.

Assuming constant threadline tension and yarn properties, yarn torque should correlate with yarn twist. Lunenschloss et al. [71, 117] demonstrated the correlation between on-line torque readings and photographically determined twist levels. Similar data were generated by Brookstein [52] who also measured the tension simultaneously.

The possibilities for using on-line torque or twist choking force measurements for control of yarn twist are little better than for the direct twist measurement schemes. These methods show variations in torque of 8×10^{-7} out of 4×10^{-5} NM (2%) and in choking force of 9 out of 120 millinewtons [7.5%]) for a change in twist of 2 TPI in the commercial range. The choking force measurement requires the trapping of twist and would therefore have to be located at the entrance to the texturing zone where the cold twist is much lower, especially during draw texturing. The high sensitivity of the choking force measurement in the range of 40-65 TPI (basic) disappears at the low twist levels (10-25 TPI basic) of the cold zone. In addition, the correlation between cold zone twist and hot zone twist will be poor in the presence of fiber, heater, or guide friction variations [74].

Any control scheme based on monitoring yarn tension alone and using it to control the level of yarn twist is doomed to failure. Mutschler [75] found only a 56% correlation between yarn tension and textured yarn crimp. Nonetheless, several machine and equipment manufacturers offer elaborate systems for monitoring tension. It is their belief that non-uniform yarn will be produced as a result of threadline tension variations. One of these systems, the Tenscan Tension Monitor System [81], automatically scans the tension readings of the threadlines and compares the value with set control limits. Mutschler found that a 7.5%

variation in tension could produce on the average a relative crimp variation in textured yarn of 2.5% (or just below the threshold for single end barré production. Some yarns produced within 7.5% tension variation showed up to 5%, or twice the design level, of crimp variation. On the other hand, some yarns with higher tension variations showed only 1.5% crimp variation.

The control element for use with any of the twist measuring systems described above would provide an independent speed change of the individual twister with respect to the yarn throughput speed, or a change in its geometry, in order to produce subsequent changes in yarn twist. Changing the speed of each twisting unit in a continuous and stable fashion would be possible through the use of expandable drive rollers that run on the machine power belt, or any of the other common variable speed drives based on cone or cone transmission. Similar changes could be accomplished for friction disc units by changing the penetration of the discs (adjusting the center spacer) and thus the wrap angle.

C. Yarn Orientation.

The orientation of the filaments in the yarn is virtually impossible to measure by the standard techniques of birefringence. This is because of torsion and flattening in the filaments and yarn twist. It would require simultaneous knowledge of the filament/yarn geometry to separate the optical and geometric effects and deduce the orientation

of the yarn. Sonic modulus measurements do correlate well with filament orientation, but similar twist knowledge would be required to assess accurately the orientation of the filaments in the zone. The torque in the hot threadline is composed primarily of filament tension contributions. The filament tension will be a function of orientation, setting, and temperature. Therefore, the torque in the threadline should, for constant yarn twist, be related to the filament orientation. No single measurement of textured filament orientation on the running, twisted threadline is feasible.

Control elements for changing filament orientation could involve either twist, texturing draw ratio, or quench rate. It is impossible to change draw ratio or yarn quench rate without affecting yarn twist.

D. Feasibility of On-Line Control.

We have seen that on-line control of textured yarn crimp and dyeability requires on-line measurement and control of twist ($\pm$ 1 TPI), temperature ($\pm$ 1/2°C), and fiber orientation. The control limits for all quantities are small. Most of the measurement systems available, because of this, suffer from gross deficiencies in one or more of these important qualities:

(1) correlation of measurement with desired parameter,

(2) sensitivity,

(3) ruggedness, reliability,

(4) safety,

(5) price.

These limitations in measuring devices make on-line control unlikely. The added expense of individual control elements (over and above the cost of individual measuring devices) makes the prospect of on-line control even more unlikely. Further, we have only limited knowledge of the combined effect of such hypothetical control actions on textured yarn quality.

To reap substantial benefits from an on-line monitoring approach in contrast to the on-line control approach, one would have to check several operating parameters on a regular basis at each position around the machine. The same measurement problems encountered in on-line control schemes as discussed above, obviously apply to on-line monitoring. On-line monitoring has been found to be capable of detecting only gross failures in machine action or large changes in feed yarn properties which lead to rogue yarns grossly different from normal production yarns. Rogue yarns amount to less than 1/2% of normal production on well-maintained machines and are easily removed by yarn packers during their "hand" inspection. A combination of several measured yarn parameters could provide a basis for on-line "go/no-go" evaluation of production. Unfortunately, the theoretical basis for combining these measurements to predict yarn quality is not at hand.

We conclude that neither on-line control nor monitoring to assure yarn quality is technically or economically feasible. At this time we must examine the possibilities for off-line control of yarn crimp and dye properties.

5. Off-Line Control Methods.

Fabric faults are due to dye and geometric differences in textured yarns. Off-line laboratory testing of textured yarns can be conducted to determine the bulk, length, and dye uptake of the yarn in the fabric as finished, or after treatments intended to simulate yarn bulk development and dye uptake in fabric form.

A. Knit-Dye-Grade Method.

The most common form of textured yarn quality control is based on the method suggested by Clements [12], who felt that the best way to examine the dye behavior of textured yarns is to knit and dye a tight hoseleg with adjacent segments from the different yarn packages to be tested. He further recommended the inclusion of a control sample at regular intervals throughout the hoseleg. The hoseleg is then atmospherically dyed with a "critical" dye. Junctions between segments are compared to a reference junction (4/5 on the AATCC International Grey Scale) and numerical values are assigned accordingly. Yarns that produce junctions more severe than the 4/5 reference are removed from the lot prior to shipment. The inclusion of the reference package in the hoseleg is important to assure valid rejection of varying

packages in the presence of minor differences in dyeing procedure.

The apparent dye shade in finished fabrics is also affected by filament geometry in the fabric [47]. Therefore, a looser knit than that recommended by Clements, which allows both geometric and dye differences to be assessed, is most often used in industry. Observations are made in transmitted and reflected light. Differences in appearance of hoseleg segments that are more obvious in reflected light are due primarily to dye differences, while those seen in transmitted light are primarily due to yarn bulk differences [20].

Yarn grading by this knit-dye technique has one very large advantage over other methods, namely it is based on yarn performance in dyed fabric form. If the knitting and dyeing procedures used during the test method match those in subsequent yarn processing, little question can be raised regarding the validity of the test. It turns out that the laboratory knitting machine (F.A.K., Lawson-Hemphill) used in industry has special stitch cam compensation to maintain uniform stitch tension in the presence of yarn extensibility differences. This type of compensation is not used on commercial knitting machines. Further, there is substantial room for the operator's visual interpretation in the test method as usually practiced. This often leads to poor reproducibility between operators [19,87]. The knitting, dyeing, grading, and selecting procedures require substantial time

(12 hours) and technician activity. In addition, storage areas must be provided for the material during the testing period. Thus, a considerable increase results in the quantity of material in process.

B. Dye Uptake Measurements.

Instrumentation is available from Toray Industries [88] to measure the average and variation in dye uptake of textured yarns. The most advanced system selects yarn samples from textured packages, ties the samples together, scours, atmospherically dyes (10 minutes), and rinses the yarn before measuring dye uptake optically. The dyed yarn is twisted at constant tension to provide for uniform yarn presentation to the panchromatic light beam. The reflected light is split into two filtered beams. The square root of the ratio of visible light intensity to infrared light intensity is the fundamental output of the device (FYL value). Higher FYL values correspond to lighter dye shades, and vice versa. Calculations are made of the average FYL value and the standard deviation for each sample. The device measures 20 meters of yarn per minute. The length of yarn sample taken from each package is established by experience and the required throughput (number of packages/shift).

Other methods of evaluating the dye uptake of textured yarns are based on measuring the light reflected from the surface of a dyed fabric, e.g. a commercial instrument called the Color Eye is available from Kollmorgen Corporation and is widely used. According to the Kubelka and Munk theory [in 27]

$$K/S = (1 - R)^2/2R,$$

where K = coefficient of adsorption

S = coefficient of scatter

R = reflectance.

Reflectance is measured photoelectrically and the calculated K/S value is directly related to dye uptake for a particular dye. Dye shade predictions for a given dye may be made based on K/S values determined for another dye, if the two dyes are applied under conditions that allow equal approaches to dye uptake equilibrium [57]. It is estimated that 37% variation in K/S values can be caused by differences in fabric structure, filament flattening, delustrant content, or angle of illumination [57].

Of course, more (laborious) direct methods of determining dye behavior of textured yarns are possible. One such procedure involves dyeing the yarn and then extracting the dye from the yarn. Optical density of the extracted dye solution is measured and the dye absorption calculated. Alternately, a mass of yarn can be introduced into a bath of known volume at a given dye concentration. The change in optical density of the dye bath liquor after removal of the dyed yarn will then be inversely related to the dye in the yarn. Dyeing is a slow process (hours) and therefore any individual treatment of yarns from each textured package is simply impractical due to labor and time requirements.

Since most industrial dyeing procedures are not carried

out to equilibrium, dyeing rate can be used as a critical parameter to anticipate barré. A recently developed method for rapidly evaluating dye rate differences involves the use of a fugitive tint [57]. The tint is sprayed onto the yarn samples and rinsed off after a given time (from 30 to 300 seconds). Those yarns that are more deeply shaded are expected to dye darker. The details of the composition of the tint are unavailable. If there is no fiber swelling agent in the formulation to allow for relaxation of the fibers (as occurs during scouring and bulk development), then the correlation between the tinting and the actual dye uptake may suffer. Thorough scouring of the yarns to remove coning oil seems to be critical in achieving any success with this technique.

Other chemical and physical methods that correlate with fiber structure and dye uptake have been developed. Chief among these are fiber density and critical dissolution time (CDT) methods. CDT is the time required for yarn failure under a constant tension while subjected to chemical attack. Several workers have shown good correlation between log CDT and K/S values [27]. Unfortunately, the (dye uptake) K/S values show a minimum at texturing temperatures around 180-200°C, while the log CDT values increase almost linearly with temperature throughout this region. Prior knowledge of the non-linear relationship between dye uptake and log CDT is required. Also, yarn failure will occur at the weakest

point in the yarn, and thus many tests (30) are needed to obtain reproducible results. Finally, each test requires a different length of time (10-1000 seconds) which makes automation difficult [42] and slows the testing process considerably.

Fiber density measurements also can be used to predict dye behavior of textured yarns. Density increases directly with increasing fiber crystallinity in the range 1.335 to 1.455 gm/cc [83]. As mentioned earlier, dye uptake vs. density shows a minimum in the region of 55-60% crystallinity [26,37]. If the dependence of dye uptake on crystallinity is established for each yarn type, then fiber density measurements can be used to predict yarn dye behavior. Additional crystallization occurring during the dyeing and finishing operations will obviously affect the validity of predictions. ASTM standard number based on pre-dyeing densities (D1505) describes a method for measuring density using a density gradient column and calibrated floats (e.g. available from Scientific Glass Apparatus Company). Excellent sensitivity ($\pm$ 0.0001 gm/cm^3) is afforded by the equipment, but it is a rather slow process (15-30 minutes to equilibrate) and requires periodic removal of the test samples (a 24-hour process) from the column.

Measurements of breaking strain and tenacity (ratio of breaking force to linear density) of textured yarn represent another quality determination for yarns. When yarns are textured at different temperatures, their subsequent breaking

strain exhibits a minimum, while their tenacity and modulus both exhibit a maximum for texturing temperatures of about 200°C. The decrease in tenacity and modulus above 200°C is due to a loss of amorphous orientation and increased chain folding [42,94]. Tenacity and strain-to-break measurements lack the sensitivity to detect minor temperature variations during texturing--these minor variations are much more apparent in crimp measurements [58].

C. Crimp Measurements. Crimp measurements on textured yarns are very commonly used as a basis for quality control, since the yarn crimp is directly related to fabric bulk, fabric stitch density, and other mechanical properties of the fabric [38,40,89]. Crimp is simply the percentage of excess fiber length in a given yarn length when lengths are measured under specified loads.

$$\text{Crimp}^{\text{Index}} = \frac{\text{Filament Length - Yarn Length}}{\text{Yarn Length}} \times 100\%$$

$$\text{Crimp Contraction} = \frac{\text{Filament Length - Yarn Length}}{\text{Filament Length}} \times 100\%.$$

For example, a yarn composed of parallel straight filaments has no crimp, since the fiber length is equal to the yarn length for any applied load. However, a yarn made up of filaments having a planar zig-zag shape inclined to the yarn axis at an angle "α", when α is measured under a given load, does have crimp. The crimp index of such a hypothetical yarn is just secant α-1 for that load. This crimp index and the associated crimp angle will decrease as the applied load is increased.

The crimp in false-twist textured yarn is due to the filament memory of the helically-twisted geometry heat set during texturing. When the textured yarn is untwisted and straightened, then allowed to contract, the individual filaments will attempt to resume the original three-dimensional paths and thus contract. The exact geometry of the filament paths and their torque and tension during this crimp development stage have been the subject of a number of studies [53,90,91,92,93].

These studies show that filaments set in a helical geometry consistent with that used in commercial texturing will collapse into (left- and right-handed) helices with reversals. The radii and helix angles on either side of the reversal point are, in general, different. Assumptions governing the mechanics or geometry of the reversal point determine the relative fiber lengths, helix angles, and radii in the reversed and equi-helices. In addition, filament snarling (self-plying) to relieve torsional energy is observed on occasion, especially for yarns textured at low twist levels or unrealistically high contractions.

The extension of treatments for ideal elastic single filaments to the case of crimp (bulk) development for a multifilament draw-textured yarn in fabric is limited by numerous non-ideal complexities at the filament, yarn, and fabric level. First, the filaments have not been set in precise helical paths due to filament radial migration during texturing twisting. Second, filament cross sections do not

remain round during draw texturing, and the effect of flattening on EI and GI_p of the filaments can be severe. Third, considerable interfilament frictional interaction and geometric interference in the yarn during bulk development are to be expected. Yarn bulk will be somewhat lessened as "cooperatively" formed equi- and reversed-helices occur. This phenomenon is sometimes called "follow the leader" crimp. Fourth, the constraints imposed on free bulk development by the neighboring yarns and the stitch pattern in the fabric will also influence crimp and bulk development.

Over the years, many crimp (bulk) measurement schemes have been devised. These are well summarized in articles by Schubert [95], Latzke [96], Lunenschloss [97], and Lang and Haller [89]. An important distinction should be made between crimp testing of undeveloped as against "developed" crimp. Testing of undeveloped crimp is generally conducted on yarns as removed from the textured yarn package. Testing of developed crimp is conducted after a mechanical, and/or thermomechanical treatment of that yarn. In general, there is good correlation between "developed" and "undeveloped" crimp [44,61]. However, winding tension in the texturing process will influence undeveloped crimp to a larger extent than developed crimp [63].

To achieve crimp measurements which are meaningful for judging yarn quality:

(1) crimp development must take place under

controlled conditions equivalent to those during crimp development in the fabrics,

(2) the crimp measurement employed must provide maximum selectivity between yarns and should be reproducible.

For practical use, the method must also be quick, require minimum technician skill, and (ideally) be automatic in operation to increase the reproducibility of the measurement.

Crimp tests may be performed on single filaments, single yarns, or yarn hanks. The measurement may focus on filament geometry, yarn bulk, yarn torque-liveliness, specific aspects of the load-elongation behavior (filament, yarn, hank), or length changes (skein or yarn) as a result of crimp development.

1. Direct Observation of Filament Crimp Geometry or Yarn Geometry. The three-dimensional path of a crimped filament in a textured yarn potentially contains far more information than that contained in a simple crimp (index) measurement. The crimp amplitude, crimp frequency, local filament curvature, and torsion, can be calculated from measurements of filament geometry. These measurements can be coupled with load/extension measurements. These results can be helpful in analyzing the cause of faulty yarns. Semi-automated systems for measurement and calculation of crimp-related parameters are available at two major U.S. fiber producers. One system uses a projection microscope with image

analysis and associated transport and loading devices for filaments or yarns. The cost of the devices and time and expertise required for testing have limited their wide use in quality control.

2. Yarn Bulk Measurements. Optical measurements of yarn width or yarn opacity have been reported [109]. As shown in Fig. 15, this measurement requires very accurate control of yarn tension in the range of 10 mgpd to give results in the region of highest bulk sensitivity [97]. A special yarn width measuring device has been constructed by the author for detecting variations in yarn width corresponding to tight spots in the yarn. This device uses a microscope with a projection eye piece to form an image of the moving yarn on the 64-element photodiode detector. The voltage output from each detector is compared to a reference voltage corresponding to the presence of the yarn. The number of "light" detectors (proportional to yarn width) is counted. Details of the circuitry and a photograph of the operating unit are included in Appendix 2.

Another method of yarn bulk testing is based on the specific volume of textured yarn. Yarn is wound onto an empty spool of defined volume and mass under accurately controlled tension. The full spool is weighed and the specific volume of the textured yarn is calculated. The testing is conducted on yarn with undeveloped crimp.

Still another measure of yarn bulk is provided by the

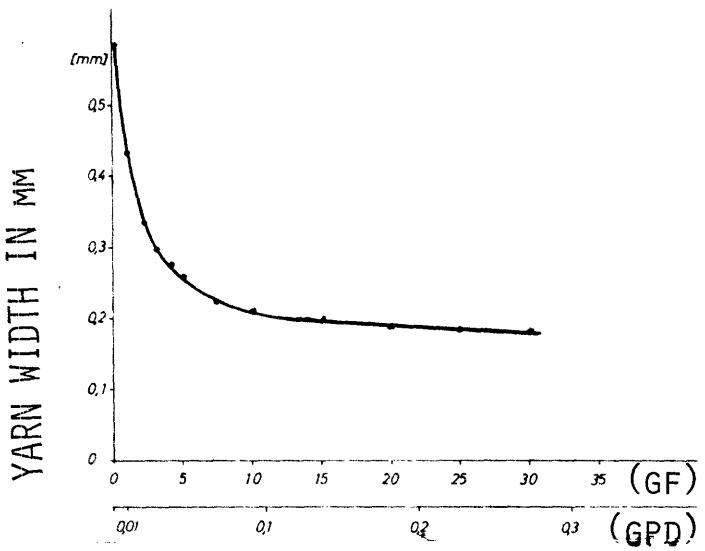

FIGURE 15. MEASUREMENT OF YARN BULK (POLYESTER 100 DEN/20 FIL) [97]

AKZO-Bulkiness Tester [110]. The volume of 10 grams of yarn is measured under a hydrostatic bladder pressure of 0.1 atmospheres. The method will accept fiber, yarn, hank, or fabric samples.

3. Yarn Torque-Liveliness. Two methods are most commonly used to determine the torque-liveliness of the textured yarn. The first method involves tangentially removing a length of yarn from the textured package and hanging a small weight in the center of the span. The ends of yarn are brought together and the weight spins as the yarns ply on one another to shed their torsional energy. The number of turns/meter in the plied yarn is an indication of the yarn's torque-liveliness. A good correlation is claimed between torque-liveliness obtained by this method and crimp contraction (e.g. 20% crimp contraction gives 70 T/M twist. However, the sensitivity of the method in the region of interest (crimp contraction >15%) is low [111].

The second method involves tangentially removing the yarn and clamping a length of yarn under tension. The clamps are brought together until a snarl develops. The distance between the clamps is the measured value and is related to yarn torque-liveliness [112].

Other more complicated methods for measuring torsional behavior of yarns have been developed [113,114,115,116]. Their application is limited chiefly by equipment cost, length of test time, and the operator skill required. Due to

the variability of textile materials, it is expected that many torsional tests would be required to obtain meaningful averages.

4. Load/Elongation Properties of Textured Yarns. As stated, the textured filaments in a tensionless condition follow paths describing alternating helices of varying radii and helix angle. Obviously, the length of such a system of springs will depend on the load applied to the system. The degree of contraction (crimp) will increase as the force on the yarn is decreased. The yarn force is determined by the contributions of individual filament tension, bending, and torque components. This force will depend on the material constitutive (σ/ε) relations, the stress-free (set) geometry of the filaments, the imposed geometry (length), and the degree of filament entanglement or interference.

A typical load/elongation curve for a textured yarn is shown in Figs. 16a,b [97]. Since reproducibility is very poor if load elongation testing is conducted from a zero starting load, a small pre-load of about 1-2 milligrams per denier (0.9-1.8 millinewtons/tex) is used. The initial extension from this low load is accommodated by straightening, or unrolling of filament helices and it requires little additional load. As the helices are further straightened, the load begins to increase more rapidly. Somewhere in the region of 100-200 mgd, the crimp is essentially removed with only negligible filament extension. However, some kinked

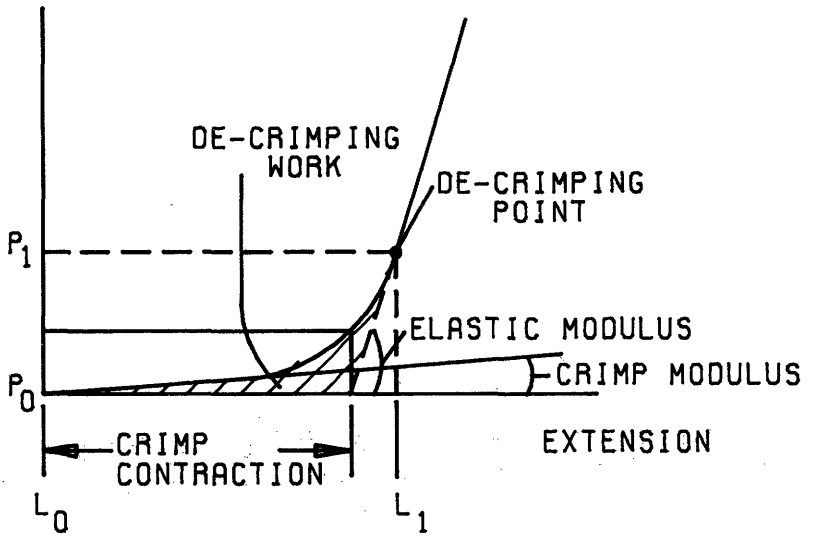

FIGURE 16A:

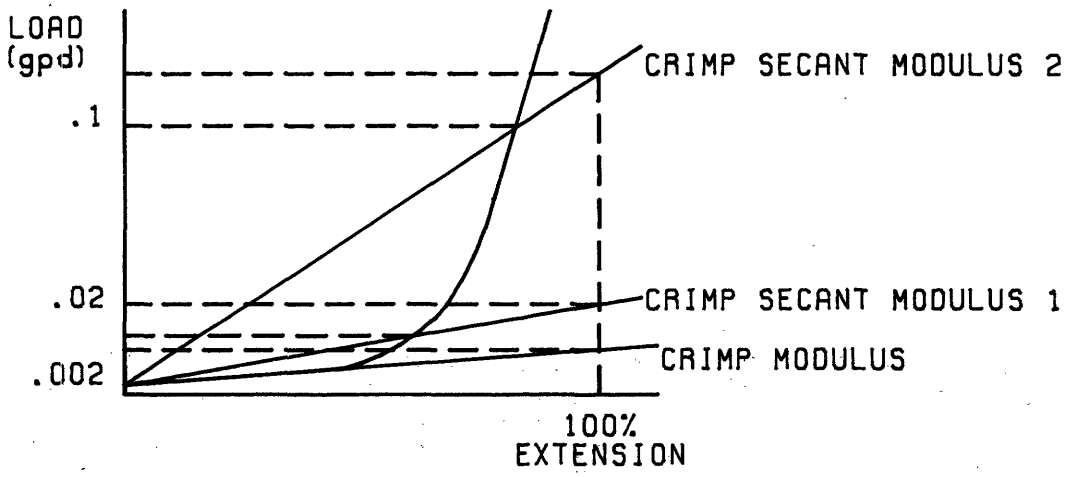

FIGURE 16B:

VARIOUS QUANTITIES DERIVABLE
FROM LOAD ELONGATION CURVES OF TEXTURED YARNS

filaments are still present up to loads of 370 mgd [51]. At higher extension the filaments themselves are extended, and such extensions are accompanied by a much faster load buildup corresponding to the modulus of the filaments. Several quantities related to the load-elongation curve can be calculated as shown in Figs. 16a,b.

Quantities related to load/extension properties of textured yarns can be measured on continuous testers. These testers operate from a fixed inlet tension and measure either the tension increase of the yarn for a given extension [118], or the extension change in the yarn for a given change in load [119]. The bases for these tests are extension or load increases as shown in Figs.17a,b. The major differences in results will occur between such loading and unloading methods, due to material hysteresis or friction and geometric interference.

Additional information is contained in loading and unloading versus extension curves as shown in Fig. 17c. The decrimping (extension) work and the elastic recovery work can be related to the crimp characteristics [97]. Changes in extension after repeated cycling between two load levels have also been used as a basis for testing crimp and crimp stability of textured yarn [120]. These changes may also relate to the yarn crimp which may be expected in knitted fabrics before finishing, just after the cyclic tension of

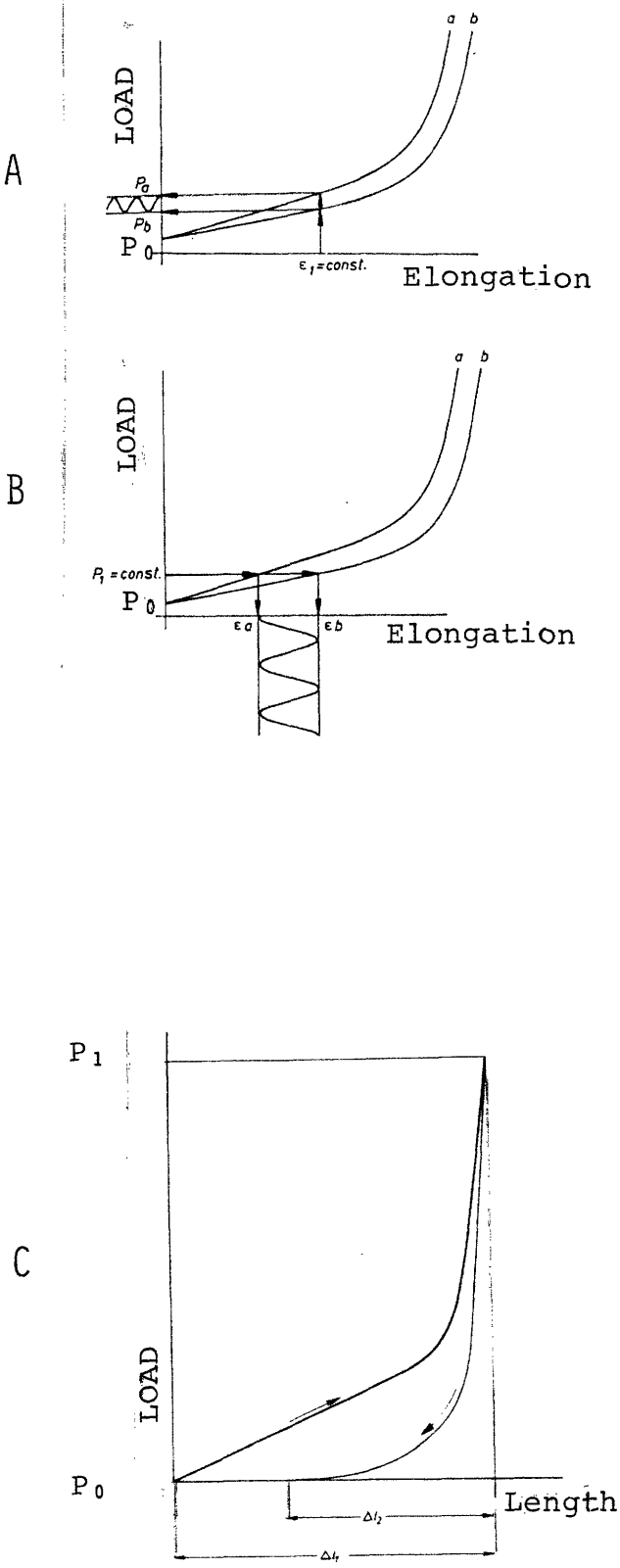

FIGURE 17. TESTING TEXTURED YARNS WITH RESPECT TO LOAD/ELONGATION BEHAVIOR [97]

knitting.

5. Length Changes during Crimp Development. By far the most popular methods for assessing the crimp potential of textured yarns in fabrics are those involving length changes in a skein of yarn as a result of crimp development and filament shrinkage. Table 9 from Latzke [96] summarizes the more popular methods. All methods are based on winding a skein of yarn, measuring the initial skein length, exposing the yarn to mechanical and/or thermal action to allow for crimp development, and measuring the final skein length under various loads. The methods differ in the loads used to measure the skein lengths and the conditions of crimp development. However, a high correlation exists between the methods. Because of manual winding, loading and measuring, the tension-time history of the yarns is often very different. The strong time dependence of yarn creep, or delayed elastic recovery, makes these differences in handling conditions important [98,121]. Two automated devices greatly improve the reproducibility of the crimp determinations.

D. Thermal Test Methods. A great deal of information regarding the molecular fine structure of fibers can be obtained using thermal test methods. Heidemann and Berndt [122] have summarized these methods and their application to textured yarns. Pure thermal or thermomechanical tests are available.

1. Pure Thermal Tests. The pure thermal

TABLE 9. VARIOUS METHODS TO MEASURE CRIMP DEVELOPMENT IN TEXTURED YARNS

Test method	Heberlein	DIN 53840	A.R.C.T.	C.R.S.I.T.	H.A.T.R.A.	Kerilon	Hoechst	Bancroft	Leesona
Hank length Hank count Pre-tension in winding	10 m variable 1 cN/tex	variable 2500 dtex 1 cN/tex	variable 9200 dtex not defined	variable 6600 dtex not defined	variable 1500-5000 dtex not defined	variable 4400 dtex not defined	variable 11000 dtex 0.5 cN/tex	variable 13500 dtex not defined	approx. 100 m variable 1 cN/tex
Crimp development	Nylon: 10 min, distilled water, 60-70°C, hydro-extract,* dry. Polyester: 10 min distilled water, 60°C, boil 15 min, hydro-extract, dry.	Nylon, polyester: 10 min hot air 120°C. Acrylic: 80°C.	10 min boiling water + soap, hydro-extract, dry 10 min at 65°C, condition for 5 min	5 min boiling water, dry for 90 min at 110°C, condition for 12 hr.	During measurement: Polyester: pre-bulk, immerse in water at 20°C, bring to 80°C, treat for 20 min, dry.	During measurement:	Load hank to 0.01 cN/tex 5 min in hot air at 130°C.	Load hank to 0.01 cN/tex 15 min in hot air at 120°C.	During measurement:
Determination of first measured value	30 sec in water at 60°C, (2 g/l wetting agent) 1.8 cN/tex load for 1 min Measure L_o	Load to 0.01 cN/tex and 0.99 cN/tex Measure L_o after 10 sec	2.5 cN/tex load for 2 min	2.5 cN/tex load for 2 min	Load to 0.02 cN/tex and 1.0 cN/tex immerse in water at 20°C (2 g/l wetting agent) Measure L_o after 2 min	Load to 0.02 cN/tex and 0.9 cN/tex immerse in water at 22°C (3 min) (Time not defined) Measure L_o	 Measure L_1 after 5 min	 (Time not defined) Measure L_1	Reel $\frac{\text{circumference}}{2}$ $= L_o$
Determination of second measured value	Dry for 60 min at 50-60°C Cool for 60 min Load to 0.018 cN/tex Measure L_1 after 1 min	 Reduce load to 0.01 cN/tex Measure L_1 after 10 min	 Reduce load to 0.02 cN/tex Measure L_1 after 60 min	Reduce load to 0.02 cN/tex Reduce load to 0.02 cN/tex Measure L_1 after 30 min	 Reduce load to 0.02 cN/tex Measure L_1 after 2 min	 Reduce load to 0.02 cN/tex (Time not defined) Measure L_1	 Load to 1 cN/tex Measure L_o after 30 sec	 Load to 1 cN/tex (Time not defined) Measure L_o	Load to 0.016 cN/tex Treat in water at 65°C for 10 min Dry at 65°C, condition Measure L_1 after 24 hrs
Calculation formula	$KK = \frac{L_0-L_1}{L_0}$	$E = \frac{L_0-L_1}{L_0}$	$E = \frac{L_0}{L_1}$	$C = \frac{L_0-L_1}{L_0}$ $E = \frac{L_0-L_1}{L_1}$	$CR = \frac{L_0-L_1}{L_0}$	$E = \frac{L_0-L_1}{L_0}$	$E = \frac{L_0-L_1}{L_0}$	$K = \frac{L_0-L_1}{L_0}$	$S = \frac{L_0-L_1}{L_0}$

* hydro-extraction by centrifugal method

analyses focus on the changes in specific heat that occur when a semi-crystalline polymer is heated. The two most common tests employed are the Differential Thermal Analysis (DTA) and the Differential Scanning Calorimetry (DSC). The DTA instrument detects changes in temperature difference between a reference and a fiber sample while both are lodged in a thermal mass which is heated at a constant rate. The DSC instrument measures the difference in power required to heat a reference and a (fiber) sample. The temperature of the reference and sample are maintained equal during the test. The rate of temperature rise is controlled. The DSC device is the more sensitive and can also give quantitative results.

Major changes in specific heat occur during crystallization and crystal melting. Minor changes in heat capacity also occur in the absence of phase changes. For example, the slope of the specific heat vs. temperature curve changes at T_g, where the amorphous regions acquire more mobility and therefore the ability to store more thermal energy. These minor changes in specific heat, and evaporation of water or finishes lead to baseline "drift". Both DSC and DTA results depend on the rate of testing (i.e. rate of heating). Heating rates greater than 20°C/min are desirable to avoid continuous crystallization and recrystallization processes during the test. However, there are limitations to the heating rate. The melting of crystallites will appear to occur at higher temperatures when higher heating rates are used due to the

presence of thermal gradients in the sample and kinetic melting effects. A heating rate of 20-30°C/min will accurately reflect the temperature of crystal melting [122].

During heat treatment of a yarn, a network of crystallites is formed throughout the fibers. These crystallites are of different sizes and of varying degrees of perfection. Consequently, they melt at different temperatures. The thermal stability of the crystallites in a fiber not only gives an indication of the previous heat treatments, but also can help predict the response of that fiber to subsequent thermal treatments.

Effective temperature is an important concept that characterizes fiber thermal stability. According to Heidemann and Berndt [122], the effective temperature corresponds to the location of the largest endothermic peak on the DTA or DSC trace below the main melting peak at 256°C. Several interesting results that tie in with experience have come out of thermal (DTA) testing of yarns:

(1) The effective temperature of the yarn is not determined solely by the previous heater (or process) temperature.

(2) The time of treatment is also important in determining the effective temperature of the heat set yarn. As shown in Fig. 17a [123], the effective temperature is increased with increasing heat treatment time. Similar results

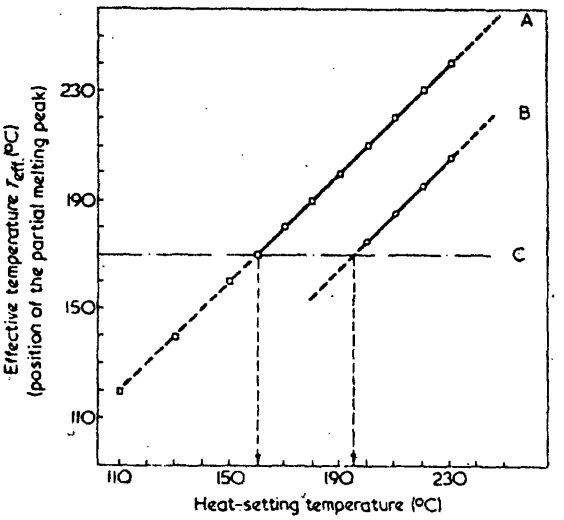

Influence of heat-setting temperature, time of treatment and high temperature dyeing on the effective temperature. A, heat setting 20 sec in hot air (□); B, heat setting 0.2 sec in hot air (○); C, high temperature dyeing at 130°C, 90 min (· – · – · –)

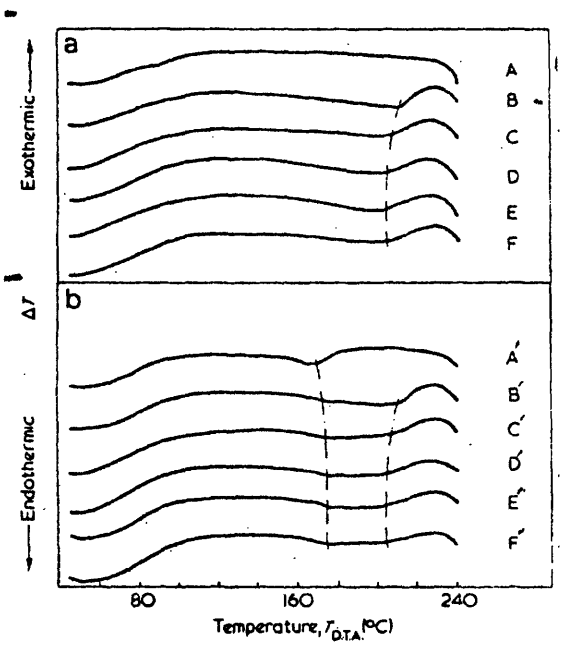

(a) D.t.a. traces of PET fibres heat set (hot air, 20 sec, 200°C) at the various indicated tensions (N/tex): A, original; B, 0.00; C, 0.01; D, 0.02; E, 0.05; F, 0.10. (b) As (a) and high temperature dyed (90 min, 130°C). Tensions (N/tex): A′, original; B′, 0.00; C′, 0.01; D′, 0.02; E′, 0.05; F′, 0.10

FIGURE 18. THE EFFECTIVE TEMPERATURE OF POLYESTER FIBERS AS A FUNCTION OF THEIR PROCESSING HISTORY [123]

have been reported by Coppola and Frediani [99]. The dwell time required to produce an effective temperature equal to the heater temperature is seen to be about 3 seconds.

(3) The effective temperature of the yarn is reduced as the tension during setting is increased, as shown in Fig. 17b [123].

(4) The effective temperature of a process is reflected by the melting point of the crystallites formed during the process. High-temperature dyeing (130°C, no carrier) was found to have an effective temperature of 170°C. In general, 90-minute hydrothermal treatments of polyester produced effective temperatures about 30°C higher than the water temperature [124].

2. Thermomechanical Tests. More information about fine structure of the fiber can be obtained when shrinkage force or shrinkage (length change) measurements are made on the textured yarns as a function of temperature. A force develops when a textured yarn with latent crimp is clamped at fixed length and heated above its T_g (≃100°C). At temperatures below about 150°C the force comes from the imposed deformation with respect to the reawakened memory of the helically set geometry of the filaments (i.e. their stress-free geometry). This low temperature contractile force is therefore referred to as a "crimp contraction force"

and is the basis for a number of static and continuous test methods [89,97,118,124]. In these tests, the yarn is fixed at zero or a small contraction, and subsequently heated. The resulting contractile force can be as high as 0.5 gpd. Such large contraction forces make measurements easy, but it has been found that these measurements do not correlate with yarn crimp development in fabric [40].

The reasons for the lack of correlation can be found in the mechanics of textured yarns and the physics of thermal contraction forces. First, tension in a straightened textured yarn before heating is due primarily to filament bending stresses. The tension in a highly crimped yarn is due primarily to filament torsional stresses [53,91,92,93]. The "crimp' contraction force measurements which are carried out on relatively straight yarns therefore rely on different components of filament stresses than those which are important for high-level crimp development as in finished fabric. Second, as the temperature of the filament is raised above T_g, the mobility of its extended molecules is increased and rearrangements into a more coiled molecular configuration are energetically favored. If the fiber is kept at fixed length, an increasing force will be required to maintain its extended molecules at increasing temperatures (thermo-elasticity). The magnitude of axial filament shrinkage required to reduce this force dramatically is only a few per cent compared to the potential crimp level of 10-60%.

This force, then, is not truly related to crimp contraction either.

In spite of the lack of correlation between yarn crimp development in fabrics and contraction force measurements, contraction force testing devices abound [89,97]. Most notable among these is the DYNAFIL [125]. Extensive testing by Stein and coworkers [126] has recently been conducted using this device. There is little doubt that intra-yarn variations are easily spotted by the test device.

Shrinkage force measurements are aimed at the yarn forces which develop at temperatures high enough to destroy part of the previous permanent set. As the crystals developed in the previous setting operation are melted, the tensions present during the crystal formation are released. Additional tension representing the chain folding (recrystallization) tendency of the molecules at high temperatures is also present. The effective tension is defined as the tension (shrinkage force) that develops at the effective temperature.

Shrinkage force measurements are useful diagnostic tools for detecting severe variations in processing temperatures or tensions, but their direct application for detection of minor variations in texturing parameters is doubtful. In addition to the DYNAFIL instrument, the KANEBO Thermal Stress Analyzer [127] and the Thermofil devices [128] are available for measuring thermal shrinkage forces.

3. Thermal Shrinkage Tests. The length change of a heated yarn can be used as an indication of the

previous thermomechanical history of the yarn. Shrinkage will be greater for yarns with higher amorphous orientation [25]. If these oriented amorphous molecules are partially stabilized by the presence of crystallites, the full relaxation shrinkage will occur only after these crystallites have been melted. The total shrinkage of a yarn will depend on the amorphous volume fraction, the amorphous orientation, the temperature of the shrinkage test, and the tension on the yarn during testing. Thermal length changes are most easily followed using the Thermomechanical Analysis (TMA) attachment on the du Pont Model 900 DTA instrument. Latzke describes a similar device [127]. Both devices rely on an LVDT to monitor yarn shrinkage while heating the sample in air or in an inert atmosphere.

6. Summary.

Barré has been shown to be the result of light reflection differences due to geometric or dye differences between courses or groups of courses in knit fabrics. The magnitudes of the relative differences required to produce barré are small. The processes which are most likely to contribute to barré are fiber spinning and texturing. The key process parameters have been outlined. The sensitivity of textured yarn geometry and dyeability to variations in these parameters has been stated. The required control levels for spinning and texturing variables have been developed and are found to be within the normal (open-loop) control limits for the texturing

machine and spinning operation. Since barred fabrics are still being produced with machines and feed yarns having the required open-loop controls, it was proposed that either interactions between machine variations and feed yarn variations within the normal control range, or changes in the transmission of machine settings to yarn parameters during texturing are responsible for the faulty yarns and fabrics.

The closed-loop control of yarn quality was, therefore, considered and subsequently rejected on the basis of technical and economic reasons. On-line monitoring was similarly rejected, since it has the same problems in sensitivity of measuring devices and correlation between the measured variables and yarn properties.

Off-line quality control methods have been reviewed and found to be too slow, or to lack sensitivity and correlation with yarn performance in fabric, or to involve too much operator judgement.

In light of these findings, the design and construction of a rapid automatic tester to predict yarn performance in finished fabric was undertaken.

CHAPTER II

DEVELOPMENT OF A CONTINUOUS TESTING INSTRUMENT FOR OFF-LINE CONTROL OF TEXTURED YARN QUALITY

1. Scope of the Development.

The work reported in this chapter proceeded in three stages. First, the basis for a rapid off-line test method was sought. Such a method should focus on the geometric and dye potential of the textured yarn in fabric. This stage emphasized the correlation of results of various "batch" yarn testing methods with yarn evaluations provided by the knit-dye-grade procedure mentioned earlier. Commercially draw-textured yarn samples were provided by UNIFI, Inc. These yarns had been graded according to the classifications of normal, select, dark, light, high bulk, low bulk, or second quality. There were 132 individual textured yarns in all, divided into nine sample lots. Details of these yarns have been given elsewhere [69]. These samples were textured and given a "setting" heat treatment as a second stage on the same texturing machine to reduce yarn torque-liveliness and stretchiness. The setting operation and its influence on yarn geometric properties is discussed in Chapter III. Yarns that are textured with exposure to a single heater are called stretch, or high extension yarns. When such yarns are subsequently exposed to a second heater, they are called set yarns.

The second stage of the development served to convert the most promising "batch" testing methods into a continuous

dynamic tester. The results from such tests were correlated with the results of the knit-dye procedure with a view toward predicting yarn performance in fabric.

In the third stage of the development, actual doffs from a commercial texturing machine were graded on an improved continuous tester. The grading was done on the basis of the statistical deviation of individual packages from the doff average. Subsequently, several fabric trials were conducted to test the validity of predicted yarn response in fabric.

2. Batch Test Methods.

The complete data generated during this exploratory phase of mechanical and thermomechanical testing on discrete lengths of textured yarns are contained in a previous report [68]. The excerpted data discussed herein represent the most significant findings.

A. Load/Elongation Tests. Stretch Yarn. The load elongation behavior of textured yarns with known processing conditions is shown in Fig. 19. These samples were textured by C.E. Bell on the laboratory (MITEX) texturing machine described elsewhere [44]. We now consider load elongation results on two samples: one textured with high twist and high machine draw ratio, the other with low twist and low draw ratio.

The length of a textured yarn is a strong function of its tension especially at light loads. The "zero load" length is not reproducible, and for this reason, the reference length of 10.00 inches was established at a "stress" of 0.1

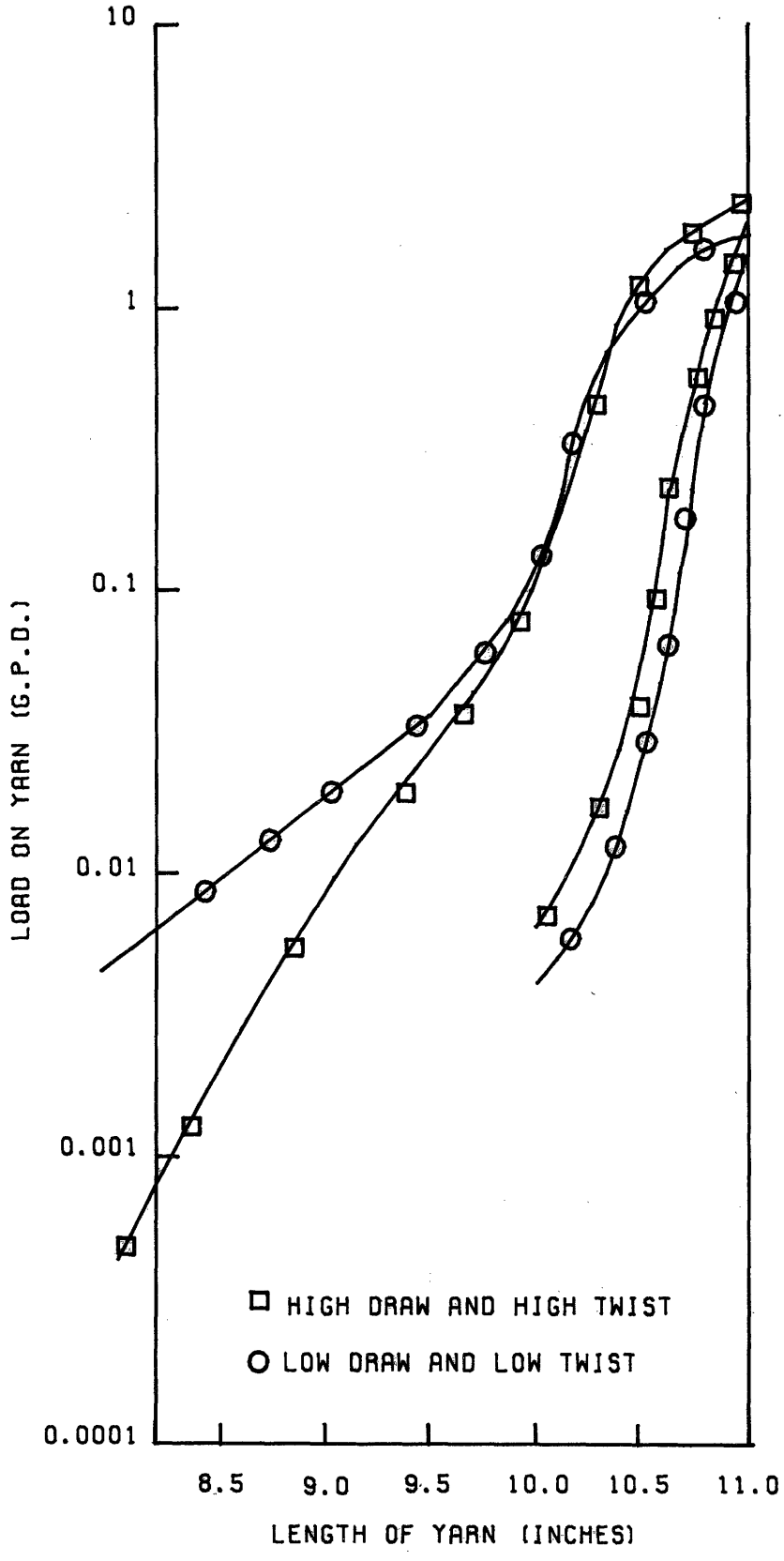

FIGURE 19: LOAD ELONGATION OF STRETCH TEXTURED YARNS WITH DIFFERENCES IN TWIST AND DRAW RATIO

gram per denier. This "stress" is widely regarded as that necessary to straighten but not stretch the yarn. The yarns were first contracted until the load reached zero on the Instron scale. The yarns were then extended at 1%/minute to a length of 11 inches. Finally, the yarns were contracted back to 10 inches in length. The load elongation curves as shown in Fig. 19 illustrate the large differences in load which occur from an arbitrary contracted length of 8.2 inches to the original length of 10 inches. These differences are a consequence of the large differences in the geometry of the yarn as textured. In this region yarn extension serves to decrimp the filaments.

In the elongation region, from 10 to 10.4 inches, the yarns behave very similarly. For here the yarn extension is equal to filament extension. At lengths from 10.4 to 11.0 inches "yielding" or drawing of the fiber occurs and the difference in the texturing draw ratio of the filaments becomes evident. The yarn with higher draw ratio during texturing has a higher yield stress than the low draw material. During unloading, both yarns exhibit permanent deformation as indicated either by the increase in length at 0.1 gpd force, or by the decrease in load at 10.0 inches. The high draw-high twist yarn was less affected by the extension cycle than the low draw-low twist yarn. The gross differences in yarn texturing conditions are clearly reflected in load/elongation behavior of the textured yarns. Such

gross differences in texturing conditions normally do not occur on well maintained, properly operated texturing machines.

B. Load/Elongation Tests. Set Yarns. The load/elongation behavior of commercially set-textured yarns (Shipment A) was also investigated. Yarns were tangentially wound off a package under a tension of 1.5 gm on 150 denier yarns. Measures were taken to insure against loss of twist in unwinding. The connection to the package was then severed and the yarn mounted in the Instron with a gage length of 10.0 inches at 1.5 gmf (0.01 gpd). The total time from unwinding the yarn to the start of the extension cycle was 4 minutes in all cases. The elongation rate during subsequent extension and contraction tests was 1%/minute.

The test cycle consisted of: (1) mounting the yarn under tension at a fixed gage length; (2) extending the yarn until 100 gf developed; (3) immediately contracting the yarn back to its original gage length. The load and elongation were recorded throughout the test.

Figure 20 contains example load vs. extension curves for groups of three yarns which had been graded by the knit-dye process as dark, normal, or light. Figure 20A shows the yarn behavior during the loading part of the cycle, while Fig. 20B illustrates the unloading behavior. As mentioned previously, the load elongation behavior of textured yarns can be characterized by changes in extension, E, for given changes in load, P, or vice versa. Tables 10 and 11, respectively,

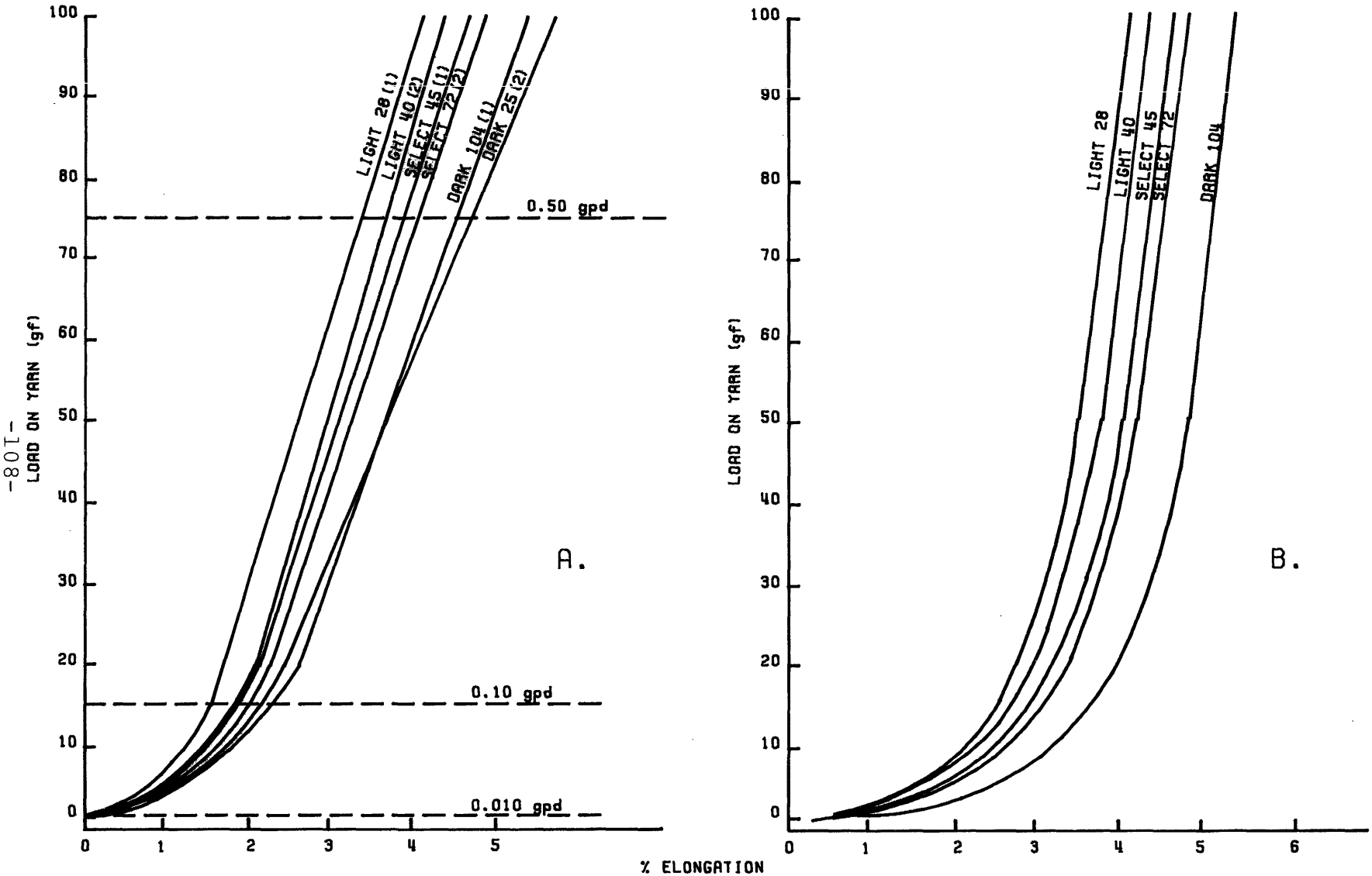

FIGURE 20:
LOAD-ELONGATION BEHAVIOR SET YARNS WITH DIFFERENT FABRIC APPEARENCE

TABLE 10. ELONGATION CHANGES FOR A GIVEN CHANGE IN LOAD

Stage of Test	Darks (104,25,20)*		Selects (72,69,45)		Lights (40,28,6)		Fixed Change in Load
Loading	4.96%	(0.69)**	4.61%	(0.42)	4.24%	(0.38)	ΔP, 1.5 → 100 gf***
	3.38	(0.50)	3.08	(0.25)	2.84	(0.16)	10 → 100
	2.50	(0.40)	2.25	(0.16)	2.08	(0.10)	25 → 100
	1.61	(0.26)	1.44	(0.09)	1.35	(0.05)	50 → 100
	0.80	(0.12)	0.73	(0.03)	0.70	(0.02)	75 → 100
Unloading	-2.22	(0.15)	-2.18	(0.11)	-2.11	(0.07)	ΔP,100 → 10
	-1.31	(0.06)	-1.28	(0.03)	-1.26	(0.02)	100 → 25
	-0.70	(0.04)	-0.67	(0.01)	-0.67	(0.005)	100 → 50
	-0.29	(0.005)	-0.29	(0.004)	-0.29	(0.003)	100 → 75
Cycle Difference	1.17	(0.36)	0.91	(0.17)	0.73	(0.11)	ΔP, 10 ⇄ 100
	1.20	(0.34)	0.96	(0.13)	0.81	(0.09)	25 ⇄ 100
	0.92	(0.24)	0.77	(0.09)	0.68	(0.05)	50 ⇄ 100
	0.51	(0.11)	0.45	(0.025)	0.41	(0.02)	75 ⇄ 100

* Sample numbers

** (Standard deviation)

*** On 150 denier yarn.

TABLE 11. LOAD CHANGES FOR GIVEN ELONGATION CHANGES

	Elongation*	Load at Elongation (gf) Darks		Selects		Lights	
During Extension**	1%	5.6	(1.1)++	5.5	(0.9)	6.2	(0.8)
	2%	16.7	(5.2)	17.7	(4.6)	21.2	(4.9)
	3%	41.3	(13.4)	45.3	(11.0)	54.5	(9.7)
During Contraction***	1%	2.3	(0.8)	2.7	(0.4)	3.2	(0.5)
	2%	5.9	(3.0)	6.9	(1.9)	8.9	(2.0)
	3%	16.0	(12.0)	19.0	(8.0)	27.0	(9.0)
Cycle Difference	1%	3.2	(0.6)	2.9	(0.6)	2.9	(0.65)
	2%	10.9	(2.4)	10.7	(2.7)	12.3	(3.1)
	3%	24.2	(5.1)	26.0	(3.3)	26.8	(2.9)

* Measured from length at 0.01 gpd.

** During Loading to 100 gf on 150 denier yarn.

++ Standard deviation.

*** During unloading from 100 gf.

summarize these quantities derived from the curves. Although no statistically significant (95% confidence level or greater) differences existed between yarns of different grade, slight consistent differences did exist between the various yarn grades.

As shown in Table 10 for any change in load, dark graded yarns always had the largest associated change in elongation. Selects had intermediate elongations, and lights always had the smallest change in elongation. Conversely, in Table 11 darks had the least increase in load for a given increase in extension. Selects had intermediate load increases and lights had the largest load increases.

These rankings may be compared to the load elongation behavior of yarns textured with high draw-high twist, or low draw-low twist, as shown in Fig. 19. On this basis we see that the softer behavior of the dark yarns corresponds to the lower effective modulus of the low draw-low twist textured yarns. This is in keeping with the expected decrease in dye uptake for yarns textured at increased draw ratio. But, of course, many factors (including texturing draw ratio) determine dye uptake and load elongation behavior.

It is also interesting that the load elongation tests between yarns with dye differences show the greatest differences in elongation in regions where crimp deformation occurs. This means that crimp and dye differences appear to be related for these samples. Texturing heater variations

could be responsible for these differences.

C. Thermomechanical Tests. During scouring, dyeing and finishing, the textured yarns in fabric are exposed to hydrothermal and chemical (swelling) actions that will change the yarn crimp and filament lengths. In this series of experiments, the tensile response of textured yarns to changes in length and temperature after various levels of cold working are examined. Of the various tests run one was found to correlate well with yarn dye grades. This parameter related to the shape of force buildup in the heated yarn. En route to discovering this parameter, several other less significant correlations were found. These are included in Appendix 3.

Sample yarns graded dark, normal, and light were used in this series of tests. Yarn was tangentially wound off its package under a controlled cold-working load (from 15 to 150 gf) and held under this load for 5 minutes. The load on the yarn was then reduced to 15 grams force (0.1 gpd) and the yarn was wound onto two cardboard tabs which had previously been taped together. Thus, two "identical" samples were produced. Dots of epoxy resin were applied to mount the yarns securely to the cardboard tabs and to establish the gage length under the winding load. Because wicking of the epoxy along the textured yarns occurred, careful measurements of the actual gage length were made using a microscope. The time from mounting to testing was approximately 24 hours.

During the test cycle, the yarn was mounted in the Instron and extended until the (slightly relaxed) load again reached 0.10 gpd. This load was maintained for two minutes. The yarn was then contracted by 2.2 $\pm$ 0.1% based on the gage length of the tab-mounted specimen. The contraction rate was 10% per minute. After one minute, an electrical heater at 130 $\pm$ 1°C was positioned in near contact with the yarn and left in place for 10 minutes. A shield against room drafts was provided for the otherwise open heater. The force exerted by the yarn was monitored continuously throughout the cycle.

Two characteristic shapes of the resulting force time curves are shown in Fig. 21. The upper curve corresponded to tests where small (0.10 or 0.5 gpd) cold-working loads had been applied. The lower curve was typical of the behavior after heavy (1.0 gpd) cold working. It is noted in these curves that the yarn tension increases rapidly when the 130°C heater is brought into contact with the yarn. The "peak" tension is reached after a short time (<1 minute). The final tension is measured after 10 minutes of heating. The tension rises rapidly as the mobility of the extended chains bridging crystallites is increased above their T_g. When these "tie" molecules become unentangled after longer periods of heating, a general creep, or flow, of the structure can begin. These two competing processes account for the occurrence of the tensile peak or overshoot. An additional

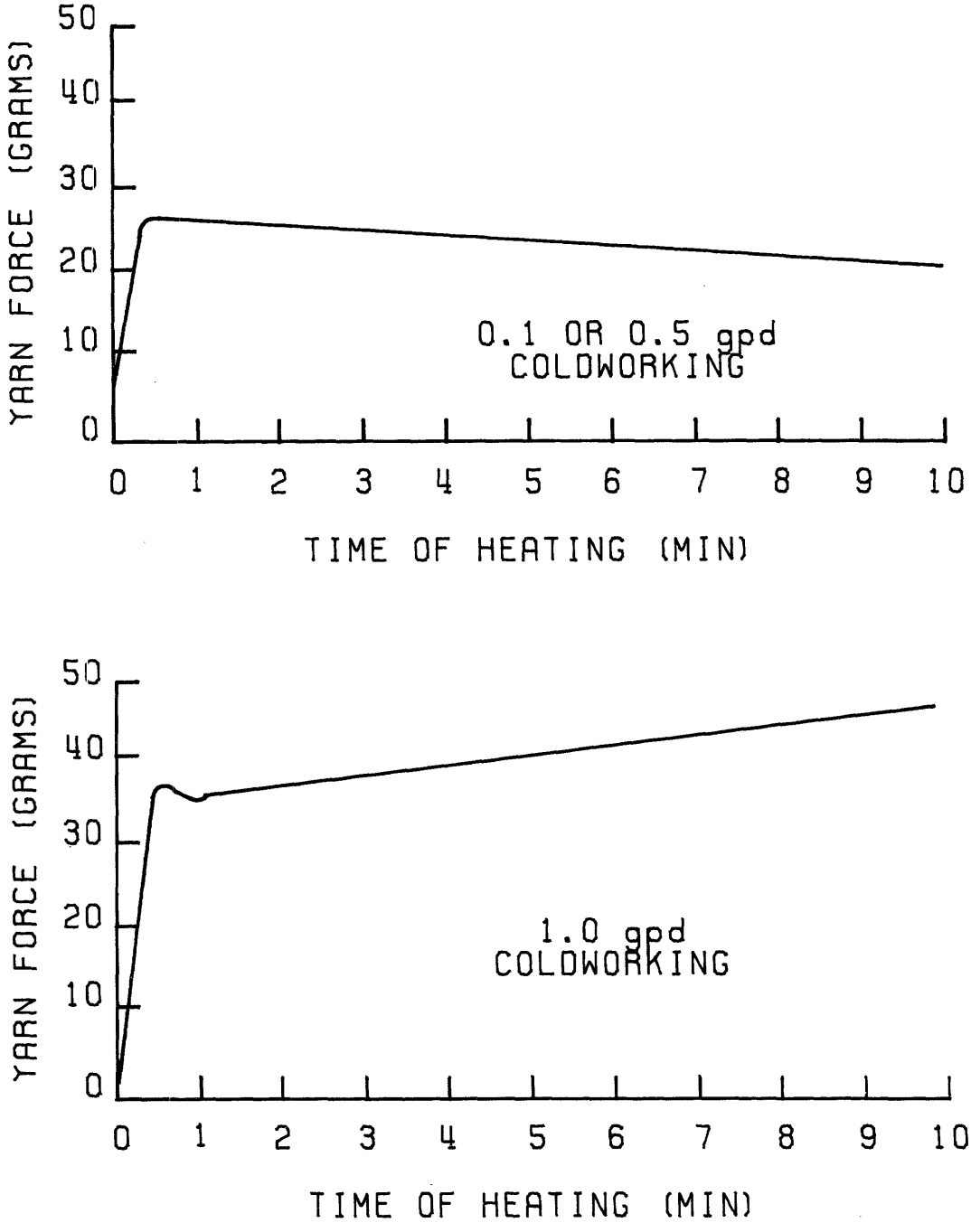

FIGURE 21:
THERMALLY INDUCED FORCE IN YARNS AFTER COLDWORKING (HEATER 130 °C 150/34 PET)

small reduction in tension may be expected to result from continuing flow under the combined action of temperature and force at longer times.

If one calculates the overshoot in hot tension as given below, the statistically significant results as shown in Table 12 are obtained. These results are for yarns subjected to 0.1 gpd cold working:

$$\text{overshoot in hot tension} = \frac{\text{peak hot tension-final hot tension}}{\text{final hot tension}} \times 100\%.$$

The physical basis for this overshoot value can be better understood by treating the peak tension and the final tension separately. The peak tension is determined to a great extent by the amount of amorphous material in the fibers and its orientation. The final hot tension depends on the stability of the crystallite network. On this basis, dark samples which show the largest overshoot reflect the presence of more amorphous material and/or a less stable crystallite network. Both of these conditions favor higher dye uptake as outlined previously. Conversely, light samples can be expected to have less amorphous material and/or a more stable crystallite network, which would act to restrict dye uptake. Normal yarns should have intermediate properties.

Thus, our discontinuous thermomechanical tests have provided one parameter : the hot tensile overshoot, which ranks yarns, subjected to 0.1 gpd, in a manner consistent

TABLE 12

HOT TENSILE OVERSHOOT FOR SHIPMENT "A" YARNS

Grade (Sample)	Overshoot % Mean	σ
Dark (104)	45.75	0.021
Select (45)	37.38	0.14
Light (28)	33.57	0.15

with dye grade and with high confidence in the ranking. However, the testing procedure is too long and exacting to be used as a routine quality control test. Significant differences and often reversals in ranking of the graded yarns occur as the cold working load is increased to 0.5 and 1.0 gpd. It is also possible that some of the less significant results of experiments as discussed in Appendix 3 of this series may be more significant when a longer sample of yarn is tested, as in a continuous tester.

D. Other Exploratory Tests. Tests were also conducted to measure yarn-on-metal friction and the coning oil content. Some fortuitous correlation existed between oil content, and/or coefficient of friction and yarn dye grade, but the scatter in the data precluded further use of these tests. C.D.T. tests were also conducted and gave highly variable results lacking in correlation with dye grade [68].

Measurements of torque-liveliness (equilibrium retwist under 2 mgpd stress) were conducted on the yarns, but the results were not reproducible and lacked clear correlation with the dye grade. The retwist level observed was 1-2 TPI, which is in agreement with the data reported by Schubert [96].

In summary, certain aspects of the load-elongation behavior of textured yarns prior to crimp development could form a suitable basis for quality control of textured yarns if the scatter in the test results can be reduced by continuous testing. Likewise, highly significant correlation was found

between aspects of the hot yarn tension vs. time curve, and the yarn dye grade. It was therefore decided to conduct continuous tests emphasizing the aspects of textured yarn behavior that were found to correlate with yarn dye grade. It was recognized that additional testing on an expanded sample set with various texturing conditions would be required to assure the general application of the test method in industrial quality control of textured yarns.

3. Continuous Tests with a Laboratory Instrument.

The complete data generated during this phase of the continuous testing with a laboratory prototype instrument are contained in a separate report [69]. The excerpted data presented here are representative of the findings in that report.

A laboratory texturing device described fully in [131] was converted to a two-zone, continuous yarn tester as shown schematically in Fig. 22. All three pairs of nip rollers were driven by the same variable speed motor. The speed of each set of feed rollers was adjusted with respect to the main drive speed by reduction gears. This feature allowed any ratio of feed speeds to be selected independently of overall tester speed. Each zone had provision for heating the yarn. In the first zone the heater was a curved, groove-type, electrical heater taken from a Scragg Minibulk texturing machine. The second zone heater was a 1.25"-wide electrically heated model manufactured by Rosemount.

FIGURE 22: LABORATORY TESTING INSTRUMENT

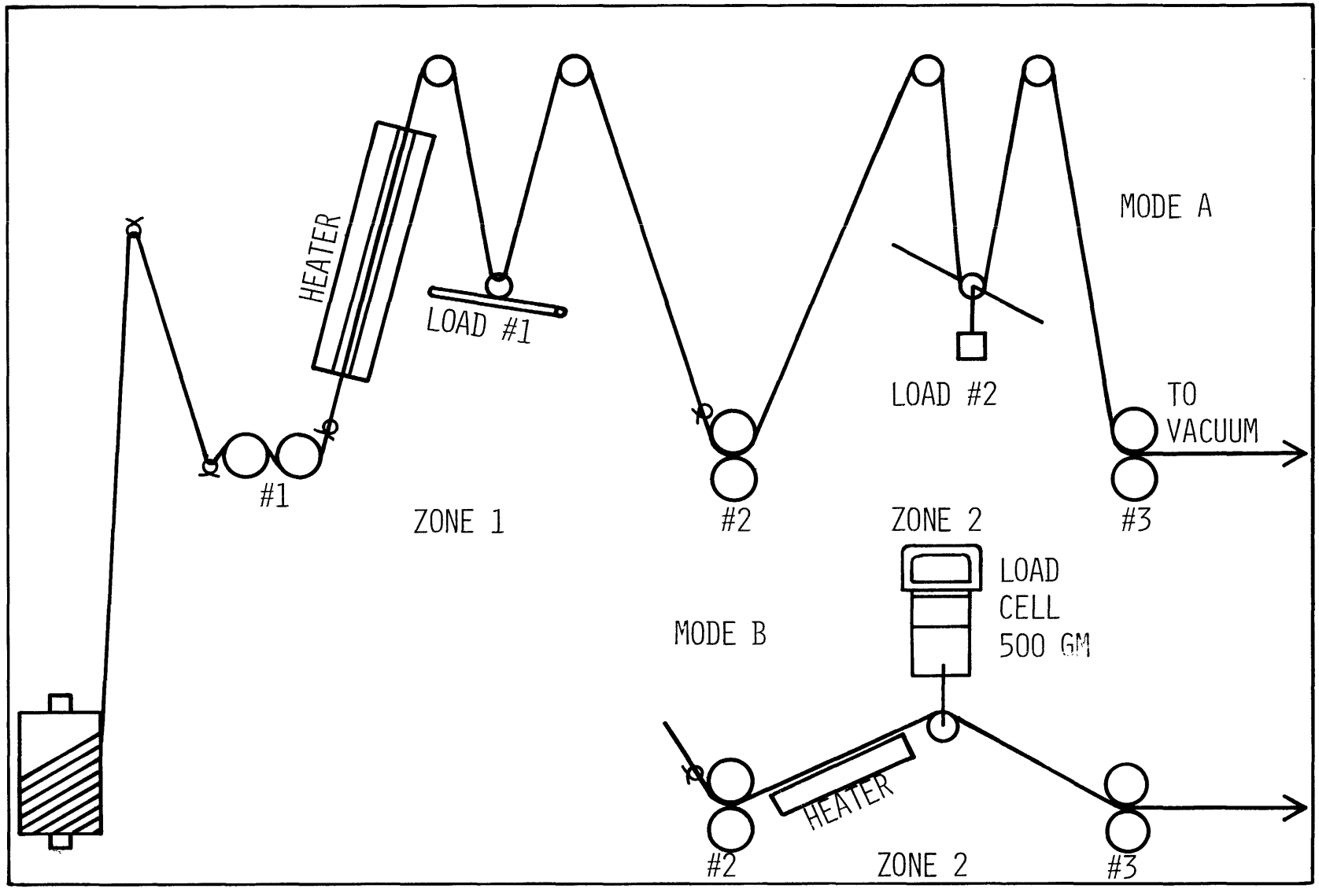

As shown in the upper part of Fig. 22, the yarn path in each zone was "M"-shaped. The two peaks of the "M" were pulleys mounted on low friction ball bearings. At the center of the "M" a weight was hung to control the yarn tension in the zone. Heavy loads were suspended with the yarn running in a ceramic guide or over a pulley mounted in a ball bearing. Light loads (i.e. 2 gms or less) precluded the use of a pulley and sliding contact with the yarn was unavoidable. The second stage could be modified as shown in the lower part of Fig. 22 by removing the weight and including a 500 gm load cell with a ball bearing pulley for the yarn to run over.

A. Load/Elongation Tests. The tester was configured to measure changes in elongation for changes in load. In this mode of operation, the yarn was drawn off the package into the first zone. A 2 gm weight (Load #1) was suspended on the yarn. Due to the sliding friction of the yarn around the suspended weight, there was a tension difference between the yarn entering and exiting zone 1. An estimate of the tension ratio was made on the basis of the previously measured friction behavior for the yarns [68]. On the basis of this calculation we estimate that the entering yarn was acted on by about 5 mgpd, while the exiting yarn was under about 7.5 mgpd for the 150 den yarn. The yarn then entered the second zone and here supported a weight of 120 gms (Load #2). This corresponded to a stress of about 300 mgpd on the yarn entering the second zone and about 500 mgpd on the exiting yarn. This load level

was more than sufficient to straighten the filaments and probably resulted in some filament extension as well. In this testing scheme the yarn is continuously exposed to a light load followed by a heavy load in order to determine resulting yarn elongation. One need only measure the change in height of the weight in the second zone as a function of time to calculate the elongation of the yarn by use of length continuity:

$$\frac{dH}{dt} = \frac{V_3}{2} - \frac{V_2}{2}\ (1 + \Delta E_{12})$$

or

$$\Delta E_{12} = \left(\frac{V_3}{V_2} - 1\right) - \frac{2}{V_2}\left(\frac{dH}{dt}\right)$$

where

V_i = linear rate of yarn delivery of "i^{th}" set of nip rollers,

$H(t)$ = height of weight in zone 2 as a function of time,

$\frac{dH}{dt}$ = derived rate of change of height,

ΔE_{12} = change in elongation from load 1 to load 2.

If the total height change (ΔH) is measured for an extended Δt (e.g. 10 minutes or 450 ft. of yarn), the average elongation over this period can be calculated using $\Delta H/\Delta t$ in the equation. Typical results for shipment B yarns with and without coning oil are shown in Fig. 23. Good grouping of the yarns by dye grade is seen and oil on the yarn does not influence the reading. This average value does not take into account the pronounced cycles in elongation as shown in Fig. 24. This figure was obtained by measuring the time associated with a given rise in the zone 2 weight, hence the

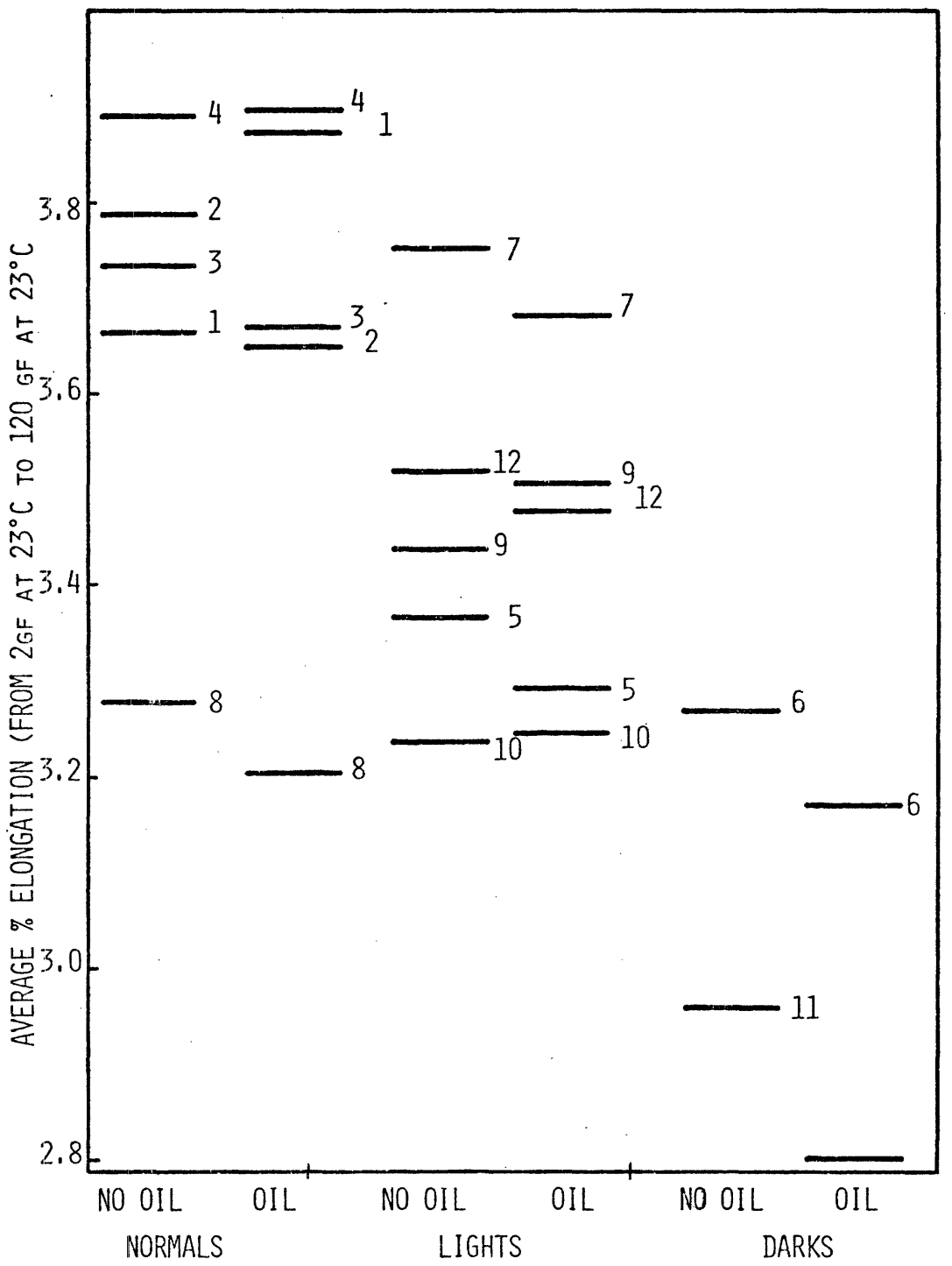

FIGURE 23. AVERAGE ELONGATION FOR SET B

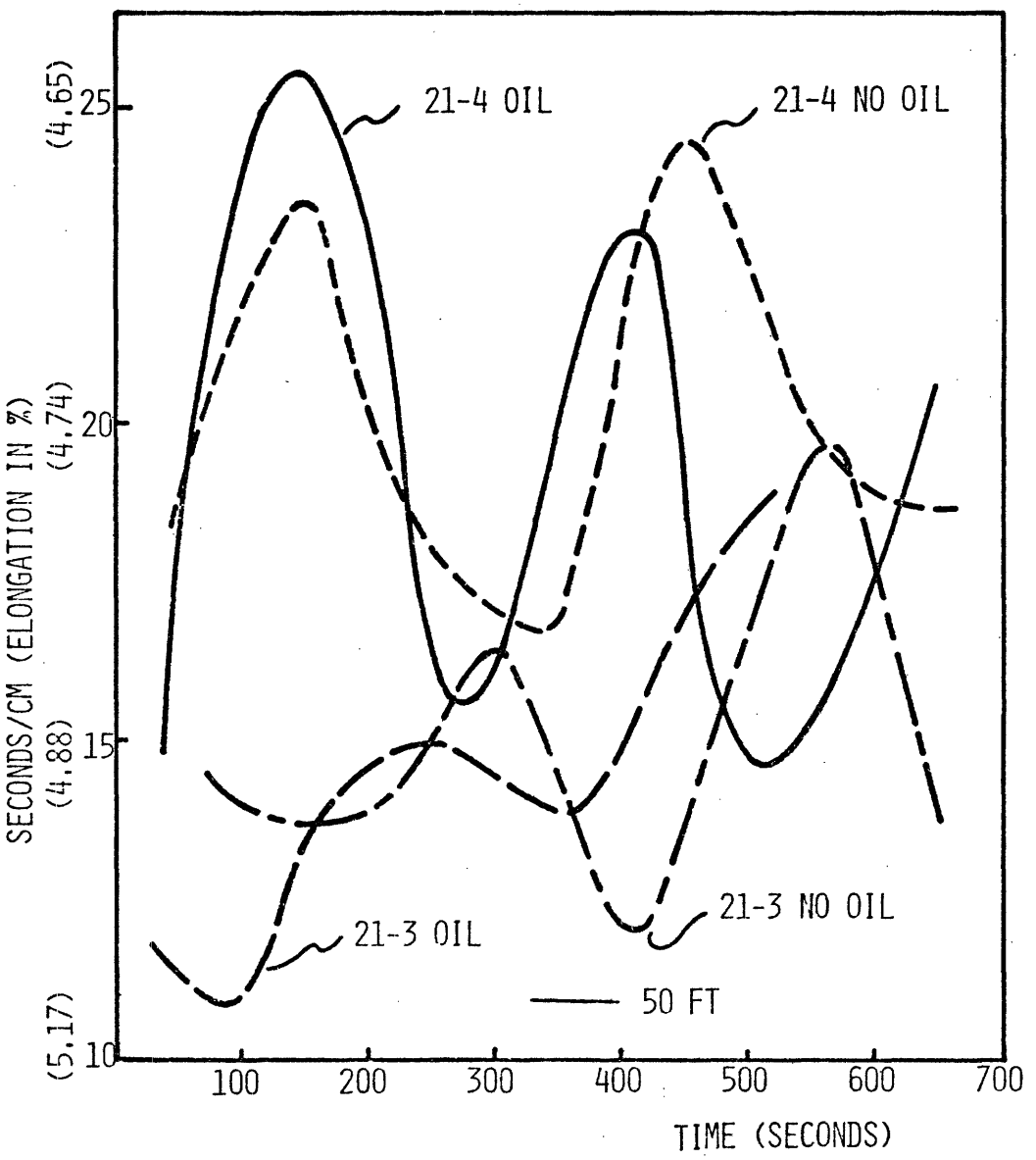

FIGURE 24. CYCLIC BEHAVIOR OF SET B
(FROM 2 GF AT 23°C TO 120 GF AT 23°C)

vertical axis is marked off in units of seconds/cm. The associated values of elongation are shown in parentheses. The resulting vertical scale for elongation is not linear. These "cycles" in extension had the same period and similar amplitudes for all samples in the yarn shipment. It seemed unlikely that these regular cycles were the result of threadline instability during texturing and, in fact, they were traced to the period associated with speed changes of the winding traverse on the texturing machine. To form a more stable cylindrical package, the winding angle of the yarn is generally changed slightly in a cyclic manner. Calculations on the length of textured yarn wound up during one of these cycles in traverse speed agreed well with the observed cycles in elongation. Schubert [95] discusses the elongation changes during winding as a function of the changing angle of winding.

Since we want a measure of crimp (as developed in the fabric), which has been shown to be independent of winding conditions [63], a series of tests on yarns after crimp development was undertaken.

B. Thermomechanical Tests. In the first series of tests, the zone 1 heater was operated at 150°C $\pm$ 2°C to develop the latent crimp in the yarn. The same 2 gm weight was used to control the tension during crimp development. The second zone weight was again 120 gms. Thus, elongation changes in textured yarns after crimp development were measured. Figure 25 shows the results on shipment B yarns

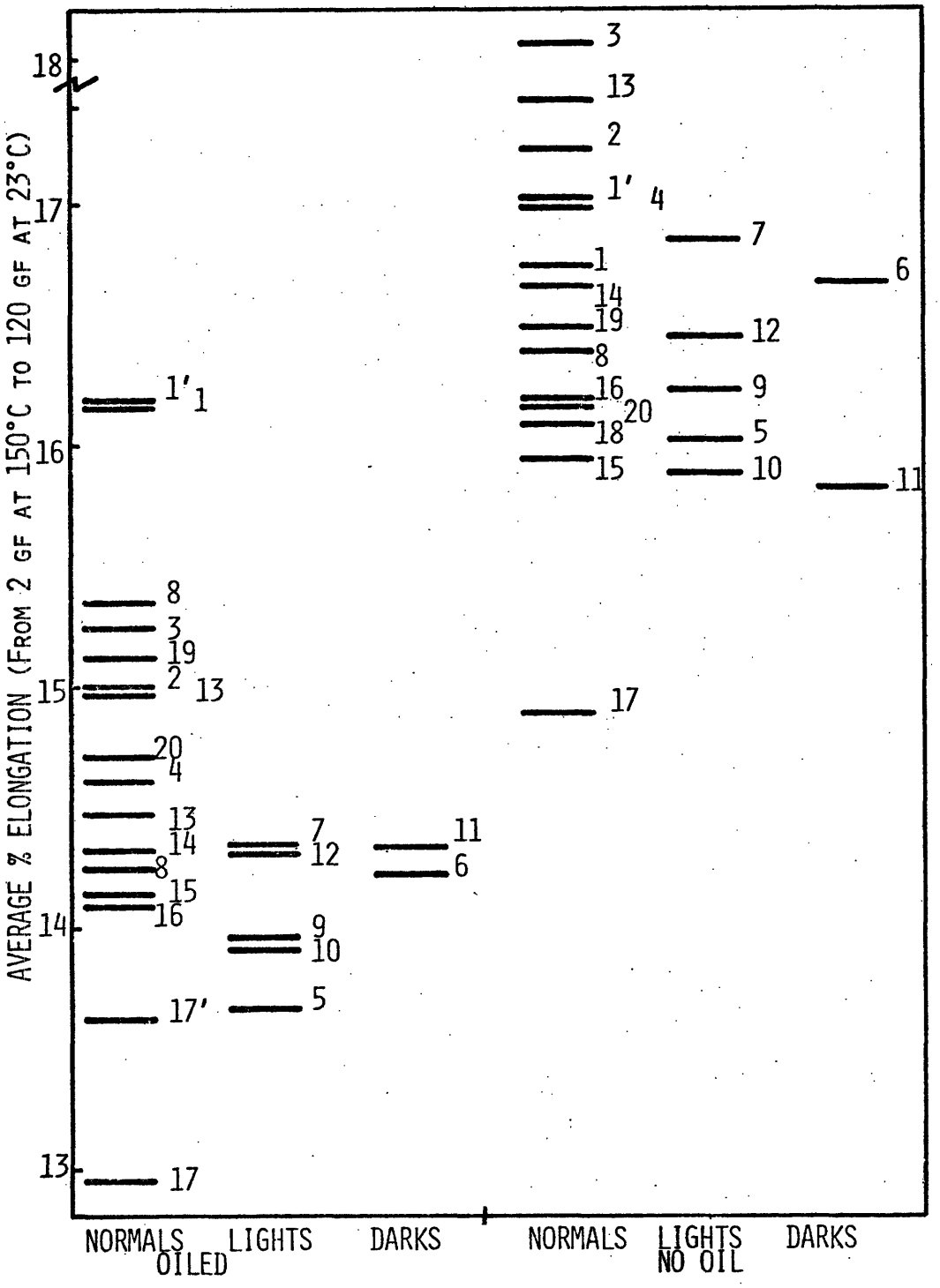

FIGURE 25. AVERAGE ELONGATION FOR SET B

with and without oil. Much greater elongations (indicating higher crimp) were obtained in this series (Fig. 25) as compared to the previous series (Fig. 23). Very large overlaps in measured elongations existed between the various yarn grades. It is unclear whether the test method was not sensitive to the proper differences between yarns, or whether the yarns had significant variations along their length, or whether the initial yarn grading method was inaccurate.

The large difference in crimp elongation between the oiled and non-oiled samples can be attributed to differences in yarn friction on the 2-gram weight; the lower the friction, the higher the load in the crimp development region. The resulting lower crimp development on oiled yarns reduced their measured elongation as shown in Fig. 25. The oil content of each of the oiled yarns was determined, but no clear correlation was found between amount of oil on the yarns and their crimp elongation. It appears that if there is enough oil (>1/2-1%), the yarn friction, crimp development and elongation are relatively insensitive to the level of oil.

Additional tests were run using this crimp development, and loading scheme on yarns from shipment A. Figure 26 shows the results from shipment A. On the left are measured elongation data from 3 successive doffs of the same texturing machine position. The yarns with the same dye grade come from the same texturing position, and the same feed yarn package.

The elongation for different doffs from the same

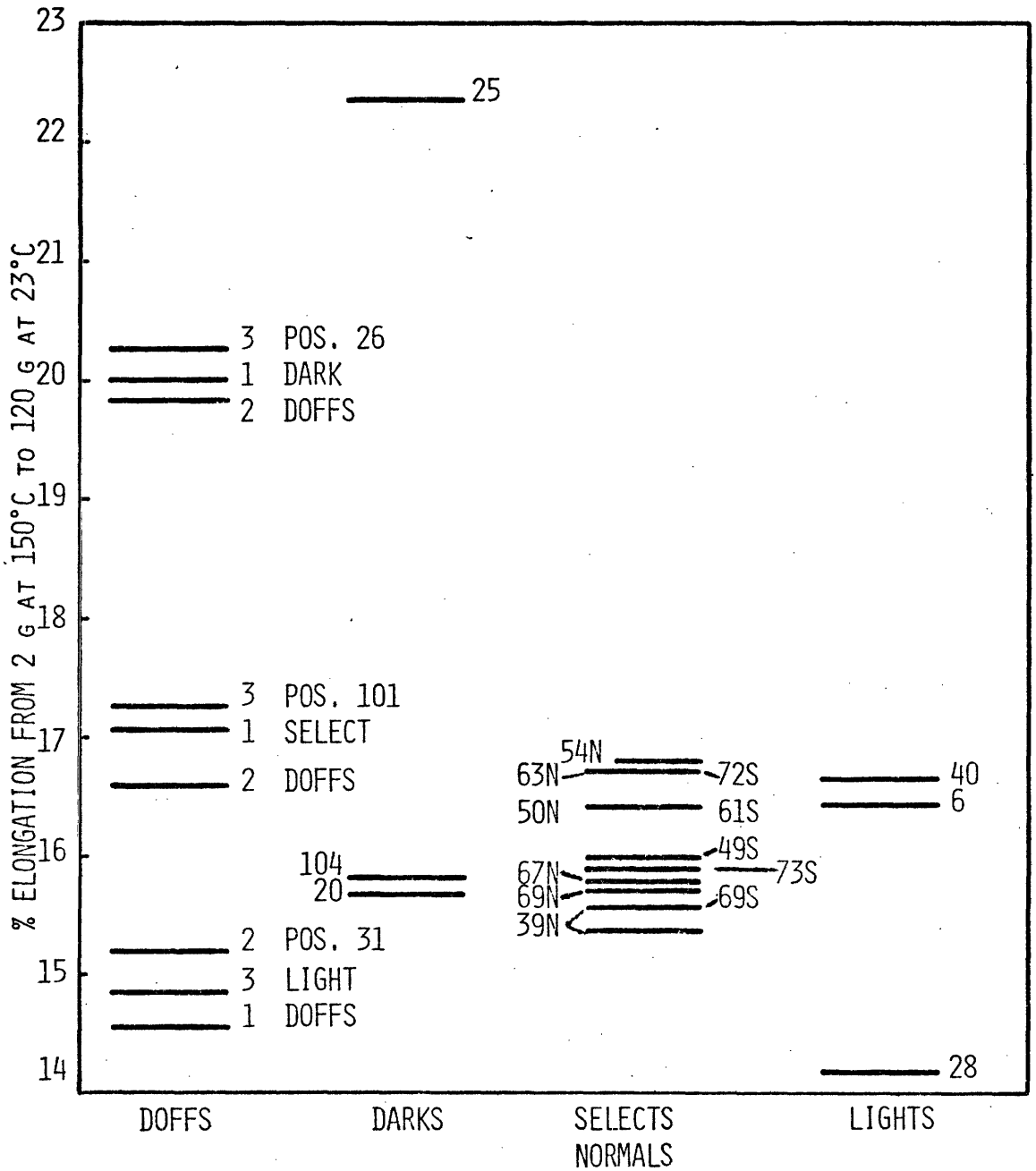

FIGURE 26. AVERAGE ELONGATIONS FOR SAMPLE SET A

texturing position was very similar and the difference in elongation between dye grades was also good. When additional packages from shipment A were tested, as shown on the right in Fig. 26, the results were mixed. Light 28 and dark 25 were clearly different from the group of selects and normals, but other lights (40,6) and darks (104,20) were no different. These packages were regraded and they showed the same apparent dye shades as in the previous grading.

All the continuous tests described thus far have relied on measuring the change in weight height and calculating yarn elongation. The process was tedious and did not provide permanent records. To remedy these shortcomings, the elongation imposed on the yarn entering the second zone of the tester was increased to about 19%. The weight was then replaced by a load cell as shown in the bottom of Fig. 22. The crimp was developed at 145°C and at a load of 0.8 gms. This load gave an estimated 2 mgpd crimp development tension and exit tension of about 3.5 mgpd from zone 1. By this method, yarns that contract less will show higher yarn extension forces (Y.E.F.) when subjected to the fixed extension of the second zone. This test was conducted on all 9 sample sets. Correlation between dye grade and the measured (average) yarn extension force was good for shipments D,F,H,I; fair for shipments B,C; and poor for shipments A,E,G. No clear statement can be made regarding the effect of feed yarn, or texturing conditions on the level of

correlation between yarn extension force and dye grade.

Figures 27 and 29 show yarn extension force values grouped by dye grade in Fig. 27 and by increasing average yarn extension force in Fig. 29. The bars indicate maximum, visual average, and minimum yarn extension force values for each sample tested. Several hundred feet of yarn were tested for each sample. In Fig. 27, the grouping by average yarn extension force and dye grade is very good with the exception of yarn from position 136. Intra-package variability of this yarn was suspected and it was checked by reknitting, dyeing, and grading position 136 in comparison with positions 83 and 92. Using this procedure, yarn from position 136 was re-graded as slightly dark once, and light twice, thus confirming its intra-package variability. The ranking seen in Fig. 27 is consistent with a non-linear dye uptake curve vs. (texturing) heater temperature as shown in Fig. 7 (Chapter I), and a linear increase in crimp, or decrease in yarn extension force, with texturing heater temperature. These three curves are superimposed in Fig. 28. On the basis of texturing temperature effects on dye shade alone, the possible ranking of dye grades on the basis of Y.E.F. would be D>S>L>S>D. Therefore, select yarns (those having average knitted and dyed appearance for the textured yarn lot) could theoretically occur at either S1 or S2 on the dye uptake curve. The two select samples of this yarn lot are apparently of the S1 variety. Other yarn lots showed the bimodal distribution of

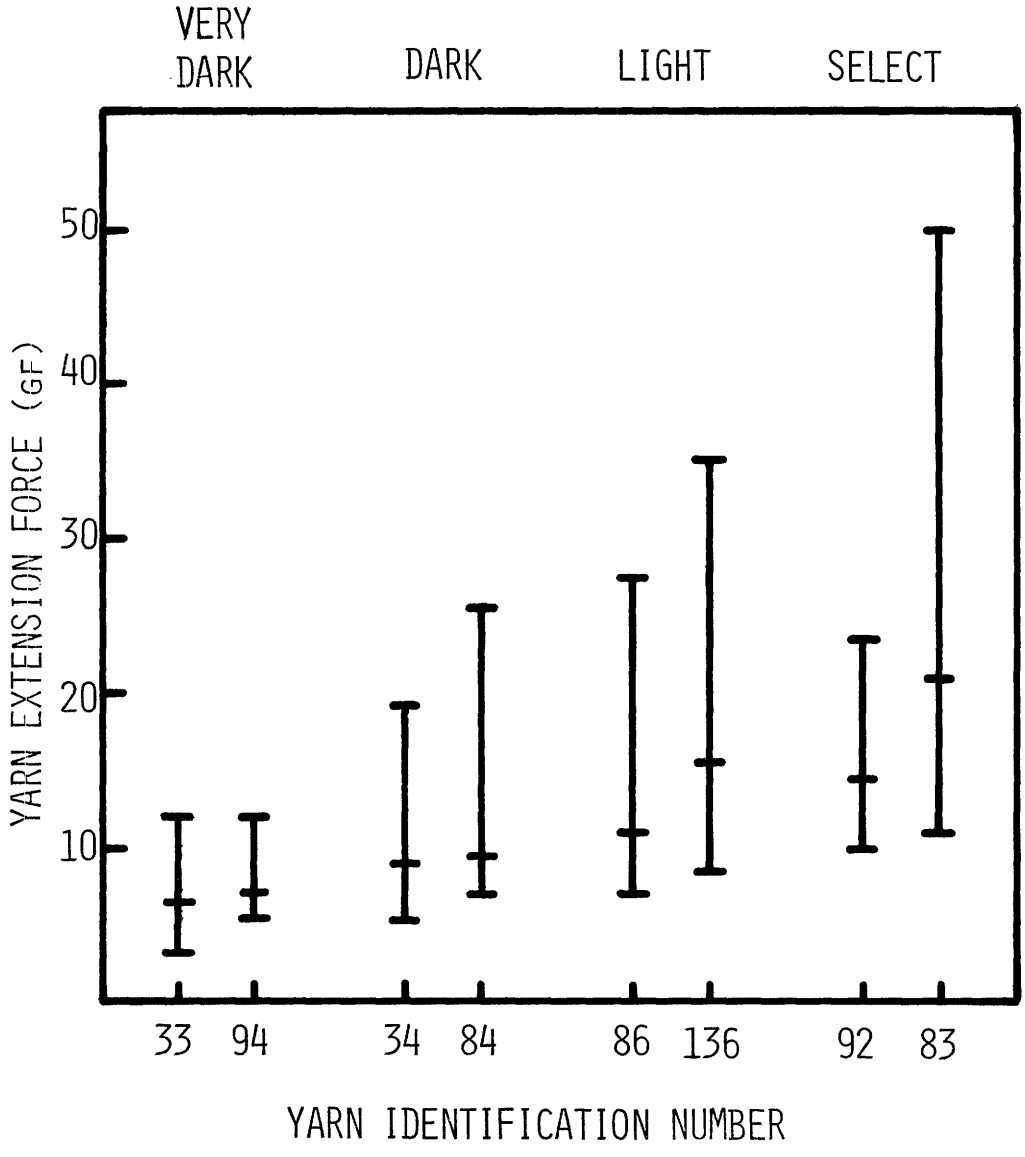

FIGURE 27. YARN EXTENSION FORCE AFTER CRIMP DEVELOPMENT AT 145°C AND 2 MGPD IN SAMPLE SET D

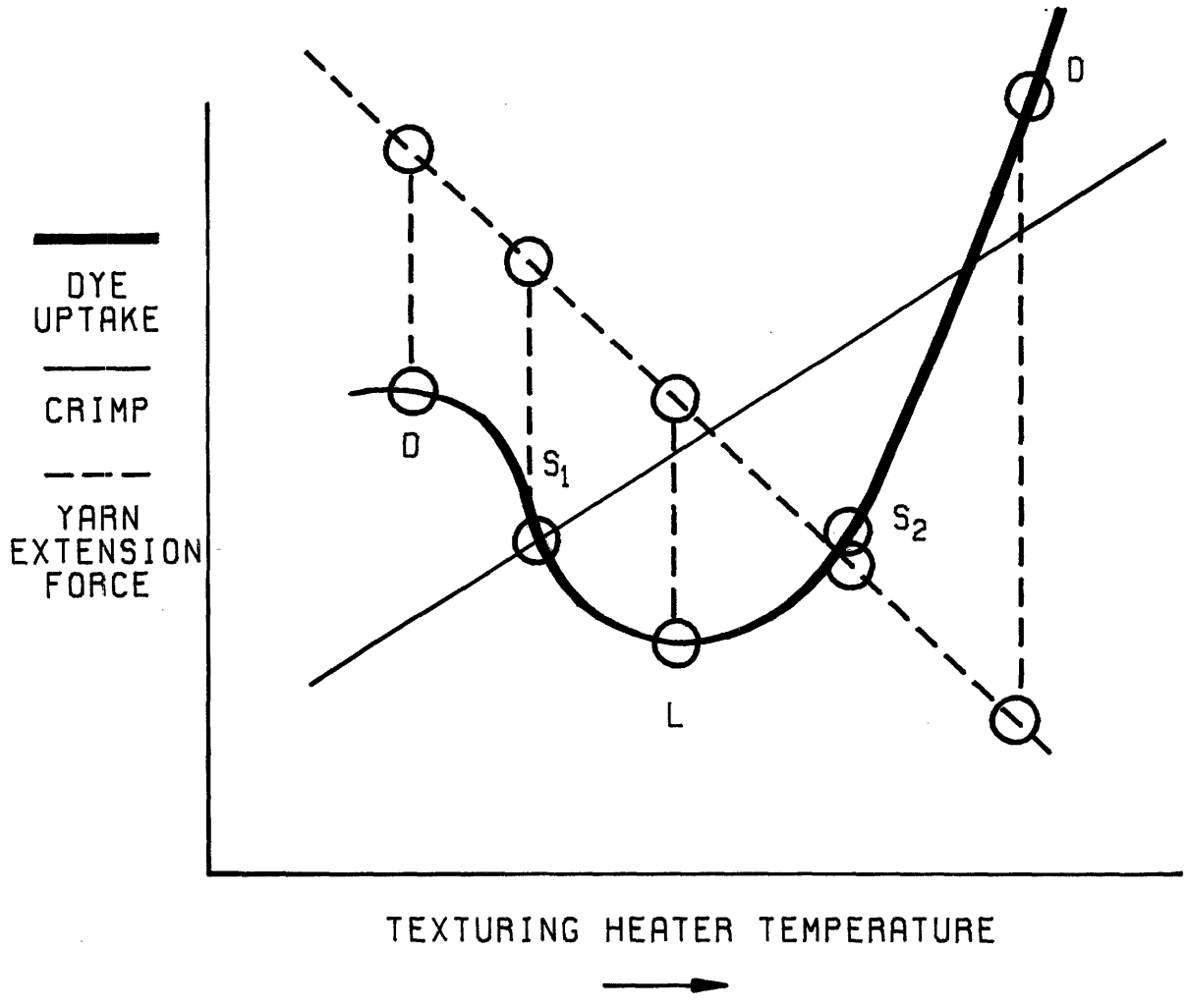

FIGURE 28: THEORETICAL CORRELATION
BETWEEN DYE UPTAKE AND YARN EXTENSION FORCE
AS A FUNCTION OF TEXTURING HEATER TEMPERATURE

BULK DEVELOPED AT ≈2MG/DEN 145°C. TENSION MEASURED AT 19% U.F. FROM LENGTH AT 0.5 G/150 DEN.

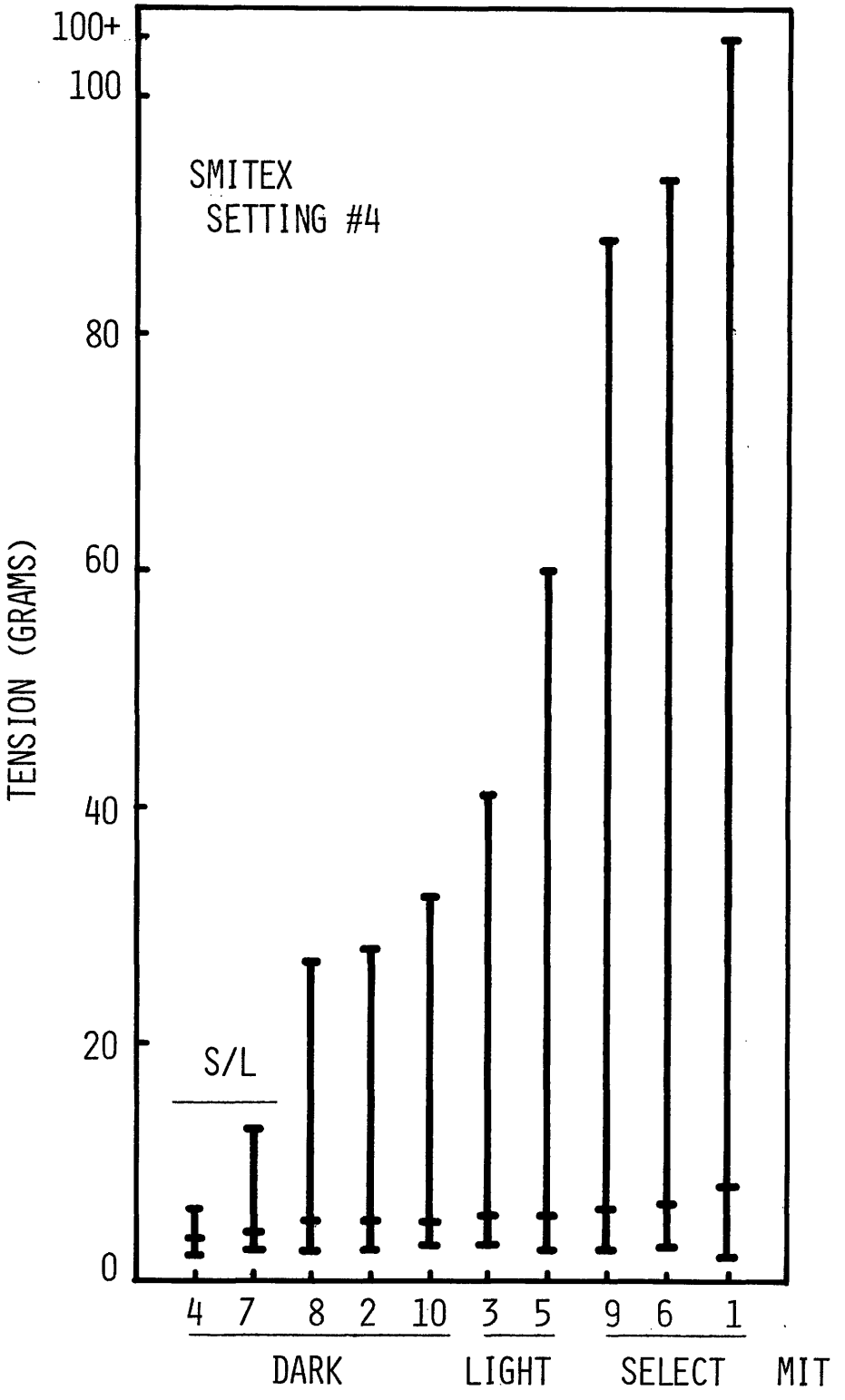

FIGURE 29. YARN EXTENSION FORCE TESTS ON SPLIT PACKAGES IN SAMPLE SET F

select and dark yarns. Industrial experience has shown that dark yarns can be either extremely low in bulk, or very high in bulk. Temperature of the yarn during texturing, or the crystallization of the yarn in response to the texturing temperature, are implicated as sources of property variation in textured yarns.

Figure 29 shows the results of yarn extension force testing on a series of 10 textured packages made by rewinding two smaller packages from each of the five original textured packages. Packages 4 and 7 came from a very dark package; the pairs 8 and 2 and 10 and 3 came from two textured packages which were dark dyeing; 5 and 9 came from a light dyeing package; and, finally, 6 and 1 came from a select package. Good agreement is shown between measured values of yarn extension force for pairs of packages. The ranking of dye grades on the basis of yarn extension force was, again:

select > light > dark > dark second quality.

The Y.E.F. was found to vary considerably along the yarn length for all yarns. Figure 30 shows the pattern of variation in yarn extension force and the locations where tight spots were observed in the bulked yarn. A tight spot is simply a yarn segment that was never untwisted during texturing. Tight spots are produced whenever there is a large change in the yarn translational speed through the twister with respect to yarn rotational speed (as driven by the twister). Tight spots can result from changes in feed speeds, in twister

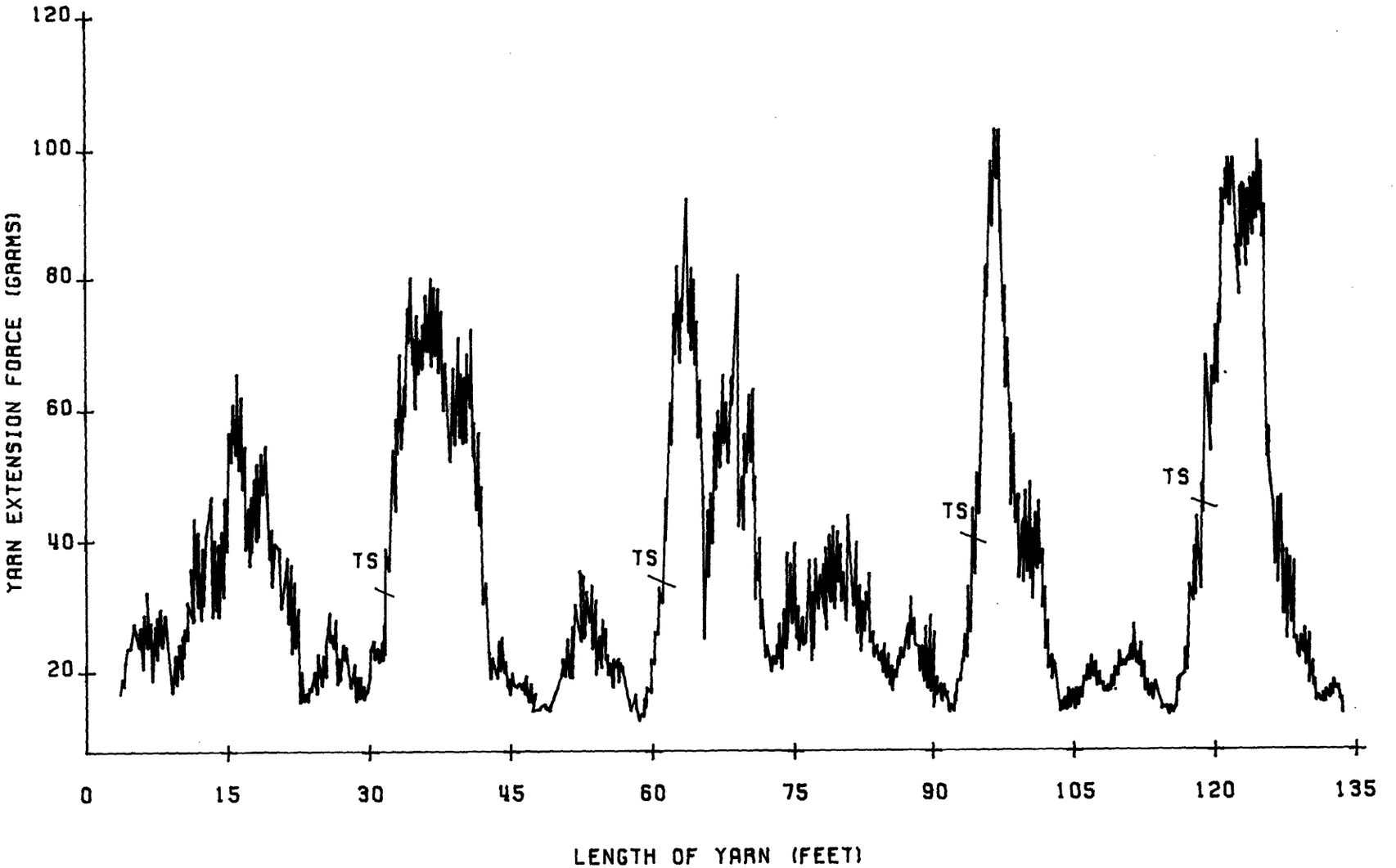

FIGURE 30: LOCATION OF TIGHT SPOTS IN TEXTURED YARN.
(150/34 PET, 19% EXTENSION FROM 1 mgpd AT 23 °C)

speeds, or in rotational slippage of the yarn on the twister.

Whatever was the cause of the observed tight spots, we expect such a disturbance in the torque/tension/twist/velocity equilibrium of the threadline to produce a transient disturbance in all these threadline parameters and therefore in the yarn crimp. Figure 30 shows that the yarn extension force reflects this type of threadline transient response.

The machine recovery from these disturbances was seen to occur in about 10-25 feet. The surges (slippages) occurred randomly and were from 30-150 feet apart, depending on the yarn and its processing conditions. The texturing machine "time" constant for recovery from a disturbance is about one machine length (10-15 feet for the texturing machines considered here). The observed length of yarn required for a recovery as seen in Fig. 30 is in good agreement with this value. In addition, the texturing machine surging period as measured here is in good agreement with the 5-10 machine lengths observed in [50].

Fluctuations in yarn extension force were also observed to occur at much smaller (5-10 feet) and at much larger (450-1000 feet) periods through the textured yarns. The shorter disturbances are expected to arise from any of the higher frequency machine actions (e.g. spinning wind-up traverse, cyclic twist buildup and dumping at the entrance to the texturing machine, draw point motion, splices in machine drive belt, changes in yarn balloons, filament

snagging on worn guides). The hot draw force for POY-PET feed yarns was measured [50] and found to have variations in the range of 10 feet (drawn length).

In one case, variations in yarn extension force with longer periods were found to be due to a 10% denier variation in the feed yarn. This denier variation was further traced to a missing gear tooth in a fiber extrusion pump. Other sources of variations in yarn properties occurring at long repeat periods are the lower frequency machine actions, such as the action of traversing a worn feed roll or belt, the change in yarn position entering the second heater due to the traverse action on the intermediate feed, heater temperature cycling about the control point, line voltage fluctuations (overall machine speed), or changes in twister, guide, or heater finish buildup.

Undoubtedly, a great deal of information is contained in the pattern of variation in yarn extension force that can be used to fine tune machine settings so that intra-yarn variations can be minimized. It is not known to what extent the action of eliminating intra-yarn variations would reduce the inter-yarn differences which are most important in barred fabrics. Research on intra-yarn variations will be left for future workers, since the subject of this study is inter-yarn differences.

C. Retexturing Tests. Self-induced texturing machine instability, or surging, is known to depend on yarn

properties as do the threadline torque and tension during texturing. It was proposed that retexturing of a previously textured yarn could provide a very sensitive indication of both the geometric and thermomechanical properties of the yarn and therefore form a continuous test of yarn quality. Experiments were conducted by Bell [50,52,68] to investigate this possibility and his results are discussed here.

The steady-state torque and tension of the previously textured yarns during retexturing did not show significant differences despite significant differences in their dye grades. The period of surging in the laboratory texturing machine was found to be different for the differently graded yarns of sample set A. Dark yarns cycled at the highest average frequency (the shortest period) and light yarns at the lowest average frequency (the longest period). Select yarns showed intermediate cycling behavior. This ranking was consistent with the rankings based on crimp extension force results obtained for the same samples.

Bell and Backer [50] based their explanation of the correlation between dye grade of textured yarns and the period of cycling during retexturing on postulated differences in stored torsional energy in the threadline during retexturing. These differences in stored torsional energy can exist in the absence of differences in yarn twist, since the stored energy depends on the deformation from a stress-free geometry. If a given textured yarn has been exposed to different texturing

temperatures and stresses than another yarn, we may expect the fine structures in the previously textured yarns to respond to a re-texturing operation in different ways. Textured yarns with crystallite networks that are more stable to the heat and stress of the retexturing operation will not readily be "set" into the new twisted configuration during retexturing. These yarns will, therefore, have more stored and recoverable elastic energy at a given yarn twist during retexturing than yarns with a less stable crystallite network. The heat and stress stability of crystallite networks in fibers increase with previous heat treatment temperature of the fibers [35,36,123].

D. Shrinkage Force Tests. A more direct measurement of the temperature and stress history of the textured yarns can be obtained by measuring the force on a heated running threadline. To measure these shrinkage forces, the first zone of the laboratory testing instrument was operated at an underfeed, with the heater at room temperature, and with load controlled by a dancer weight of 60 gmf. The second zone was operated at 0% overfeed, with a 1-1/4"-wide contact heater, and the 500 gm load cell. In passage through the first zone of the instrument a textured yarn is decrimped by the action of the dancer weight (0.2 gpd) and is delivered in a straightened condition to the second zone. Only part of the second zone is heated (1-1/4 out of 16 inches), so three distinct subzones corresponding to yarn states exist within this zone. The cold entering yarn, the hot yarn over the heater, and the cooled

yarn exiting the second zone must be in force equilibrium. Although the overall elongation imposed by the zone overfeed is known to be zero, the length contractions of the entering and hot yarns need not be zero. This is not a well-controlled test, since the zonally imposed deformation of the yarn is not operative at the point of yarn heating. Furthermore, the measured force will depend on the properties of the entering and exiting yarn, as well as the response of the hot yarn.

In the face of these obvious drawbacks in yarn control during testing, thermal shrinkage force tests on the laboratory instrument were conducted over the temperature range 60-250°C. The results obtained for sample set D are shown in Fig. 31. This sample set shows the characteristic shape of the shrinkage force vs. temperature curve. From 60°C to about 140°C, the measured shrinkage force decreases in keeping with the lower modulus of a partially amorphous polymer above its T_g. The shrinkage force is constant from about 140-170°C. The shrinkage force increases starting at about 170°C and is constant from about 200-240°C. Above 240°C, the shrinkage force declines as the melting point of the fiber is approached. Although the variations in dye grade of yarns within a shipment could not be reliably predicted by shrinkage force measurements, gross differences between yarn shipments were seen.

Figure 32 shows the marked difference in shrinkage force (at 0% overfeed following a pre-stress of 0.2 gpd) for two

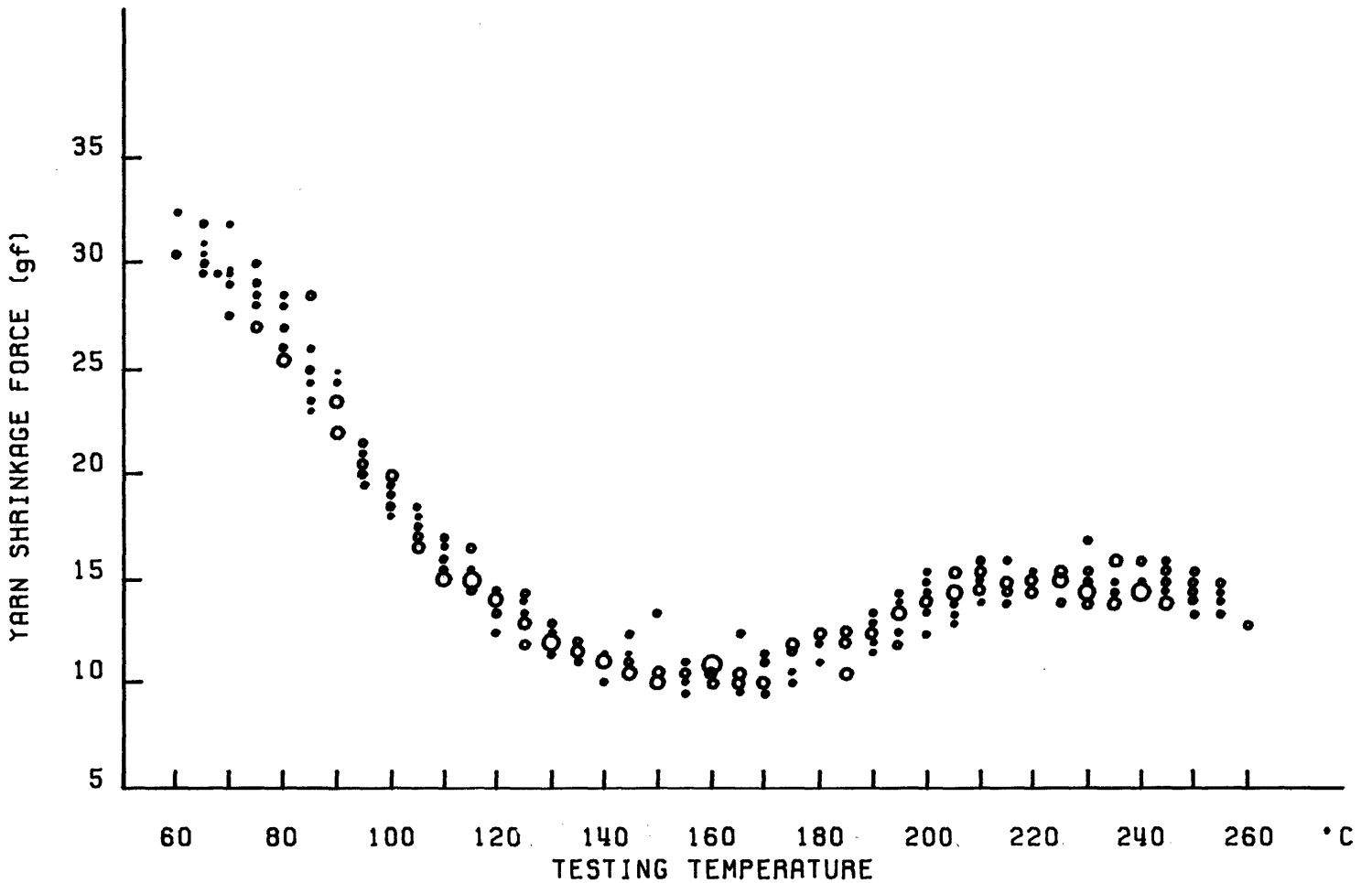

FIGURE 31:
SHRINKAGE FORCE FOR SAMPLE SET "D" AS A FUNCTION OF TEMPERATURE
(0% OVERFEED FROM 30 GRAMS PRETENSION ON 150/34 PET)

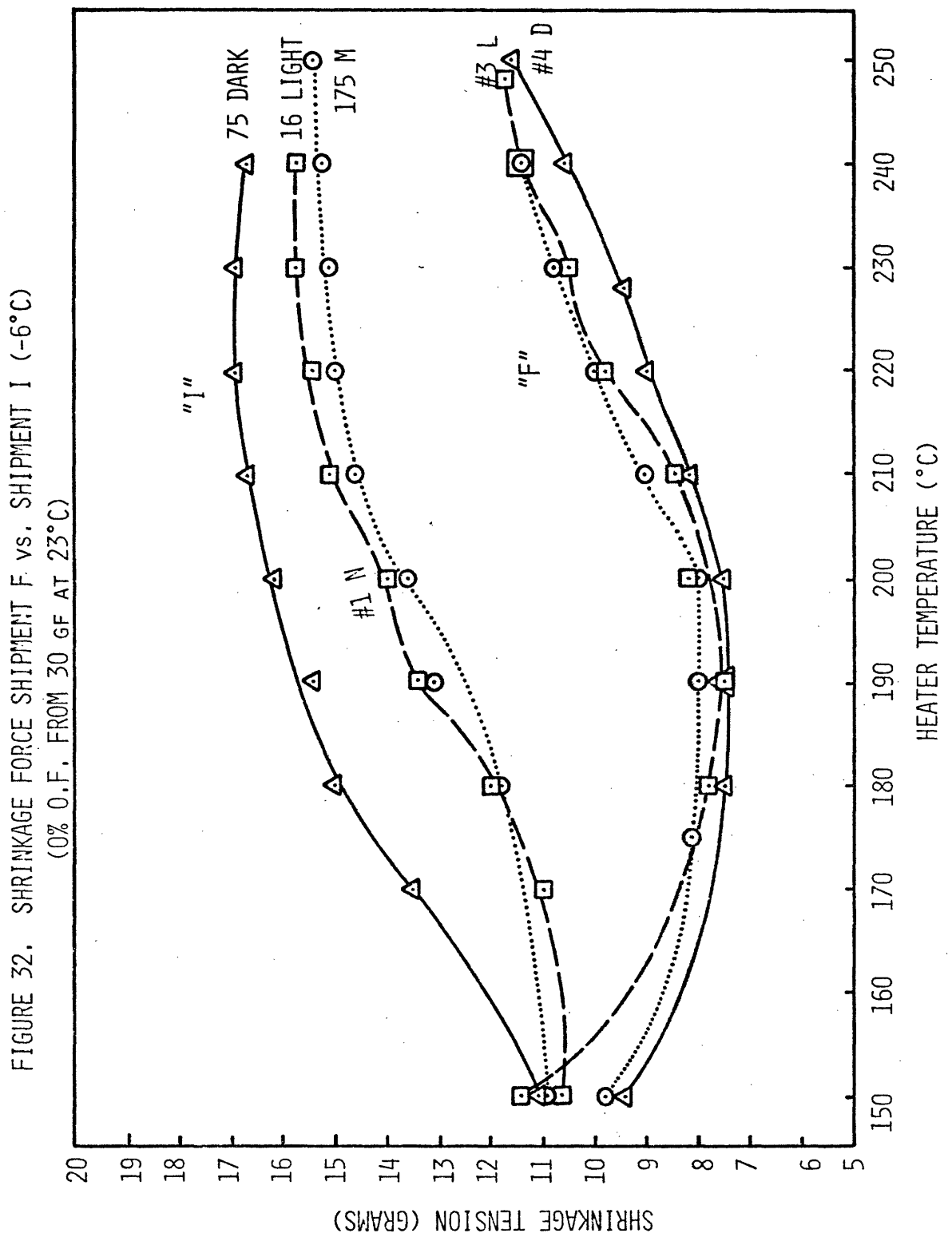
FIGURE 32. SHRINKAGE FORCE SHIPMENT F vs. SHIPMENT I (-6°C)
(0% O.F. FROM 30 GF AT 23°C)
SHRINKAGE TENSION (GRAMS)
HEATER TEMPERATURE (°C)
"I"
"F"
75 DARK
16 LIGHT
175 M
#1 N
#3 L
#4 D
20
19
18
17
16
15
14
13
12
11
10
9
8
7
6
5
150
160
170
180
190
200
210
220
230
240
250

textured yarn shipments. The yarns labelled "I" were textured at 180°C and 165°C for the primary and secondary texturing machine heaters, respectively, while the yarns labelled "F" were exposed to 225°C and 195°C during texturing. The 45°C difference in primary texturing heater temperature between the two yarn lots is clearly reflected in the much higher tensions of the "I" yarns. In addition the rise in shrinkage force to the high temperature plateau occurs some 30-40°C lower for the "I" yarns.

The relative positions of the yarns within the two shipments in Fig. 32 show some consistent differences, but in light of the scatter seen in Fig. 31 for a larger sample set, no interpretation of the relative positions will be made except to note the large difference in shrinkage force between yarn number 75 and the other two in lot "I". It was disclosed to us that 75 dark was textured with its primary texturing machine heater 6°C lower than that used for the other yarns. This lower primary heater temperature is reflected in a 20°C earlier rise in shrinkage force and a 10% higher shrinkage force level at temperatures over 150°C.

In summary, we have seen that continuous testing of textured yarns using a crude laboratory device has given some results which correlate well with the performance of textured yarns in a laboratory fabric. The ranking of the variously graded yarns using <u>average</u> yarn extension force values was similar for all shipments (D < L < S < D). It was shown that

this ranking is consistent with expected dye shade or crimp development changes due to variations in yarn temperature or yarn (crystallization) setting during texturing. Surging of the texturing machine, periodic variations in feed yarn denier, or hot draw force, and periodic variations in textured yarn windup tension were also detected during measurements of the textured yarn.

The average yarn extension force showed strong sensitivity to the amount of coning oil on the yarns. This resulted from differences in friction on the dancing weight which produced changes in the crimp development force and, therefore, in the amount of crimp developed. The cycling behavior during re-texturing also showed this oil sensitivity.

4. Continuous Tests with "Production" Quality Control Instrument.

A. Design Features of the Instrument. The laboratory testing device described in the previous section was sensitive to friction differences in oil, required constant zone overfeed adjustments to accommodate the differences in yarns, and used yarn extension force as a measure of the yarn shrinkage in the first zone. These shortcomings were rectified in a "production" thermomechanical tester for textured yarn. The device was conceived, designed, and constructed by the author in conjunction with Jan Krizik of IDR, Incorporated. The instrument was configured, as shown in

Fig. 33. The key components of the system are the yarn feeds (1,2,3), the yarn heater (which could be positioned in either of the zones),the first yarn force sensor, the second yarn force sensor, and the circuitry for calculating average values of the measured quantities. The first feed speed is varied with respect to the constant speed of the second and third feeds to keep the force on the yarn in the first zone constant. The ratio of the second to third feed speed is adjusted by changing the roll size of the third feed, with respect to the roll size on the second feed. Both second and third feeds are driven by AC synchronous motors. The first yarn force sensor consists of a balance beam using an air bearing for a pivot. One arm of the beam is acted on by the force of the yarn; the other arm of the beam is acted on by the desired crimp development force (a fixed weight). A slight pendulum effect exists in the sensor which provides stability in operation without significant changes in crimp development force.

To eliminate sliding friction between the yarn and the beam, a pulley running in an air bearing was mounted on the balance beam. The balance beam was lightly damped to control free oscillations at one cycle per second. A photoelectric measurement of the position of the balance beam was used as an indication of the force on the yarn in the zone and as a feedback to change the speed of the first yarn feed. Thus, the first yarn force sensor maintained the yarn at very low

FIGURE 33. TESTING INSTRUMENT

A. YARN TENSIONER (40 GF).

B. FIRST YARN FEED. VARIABLE SPEED.

C. YARN HEATER. CLOSED TUBE, NON-CONTACT. POSITIONED FOR YARN CONTRACTION (c), OR YARN SHRINKAGE FORCE (c').

D. FIRST YARN FORCE (LENGTH) SENSOR (150 MGF).

E. SECOND YARN FEED. FIXED (75 FEET PER MINUTE) SPEED.

F. SECOND YARN FORCE SENSOR (0-300 GF).

G. THIRD YARN FEED. FIXED RATIO WITH RESPECT TO SECOND YARN FEED.

H. SPEED CONTROL SYSTEM. POWER AMPLIFIER, D.C. DRIVE MOTOR, TACHOMETER.

I. ROTARY SHAFT ENCODER MEASURES LENGTH OF YARN DELIVERED TO FIRST ZONE.

J. SIGNAL CONDITIONER. V/F CONVERTER AND AMPLIFIER.

K. SIGNAL AVERAGING CIRCUITRY. DIGITAL COUNTERS, GATE TIMING.

L. NUMERIC DISPLAY OF AVERAGE VALUES.

M. SIGNAL CONDITIONER. F/V CONVERTER.

N. ANALOG OUTPUT BUFFERING.

O. TEMPERATURE CONTROLLER. THERMISTOR SENSOR 80-300°C.

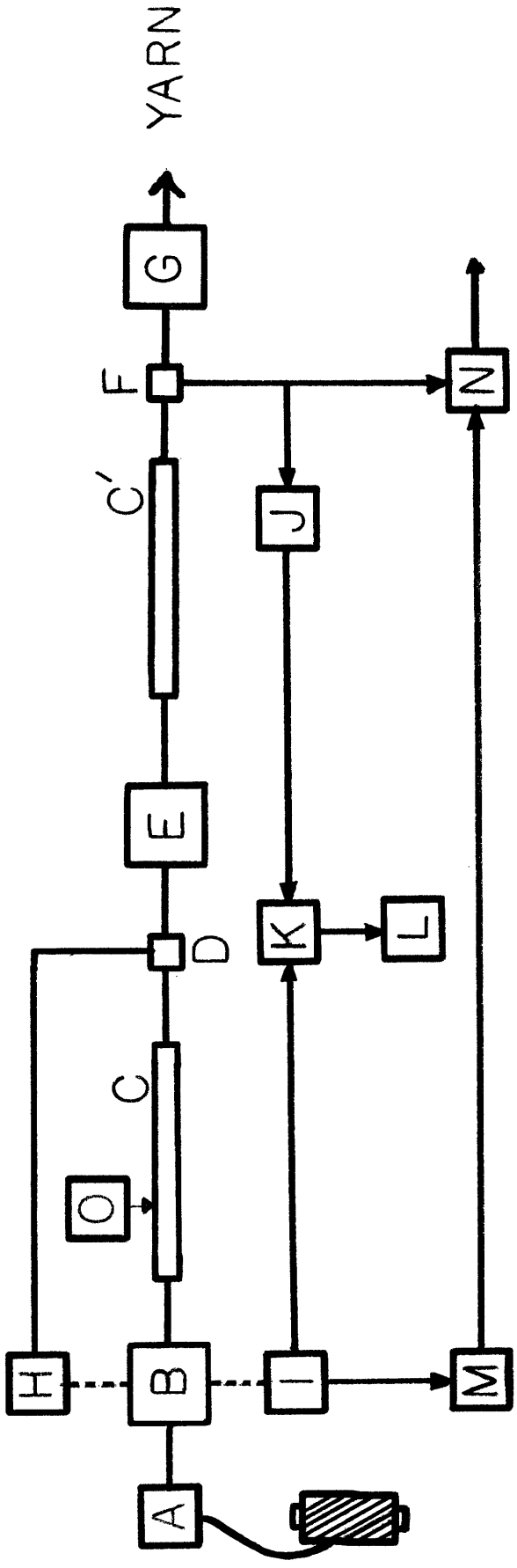

FIGURE 33

threadline tensions of about 1 mgpd, or 150 mg on 150 denier yarn. It was rugged enough to withstand several hundred grams of force (the breaking strength of the yarn) in the event of an instrument malfunction.

The output of the photoelectric cell by the balance beam was dictated by the length of yarn in the zone and was used as a command signal to the controller of the low inertia d.c. drive motor in the first feed. The motor speed was monitored by a tachometer (to provide system damping) and rotary shaft encoder to indicate the amount of yarn fed into the first zone.

The yarn was heated by passing it through a meter-long, electrically heated, small diameter tube. A temperature controller using a thermistor sensor was calibrated against a thermocouple to give heater temperatures from 80°C to 300°C. The yarn was in the heater about 2.4 seconds.

Yarn tension in the second zone was measured on a sensor using capacitance changes to produce voltage changes. The yarn ran over a pulley mounted on a ball bearing which was mounted on one end of a beam. The beam was, in turn, mounted on a torsional pivot with a highly linear spring constant. The other end of the beam was shaped like a flag, which moved between two parallel plates in response to yarn force changes, thus forming a two-element capacitance bridge. A suitable electronic circuit was employed to convert the changes in capacitance to voltage changes. A voltage-to-frequency converter was used to make the yarn load

signal compatible with the signal averaging circuits.

Since the average value of yarn properties is most important in determining whether barré will occur or not, the average value of the measured quantities should be determined. The total test time of 100 seconds precluded the use of normal ("op amp" type) analog integrators to determine the signal average, so a digital "window" counting circuit with associated timing circuits was designed and constructed. A numeric display was provided for the total counts from either the encoder or the load signal (converted to frequency).

B. Results from Prototype "Production" Testing Instrument. To assess the performance of a textured yarn in finished fabric accurately, the thermomechanical tests conducted should focus on the geometric and/or dye uptake behavior of textured yarns under conditions that simulate those the yarn will be exposed to during fabric formation, dyeing, and finishing. The following processing conditions prevail in commercial practice. During knitting, the maximum stress normally encountered by the textured yarn is about 40 gms for 150 denier yarn [133]. After knitting, the yarn is gradually heated from room temperature up to 130°C in a pressurized dye bath as shown in Fig. 10. It is held at 130°C for 30 minutes and then cooled. The presence of water and carriers raise the effective treatment temperature. During this time, constraints to free yarn contraction due to neighboring yarns exist. The fabric constraints can be

simulated by the application of a small load (1-5 mgpd) during crimp development. After dyeing, the fabric is set on a tenter frame for a few seconds at 170-190°C to remove wrinkles and to fix the fabric dimensions. This tenter setting operation occurs at fixed fabric extension (2-D).

The testing instrument described in the previous section is designed on the assumption that differences in appearance of yarns in fabric are due primarily to differences in geometry. It is further assumed that any differences in dye uptake can be correlated with differences in geometry. This is a very large assumption, but it has been borne out by extensive experiments under controlled conditions. Furthermore, geometric changes in textured yarns can be induced much more quickly (by heat and stress) than equivalent changes in dye uptake. Therefore, they form a convenient basis for testing textured yarns. The total contraction of the yarn in fabric is the sum of:

(1) filament shrinkage, and/or

(2) yarn crimp development.

Since crimp development is usually conducted at temperatures where negligible filament shrinkage occurs, yarn contraction is considered to result solely from crimp development in the yarns. Latzke and Hesse [130] found that yarn bulk in fabric is directly related to crimp development for crimp development less than 40%. Differences in yarn contraction will alter the course spacing (as shown in Fig. 34),

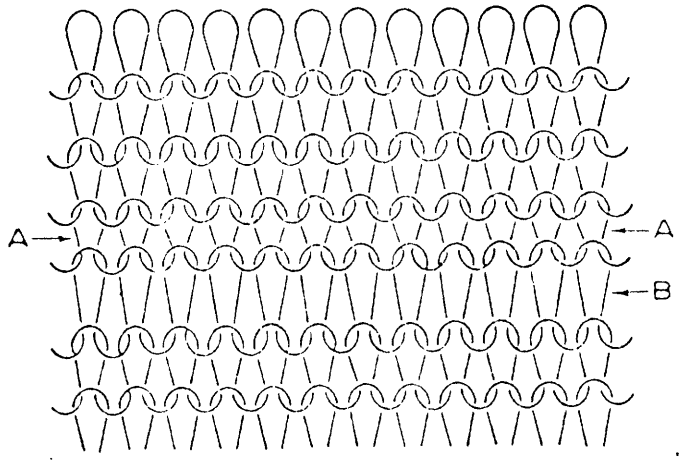

YARN IN STITCHLINE A CONTRACTED MORE FORMING A LINE OF SMALLER LOOPS.

YARN IN STITCHLINE B CONTRACTED LESS FORMING A LINE OF BIGGER LOOPS.

FIGURE 34. BARRÉ CAUSED BY DIFFERENCES IN YARN CONTRACTION

the local fabric bulk, and the local dye shade.

It was not possible to predict a priori what combination of crimp development conditions should be used to obtain the best correlation between yarn contraction and knit-dye grades; accordingly, several tests were conducted to establish the optimal conditions. In these tests the yarn contraction in the first zone of the instrument was computed as follows:

$$\text{Yarn Contraction} = \frac{L_{in} - L_{out}}{L_{out}} \times 100\%$$

where L_{in} = length of textured yarn fed into the first zone under tension of 40 gms for 150 denier,

L_{out} = length of textured yarn removed from first zone after yarn contraction.

Additional information regarding the magnitudes of the crimp component and of filament shrinkage in the total yarn contraction were obtained by measuring the yarn extension force at 19% extension in the second zone. Only average values of these quantities are shown in the following figures. The limits shown for each point represent the mean value of the averages $\pm$ the standard deviation of the mean.

Figures 35a,b show the temperature dependence of yarn contraction at two different crimp development loads. It is estimated that the tension in Fig. 35a was about 5 mgpd and about 6 mgpd in Fig. 35b. These tests were run while the balance beam was being debugged.

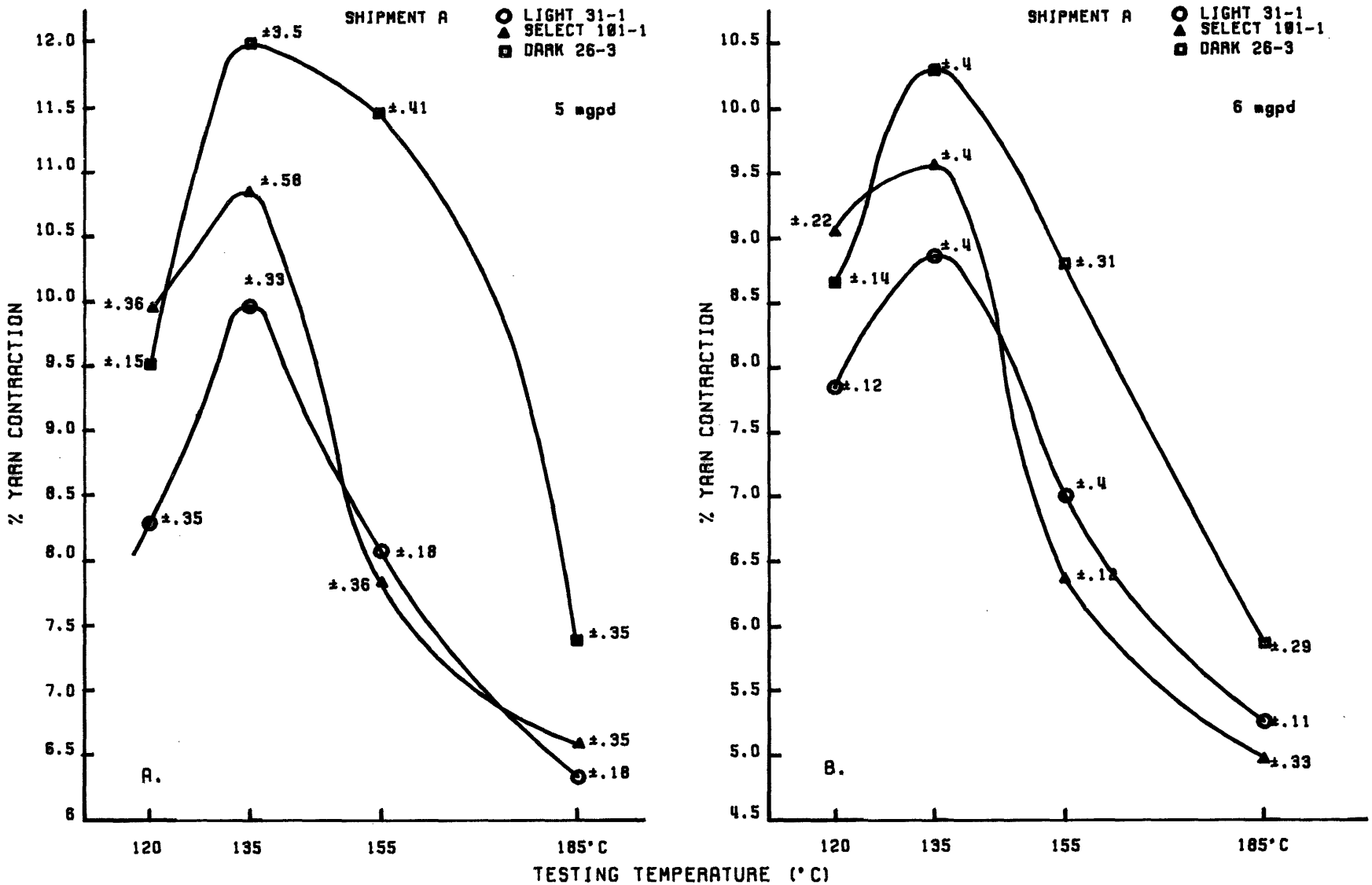

FIGURE 35: YARN CONTRACTION AS A FUNCTION OF CRIMP DEVELOPMENT AND LOAD

In both Figs. 35a,b the dark yarn showed the most yarn contraction above 135°C. The yarn contraction increases with temperature up to 135°C due primarily to higher crimp development. Above 135°C part of the driving force towards higher crimp development is removed by the combined action of heat and stress. It is highly likely that part of the original crystallite network produced during texturing is removed, even at temperatures as low as 135°C. Many workers have shown that crystallites melt at approximately the temperature they were formed. What fraction of the crystallites in a textured yarn is formed at low (<150°C) temperatures? Smith and Steward [135] found that the crystallization half time for PET with birefringence of 0.08-0.150 is on the order of 10 milliseconds or less at 120°C, or lower. On this basis, it seems likely that a large fraction of the network nucleates and grows at low temperature. Lunenschloss and coworkers [71] have measured the temperature at the drawing and up-twisting point during draw texturing of POY-PET. They found that the draw point occurred at a yarn surface temperature about 155°C and that substantial increases in fiber density (which can only result from crystallization) occurred before the yarn surface temperature exceeded 170°C. On the basis of these combined references, it is not unexpected that a large part of the "permanent" set in textured fibers may be melted and pulled out at temperatures as low as 135°C.

As the crimp development temperature is further increased to 185°C, the yarn contraction drops rapidly at first and then

appears to begin to flatten out. This presumably occurs due to the onset of increasing filament shrinkage at higher temperatures. Some insight into the division of yarn contraction into its components (crimp development and filament shrinkage) may be obtained by measuring the extension force that develops when the contracted yarn is extended.

Figure 36 shows the relationship between yarn contraction and subsequent yarn tension at 19% extension. The packages are from shipment A and represent three sequential doffs from a given texturing machine position using the same feed yarn package. The packages from each position gave the same appearance in a knit and dyed hoseleg. The packages are clearly grouped according to appearance in the figure. Thus the appearance can be predicted on the basis of either yarn contraction or yarn extension force. All yarns fall along a curve consistent with the load elongation behavior of textured yarns. This supports the hypothesis that the primary differences between the bulked yarns are in crimp development and not filament shrinkage at this low temperature (150°C).

If the imposed elongation of the second zone (19%) is great enough to remove the yarn crimp developed in the first zone, then the curve (in yarn contraction-yarn elongation force space) representing the loci of tested yarns will be a straight line as shown in Fig. 37. The inverse of the slope of this line is the elastic modulus of the filaments. The value of E calculated from Fig. 37 is 18 gpd which is in good agreement

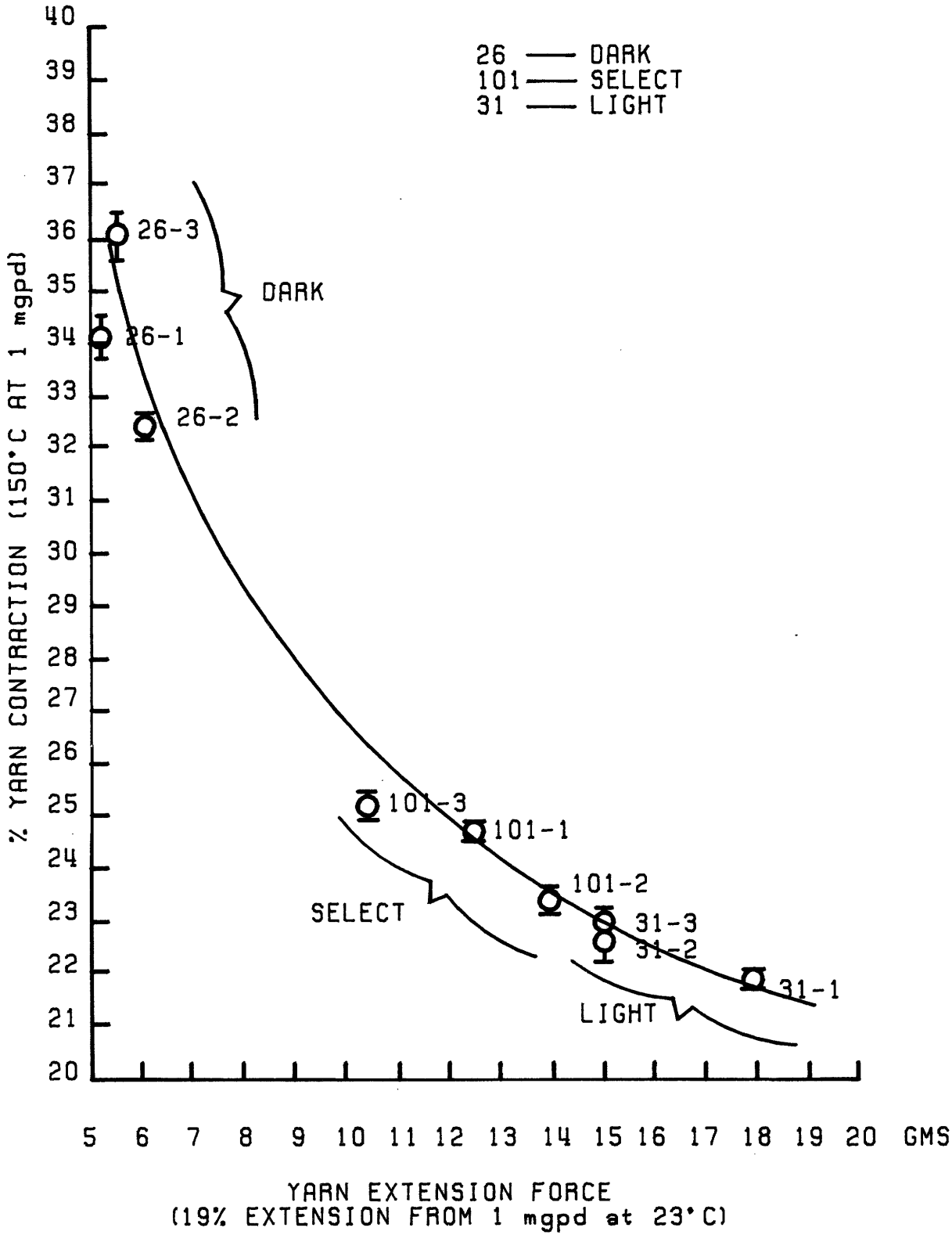

FIGURE 36: THERMOCHEMICAL TESTING OF
150/34 P.E.T. TEXTURED YARN FROM SEQUENTIAL DOFFS

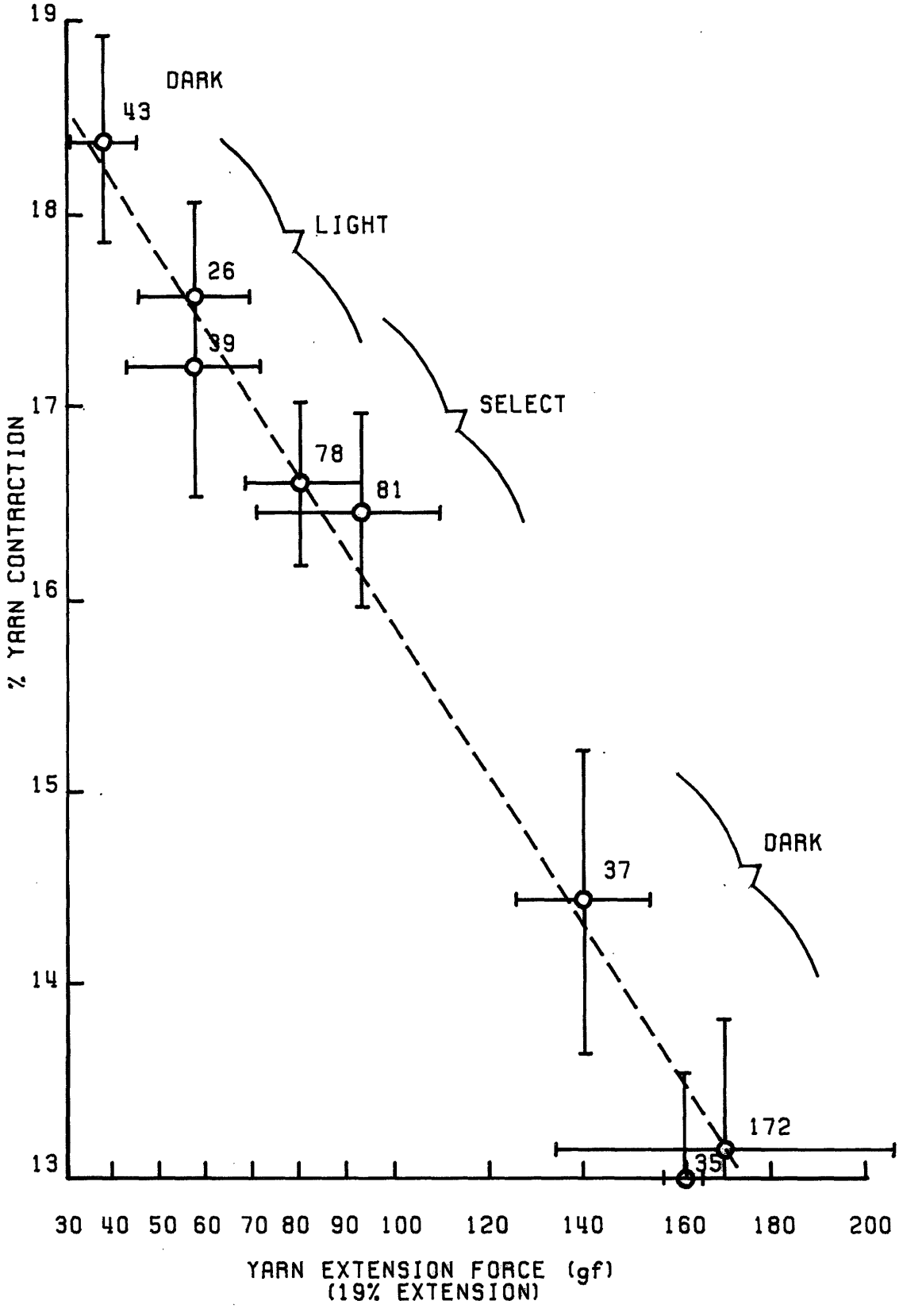

FIGURE 37: THERMOMECHANICAL TESTING OF 150/68 P.E.T. AT 150 °C AND 1 mg/den

with published values. As filament shrinkage and more severe removal of the "permanent" set from texturing increase at higher crimp development temperatures, two changes in the loci of test points occur. First, since less crimp is developed during yarn contraction, the yarn force at a fixed elongation increases. Second, the ability to predict yarn dye grade from test results is dramatically reduced at higher crimp development temperatures.

In light of these findings, crimp development conditions were standardized at 1 mgpd and 150°C. Good correlation was obtained between yarn appearance and yarn contraction (crimp development) for other sample sets as shown in Fig. 38.

C. Controlled Variation Samples. It was felt that yarn contraction and yarn extension force formed a suitable basis for predicting the apparent dye shade of textured yarns in fabric. To determine the sensitivity of the device to changes in texturing machine settings (and therefore yarn parameters during texturing), a series of tests was conducted on a set of yarns textured with known variations in texturing machine settings.

The draw-textured yarns were produced by the research and development staff at UNIFI, Inc. on a Barmag Model FK-6 set-texturing machine. The details of the variations and running conditions are shown in Table 13.

Figures 39, 40, 41, 42 show the effects that variations in primary texturing heater temperature, secondary texturing

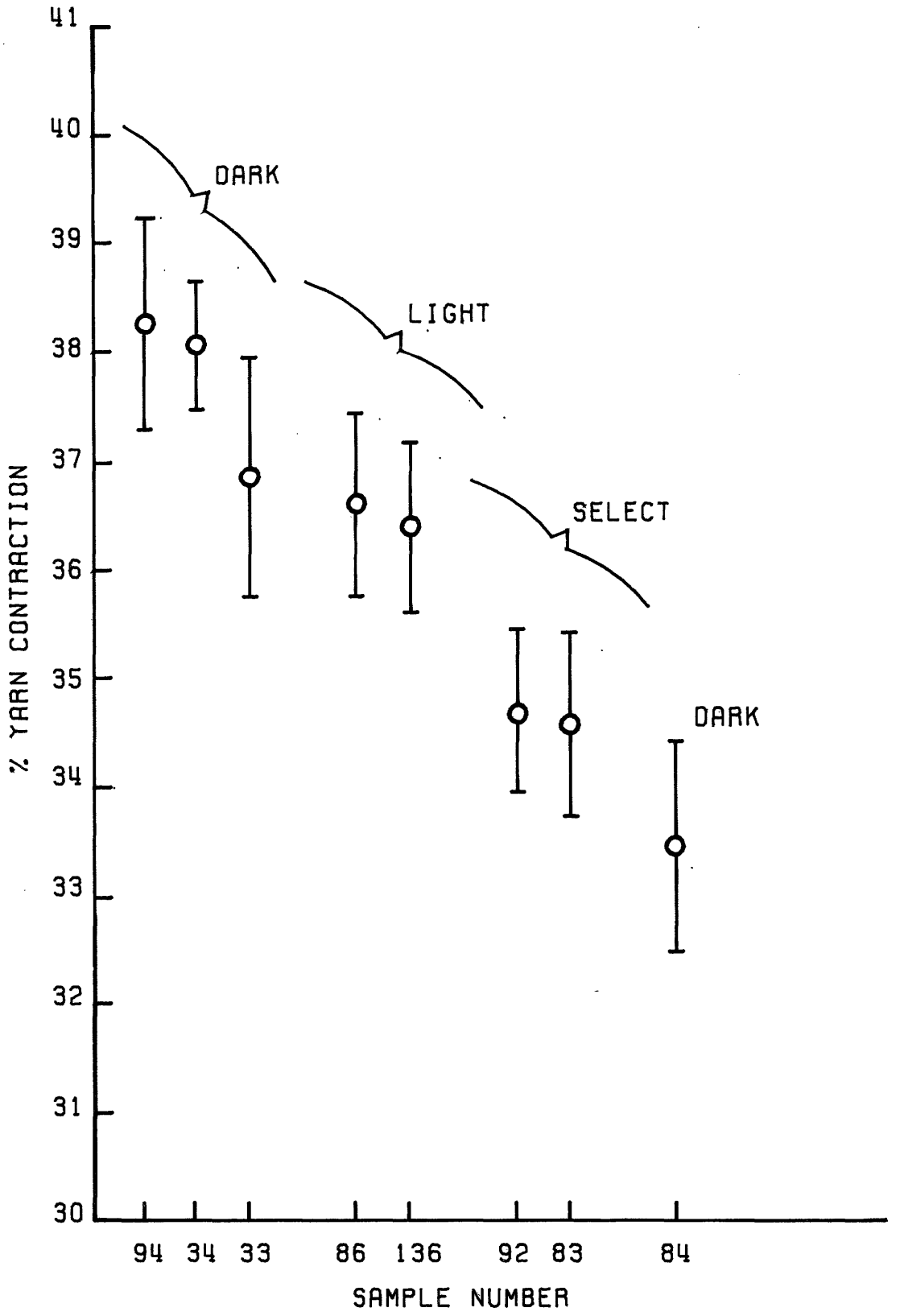

FIGURE 38: TEST RESULTS FOR SHIPMENT D. CRIMP DEVELOPMENT AT 150 °C AT 1 mgpd, 150/34, POLYESTER

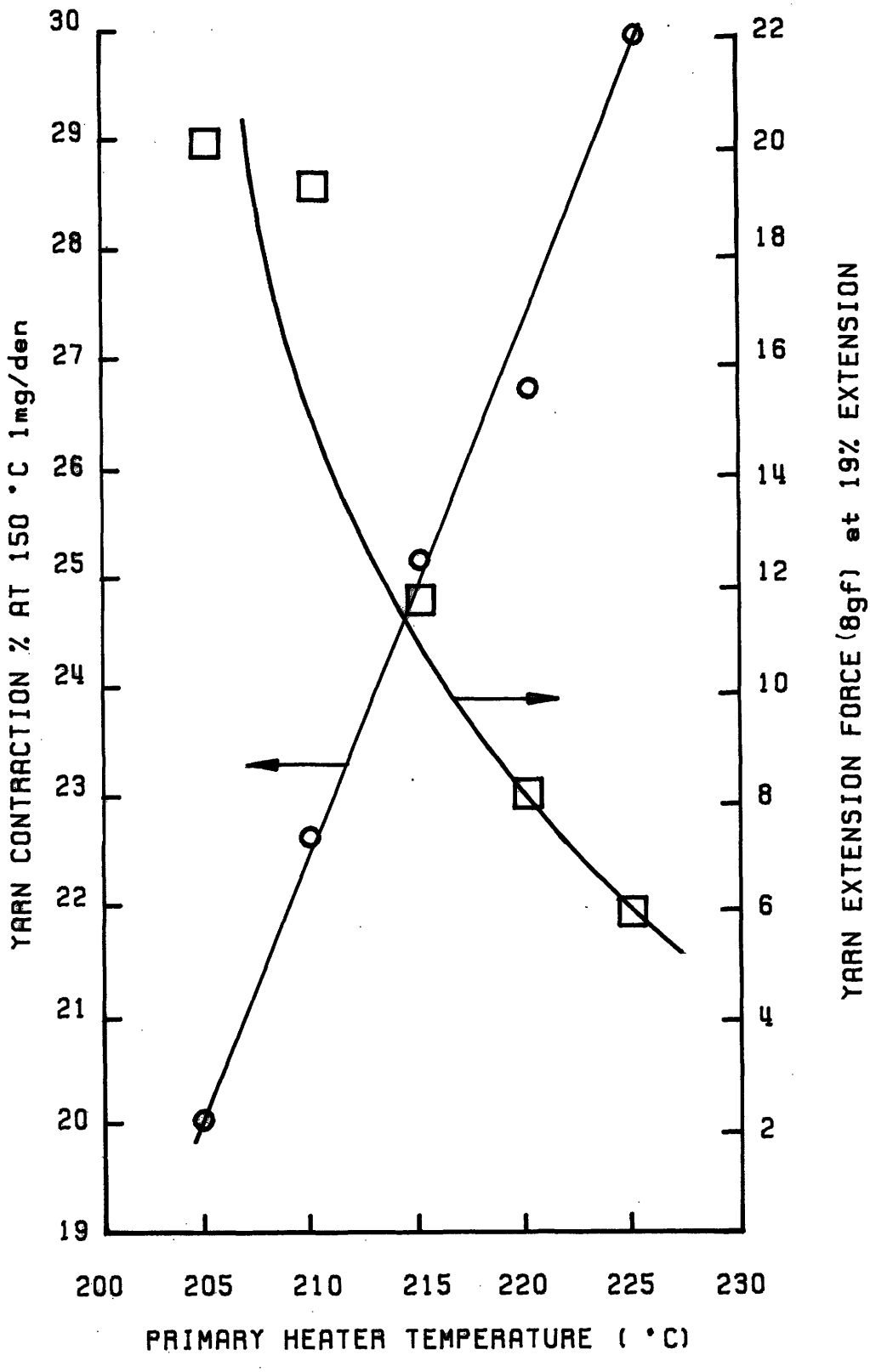

FIGURE 39: YARN CONTRACTION AND EXTENSION FORCE AS A FUNCTION OF TEXTURING MACHINE SETTINGS. (150/34, PET, 150 °C, 1 mgpd)

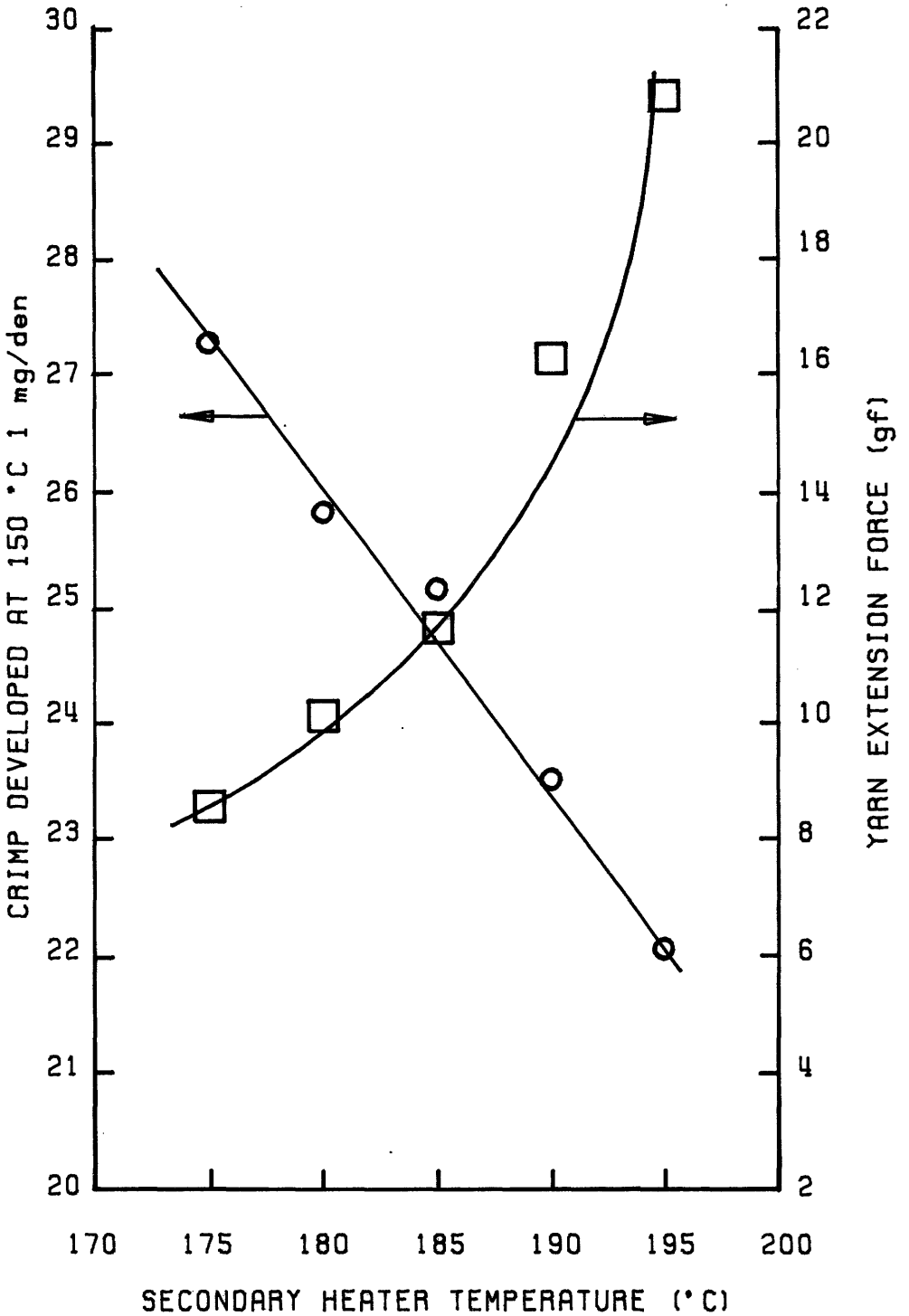

FIGURE 40: YARN CONTRACTION AND EXTENSION FORCE AS A FUNCTION OF TEXTURING MACHINE SETTINGS. (150/34, PET, 150 °C, 1 mgpd)

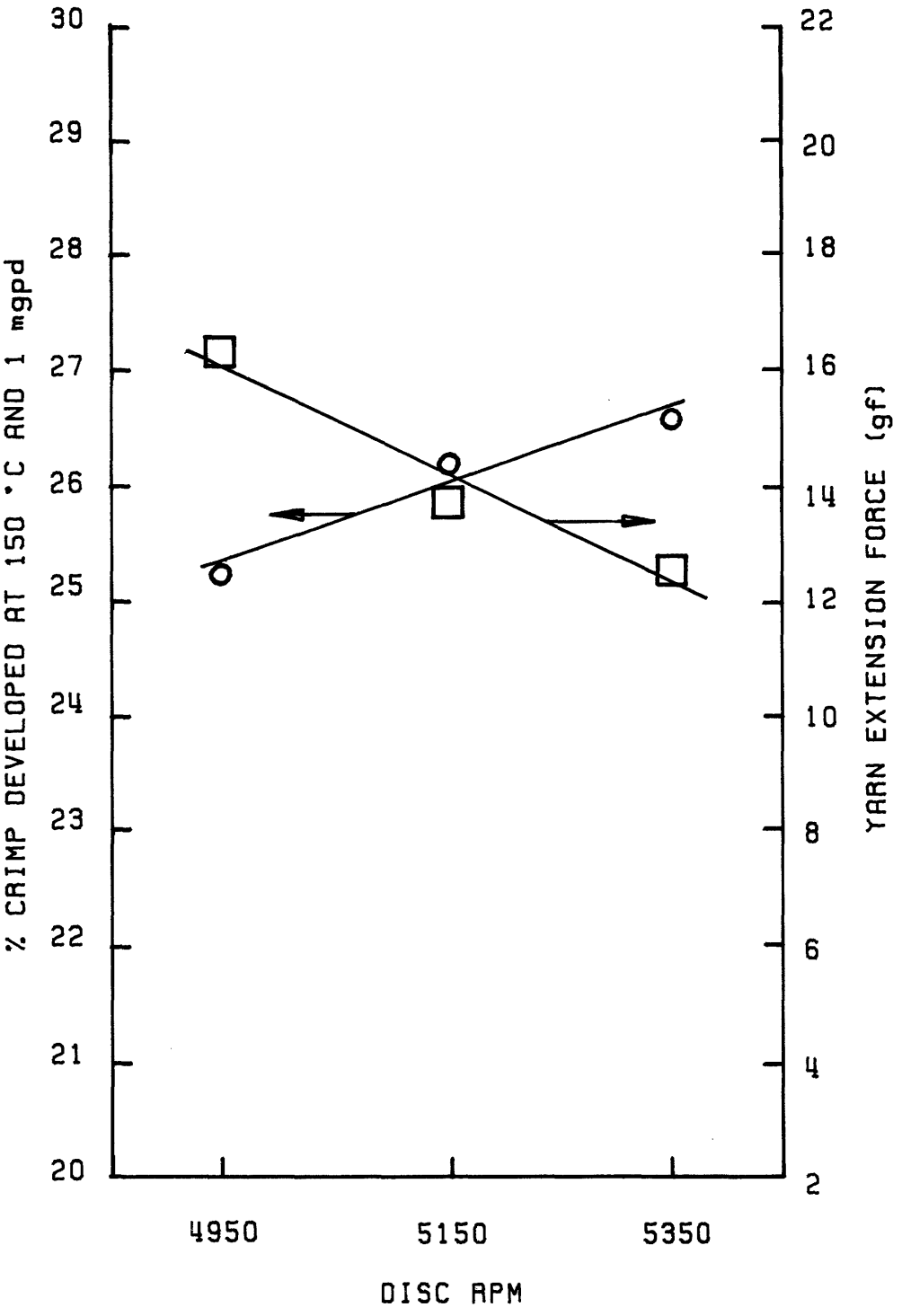

FIGURE 41: YARN CONTRACTION AND EXTENSION FORCE AS A FUNCTION OF TEXTURING MACHINE SETTINGS. (150/34, PET, 150 °C, 1 mgpd)

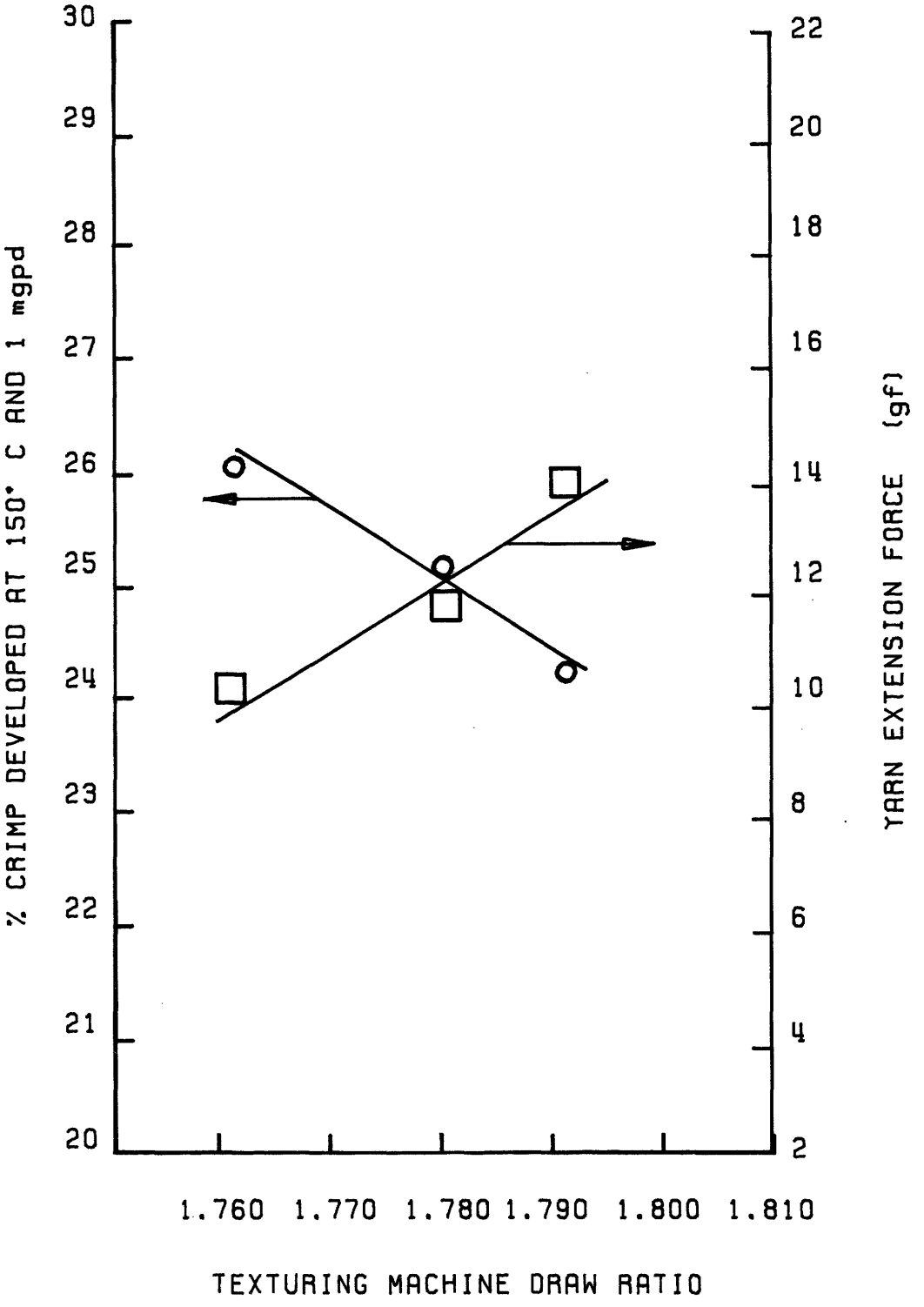

FIGURE 42: YARN CONTRACTION AND EXTENSION FORCE AS A FUNCTION OF TEXTURING MACHINE SETTINGS. (150/34, PET, 150 °C, 1 mgpd)

TABLE 13. TEXTURING MACHINE SETTINGS FOR CONTROLLED VARIATION SAMPLE SET**

Yarn Package Number	Primary Heater Temperature	Friction Disc Speed	Texturing Draw Ratio	Secondary Heater Temperature
1 (std.)	220	5150	1.790	185
2	225	*	*	*
3	230	*	*	*
4	215	*	*	*
5	210	*	*	*
6	*	*	*	190
7	*	*	*	195
8	*	*	*	180
9	*	*	*	175
10	*	5350	*	*
11	*	4950	*	*
12	*	*	1.801	*
13	*	*	1.772	*

*Standard value of this parameter applies.

**BARMAG FK-6, 1.5m Primary Heater, 1.0 meter Secondary Heater, Intermediate roll speed 445 meters/min, Second overfeed 8.85%, D/Y for first package = 1.63.

heater temperature, disc (twister) speed, or texturing draw ratio have on the measured yarn contraction and yarn extension force.

These results were obtained at crimp development conditions of 150°C and 1 mgpd. Tests were also conducted with crimp development at 130°C/1 mgpd and at 150°C/2 mgpd. The results for the former case with lower crimp development temperature paralleled those shown in the figures. The higher crimp development load in the latter case resulted in a drastic reduction (≈50%) in yarn contraction, and an associated increase in yarn extension force. The yarn contraction at 150°C/2 mgpd still showed the same trends as found at 150°C/1 mgpd, but the yarn extension force did not.

Figure 39 shows the yarn contraction and yarn extension force for yarns textured with variations in primary heater temperature (PHT). In this test at 150°C/1 mgpd, yarn contraction is seen to increase linearly with primary texturing heater temperature. The yarn extension force decreases with increased primary heater temperature. The decrease in force is related to the higher yarn crimp development during the first stage of the test and follows the usual curve associated with crimp deformation below 30 grams.

Figure 40 shows that yarn contraction <u>decreases</u> linearly with increasing secondary heater temperature (SHT). The yarn extension force is inversely related to the yarn contraction, but the same type of non-linear relation exists as in Fig. 39. The sensitivity of yarn contraction to variations in SHT is

about one-half that found for variations in PHT. This is reasonable, since the fiber fine structure originates in the primary heater in the texturing zone and is only modified by the lower temperature of the secondary heater in the setting zone.

In Figs. 41 and 42 the effects of friction disc speed (RPM) and texturing machine draw ratio on yarn behavior are shown. In Fig. 41, the yarn contraction is seen to increase slightly with increased friction disc speed. More twist in the yarn should produce more yarn contraction. In Fig. 42 the yarn contraction decreases slightly with increasing draw ratio. This is thought to be related to increased filament flattening lowering the filament EI and GI_p and hence the contraction forces.

Table 14 summarizes the results of linear regression analysis applied to yarn contraction as a function of variations in texturing machine settings. For small perturbations in texturing machine settings from the chosen operating point, yarn contraction behaves linearly for variations in any of the settings. The table also shows the relative per cent change in yarn contraction for a given change in texturing machine settings. The yarn twist was assumed to be 55 TPI (basic) at 5150 RPM of the disc. Rotational slippage of 30% at the discs was assumed on the basis of measurements in [64]. The twist change from 4950-5350 RPM is calculated to be 3 TPI.

Yarn contraction measured on the instrument shows the

TABLE 14

LINEAR REGRESSION ANALYSIS OF YARN CONTRACTION (Y.C.) DATA**

Dependence of Yarn Contraction on Changes in Texturing Machine Settings*	Relative Yarn Contraction Change from Tests	from Table 7
Y.C. (%) = 0.48 (PHT) - 80.7	+2%/1°PHT	0.8-2.2%/1°PHT
(r = .996)		
Y.C. (%) = -0.25 (SHT) + 71.7	-1%/1°SHT	-0.5%/1°C SHT [140]
(r) = - .992)		
Y.C. (%) = +0.0034 (TPM) + 7.63	+1.8%/1 TPI	+1.2%/TPI
(r) = .974)		
Y.C. (%) = -59.2 (D.R.) + 131	-2.5%/0.1 increase in D.R.	-7%/.01 increase in D.R.

** Yarn contraction measured from length at 267 mgpd/23°C to length at 1 mgpd/23°C after crimp development at 1 mgpd/150°C.

* Std. Cond.: PHT-210°C; SHT-185°C; disc speed-5150 RPM; Draw Ratio-1.79; setting zone O.F.-8.85%, 445 m/min; Barmag FK 6.

same sensitivity to changes in texturing machine settings as found by other workers using discontinuous crimp measurements. This general agreement provides confidence in the ability of the instrument to detect variations in texturing machine settings of yarn parameters during texturing.

During texturing of these yarns, tensions on the moving threadline were measured at three locations: above the twister (T1), below the twister (T2), and between the output and package (T3). The dependence of yarn windup tension (T3) on SHT was clear; the correlation between tension ratio (T1/T2) and disc speed was also clear. However, no clear trend in tension was observed for the large changes in PHT. Additional tests were conducted to measure breaking elongation, tenacity, and denier as textured. No clear correlation was found between these test results and the texturing variations.

The yarns were also knit into hoselegs with 2% carrier, and high-pressure dyed at 130°C for 30 minutes. The control package was included every third package to eliminate the Monte Carlo effect. Grading was done using transmitted and reflected light to detect primarily bulk and dye differences, respectively. The apparent shade differences were more easily seen at low (<1%) dye concentration, than at the normal (4%) concentration. The yarns were also graded for dye uptake using the Toray FYL-500 yarn analyzer described in Chapter I. The test results were provided by Mr. Tony Padgett of C. Itoh Company. A higher FYL value means more reflected light or a

lighter dyeing yarn. Table 15 compares the predictions based on yarn contraction and FYL values with the visual appearance of the yarn in dyed FAK hoselegs.

In use of the testing instrument all texturing process variations are detected by relative differences in yarn contraction. Except for variations in twist, the appearance of the yarn in the knit hoseleg is similar for reflected and transmitted light and correlates with that predicted by the difference in yarn contraction. Bulk and dye differences are indeed related for variations in PHT, SHT, and draw ratio. Twist variations seem to cause dye and bulk changes in the yarn that result in different apparent dye shade when viewed in reflected or transmitted light.

Predictions of fabric appearance based on Toray's FYL values do not correlate as well. First, no consistent trend is apparent in the FYL values for the first two sets of samples with primary or secondary heater differences. Second, the predictions made are completely opposite to the observed fabric appearance. FYL values detect lower heater temperatures in either the texturing or setting zone. Third, the FYL value will accurately predict the darker dye shade of yarns textured at lower twist or lower draw ratio. It also predicts darker yarns (than the standard yarn) for increases in twist or in draw ratio. The fabric appearance is opposite that predicted by the Toray instrument for increases in twist or in draw ratio.

TABLE 15. COMPARISON OF VARIOUS METHODS FOR PREDICTING YARN APPEARANCE IN FABRIC*

	Change in Texturing Machine Setting	Apparent Hoseleg Dye Shade Reflected Light	Transmitted Light	Relative % Change in Yarn Contraction	Dye Shade Prediction Yarn Contraction	FYL	Change in FYL-Value (Light Reflectance)
Primary	-10°C	Light	Light	-20	Light	Dark	-0.75
	- 5°C	Light	Light	-10	Light	Dark	-0.79
	+ 5°C	Dark	Dark	+10	Dark		-0.02
	+10°C	Dark	Dark	+20	Dark	(Light)	+0.03
Secondary	-10°C	Dark		+10	Dark	Dark	-0.58
	- 5°C	Dark	Dark	+ 5	Dark	Dark	-0.49
	+ 5°C	Light	Light	- 5	Light		-0.06
	+10°C	Light		-10	Light		-0.01
	+ 1.5TPI**	Light	Dark	+ 2	(Dark)		-0.32
	- 1.5TPI	(Dark)	Light	- 4	Light	Dark	-1.30
	+ .01 DR	Light	Light	- 4	Light		-0.44
	- .02 DR	Dark	Dark	+ 4	Dark	Dark	-0.90

* Appearance, contraction, dye compared to standard yarn textured at 220°C (PHT), 185°C (SHT), 1.79 (Draw Ratio), Overfeed to Setting Zone 8.85%, D/Y 1.63, Disc Speed (5150).

** Based on Change of +400RPM and 30% slippage.

The reasons for the lack of correlation between the FYL value and the fabric appearance are due to the very different dyeing conditions used in the FYL tests and in the hoseleg. The hoseleg is dyed at 130°C with carrier for 30 minutes. The FYL-rated yarns are dyed at 90°C with no carrier for 10 minutes. The integral of the mechanical loss modulus from room temperature to the dyeing temperature has been shown to be an accurate predictor of dye uptake [24,28]. The loss modulus increases slowly with temperature below T_g, increases rapidly near T_g, and declines as the temperature is raised beyond the T_g of the yarn. The point is that the mechanical T_g, which is closely related to dye uptake, is a strong function of thermomechanical history. It is suggested that dyeing at 90°C with no carrier makes the FYL value strongly dependent on the temporary components of fiber fine structure that do not remain or contribute to the dye or bulk behavior of the yarn during high temperature dyeing. An additional drawback to the FYL procedure is that the yarns are not allowed to contract freely during scouring, dyeing, and rinsing as is the case in hoseleg and commercial dyeing and finishing.

Additional crimp development tests were conducted on the yarns using various crimp tests. None of the results showed universal or consistent sensitivity to texturing machine variations. However, the Shirley tube test [139] was found to be most sensitive to changes in twist and draw ratio and totally insensitive to changes in either primary or secondary

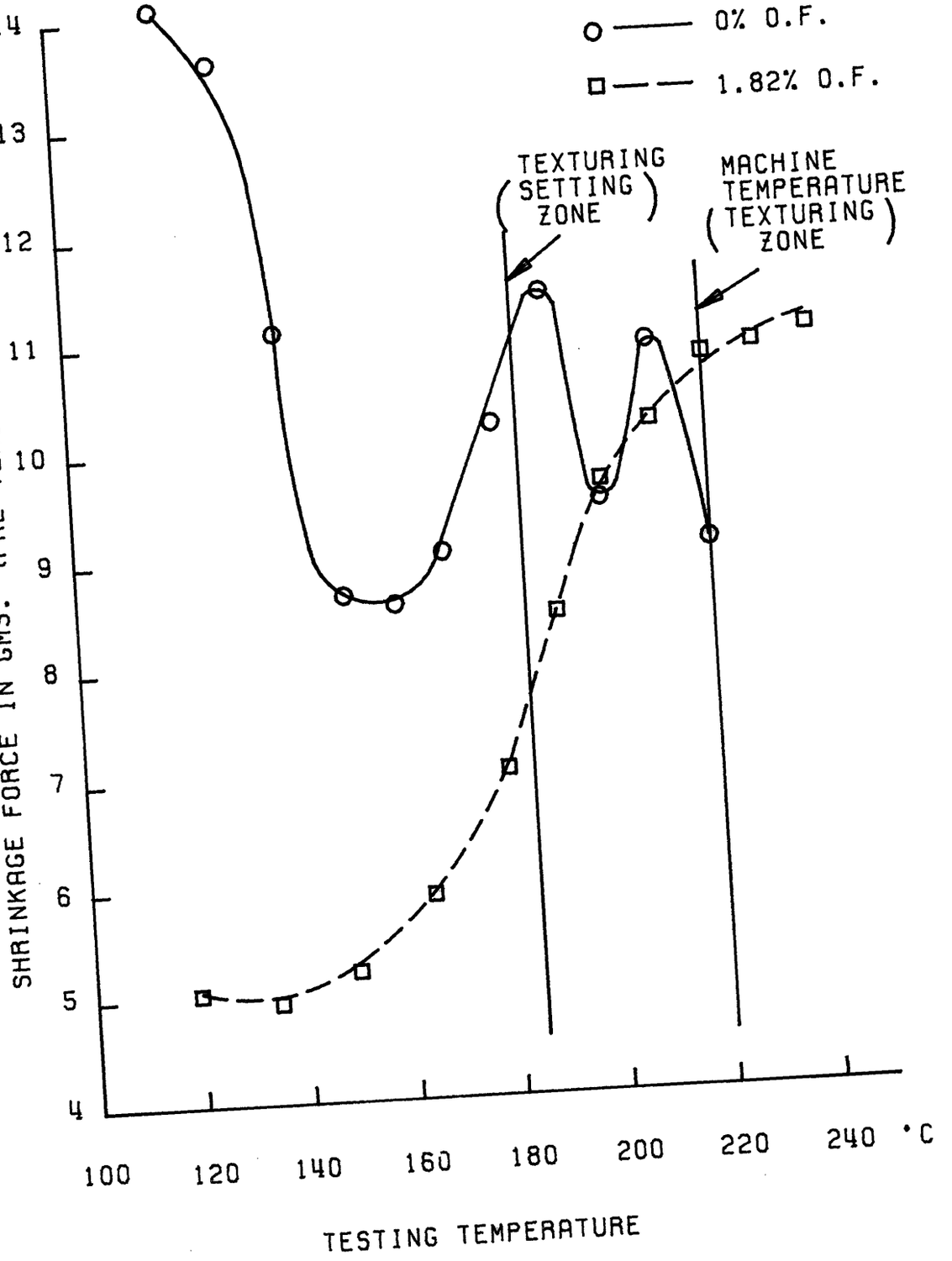

FIGURE 43: SHRINKAGE FORCE TESTING OF 150/34 POLYESTER YARN. (SAMPLE 10)

heater temperature. This test could provide a useful companion test to the continuous yarn contraction test to determine the cause of poor quality yarns.

The continuous yarn contraction measurement has been found to be an accurate predictor of yarn appearance in a knit and dyed FAK hoseleg, using a sample set of 13 yarns embodying variations in texturing machine settings.

The yarns were also continuously tested on the basis of shrinkage force as a function of temperature. The first zone of the instrument was bypassed and the heater was positioned in the yarn path between the second and third feeds as shown in Fig. 33b. The yarn was pulled off the package, tensioned to about 50 grams (150 denier), and fed into the second zone of the instrument. The yarn was conducted through the heater tube, over the second yarn force sensor, through the air to cool before exiting the zone. Either 0% or 1.8% overfeed was established in the second zone.

Figure 43 shows the shrinkage force as a function of temperature for sample 10 from the controlled variation yarns. This yarn had 1.5 TPI more twist than the control package, but the same primary and secondary texturing temperatures. At 0% overfeed, the shrinkage force drops rapidly as the yarn softens above T_g. The tension begins to increase as yarn shrinkage increases above 160°C and reaches a maximum near the temperature of the second texturing heater (190°C). The tension drops at 200°C and rises again

at 210°C, or very near the primary heater temperature of 220°C. No peaks are detected in the presence of a 1.8% overfeed. The smooth rise in shrinkage force with temperature above 150°C corresponds to increasing filament shrinkage. At 240°C the shrinkage force levels off at about 11 gms (or about 75 mgpd) as the melting point of the fiber is approached. The most rapid rise in shrinkage force at 1.8% overfeed is at 185°C. This temperature is also near the first peak in shrinkage force curve at 0% overfeed. It was felt that good discrimination between yarns should be possible at this temperature.

Figures 44 and 45 show the shrinkage force at 0% overfeed and at 1.8% overfeed as a function of texturing machine variations. The overall shrinkage forces are lower in Fig. 45 due to the 1.8% overfeed. In both figures, the shrinkage force is higher for yarns that have had lower primary or secondary heat treatments during texturing. This is due to lower relaxation of texturing stresses at these lower temperatures in the texturing machine. At zero overfeed, twist and draw ratio affect the shrinkage force more than heat history. At 1.8% overfeed, the heat history of the yarn is more important. No clear correlation can be made between the observed hoseleg appearance and the shrinkage force at this temperature and at these overfeeds.

D. Industrial Trials of the Instrument. Extensive testing of the instrument has shown the validity of predicting yarn appearance in fabric on the basis of yarn contraction and yarn

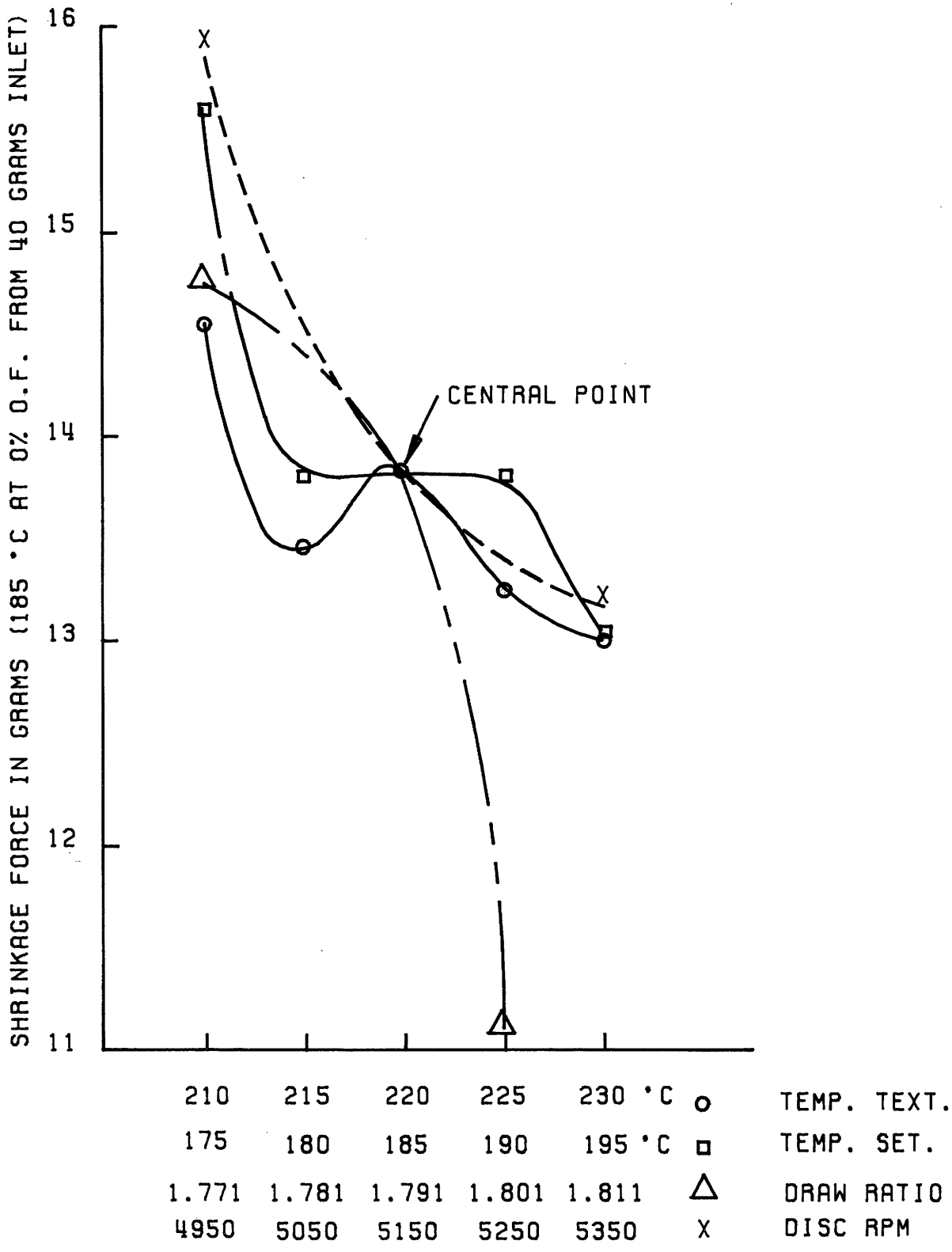

FIGURE 44: SHRINKAGE FORCE AT 0% OVERFEED AS A FUNCTION OF TEXTURING VARIABLES

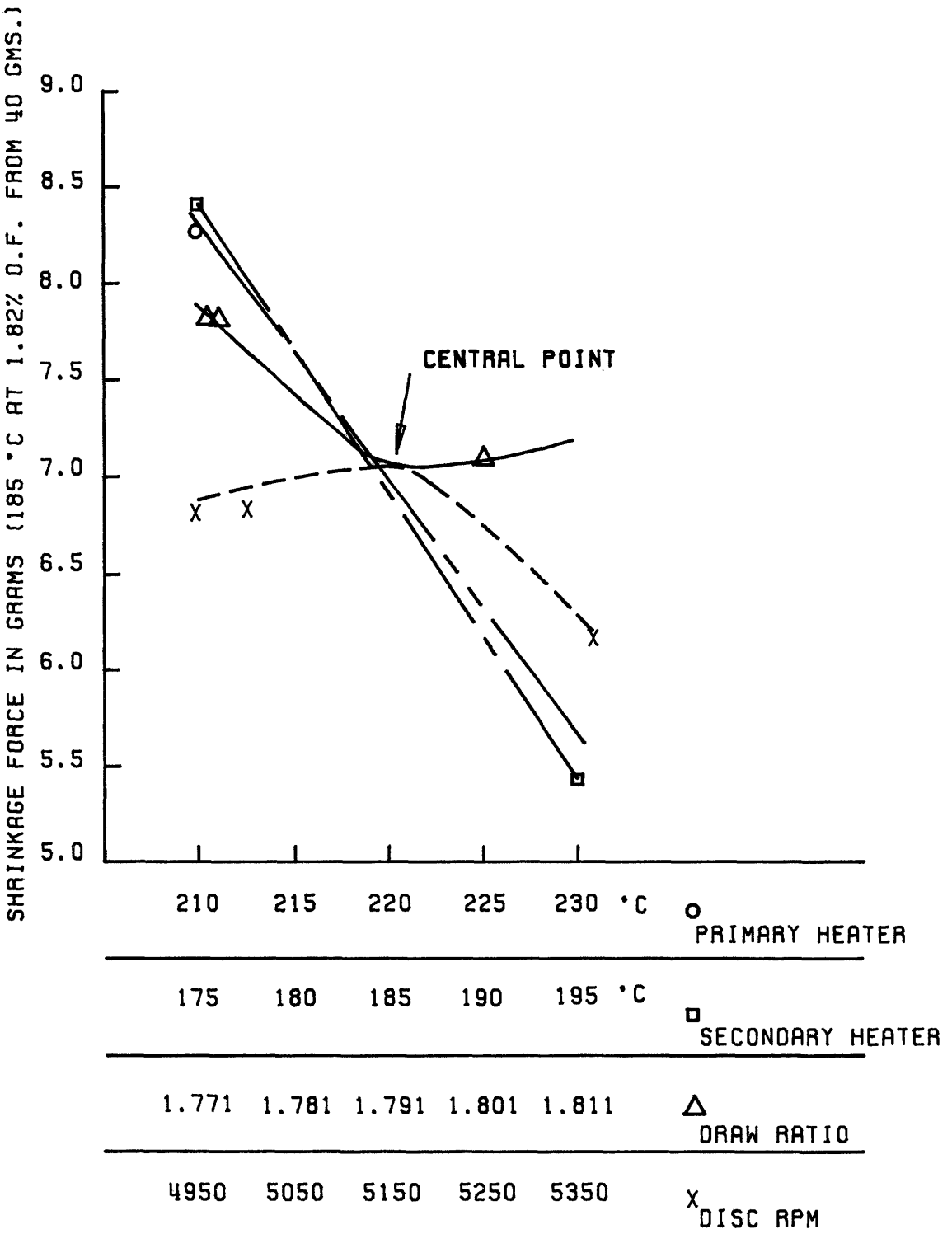

FIGURE 45: SHRINKAGE FORCE AS A FUNCTION OF PROCESSING VARIABLES

extension force. The information obtained from these tests is not the property of the author and cannot be included in this thesis. The summary of important results from these industrial trials of the device is contained in [134].

E. Recommendations for Industrial Use of the Instrument. The instrument developed here provides the basis for a fast turnaround method of grading textured yarn production with respect to its performance potential in fabric. The instrument, by virtue of its automatic handling of the textured yarn, gives a more consistent and accurate evaluation of the yarn than does the knit-dye-grade technique. To make full use of its capabilities, the instrument should be used to help establish stable running conditions for a given feed yarn lot and machine type. The inter-package variation, as measured by the standard deviation of a doff average, has been found to depend on the texturing process variables (especially primary heater temperature). Likewise, the intra-package variation will depend on process variables (especially PHT). Also, the intra-package variation will depend on the proper choice of operating conditions. The instrument provides a valuable tool for fine-tuning the texturing process to achieve uniformity from package to package, machine to machine, and within the packages.

The variation in properties within a textured yarn package can have two important consequences. First, if undetected

during inspection, variable yarns produce a "chatter" effect or intermittent single end barré in fabric. Second, if the period of variation is longer than the usual length of yarn sampled from each package for quality control, then any quality control scheme based on sampling will fail. During industrial trials, the yarns textured from certain feedlots showed high intra-package variation and could not be reliably graded by any method.

The next logical extension of quality control methods would involve preselecting feed yarn packages on the basis of their thermomechanical behavior. A suitable test might involve measuring the hot draw force at 150-210°C at the texturing draw ratio. Subsequent differences in drawn filament shrinkage or shrinkage force could also be used as a basis for selection. A simple measurement of boil-off shrinkage should provide some useful information about the fine structure and orientation of the feed yarn, or the drawn (without twist) feed yarn.

5. Summary.

The need for a rapid, continuous off-line quality control method for textured yarns was established in the first chapter. In this chapter, the development of such an instrument is chronicled. The development began with exploratory batch tests on textured yarns with known appearance differences in laboratory fabrics. The most promising of these tests were modified to form the basis of a prototype continuous testing instrument.

The continuous test methods recorded considerable

intra-yarn variability, thereby explaining the high scatter found in batch methods. Such intra-package variability was found to depend on surging (instability) in the texturing process, cyclic variations in winding on the feed of textured package, or variations in feed yarn denier and properties. Inter-package variations in (bulked) yarn extension force showed good correlation with fabric appearance variations, but were very oil sensitive.

To extend the data base, an improved version of the laboratory testing instrument was designed and constructed. The prototype production instrument was used to test many sets of yarns with known appearance or controlled texturing variations. Yarn contraction, and yarn extension force correlated well with yarn appearance in laboratory fabrics.

Industrial trials of the instrument proved its ability to predict accurately the appearance of textured yarns in commercial fabrics.

CHAPTER III

BEHAVIOR OF TEXTURED YARNS DURING CONTINUOUS THERMOMECHANICAL TREATMENT

The length change of a textured yarn during its passage through a continuous thermomechanical testing instrument has been found to correlate with the subsequent appearance of the yarn in fabric form. The response of the yarn to the treatment is measured on the basis of the final state of the yarn exiting the constant tension treatment zone. No information is provided on the transition states through which the yarn passes in arriving at the final state. Similarly, no information is available on the transition states of a yarn during the continuous setting operation on the texturing machine. It is the purpose of this chapter to report experimentally observed changes in yarn structure during continuous thermomechanical treatments and provide some insight into the physical basis for these changes.

1. The Black Box Approach to Continuous Thermomechanical Treatments.

Two types of continuous thermomechanical treatments are possible. In the first type, the contraction of the yarn is fixed and the temperature changed. Measurements of force are used to follow this process. In the second type, the load on the textured yarn is fixed while the temperature is changed. Measurements of length are employed to follow this

process. If the contraction in the former treatment and load in the latter treatment are adjusted properly, the two continuous treatments are equivalent.

We will discuss primarily the fixed contraction/fixed temperature treatment, since it has wide commercial application. The most important fixed contraction/fixed temperature thermomechanical treatment for textured yarns is the conventional second heater yarn-setting operation. This usually takes place in the second stage on the texturing machine.

Figure 46 shows the setting stage on a texturing machine. The machine settings are feed speeds (and their ratio) and heater temperature. The input to the system is an untwisted textured yarn which is straightened by the post twister tension in the texturing zone. The purpose of the setting operation is to reduce the stretchiness and torque liveliness of the as-textured yarn to a level consistent with subsequent use.

Several workers have published results relating the changes in setting zone operating parameters to changes in yarn properties. The most comprehensive examination of the output of the setting zone was conducted by Lunenschloss, Fischer, and Murata [140]. They examined the effect of changes in setting zone temperature, setting zone overfeed, and winding overfeed on yarn properties. Small changes were found in tenacity and strain at break, due to changes in setting zone conditions. The windup tension increased for

higher windup extension or lower setting zone overfeed. A small increase in winding tension was also produced at higher setting temperatures. The hardness of the wound package increased with winding tension, as expected.

The important, larger changes in crimp contraction, yarn (optical) thickness, and number of tight spots in the set textured yarn are shown in Fig. 47 as a function of setting zone variables. In the first column of graphs, the setting temperature was changed; in the second column, the overfeed was changed. The standard conditions during texturing were: temperature, 220°C; twist, 2300 TPM; speed, 130 m/min; overfeed, 1%. The yarn was 150 denier/34 filaments prior to the conventional texturing operation. The standard setting zone conditions were: overfeed, 15%; temperature 210°C.

In Fig. 47a,b,c,d, we note that crimp contraction, as measured by D.I.N. 53840, decreases for increasing setting zone temperature or decreasing setting zone overfeed. This is reasonable. At higher temperatures one would expect to reset the yarn more effectively to the geometry dictated by the zone overfeed. As the zone overfeed decreases, a geometry with less crimp is set in the yarn.

Figure 47e,f shows that measured yarn thickness is directly related to the crimp contraction. The most surprising result is the change in the number of tight spots in the yarn as shown in Fig. 47g,h. Most researchers have

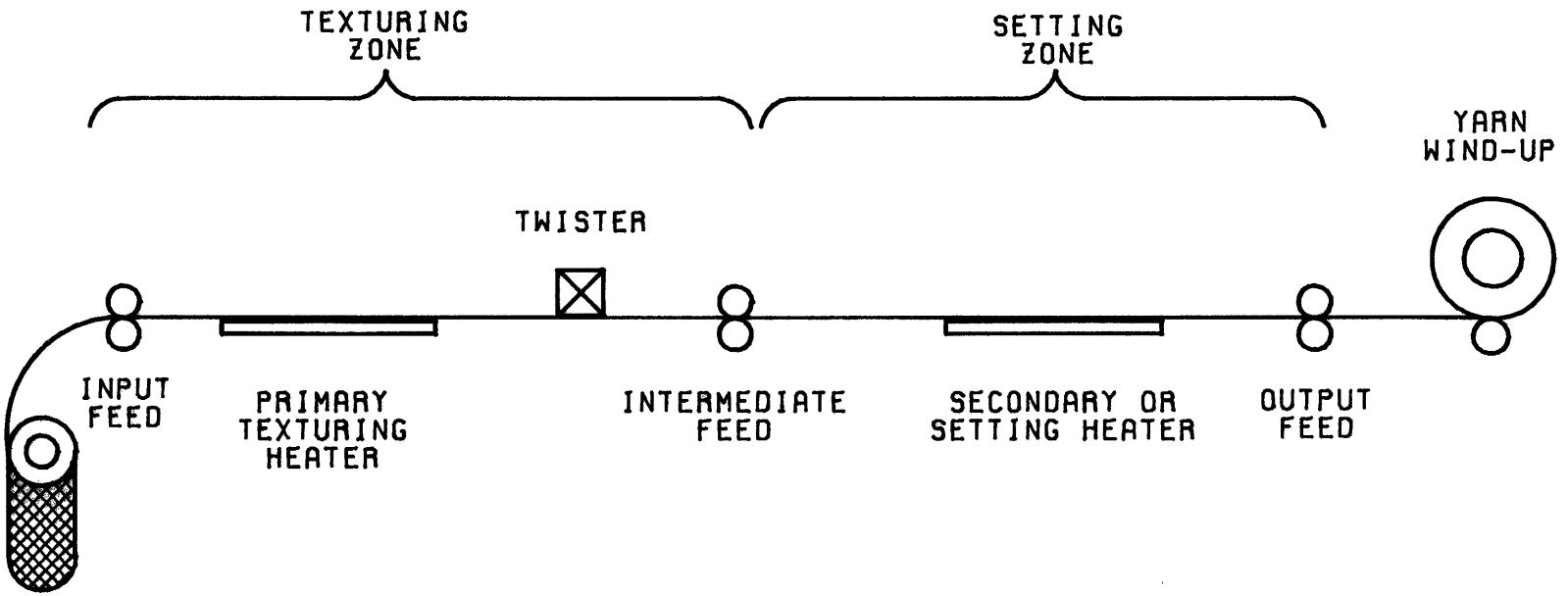

FIGURE 46: THE SET-TEXTURING PROCESS

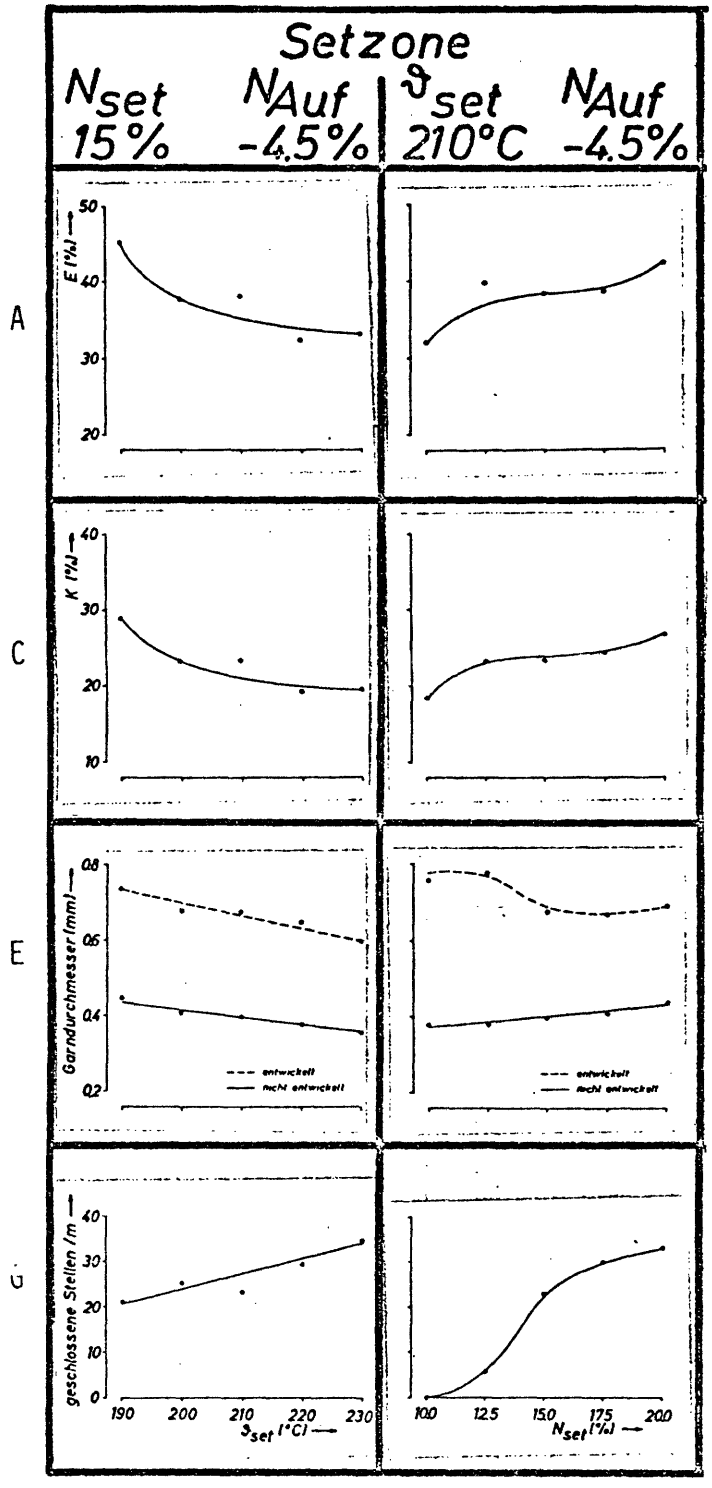

FIGURE 47. YARN PROPERTIES AS A FUNCTION OF SETTING CONDITIONS [140]

considered the formation of tight spots to be due to disturbances in the twist/velocity relationship in the texturing zone upstream of the setting zone. In these figures, Lunenschloss et al. show a strong dependence of tight spot frequency on both the setting zone temperature and overfeed. They make no explanation of the mechanism by which these tight spots are formed in a "twistless" setting process.

The results of Denton and Morris [137] are also of interest. They exposed 150/30 polyester yarns textured at 195°C to a continuous setting operation with varying temperature and time of heating. No reference is made to the setting zone overfeed used during these tests. The effectiveness of the setting operation in reducing yarn contraction (in hank form or in fabric form) and yarn torque liveliness (fabric spirality) is shown in Fig. 48a,b,c. Figure 48a shows that yarn contraction (measured after crimp development at 120°C at 5 mgpd for 5 minutes) decreases with setting temperature. A large increase in the reduction occurs as the setting temperature is raised above 180°C. This is probably close to the effective temperature of the crystallite network formed during texturing at 195°C. The yarn contraction also shows an exponential fall for heater residence times up to about 0.6 seconds for all temperatures.

Denton and Morris claimed earlier in their paper that this was the time required to bring the yarn to the heater temperature. For heating times beyond 0.6 seconds, the yarn

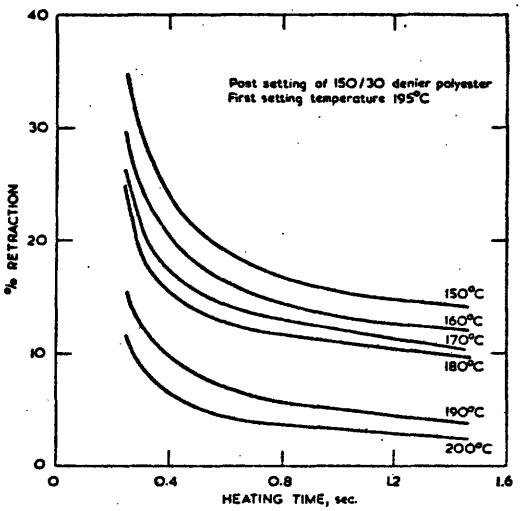

A *Post treatment; yarn retraction versus heating time at various second-heater temperatures*

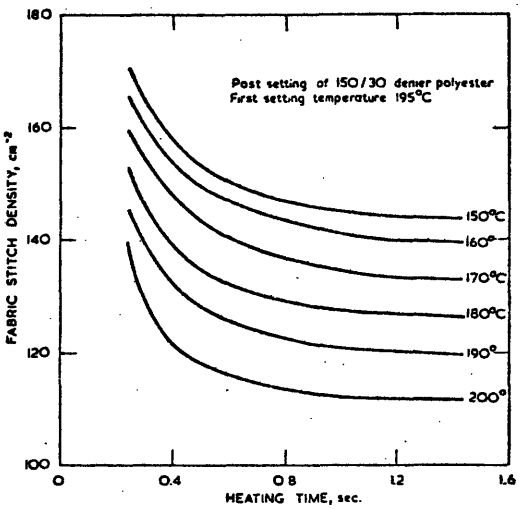

B *Post treatment; fabric stitch density for yarns post-set at various times and temperatures. Fabric stitch length 2·9 mm*

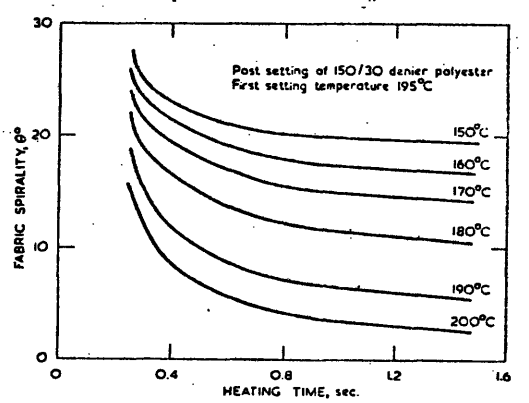

C *Post treatment; spirality of fabrics made from yarns post-set at various temperature and times*

FIGURE 48. YARN PROPERTIES AS A FUNCTION OF SETTING TIME AND TEMPERATURE [33]

contraction decreases much more slowly with time. Figure 48b and c shows the same kind of trends with temperature and heating time for the behavior of the yarn in fabric. Yarn contraction in fabric, as reflected by stitch density, decreases with higher setting temperatures or longer heating times. Yarn torque liveliness, as reflected in fabric spirality, is also reduced in a similar fashion.

These measurements of yarn properties after thermomechanical treatments are of considerable commercial importance, but they shed no light on the threadline parameters during treatment. Stein and Wallas [104,118] have made extensive measurements of the tension developed in a yarn during a continuous thermomechanical treatment on the DYNAFIL instrument. In the DYNAFIL, yarn is transported at a given overfeed through a heater (0.75 meters) and the tension is measured. The zone overfeed, yarn speed, and heater temperature can be changed to yield different testing conditions.

Figure 49 shows the force contraction behavior of two textured yarns. The solid line shows the force on a moving yarn measured in the DYNAFIL instrument. The yarn is exposed to 120°C temperature for 2.2 seconds at the test speed. At zero contraction the pretension of 25 gf is reduced to 15 gf by the softening action of the heater. Contraction serves to lower the threadline tension as expected. The other two curves are from static tests conducted on the Instron using

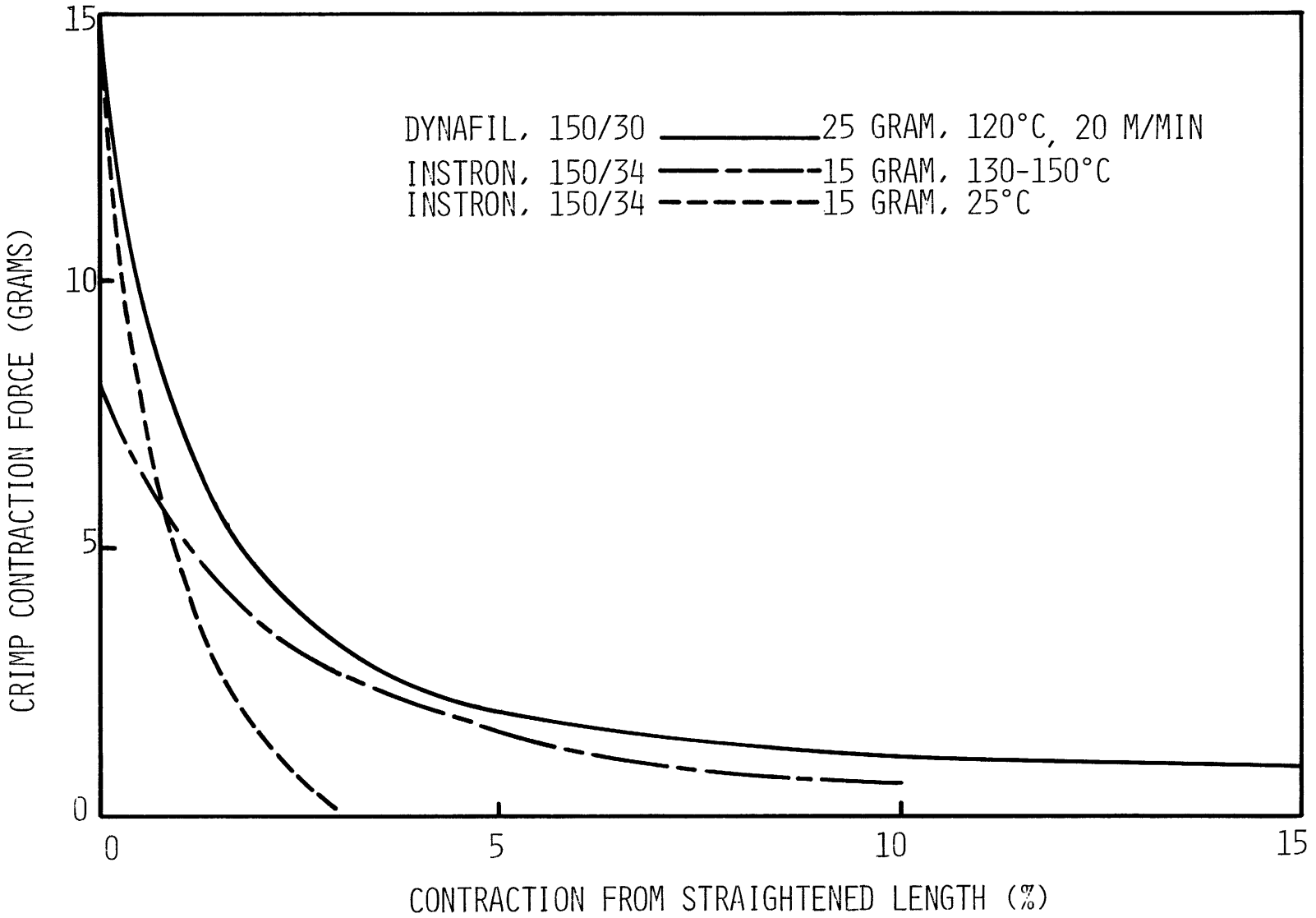

FIGURE 49. HOT CRIMP CONTRACTION FORCE OF POLYESTER YARNS [118A]

set textured yarn from shipment A. Heating the yarn at zero contraction lowers the force due to softening of the material, but at higher contractions the heat releases the latent crimp in the yarn which is reflected by an increase in the force at a given contraction. In character at least, the force/contraction curves measured dynamically on the DYNAFIL exhibit similar behavior to curves derived in static testing.

Figures 50 and 51 show a series of force curves obtained on the DYNAFIL at 5% overfeed from 25 gf pre-tension. The yarns were exposed to various testing temperatures and times depending on the machine speed. The yarn in Fig. 50 was previously set in an autoclave. Stretch yarn (unset) was used in Fig. 51. The curves in Fig. 50 show a similar shape for each heater temperature as residence time increases. There is an initial rise in force as crimp development occurs, which is followed by a decay in force as the structure responsible for crimp development is altered by the temperature and, finally, there is a rapid rise in force as the fine structure is melted and the underlying shrinkage force of the extended molecules is released.

The shapes of the force/residence time curves in Fig. 51 for the stretch yarn are different from those in Fig. 50 in that only a slight decay in force occurs after the rise in force associated with crimp development. This is because the "unset" yarn is also an "unrelaxed" yarn. At temperatures above T_g the temporary components of yarn set (e.g. quenched,

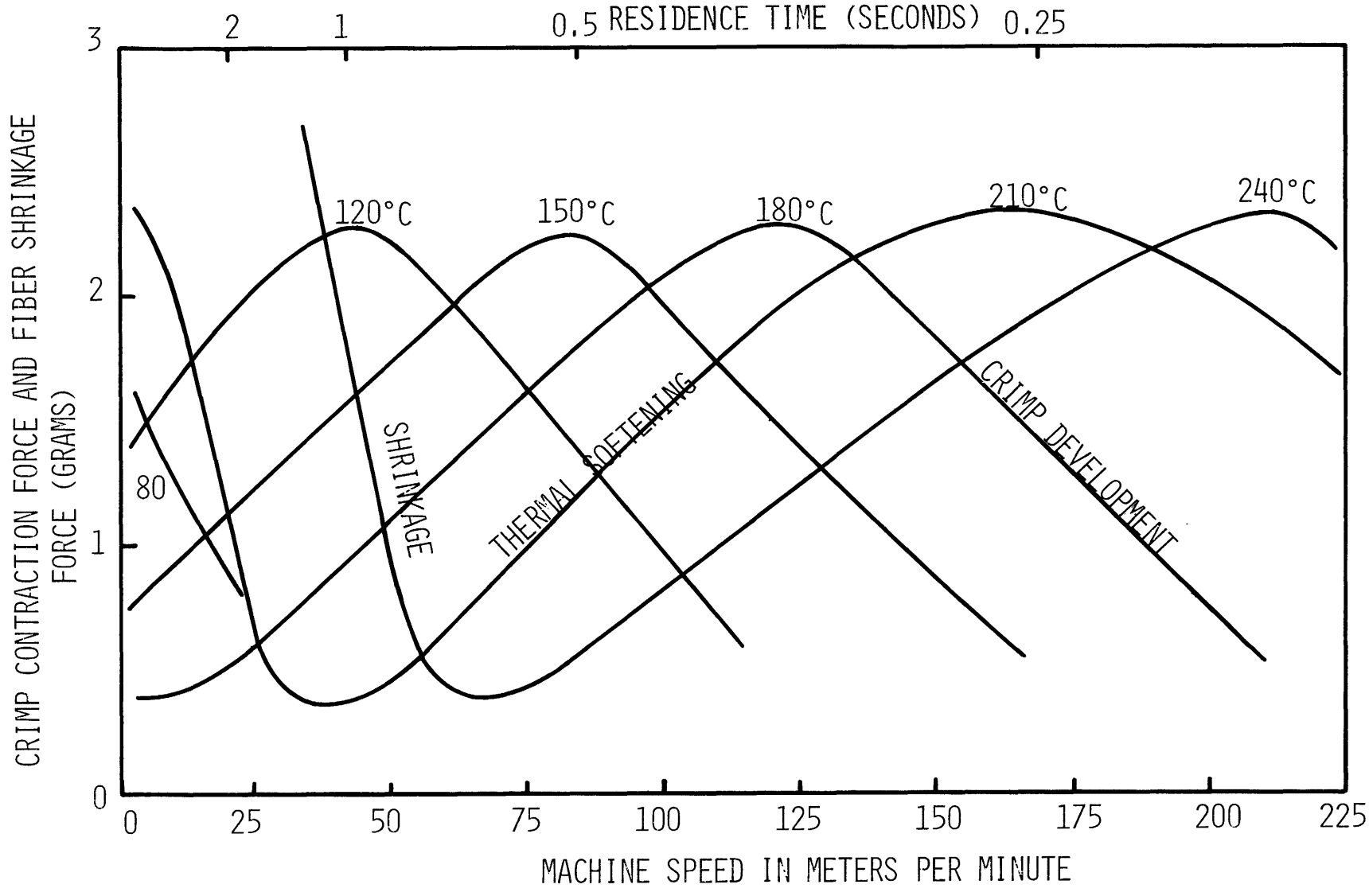

FIGURE 50. HOT YARN FORCE ON DYNAFIL (150/30PET, AUTOCLAVE SET, 5% O.F., 25 GRAM PRELOAD) [118A]

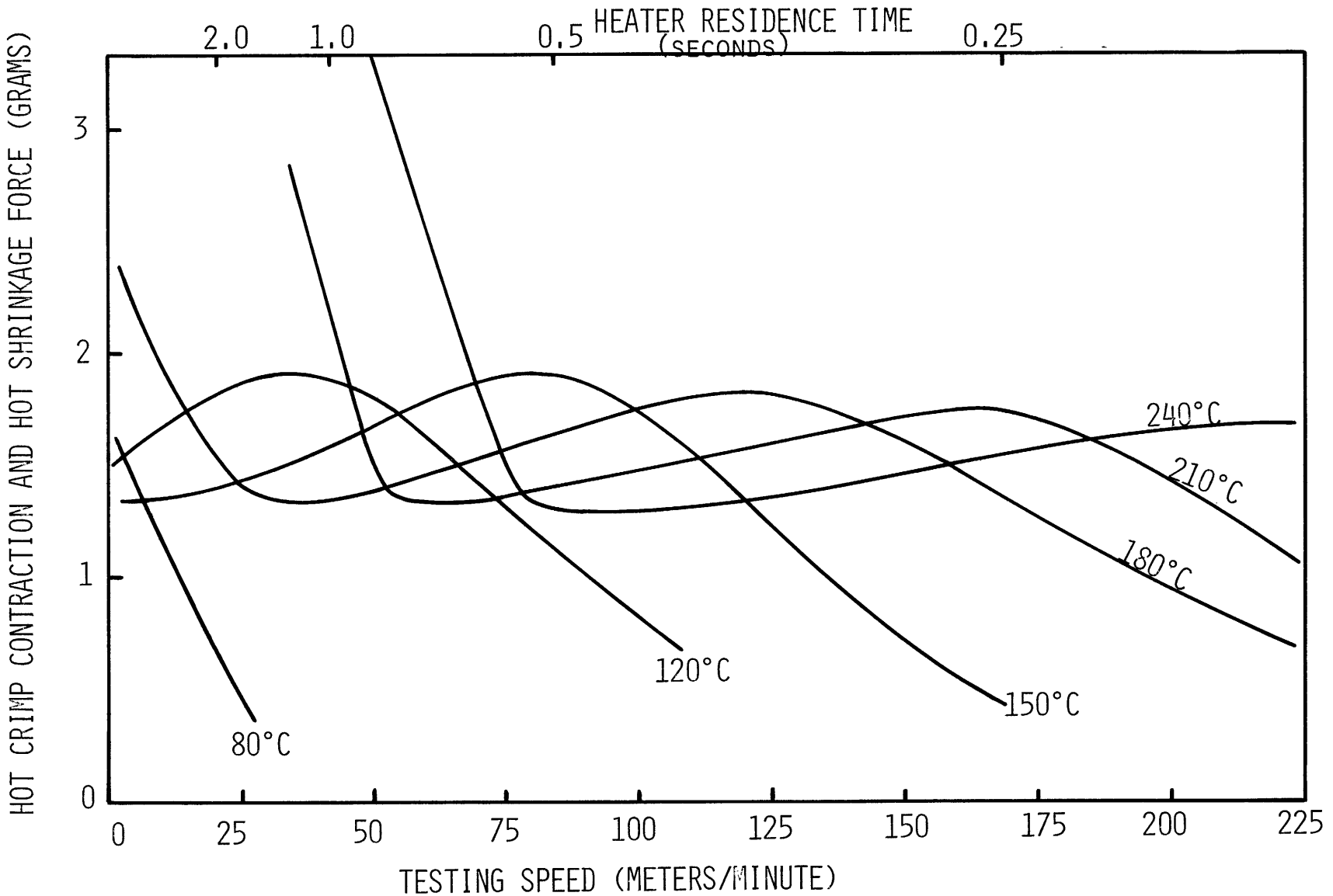

FIGURE 51. DYNAFIL TEST RESULTS ON A 150/30 PET STRETCH YARN (O.F. 5%, 25 GRAM PRE-TENSION, HEATER TEMPERATURE AS SHOWN) [118A]

extended chains) begin to exert shrinkage forces. These temporary components of set are usually lost during a high temperature (>150°C) setting operation (Hardegree & Buchanan [127]).For both yarns, the force remains fairly constant for residence times in the range of 1-10 seconds when the yarns are tested at 240-245°C.

One may take a different look at the data in Figs. 50 and 51 by replotting it as force versus heater temperature for constant heater residence time. Figures 52 and 53 are replots of the data in Figs. 50 and 51, respectively. The right hand curve in each figure is for a residence time of 0.25 seconds, or about the time allowed for setting on the texturing machine. The left hand curve is for a residence time equal to 2.5 seconds, or about the heater residence time on the testing instrument of Chapter II. The 2.5-second curve in Fig. 53 shows that shrinkage forces begin at 140°C in this stretch yarn and not until about 180°C in the set yarn of Fig. 52. This is in agreement with data reported by Hardegree. At 240°C the stretch yarn developed 8.9 gf, while the set yarn had 6.6 gf. The 0.25-second curves are similar in shape and temperature dependence for the two yarns, but the set yarn shows the highest force at about 210°C. Undoubtedly, the location of these curves depends not only on the response of the fiber fine structure to the temperature, but also on the heat transfer to the yarn. The residence time required to reach the peak tension was

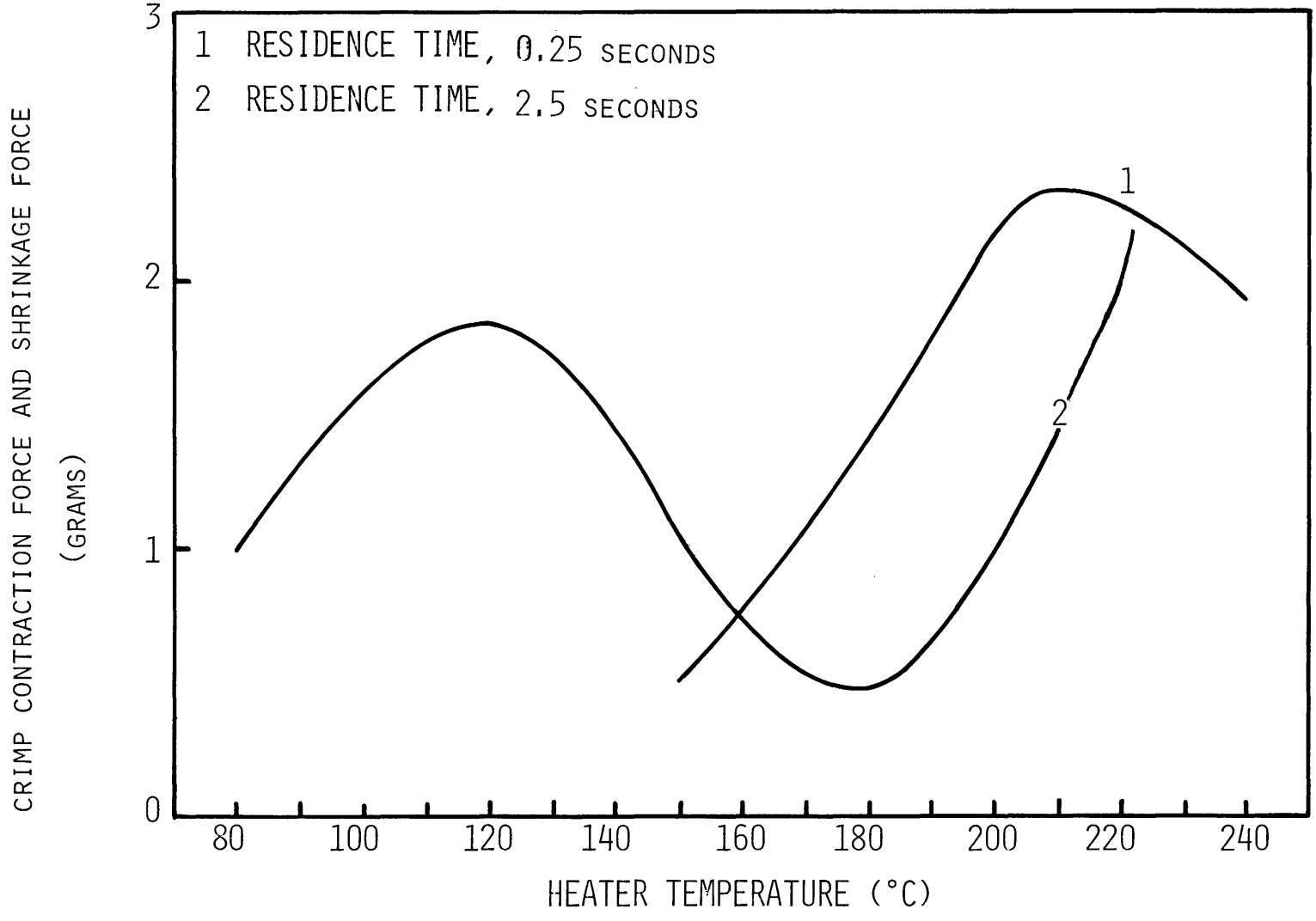

FIGURE 52. HOT YARN FORCE ON DYNAFIL (AS IN FIG. 50) [118A]

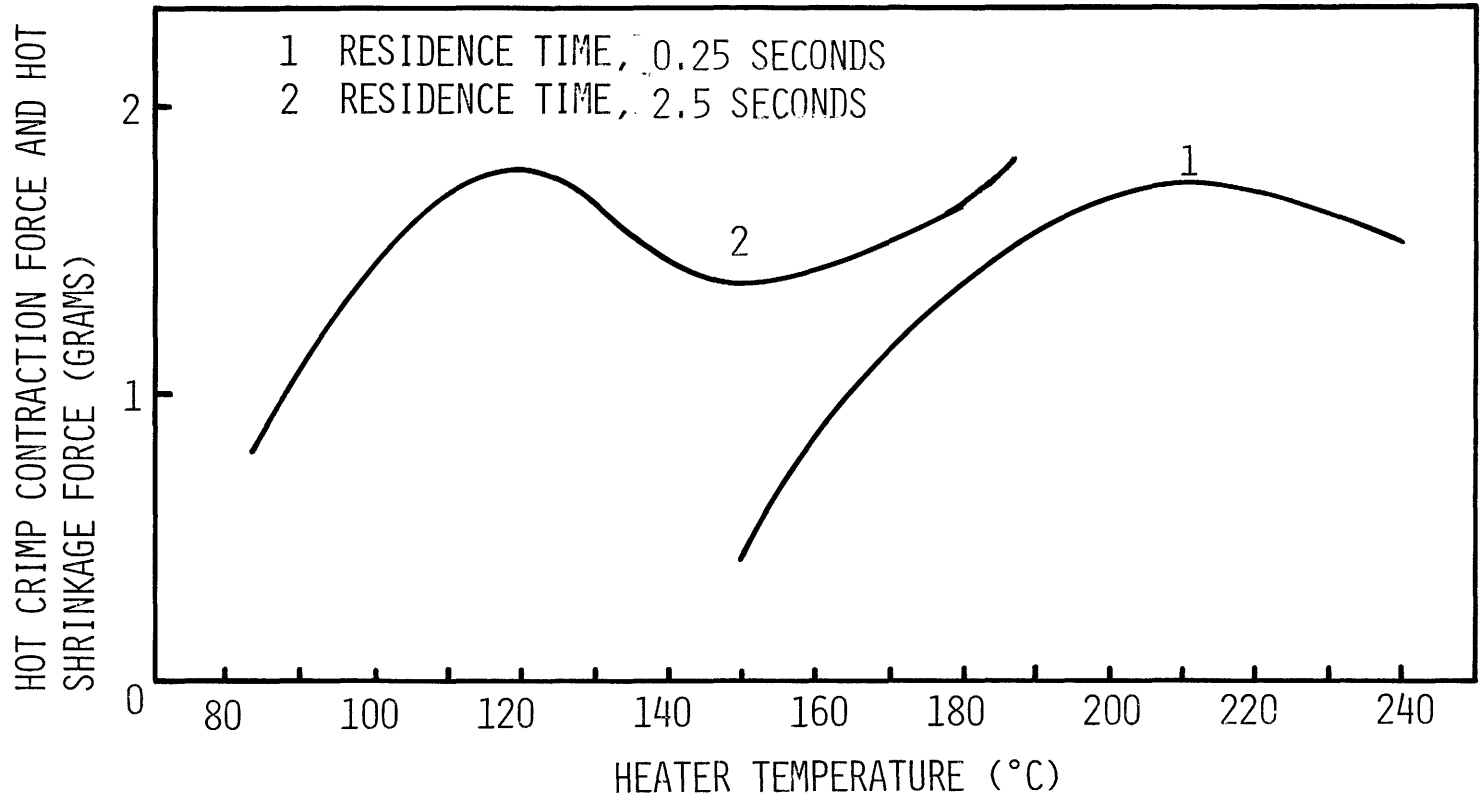

FIGURE 53. DYNAFIL TEST RESULTS ON 150/30 PET STRETCH YARN AS IN FIGURE 51 [118A]

found to have the following relationship to heater temperature:

time to peak tension (seconds) = 5.05 exp (-T/72.5)

for T in °C, r = .982.

This tension peak is not due to constant shrinkage. Ribnick's [145] relationship for time to constant shrinkage is of the form

$$t_s = \frac{C_1}{T} \exp\left(\frac{-C_2}{T}\right)$$

where C_1, C_2 are constants.

Nor can it be related to a constant temperature of the yarn. If the heat transfer coefficient is assumed to be independent of heater temperature, then the time for constant yarn temperature is of the form

$$t = -\tau \ln (1 - T_y/T)$$

where T_y is the constant yarn temperature, T is the DYNAFIL temperature minus yarn temperature, and τ is the time constant associated with heating.

Stein and Wallas [118] have also examined the effect of input yarn properties on measured threadline force during DYNAFIL testing. They selected the testing temperatures of 120°C and 245°C to focus on crimp contraction forces and shrinkage forces, respectively. Figures 54 and 55 show the separate effects of changes in primary texturing heater temperature (at two texturing overfeeds) and texturing machine twist have on crimp contraction force and shrinkage force.

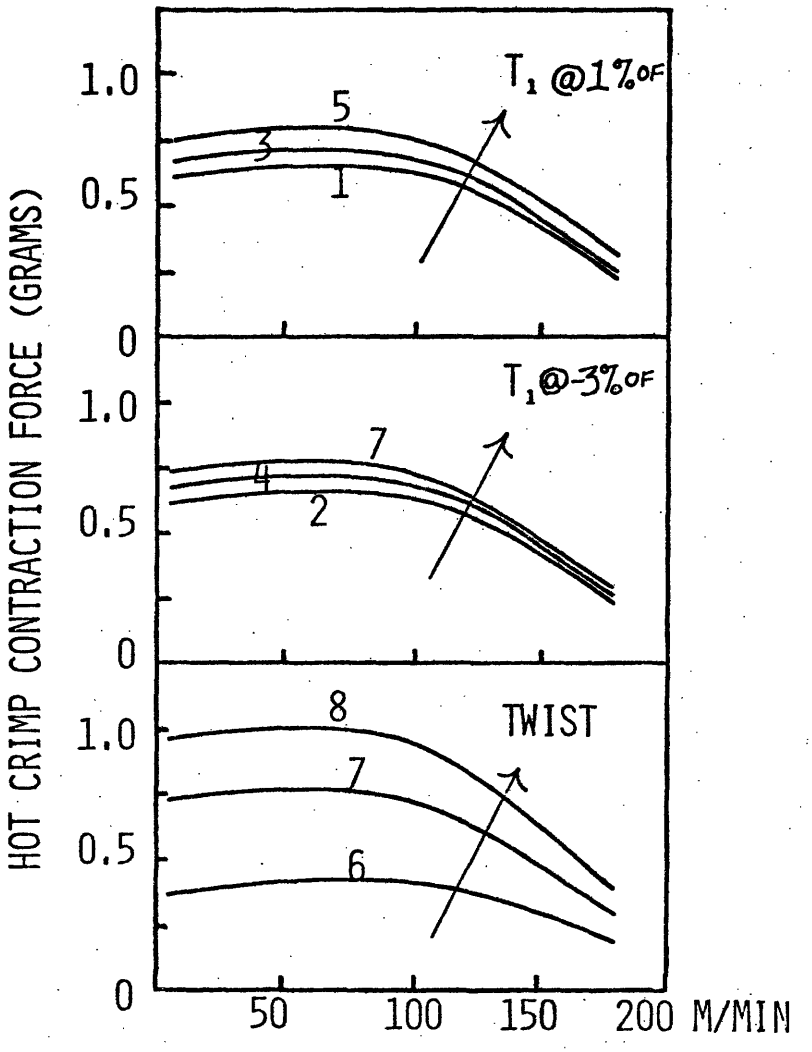

YARN	T_1(°C)	O.F. (%)	TWIST (TPM)
1	200	1	3100
2	200	-3	3100
3	215	1	3100
4	215	-3	3100
5	230	1	3100
6	230	-3	2400
7	230	-3	3100
8	230	-3	3700

FIGURE 54. CRIMP CONTRACTION FORCE OF A 70/24 PET STRETCH YARN AS A FUNCTION OF TEXTURING CONDITIONS (5%, 120°C, 12.5G). [118A]

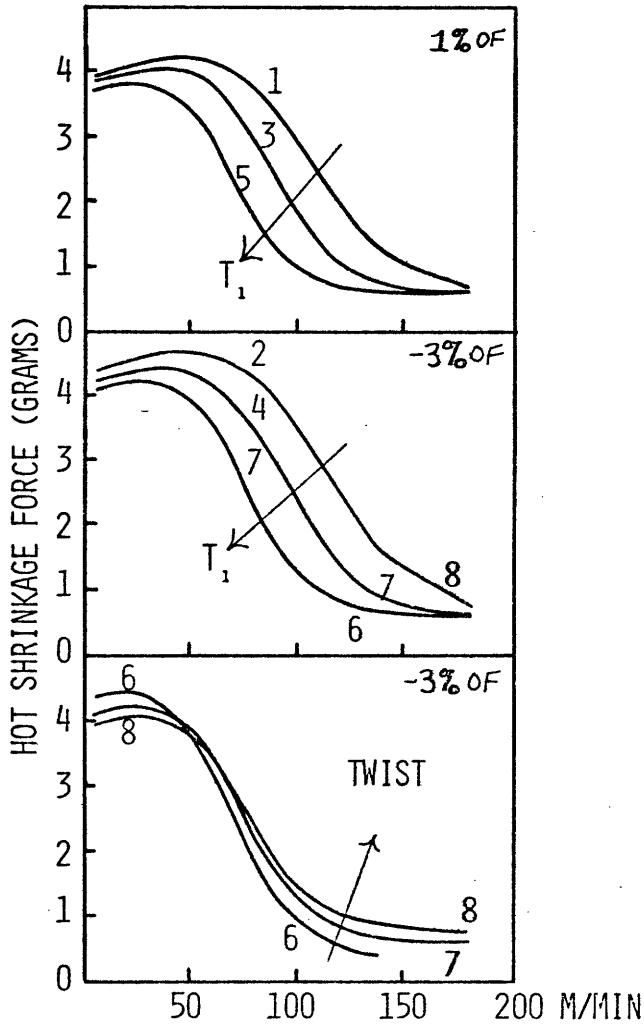

YARN	T_1 (°C)	O.F.(%)	TWIST (TPM)
1	200	1	3100
2	200	-3	3100
3	215	1	3100
4	215	-3	3100
5	230	1	3100
6	230	-3	2400
7	230	-3	3100
8	230	-3	3700

FIGURE 55. HOT SHRINKAGE FORCE OF 70/24 PET STRETCH YARN AS A FUNCTION OF TEXTURING. (DYNAFIL CONDITIONS: 5% O.F., 245°C, 12.5 GRAMS) [118A]

As seen in Fig. 54, relatively minor increases in crimp contraction force are recorded for a 30°C increase in primary heater temperature at either 1 or -3% texturing overfeed. On the other hand, twist changes from 65 to 93 TPI produce large increases in crimp contraction force as expected for such an enormous change in twist. At the higher testing temperatures used in Fig. 55, the trend is reversed for changes in primary heater temperature. The yarns textured at lower temperature show higher shrinkage forces at both texturing overfeeds. The differences in yarn force due to twist differences that were so obvious for crimp contraction force measurements all but disappear for shrinkage force measurements. The high temperature measurements are a reflection of the temperature stability of the crystallite network developed during texturing, while the low temperature measurements focus on the geometry of the fibers during primary heating of the texturing process.

Figures 56 and 57 show crimp contraction force and shrinkage force dependence on texturing variables for <u>set</u> yarns. Figure 56 shows that crimp contraction force will decrease as the temperature of the setting zone heater on the texturing machine is increased. This is in keeping with Figs. 50 and 51. The crimp contraction force also increases dramatically for a change in twist from 45-60 TPI. Maximum differences between yarns are seen at about 1 sec (45 meter/min) heater residence time in the DYNAFIL.

FIGURE 56. HOT CRIMP CONTRACTION AS A FUNCTION OF TEXTURING CONDITIONS IN 150/30 PET SET YARN. (DYNAFIL CONDITIONS WERE: 5% O.F., 120°C, 25 GRAMS) [118A]

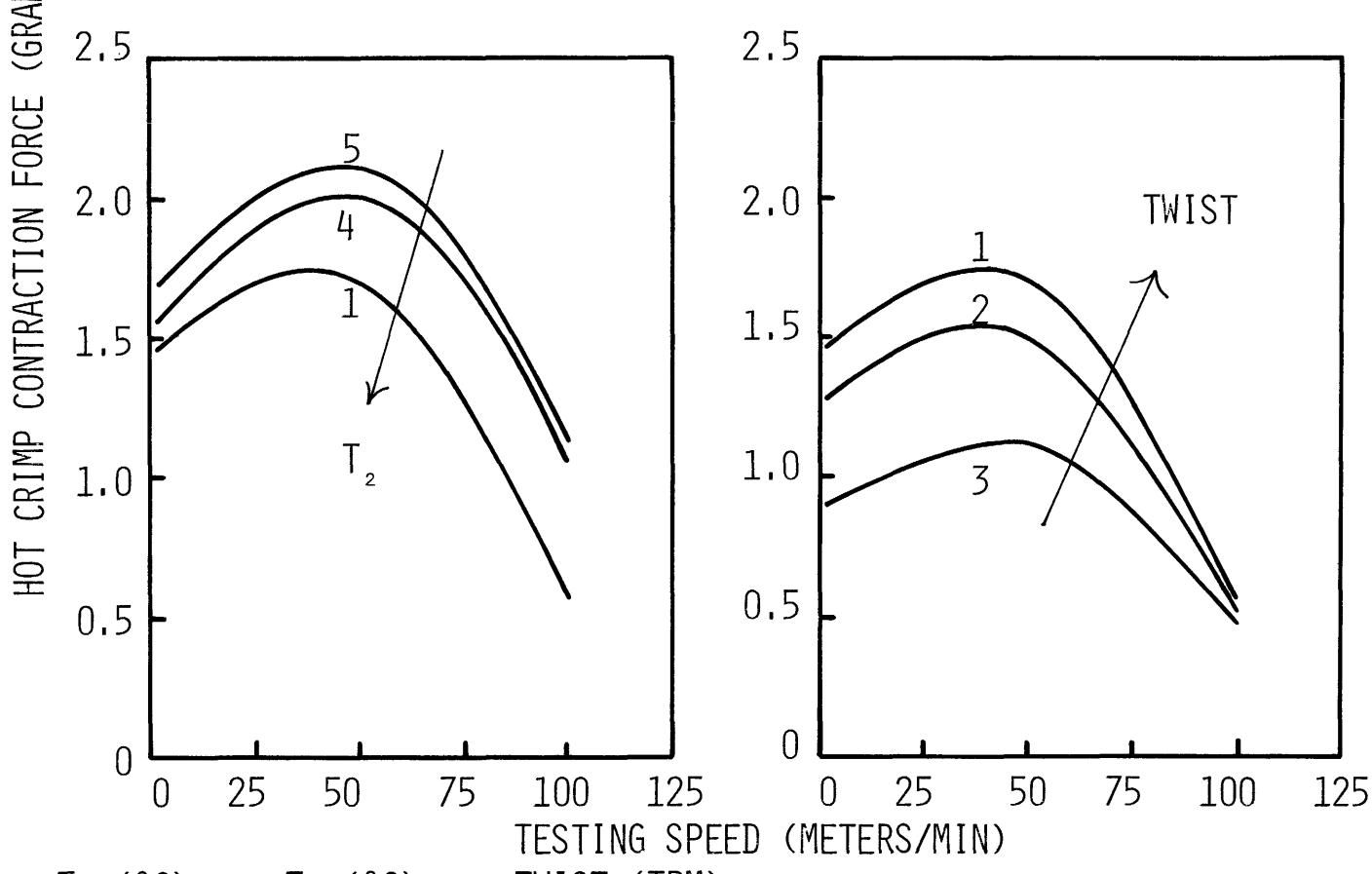

YARN	T_1 (°C)	T_2 (°C)	TWIST (TPM)
1	220	215	2400
2	220	215	2100
3	220	215	1800
4	220	205	2400
5	220	195	2400

In Fig. 57, the effect of changing the relative level of primary heater to secondary heater during texturing on the shrinkage force is shown. The curves 4, 1, and 5 show that shrinkage force has similar time dependence for changes in secondary heater temperature. The shrinkage force increases for lower secondary heater temperatures. Yarns set at lower temperatures retain more of the temporary stress components from the texturing operation. When the primary heater temperature is raised with respect to the secondary heater temperature, reversals in the shrinkage force ranking occur between curves 1 and 2, as the residence time is changed. The yarn textured at 220/190°C has the lowest shrinkage force reflecting the higher thermal stability of its fine structure.

Stein and Wallas [104] report the threadline forces at 120°C and 245°C and 5% overfeed for a yarn with deliberately created faults. The yarn was momentarily lifted off the texturing heater, thus creating gross differences in thermal history within a single yarn package. When tested at the low temperature, the faulty regions in the yarn produced lower tension, consistent with less crimp development. At the higher temperature these same faulty regions produced much higher shrinkage forces than the normal yarn. These higher forces are consistent with lower thermal stability of the fine structure.

Table 15 summarizes the trends in DYNAFIL testing as determined by changes in texturing conditions of the tested

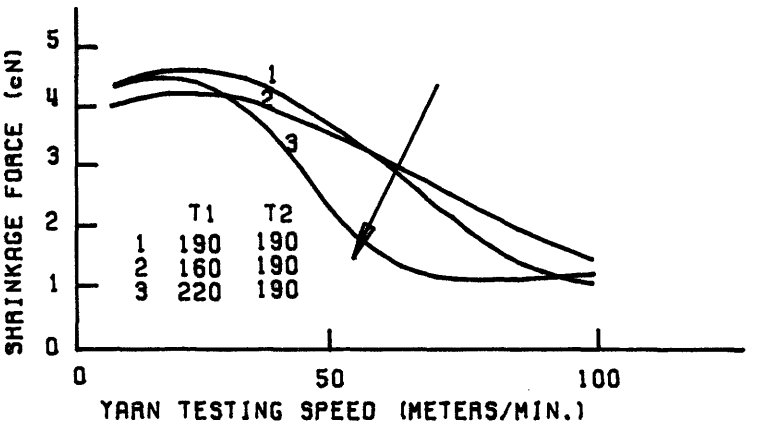

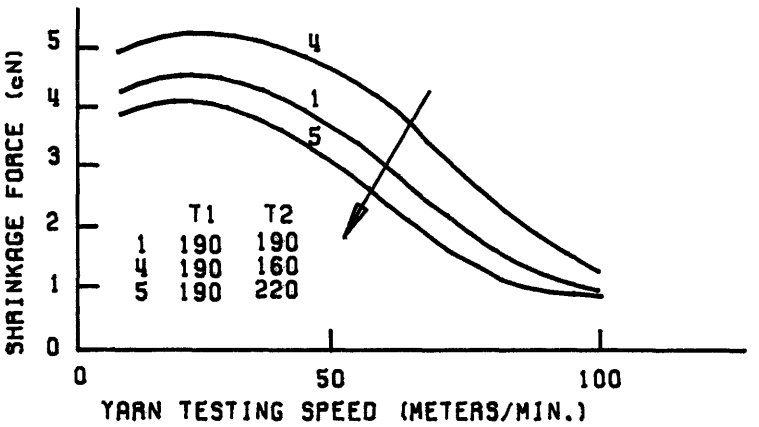

FIGURE 57: SHRINKAGE FORCE OF A SET TEXTURED YARN. (150/32, PET, 5% O.F., 245°C, 25 cN PRETENSION)

TABLE 15. DYNAFIL RESULTS

Change in Texturing Machine Settings						Change in Yarn Force during Continuous Thermo-mechanical Treatment *		
Twist	T_1	T_2	O.F.	F @ 120°C**	Reason for Change	@ 245°C***	Reason for Change
↑	---	---	---	↑	More crimp	---	No change in fine structure
---	↑	---	---	↑	More permanent set	↓	More stable fine structure
---	---	---	↑	---	Temporary orientation is lost in T_2	↓	More stable fine structure and less extended chains
---	---	↑	---	↓	Less crimp	↓	More previous relaxation of shrinkage forces

* @ 5% O.F. from .15 gpd pretension, heater residence 0.5-1.0 sec.

** Data in Figures 54,56.

*** Data in Figures 55,57.

yarns. The low temperature yarn forces during the setting operation are seen to depend primarily on the yarn crimp. The yarn forces at high temperature are dependent on the thermal stability of the fiber fine structure and the original orientation of the fiber locked in by the crystallites.

2. Predicted Behavior of a Textured Yarn during Continuous Thermomechanical Treatments.

The setting zone exposes a textured yarn to contraction and heat. The responses of the yarn to these conditions can be predicted on the basis of continuity relationships, compatibility relationships, force and torque balances, and yarn constitutive relationships. The magnitudes of yarn contraction, yarn twist, filament shrinkage, and filament crimp are the important yarn responses. The level of threadline tension and torque are also of interest. In the absence of a heater, the yarn will (within limits) contract to the level dictated by the zone overfeed. When a central part of the yarn in the setting zone is heated, four distinct sub-zones will exist (i.e. the cold (entering) yarn, the warm yarn, the hot yarn, and the cooled (exit) yarn). These sub-zones are shown in Fig. 58.

D_i = denier = mass/unit length of yarn

V_i = velocity of yarn = length/unit time

S_i = L_i/L_0 = relative length of filaments after shrinking

CC_i = $Lyarn_i/Lfilaments_0$ = relative length of yarn after crimping

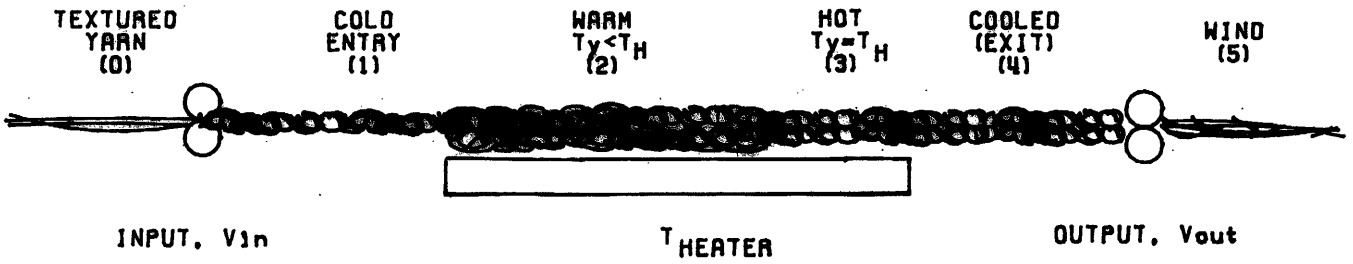

$$\text{ZONE OVERFEED} = \left(\frac{Vin}{Vout} - 1\right) \times 100\%$$

$$\text{ZONE CONTRACTION} = \frac{Vout}{Vin} \times 100\%$$

FIGURE 58: THE SUB-ZONES WITHIN THE SETTING ZONE

TC_i = $Lyarn_i/Lfilaments_0$ = relative length of yarn after twisting

ω_i = yarn rotational speed = (turns/unit time)

θ_i = yarn twist (real) = (turns/unit twisted length)

P_i = yarn tension = force

M_i = yarn torque = force x length

(ρA) = sum of (density x cross sectional area) of filaments entering the setting zone

where i = the sub-zone as defined in Fig. 58.

A. Conservation Relationships. Three conservation relationships apply to the operation of the zone, namely, mass, length, and turns. These relationships are merely a statement of the amount of mass, length, or number of turns within a fixed control volume as a function of time. The control volumes are most conveniently placed around the transition points between subzones.

The following form of the conservation equation will apply for a control volume:

Rate of change of quantity in control volume = $\frac{\partial}{\partial t}(Y)$ =

$$= \dot{Y}_{in} - \dot{Y}_{out} + \dot{Y}_{\substack{\text{added} \\ \text{externally}}}$$

where Y is quantity.

For steady state operation, the rate of change of the quantity in the control volume is zero by definition. For mass and length, the conservation relationships yield the following relationships using the subscript notation from

Figure 58:

$$(1)\quad V_0D_0 = V_1D_1 = V_2D_2 = V_3D_3 = V_4D_4 \quad \text{(mass)}$$

$$(2)\quad \frac{V_0}{S_0CC_0TC_0} = \frac{V_1}{S_1CC_1TC_1} = \frac{V_2}{S_2CC_2TC_2} = \frac{V_3}{S_3CC_3TC_3} =$$

$$= \frac{V_4}{S_4CC_4TC_4} \quad \text{(filament length)}$$

These two equations can be made identical by multiplying (2) by $(\rho A)_0$, since $D_i = (\rho A)/S_iCC_iTC_i$. The local denier divided by a constant value of (ρA) for the entering filaments is related to the local yarn length compared to the entering filament length as:

$$\frac{D_i}{(\rho A)} = \frac{1}{S_iCC_iTC_i} = \frac{\text{Lfilament}_0}{\text{Lyarn local.}}$$

The turns conservation relationship requires more careful treatment. A general control volume is shown in Fig. 59 for the turns balance. It is possible to have local twist levels that are not related to the local threadline rotational and translational speeds by the relation, $\theta = \omega/V$. This occurs whenever the yarn entering the process has been previously twisted. The previous twist then propagates through the process and is added as a constant to the twist changes produced by threadline rotations and contractions. The θ_0 term in the following turns balance relation represents real twist entering the setting zone:

$$(3)\quad \theta_0V_0 - \theta_1V_1 + (\omega_1-\omega_0) = \theta_1V_1 - \theta_2V_2 + (\omega_2-\omega_1) =$$

$$= \theta_2V_2 - \theta_3V_3 + (\omega_3-\omega_2) = \theta_3V_3 - \theta_4V_4 + (\omega_4-\omega_3) = 0$$

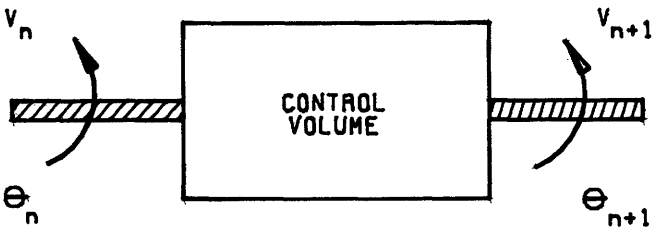

$$0 = \left(\frac{\delta \text{TURNS}}{\delta t}\right)_{C.V.} = \Theta_n V_n - \Theta_{n+1} V_{n+1} + \left(\frac{\omega_{n+1} - \omega_n}{\quad}\right)$$

FIGURE 59: TURNS CONSERVATION FROM ONE ZONE TO ANOTHER ZONE IN SETTING OPERATION.

By substituting in the known values at the entrance and exit of the zone, namely:

(1) $V_0 = V_{in}$

(2) $V_4 = V_{out}$

(3) $\theta_0 = 0$

(4) $\omega_0 = 0$

(5) $\omega_4 = 0$

(6) $D_0 = D$

we can conclude that:

(1) $\theta_4 = \theta_0 = 0$

(2) $D_4 = (V_{in}/V_{out})D = (O.F. + 1)D$

(3) $(O.F. + 1)D/\rho A = D_4/(\rho A) = 1/S_4CC_4TC_4 =$

$= 1/S_4CC_4 =$ length

since $\theta_4 = 0$.

Thus, at steady-state the exiting twist will equal the entering twist. Any twist that appears in the process will be of a temporary nature as in the false-twist texturing process. The yarn contraction in the cooled exit zone will equal the overfeed and be composed of filament length contractions due to shrinkage and crimp.

B. Equilibrium Considerations. The force and torque equilibrium equations for the setting sub-zones can be stated very simply:

$P_1 = P_2 = P_3 = P_4$.

$M_1 = M_2 = M_3 = M_4$.

We may consider the tension (P_0) and torque (M_0) of the entering yarn to be known. Once the yarn enters the setting zone, different levels of tension and torque will be established and these will remain constant as the yarn is heated and cooled. However, the constitutive relations for the yarn, i.e. the yarn torque and tension as a function of yarn contraction and twist, are expected to be a strong function of the time-temperature-stress history of the partially crystalline polymer.

C. Constitutive Relations for Textured Yarns. To gain at least a preliminary feeling for the complicated constitutive relations of the real textured yarn, we will consider Konopasek's treatment of the collapse of a single textured filament with a helical stress-free geometry from an untwisted straightened state [93]. The stress-free geometry of the filament was determined by the twist in yarn during texturing

$$\theta_0 = \frac{\tan\phi_0}{2R}$$

where θ_0 = twist set in yarn during texturing,

ϕ_0 = the helix angle of the filament,

R_0 = the radial location of the filament in the yarn.

Two parameters are sufficient to describe the three-dimensional path of a helix. Instead of ϕ_0 and R_0, the curvature and physical torsion of the filament axis may be used to define the helix.

$$p_0 = \frac{\sin^2\phi_0}{R_0} = \text{curvature of filament axis}$$

$$r_0 = \frac{\sin\phi_0\cos\phi_0}{R_0} = \text{torsion of the filament axis.}$$

During untwisting in the texturing operation, the curvature and torsion of the filaments are removed. Bending moments and torsional moments are required to maintain this deformation. By the Euler-Bernoulli equations for large deflections of slender members, we have

$$M_B = -EI_{p_0}$$

and

$$M_t = -GI_p r_0$$

The filament will contract into two helical segments joined by a torsional infection point (reversal point), if no end rotations are allowed during contraction. An equal number of coils develops in each helix. One helix has the same direction of twist as the original helix (equi-helix). The other helix is reversed in direction. The helix angle and filament helix radius are different for the reversed and equi-helix. The geometry is shown in Fig. 60 from [141]. We can calculate the curvature and torsion of the filament axes in the two helices as follows:

$$p_1 = \frac{\sin^2\phi_1}{R_1} \qquad r_1 = \frac{\sin\phi_1\cos\phi_1}{R_1}$$

$$p_2 = \frac{\sin^2\phi_2}{R_2} \qquad r_2 = \frac{\sin\phi_2\cos\phi_2}{R2}$$

where 1 is the reversed and 2 is the equi-helix.

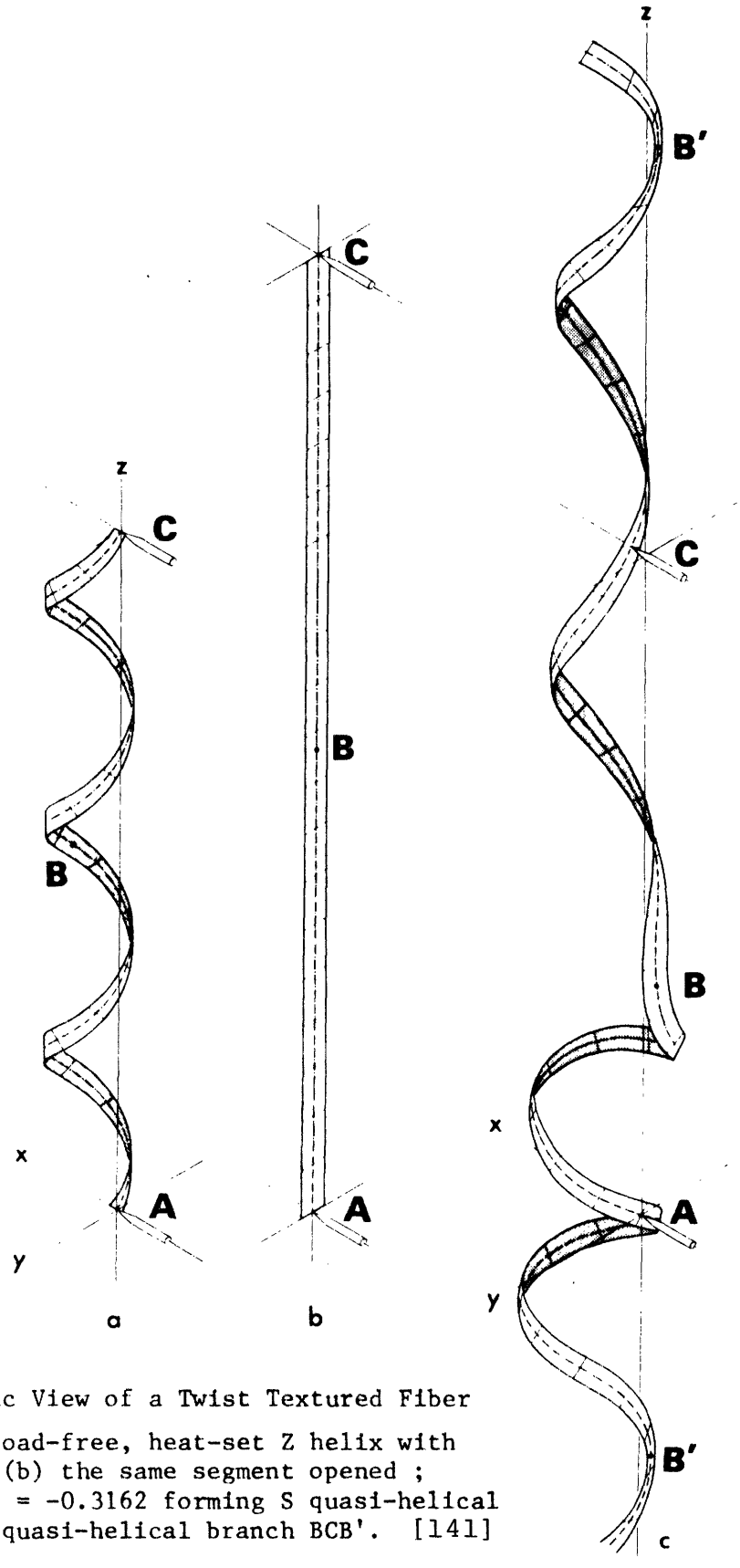

Fig. 60. Isometric View of a Twist Textured Fiber

(a) Segment of a load-free, heat-set Z helix with helix angle 45° ; (b) the same segment opened ; (c) collapsed to $\varepsilon = -0.3162$ forming S quasi-helical branch B'AB and Z quasi-helical branch BCB'. [141]

At any contraction level the two coils must be in tension and torque equilibrium with each other. Expressions for this equilibrium in terms of P, the threadline tension, and M, the threadline torque are given by Konopasek using the Euler-Bernoulli assumptions:

$$P \sin\phi_1 = GI_p p_1 (r_1 - r_0) - EI(p_1 - p_0)$$

$$P \sin\phi_2 = GI_p p_2 (r_2 - r_0) - EI(p_2 - p_0)$$

$$M = EI(p_1 - p_0)\sin\phi_1 + GI_p (r_1 - r_0)\cos\phi_1$$

$$M = EI(p_2 - p_0)\sin\phi_2 + GI_p (r_2 - r_0)\cos\phi_2$$

The length of filament in each helix can be computed:

$$L_1 = 2\pi R_1 / |\sin\phi_1|$$

$$L_2 = 2\pi R_2 / |\sin\phi_2|$$

or

$$\frac{\sin\phi_1}{\sin\phi_2} = -\lambda \frac{p_1}{p_2}$$

where

$$\lambda = L_1 / L_2 .$$

This point has been reached by several investigators [91,92,93,53]. We have 10 unknowns of interest, i.e. r_1, r_2, p_1, p_2, ϕ_1, ϕ_2, R_1, R_2, P,M, but only nine equations, i.e. 2 force equilibrium equations, 2 moment equilibrium equations, 4 equations to define the helical constraints on the filament geometry, 1 equation to assure length conservation. An additional assumption is usually made at this point. Tayebi [53] chose $R_1 = R_2$ on the basis of experimental observations. The author confirmed the apparent validity of this for polyester

monofilaments heat set at high helix angles (c. 80°). Konopasek [93], on the other hand, uses the assumption that equal lengths of filament are in each helix, or $\lambda = 1$.

As he points out, the reversal point occurs initially at the center of the span due to symmetry. However, the requirement for equal numbers of coils in the two helices demands that the reversal point move along the fiber causing $L_1 \neq L_2$, or $\lambda \neq 1$ as contraction is increased. The tenth equation should be a statement that the total potential energy in the collapsed helices is a minimum and <u>not</u> that the $\lambda = 1$. Konopasek found that the potential energy function was very shallow and that for contractions up to 30%, $\lambda = 1$ was a good assumption and greatly reduced the computation. A comparison of the various solutions for force as a function of contraction is shown in Fig. 61 from Brüggisser [141]. The difference between the various curves is small compared to the expected interfilament interactions in a real multifilament yarn.

Explicit formulae for force and moment as a function of contraction were not obtainable due to the nonlinear equations. Computer-generated, iterative solutions were obtained by all workers. Denton's [91] results are shown in Fig. 62. We see that the torque and tension required to hold the ends of the filament increase as the texturing helix angle increases. As the contraction is increased, the torque and tension decrease as shown. Tayebi [53] combined the retractive forces from

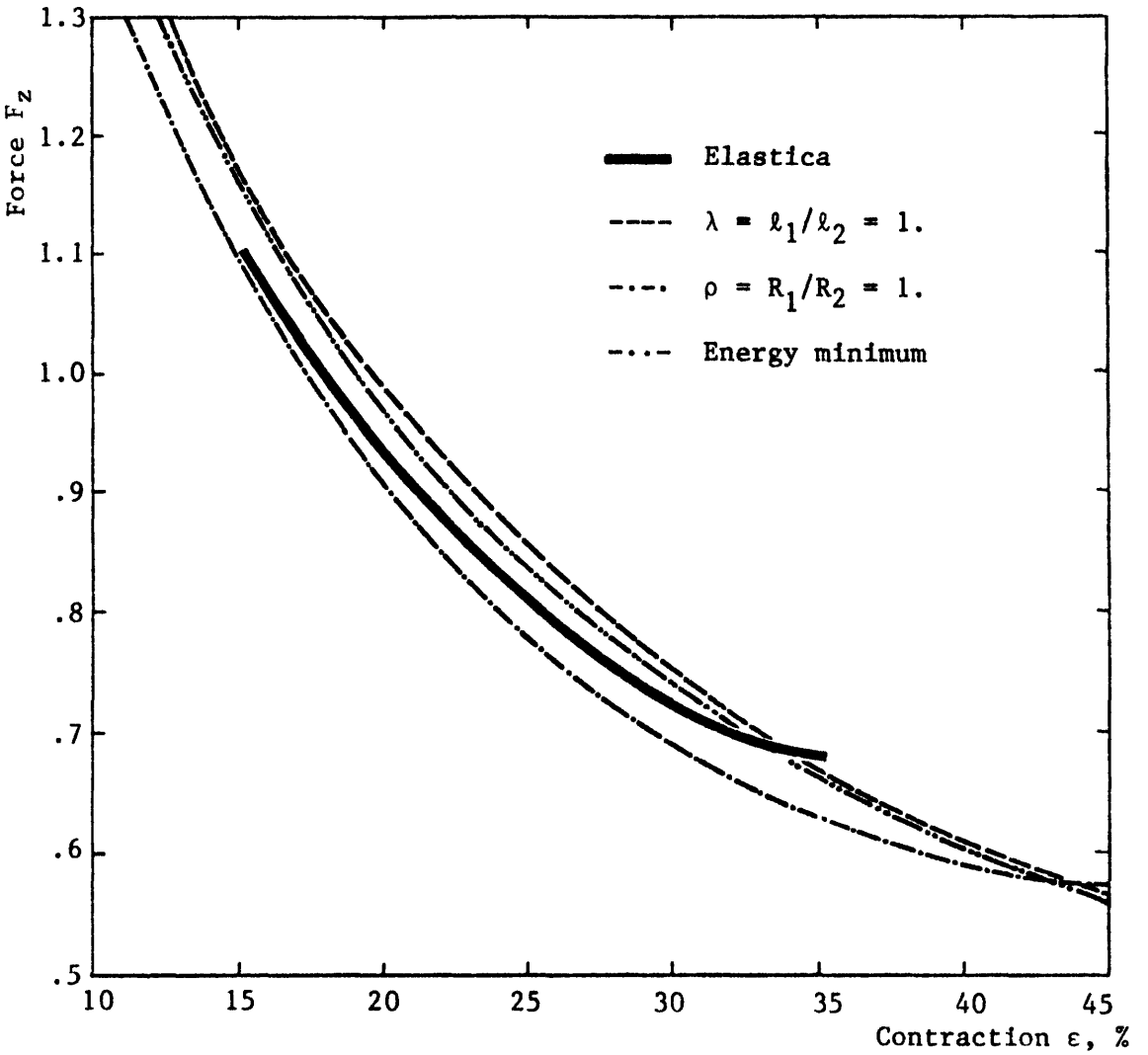

Fig. 61. Comparison of Load Contraction Behavior of Elastica Model of Twist Textured Fiber (as in Fig. 49,c) and its Helical Approximation [141].

A

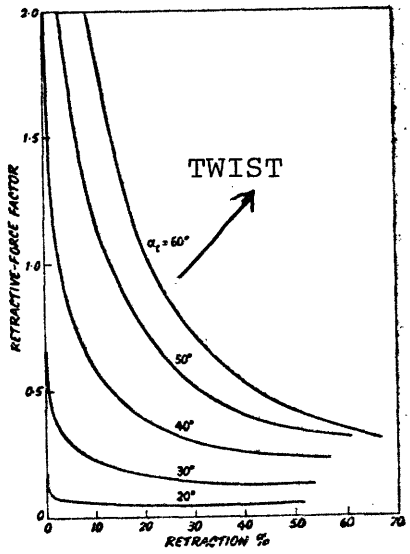

B

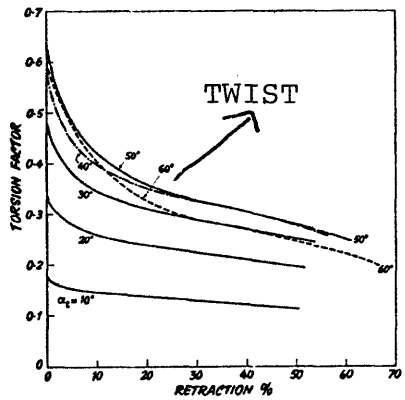

FIGURE 62. CONSTITUTIVE RELATIONS FOR TEXTURED FILAMENT [91]

many filaments, using a distribution in set grometry consistent with that in a twisted yarn. For our purposes, we will assume that Fig. 62 applies equally well to a textured yarn.

We also expect that the torque and tension in a yarn will be affected by twisting the contracted yarn. No complete calculations of the force and torque behavior of textured filaments (or yarns) during twisting are available, however Thwaites [92] did calculate the torque/untwist behavior of a textured yarn held at fixed contraction. As shown in Fig. 63, the data brackets the theory. Based on this figure only small torque changes occur for changes in twist of the contracted yarn. Okabayashi et al. [115] measured the torque/twist behavior of a 50 den/36 filament polyester yarn at a constant load of 14 mgpd. Their results are shown in Fig. 64. They found the average twisting rigidity (torque/turns/cm) to be about 0.15-0.16 dyne-cm^2 for either uptwisting or untwisting. The initial residual yarn torque at zero twist was about 2.3 dyne-cm. The retwist at zero torque was about 1.5 TPI.

Kawabata et al. [114] also examined the torque/twist behavior of a 150/48 textured polyester yarn at different testing tensions corresponding to 3.3 mgpd, 66 mgpd, and 200 mgpd. Their results are shown in Fig. 65. These results are similar to those in Fig. 64. It must be assumed that Kawabata et al. allowed the yarn to retwist since all their tests start at zero torque. The twisting rigidity is about

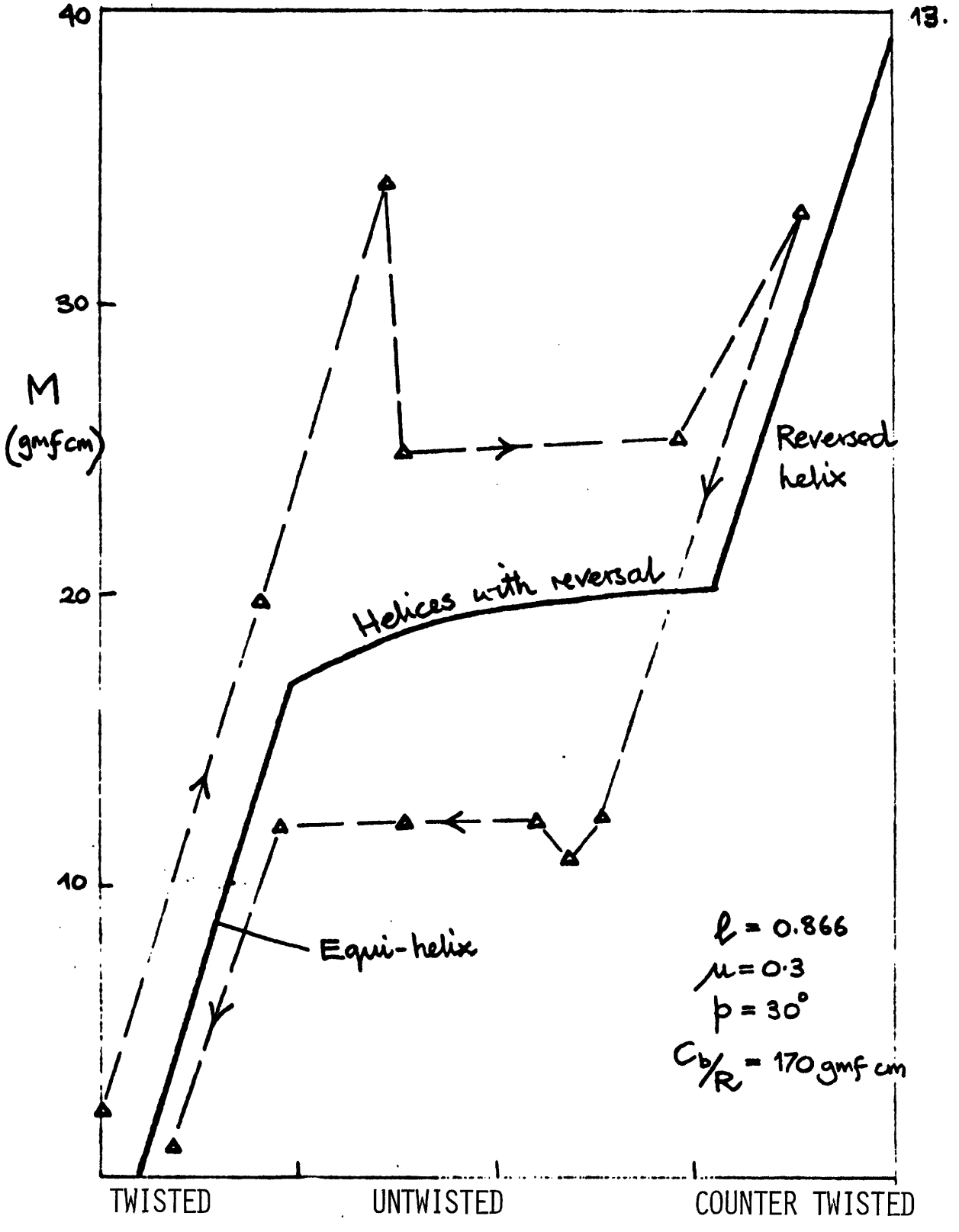

FIGURE 63. TORQUE REQUIRED TO DE-TWIST FILAMENT AT GIVEN CONTRACTION [92].

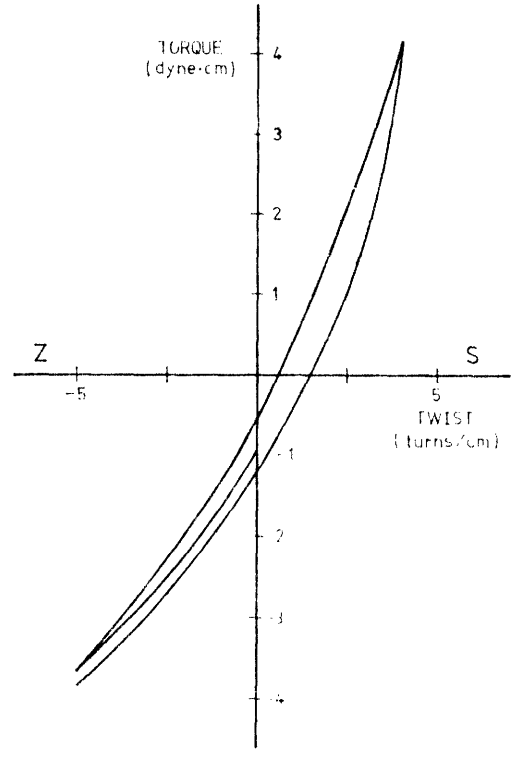

FIGURE 64. TORSIONAL BEHAVIOR OF 50/36 TEXTURED POLYESTER YARN [115].

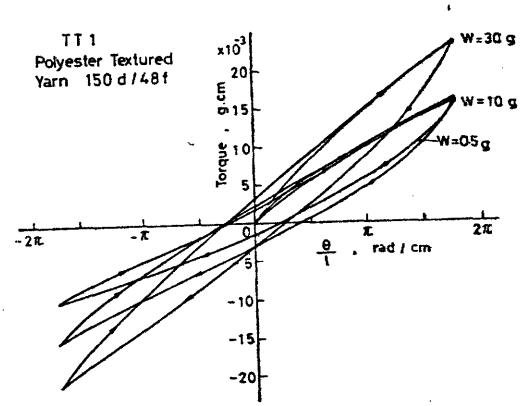

FIGURE 65. TORSIONAL BEHAVIOR OF 150/48 TEXTURED POLYESTER YARN [114].

1.5 dyne-cm^2 for the 150 denier yarn, or 10 times that found for the 50 denier yarn. The twisting rigidity for a solid rod goes up as r^4 while the linear density goes up as r^2. We calculate a 9-fold increase in torsional rigidity on this basis, which agrees well with the 10-fold increase observed. No important differences in retwisting torque exist between yarn tested at 3.3 and 67 mgpd. Since yarn contraction will change dramatically between these two load levels, we expect no difference in twisting rigidity at yarn contraction in the practical range of 5-25%.

Table 16 summarizes the qualitative aspects of textured yarn deformation. We see that the original (set) geometry plays a dominant role in determining the force and torque. The fiber deformational properties, i.e. bending modulus, ε_B, and torsional modulus, G, directly influence the force and torque as a function of deformation. Temperature can drastically change both of these parameters.

D. The Effects of Temperature on Textured Yarn Constitutive Relations. Temperature can alter the load/elongation behavior of textured yarns by changing one or more of these parameters:

(1) the stress-free geometry by removing temporary sets above T_g,

(2) the stress-free geometry by destruction of the permanent set above the Tm of the crystallites,

TABLE 16

TEXTURED YARN CONSTITUTIVE RELATIONS DURING COLLAPSE AND TWISTING

Yarn Parameter	
Force	• Determined primarily by set geometry and contraction from straightened length (Fig. 62) [91,92,93,53]. • Weak function of twisting (during test) [142]. • Depends on E and G of filaments.
Torque	• Determined primarily by set geometry and twisting (during test) [91,92,93,53]. • Weak function of contraction [91,92,93,53]. • Depends on E and G of filaments.
Residual Torque	• Weak function of load (0.5-10 mgpd) [142]. • Strong function of set geometry (texturing twist) [97]. • -1.5 dyne-cm (2.4 TPI of retwist).
Twisting Rigidity (Torque/ Twist)	• Weak function of load (3-67 mgpd) [114]. • 1.5 dyne-cm^2 for 150/48 polyester.

(3) the stress-free geometry by establishing a new permanent set,

(4) the fiber bending and torsional moduli by thermal softening and fine structure changes.

The one factor which dominates all of these interactions is the configurational stability of the molecules in the stressed and heated filament. The filaments are composed of polymer molecules with varying degrees of extension, or orientation, with respect to the random-coil configuration which is thermodynamically preferred at the melt. The extended molecules are stabilized by (1) restriction in large scale molecular rearrangements below T_g, (2) physical entanglements with other chains, (3) crystallization of chain segments with segments from other molecules. The stability that each of these mechanisms confers to the extended chain network depends on the temperature, the stresses acting on the filament, and time [33].

In what follows, we will attempt to predict the yarn contraction and twist changes in the four sub-zones of the setting process based on changes in yarn constitutive relations as the yarn is progressively heated and cooled. The stress-free geometry of the fiber entering the setting zone is determined by the twisted geometry stabilized over the texturing heater, and by the cold strains resulting from tensions in the post-twister zone or in the package. We will

assume a stress-free geometry for the entering yarn and show its behavior in Fig. 66a as curve 1. We do not know the level of threadline tension or torque that the entering yarn encounters. Immediately upon entering the setting zone, the textured yarn will contract to the level C1 as determined by the zone tension (P). The threadline also will twist, if the threadline torque (M) is other than that required to maintain the twistless configuration at C1. We may expect that threadline torque is even smaller (closer to zero) than the residual torque in the textured yarn, since the setting operation is known to reduce yarn torque-liveliness. As the yarn moves over the heater in the setting zone and is warmed, we may expect the temporary components of set to be relaxed.

Rosborough [85] makes a distinction between cold strains which can be recovered by "delayed elastic recovery" at room temperature, and the strain frozen in the molecules by quenching the extended molecules from a higher temperature. Cold strains are recovered much more rapidly as the T_g of the polymer is reached. Frozen-in strains are recovered only when the temperature is raised to the same level where straining occurred. Thus, we may expect that the original texturing set will be recovered first as the yarn is heated above T_g. This has been confirmed by Gupta et al. [63]. In addition, the moduli will decrease by about 40% as shown in Fig. 49.

The combined result of these two effects is a change

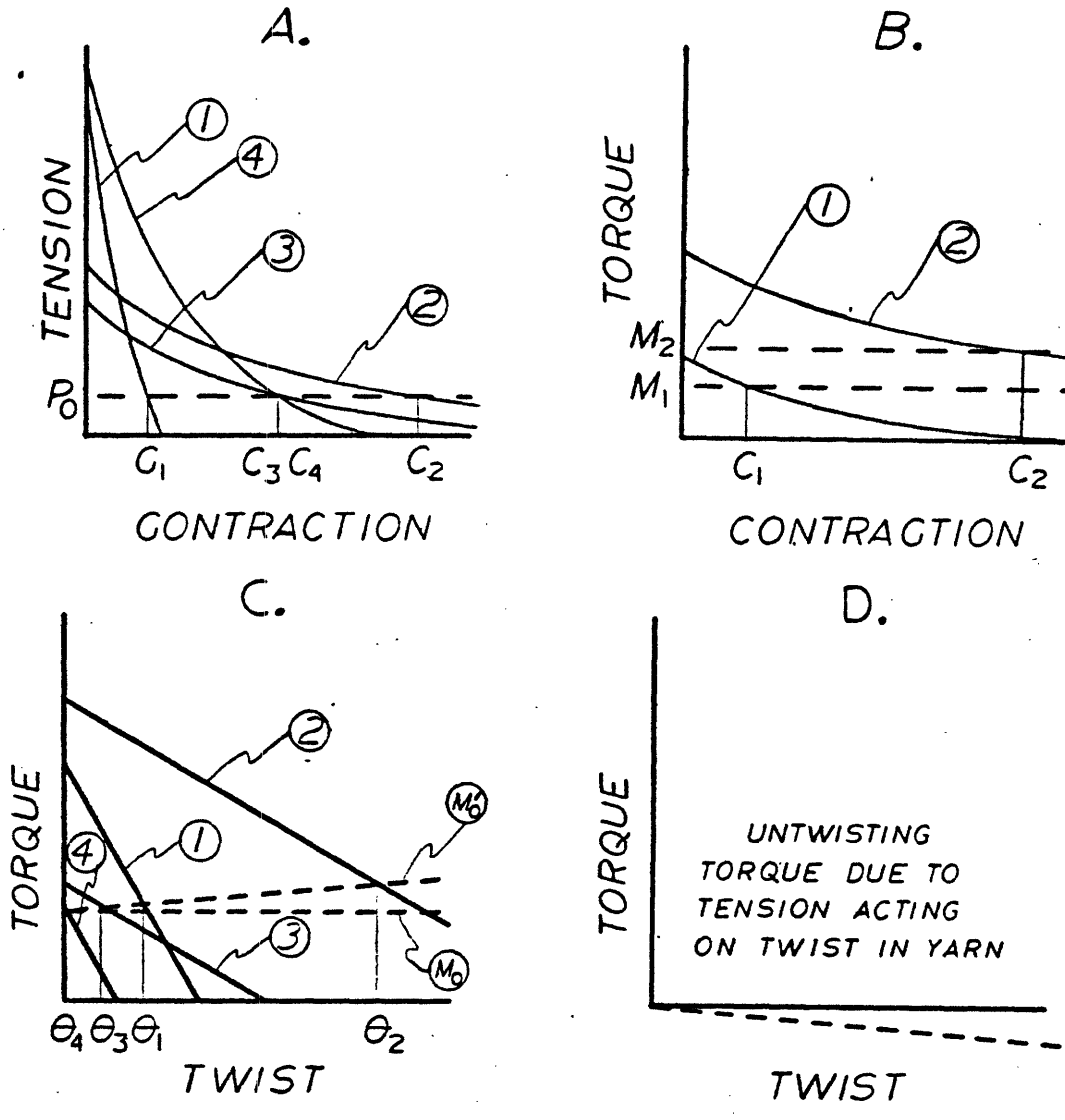

FIGURE 66. CHANGES IN TEXTURED YARN CONSTITUTIVE RELATIONS WHEN HEATED

in the load contraction behavior of the yarn from curve 1 to curve 2 in Fig. 66a. We now consider a yarn moving from the cold sub-zone (1) to the warm sub-zone (2). In order that $P_2 = P_1 = P_0$, the contraction at 2 will be greater than at 1. We find similar curves for the moment contraction behavior in sub-zones 1 and 2 in Fig. 66b. We note that at C1 and C2 the yarns have different moments. However, the physics of the threadline demands equality of moment along its length. Therefore, the yarn will twist locally to equalize the moments according to Fig. 66c as the yarn uptwists, its torque, due to components of fiber bending and twisting moments, will decline. The end point of the uptwist will occur when the residual uptwisting torque components due to fiber bending and torsion are just balanced by the untwisting torque generated by the threadline tension acting on the twisted filaments, as shown in Fig. 66d.

As the yarn reaches the heater temperature, smaller crystals from the original set will melt. According to Denton and Morris in [33], such desetting (or lack of original setting efficiency) should cause an increase in the helix radius of the "strain-free" geometry with no change in helix angle. The larger helix will be a "softer" helix, as shown by Fig. 66a, curve 3. Considerable filament shrinkage can also be expected as the temperature is increased. Filament shrinkage will undermine the original set and thereby lower the torque and tension at a given twist and extension. In addition, filament shrinkage lowers the elastic modulus,

producing a still softer helix.

As the yarn proceeds further along the hot sub-zone, it is expected that the fiber bending and twisting moments tending to uptwist the yarn will be drastically reduced as the components of set vanish at the heater temperature. As shown by curve 3 in Fig. 66d, the tensile components of torque tending to untwist the yarn will be virtually unopposed and the yarn will suddenly untwist. The crimped, but untwisted, yarn will then move out of the heater into the cooling sub-zone.

As the yarn exits the heater and cools, it will regain elastic rigidity, but lose the retractive force developed by the extended chains at high temperatures. The two effects should compensate each other and no major changes in twist or contraction should occur as the yarn cools, as shown in curve 4 in Fig. 66.

The effect of temperature on torque exerted by the yarn was unavailable in the literature. Preliminary measurements have been made in the following manner [142]. The stretch textured yarn is removed from its package and loaded briefly to 100 mgpd. A small 2-mgpd weight is used to tension the yarn during heating and prevent twist loss. The torque is measured as the yarn is brought into contact with an electrically heated surface. The torque sensor is capable of detecting torque changes as small as 1×10^{-7} in/lb. Qualitative results are shown in Figs. 67 and 68.

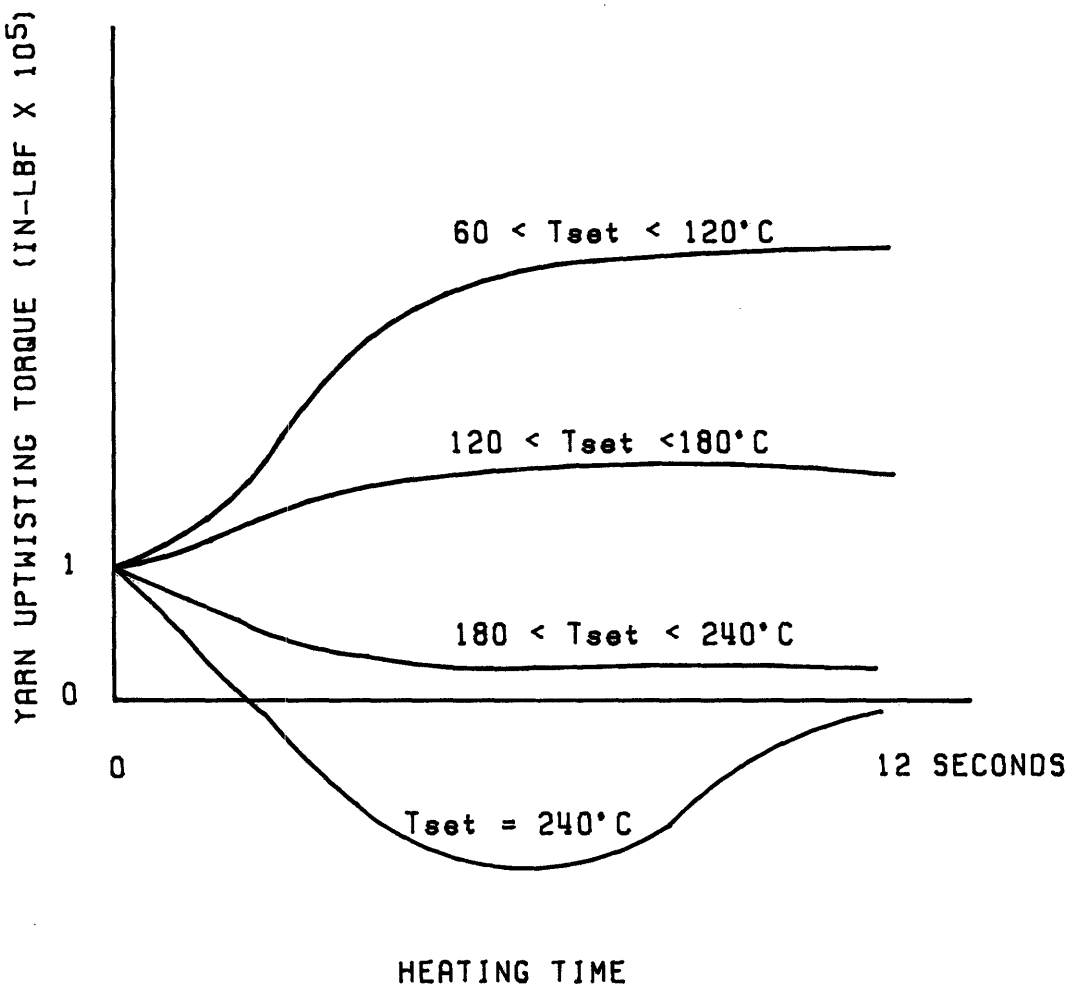

FIGURE 67: YARN TORQUE AT VARIOUS TEMPERATURES. ZERO TWIST; 2 mgpd CONSTANT TENSION; 150/34 STRETCH YARN. [142]

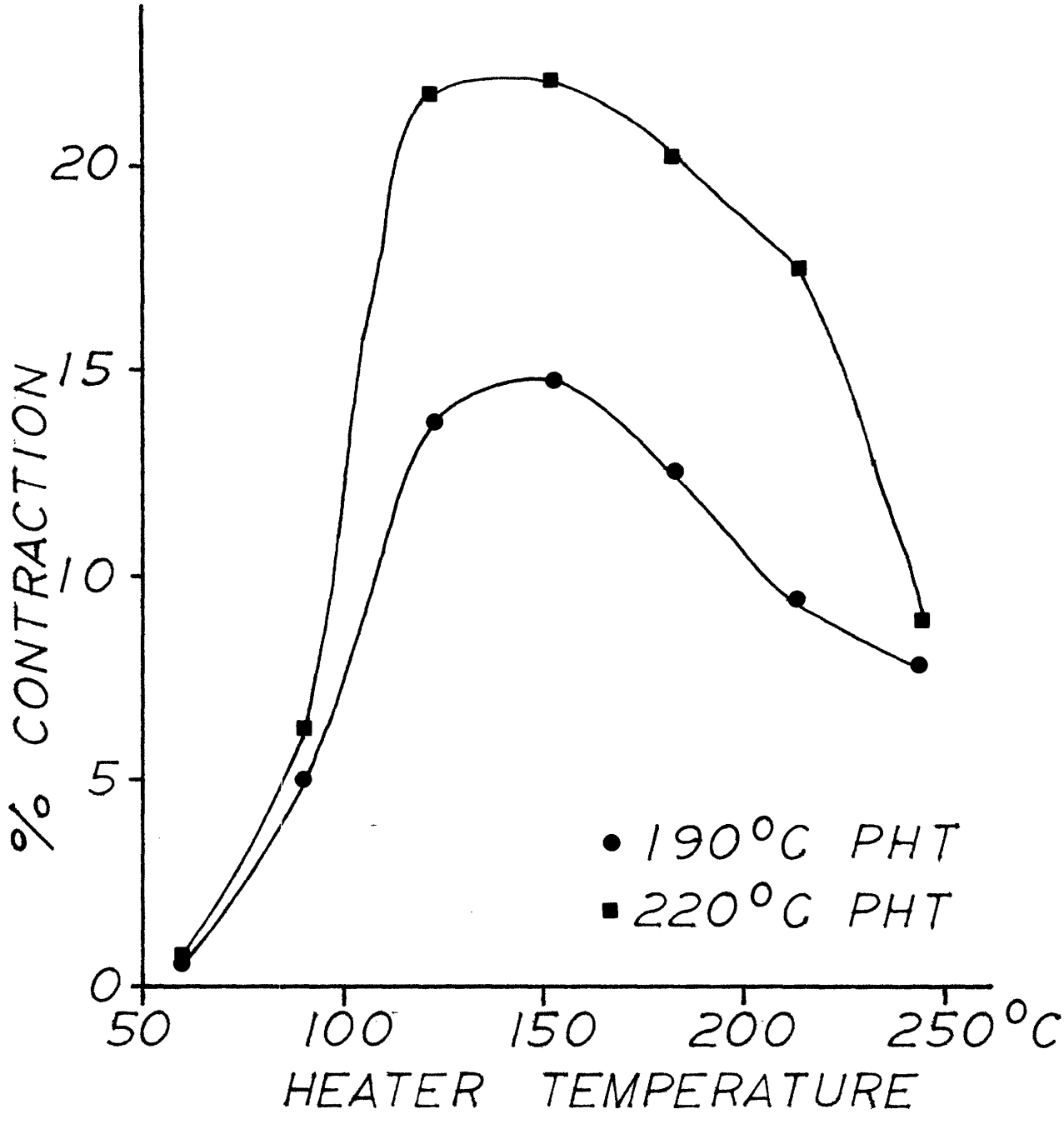

FIGURE 68. YARN CONTRACTION OF STRETCH TEXTURED POLYESTER YARNS AT 2 MGPD AND ZERO TWIST [142]

At low temperatures the influence of the package set and the 100-mgpd pre-tension is removed with an associated increase in torque as the twisted memory is restored. The yarn contraction also increases. At intermediate temperatures, the filaments soften and part of the set is apparently removed, as shown by decreased contraction. At higher temperature the torque in the yarn is removed as further desetting occurs. At the highest temperature we have observed an interesting phenomenon of torque reversal during the heating. At the end of the test, the torque is zero and the yarn contraction (primarily due only to filament shrinkage) is small.

A possible explanation for the phenomenon of torque reversal is shown in Fig. 69. The yarn is treated as a solid rod and an element of the surface is observed during texturing (steps 1-4) and subsequent heating (steps 5-7).

3. Observations of Yarn Behavior in the Setting Zone.

The mechanical behavior of the yarn in the setting zone will depend on material-process interactions and fiber-fiber interactions complicated by permanent changes in fiber structure and properties as the fiber is heated in the presence of stresses. Some general predictions of yarn behavior in the setting zone can be made. Redistribution of twist, filament length, and yarn contraction must occur between the three sub-zones in the setting zone to maintain tension-torque equilibrium. The length of yarn exiting the

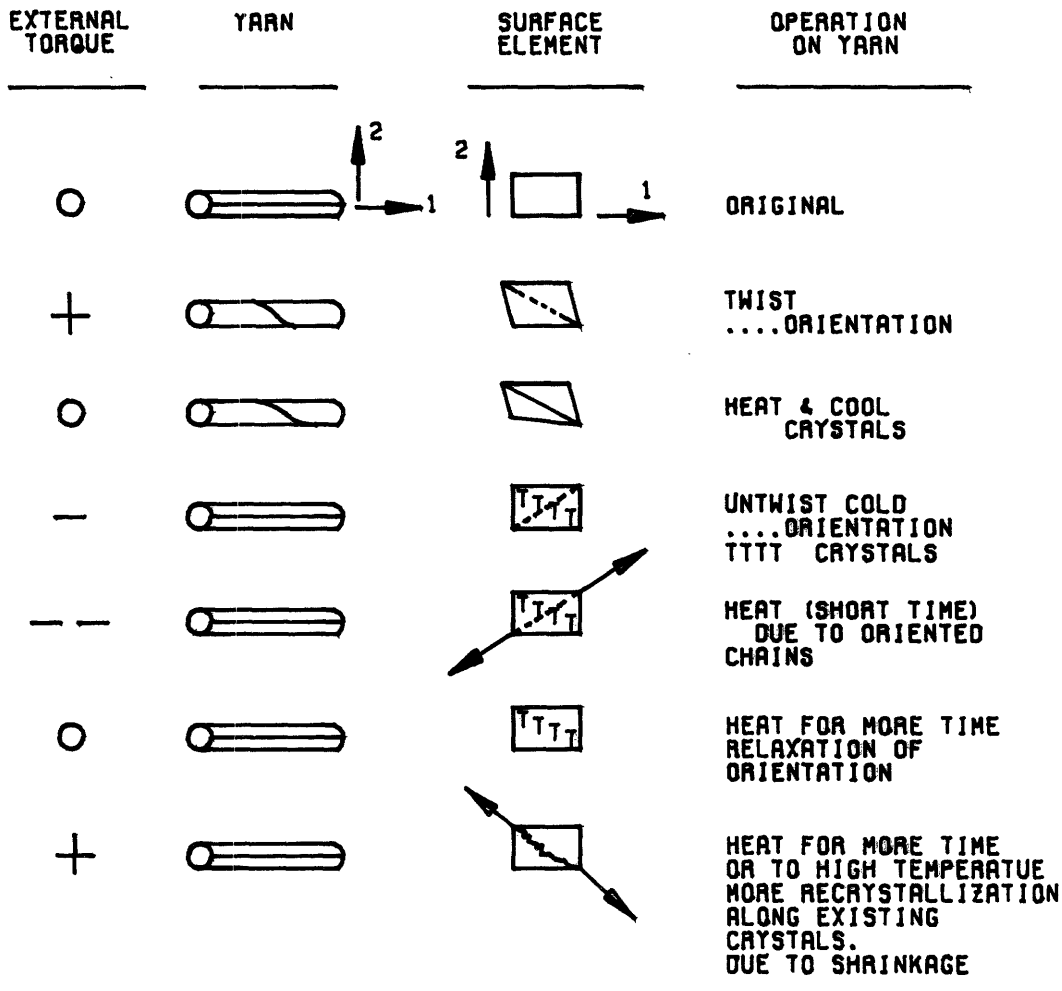

FIGURE 69: EXPLANATION OF TORQUE REVERSAL AT HIGH TEMPERATURES

zone should be dictated by the zone overfeed. The sum of filament crimp and filament axial shrinkage (in the exiting yarn at the threadline tension and torque) will equal the zone overfeed. Any twist that develops in the cold, warm or hot sub-zones cannot exist in the exiting yarn. If zero twist yarn is fed into the setting zone, zero twist yarn will exit the zone when steady-state is reached.

To test these predictions, a laboratory texturing machine, as described in [52], was modified by eliminating the twisting unit and substituting a specially constructed heater. The glass top on the 10-1/2-inch long channel-shaped heater permitted direct observations of the yarn geometry during the treatment. Sections of the glass heater cover could be removed to facilitate snatching samples of the hot yarn with a special clamp. Heater residence time was about 6 seconds. Bows and gauge marks were placed along the pre-tensioned, entering yarn so that photographic records of yarn rotations and length contraction could be made during the treatment. Longer gauge length marks (≃35") were used to determine filament shrinkage. No measurements of tension or torque were made. Three quantities were determined on the basis of yarn lengths:

L_0 = yarn length under 100 mgpd pre-tension (35 inches),

L_1 = yarn length under 3.5 mgpd (a paper clip on 150 denier yarn) after setting and at

least one hour for elastic recovery,

L_2 = yarn length under 100 mgpd after setting.

$$\text{Filament shrinkage} = \frac{L_1-L_2}{L_0} \times 100\%$$

$$\text{Residual crimp} = \frac{L_2-L_1}{L_2} \times 100\%$$

$$\text{Yarn Shrinkage} = \frac{L_0-L_1}{L_0} \times 100\%.$$

The qualitative predictions were confirmed by observations of the behavior of stretch and set textured yarns during continuous setting.

A. Behavior of Stretch Yarns. To convert bow rotations, which represent local yarn rotations, to twist, one need only realize that a moving, rotating twisted yarn screws itself through space if the twist is produced by the threadline rotation. The false-twist texturing process shown in Fig. 70 illustrates the principle. The local twist represents the local slope of the bow rotation versus length curve. Note that bow rotations do not return to zero at the untwister even though twist must return to the level in the entering yarn (in our case, zero). There are a certain number of turns "trapped", or bow rotations, in the setting zone at steady-state. Figure 71 shows the measured bow rotations and derived twist for a 150/32 polyester stretch textured yarn. A few turns per inch of twist are developed in the cold yarn. When the yarn is heated, it develops additional twist, which is removed by further heating. The yarn exits

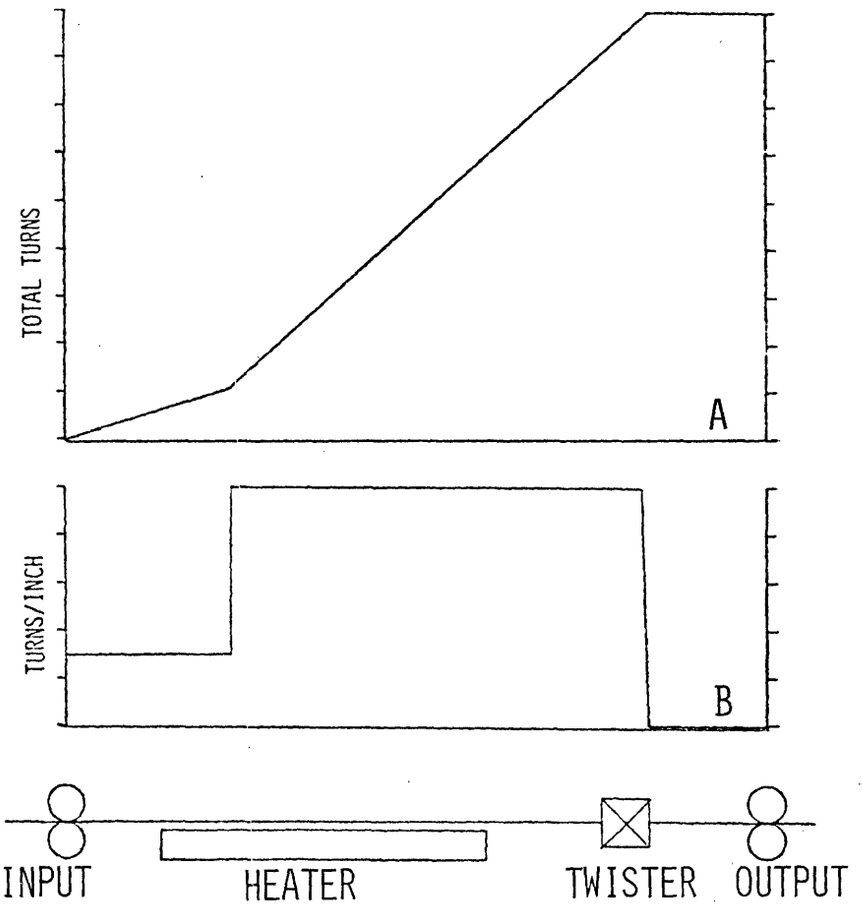

FIGURE 70. BOW ROTATIONS AND DERIVED TWIST FOR THE FALSE-TWIST TEXTURING PROCESS

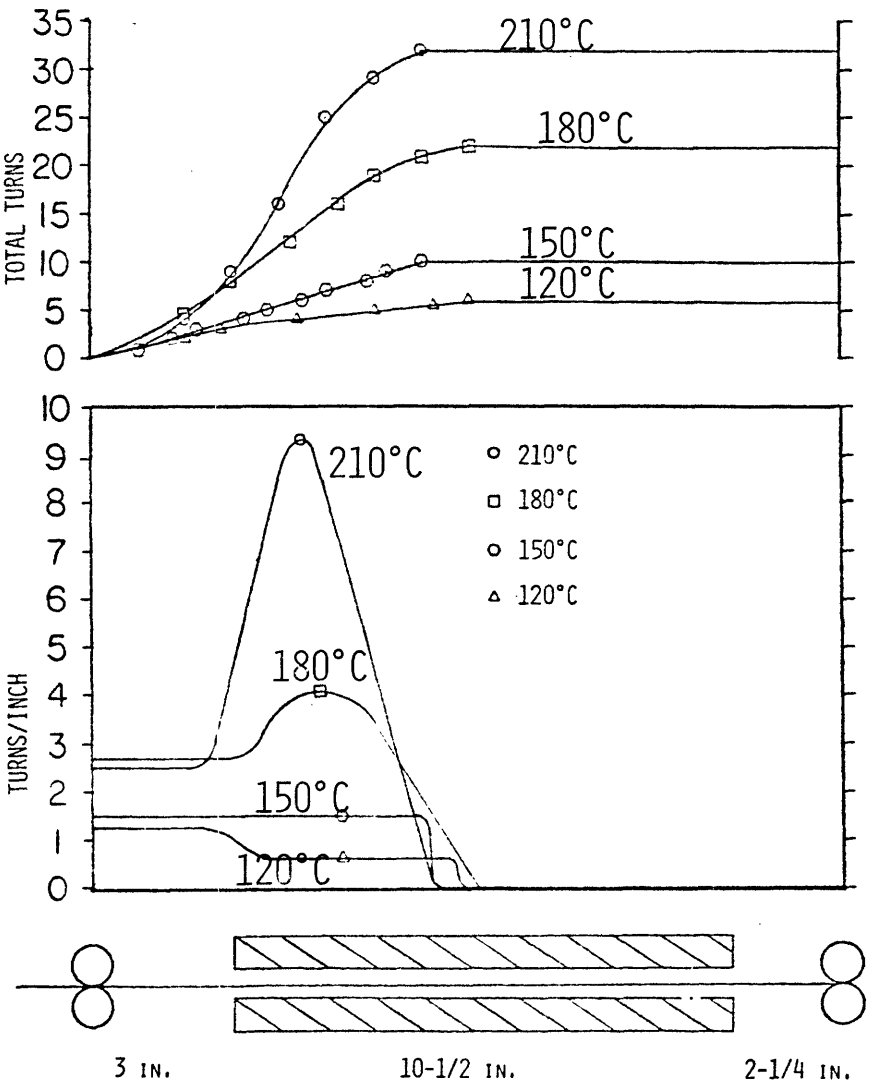

FIGURE 71. (A) BOW ROTATIONS AND (B) TWIST DISTRIBUTION DURING CONTINUOUS SETTING AT VARIOUS TEMPERATURES. POLYESTER (150/32) STRETCH YARN. SETTING ZONE O.F. = 14.6%.

the zone with zero twist.

The corresponding contraction during the setting operation is shown in Fig. 72. The zone overfeed should allow 14.6% yarn contraction at the exit. However, the entering yarn has less contraction and the warmed yarn has more contraction. This is in keeping with our predictions and measured values of contraction at fixed load and varying temperature.

The filament geometry during this process was observed by snatching samples from the running threadline. Figures 73 and 74 show the filament (yarn) geometry in the cold entry zone, at the maximum contraction and uptwist (labelled hot), and in the cooled exit zone. Some interesting differences can be seen. For example, in Fig. 73, we see that the cold zone geometry for 160°C setting zone temperature is similar to that for 205°C. At maximum yarn contraction, however, a striking difference exists between the yarns. The yarn heated to 160°C has more bulk, even though the contraction level is less than for the 205°C. The yarn heated to 205°C is seen to have a tighter structure with alternating highly twisted and untwisted regions. The cooled yarns have about the same apparent bulk (width) but the yarn heated to 160°C has shorter, tighter crimps.

Figure 74 has enlargements of the same threadline swatches shown in Fig. 73. The difference in hot filament geometry is even more apparent. The hot yarn in the 205°C

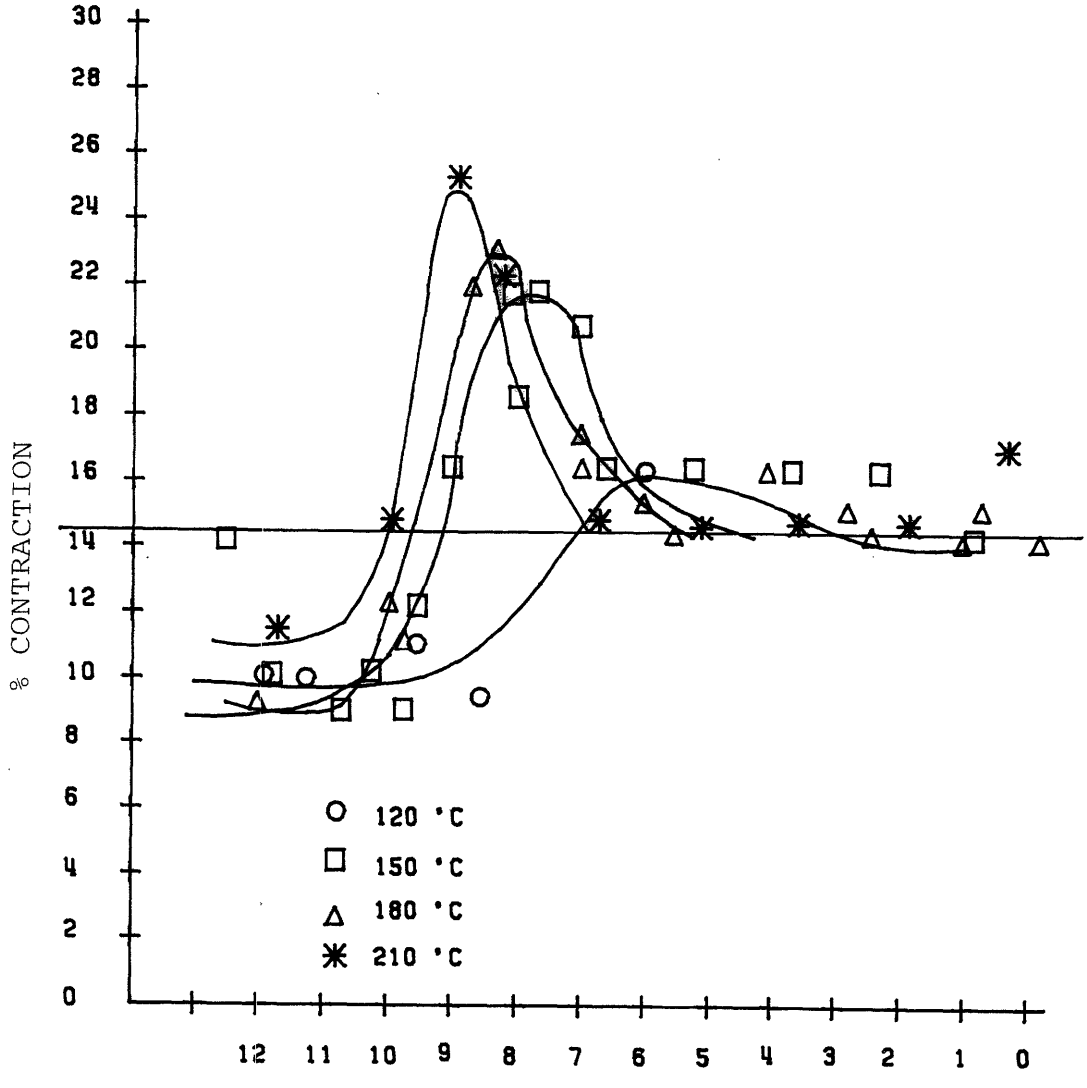

FIGURE 72: LENGTH CONTRACTION DISTRIBUTION DURING CONTINUOUS SETTING OF 150/32 POLYESTER, 14.6 % OVERFEED

FIGURE 73. THREADLINE SWATCHES 150/32 DURING SETTING

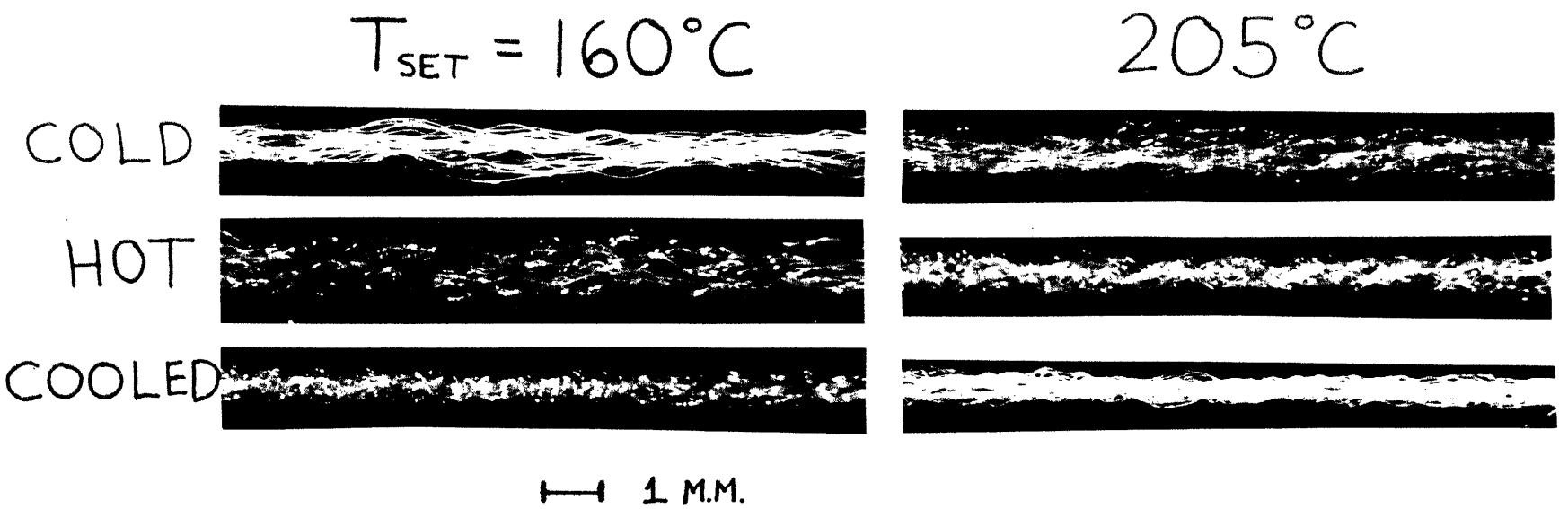

FIGURE 74. THREADLINE SWATCHES 150/34 POLYESTER DURING SETTING

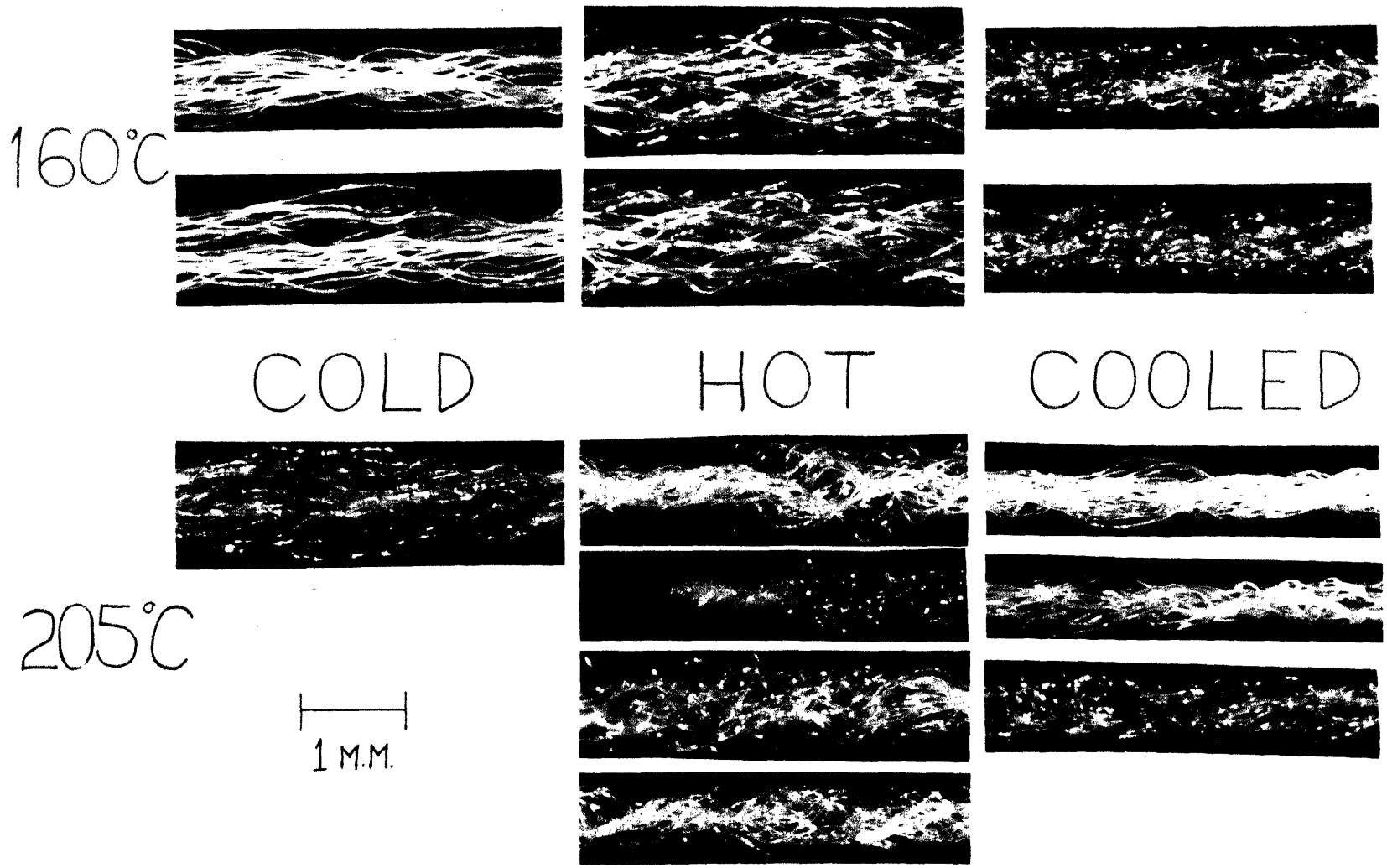

treatment is twisted about 8 turns per inch, but the twist is not apparently uniformly distributed.

This can be explained by follow-the-leader filament collapsing in the cold zone. When this occurs, all filaments in the yarn twist in the same direction on either side of a common reversal point. When this yarn is subsequently uniformly twisted, part of the yarn is uptwisted further and part is untwisted. The result would be as shown in Fig. 75. This agrees with alternating highly twisted regions (say, about twice the yarn average of 8 TPI) and regions with almost no observable twist for the hot yarn at 205°C (Fig. 74). These tightly twisted regions persist in the cooled exit yarn, thus providing a basis for the increased tight spots due to higher heater temperature in the setting zone of Lunenschloss et al. [104].

In addition to the measurements of twist and contraction during the setting process, measurements of filament shrinkage, residual crimp, and total yarn shrinkage were made and are shown in Fig. 76. The total yarn shrinkage is approximately constant and close to the zone overfeed. It may be slightly less because the tension for measuring yarn shrinkage (3.5 mgpd) is more than that during setting. The predicted interchange between filament shrinkage and residual crimp has been confirmed. The higher temperatures produce more filament shrinkage and, therefore, less crimp can remain in the exiting yarn. This tradeoff between residual

FOLLOW THE LEADER FILAMENT
COLLAPSE WITH COMMON REVERSAL POINT

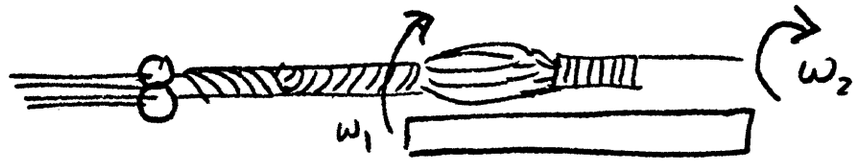

UPTWISTING OF THE YARN TO SHED TORQUE AND MAINTAIN EQUILIBRIUM WHEN HEATED

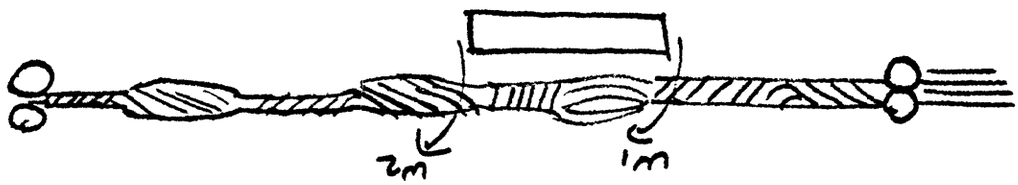

UNTWISTING OF THE YARN TO REGAIN TORQUE LOST FROM RELAXATION AND SETTING

FIGURE 75. CREATION OF APPARENT TIGHT SPOTS DURING SETTING

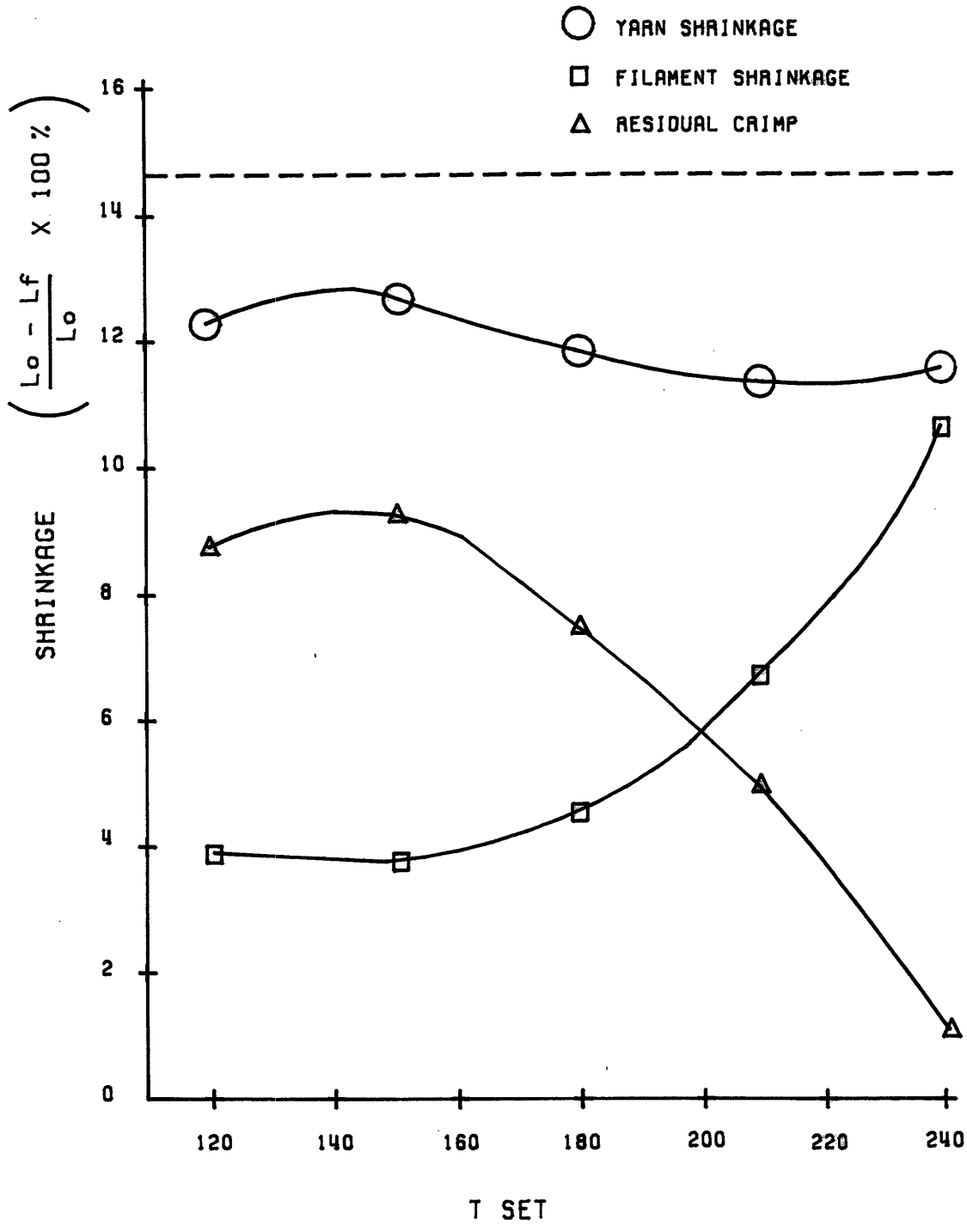

FIGURE 76: CHANGES IN YARN LENGTH AFTER SETTING AT 14.6 % OVERFEED. (LURAY STRETCH, 150/32, PET)

crimp and shrinkage was also observed at overfeeds of 6.9% and 21.2% in the setting zone, as shown in Figs. 77 and 78. At 6.9% overfeed, the zone tension at 120°C was higher than the 3.5 mgpd used to measure yarn contraction. At 240°C, virtually the entire yarn shrinkage is due to filament shrinkage. In Fig. 78, we see that yarn shrinkage measured at 3.5 mgpd falls far below the zone overfeed of 21.2%. This implies that the zone tension must have been much lower than 3.5 mgpd.

Figures 79, 80, and 81 replot these same data so that the effect of overfeed on yarn properties can be assessed. Figure 79 shows the filament shrinkage as a function of setting zone temperature. At all overfeeds, the shrinkage increases with temperature. The upswing in shrinkage above 210°C shown by the 14.6 and 21.2% overfeed curves is not seen at 6.9%, simply because the overfeed limits the shrinkage. No differences exist between the shrinkage at 14.6 and 21.2% overfeed.

The amount of residual crimp is plotted in Fig. 80. Clearly, more crimp remains in yarns processed at higher overfeeds. Since the shrinkages at 14.6 and 21.2% overfeed are similar, we may expect that the amount of desetting will also be similar. The resetting, however, will occur at higher contraction for the 21.2% overfeed and result in higher residual crimp as shown. These results are in keeping with our predictions and the data of others [33,104].

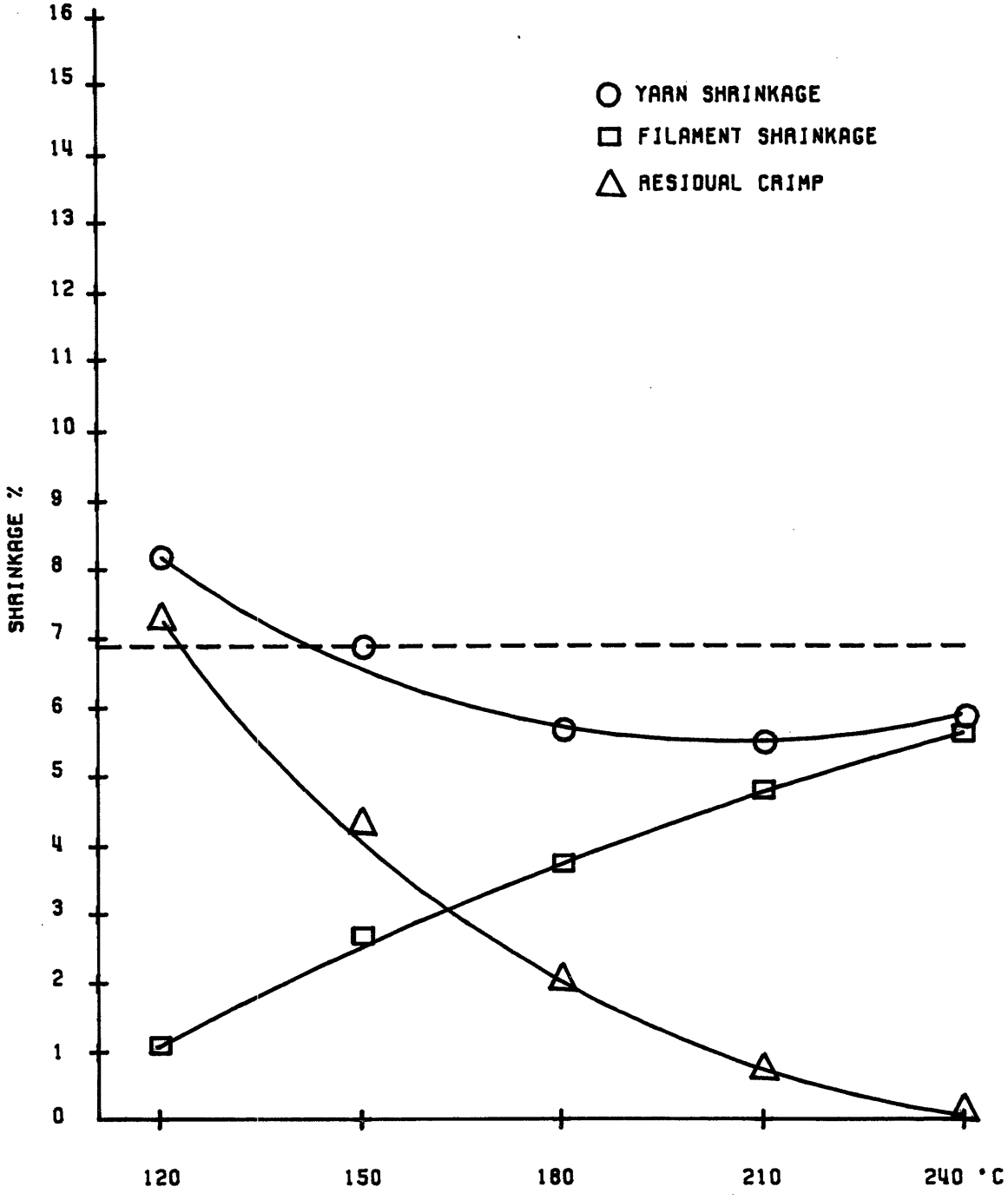

FIGURE 77: CHANGES IN YARN LENGTH AFTER SETTING AT 6.9 % OVERFEED. (LURAY STRETCH, 150/32,PET)

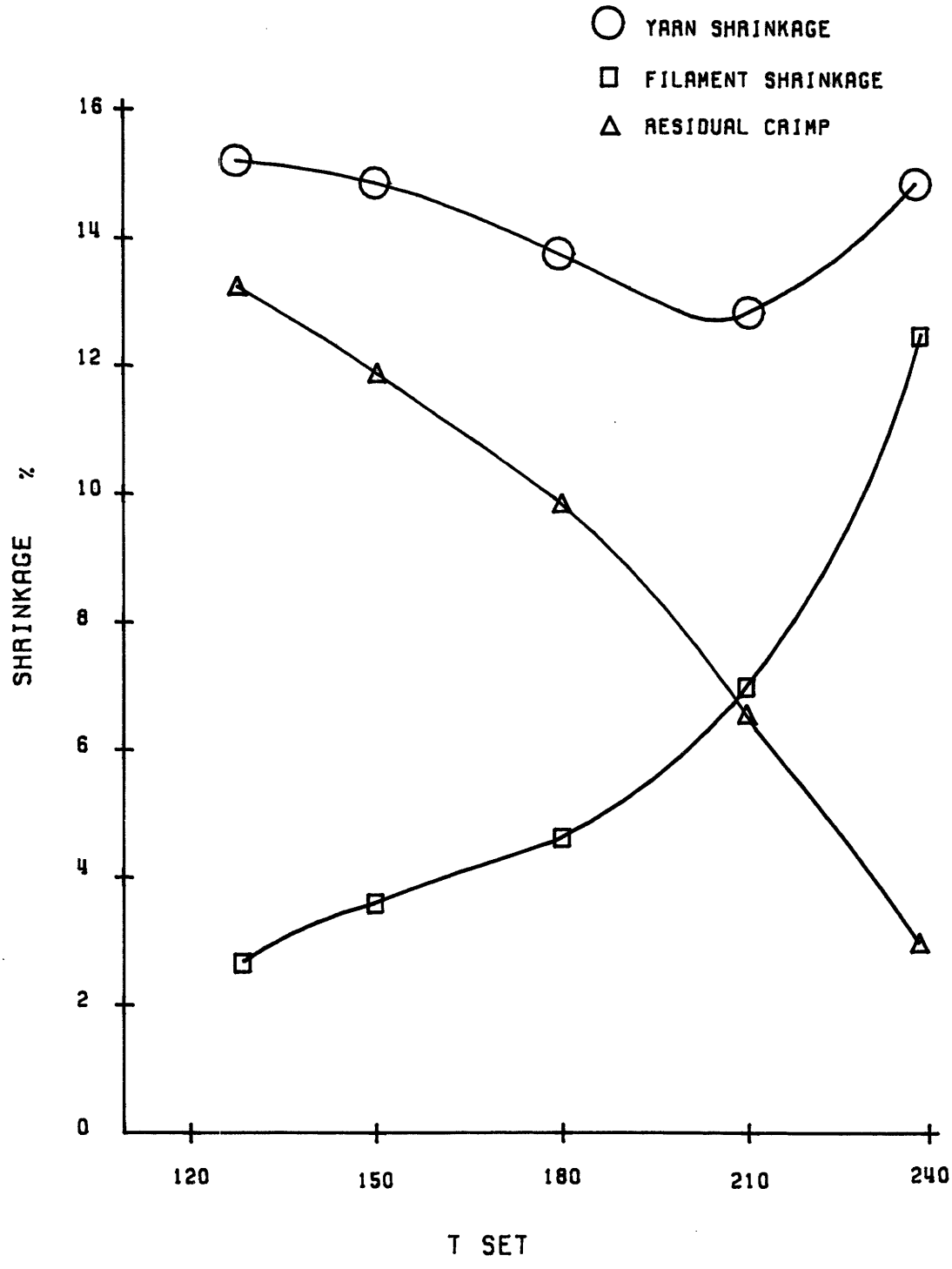

FIGURE 78: CHANGES IN YARN LENGTH AFTER SETTING AT 21.2 % OVERFEED. (LURAY STRETCH, 150/32, PET)

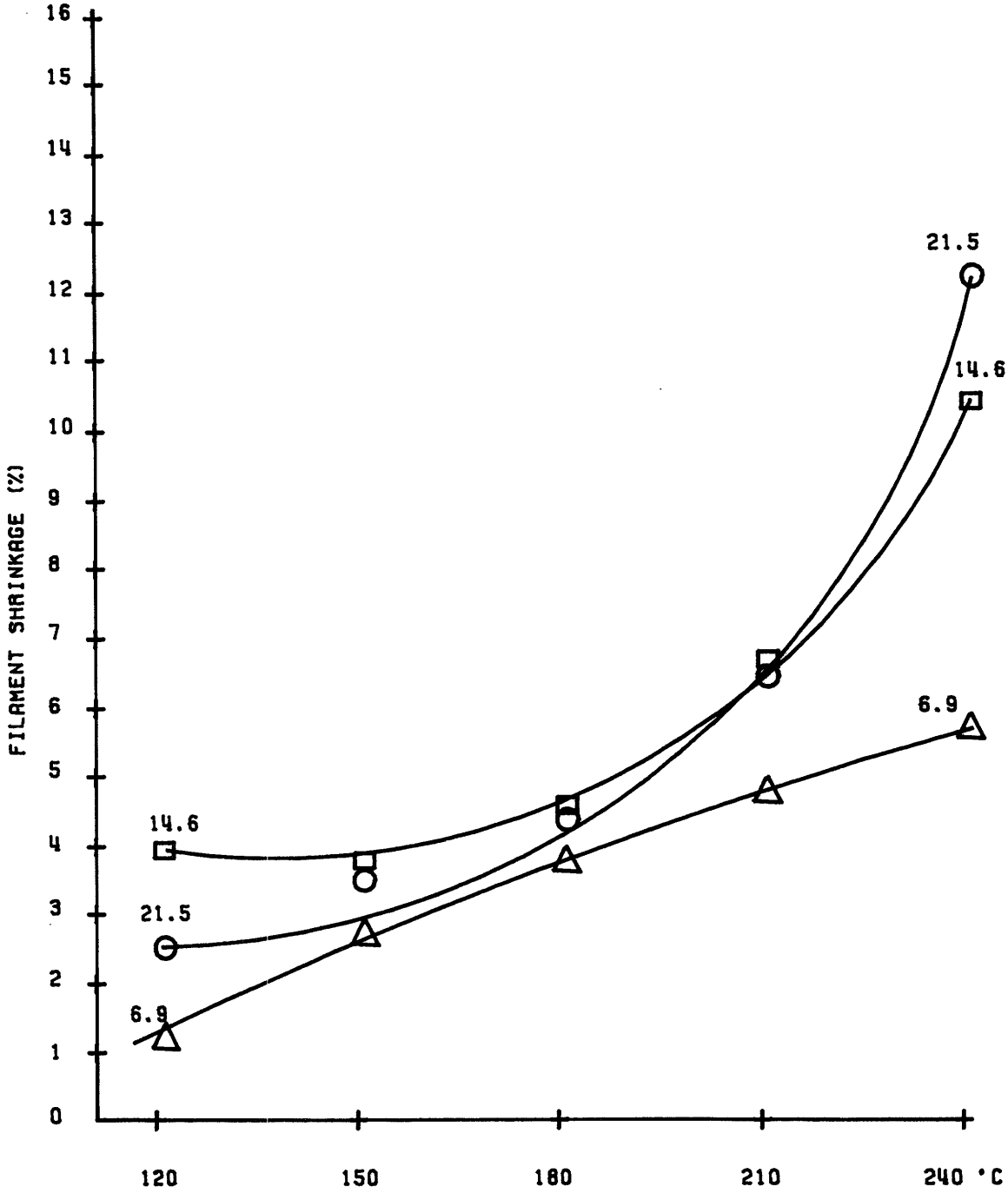

FIGURE 79: FILAMENT SHRINKAGE AS A FUNCTION OF SETTING TEMPERATURE AND OVERFEED. (LURAY STRETCH, 150/32, PET)

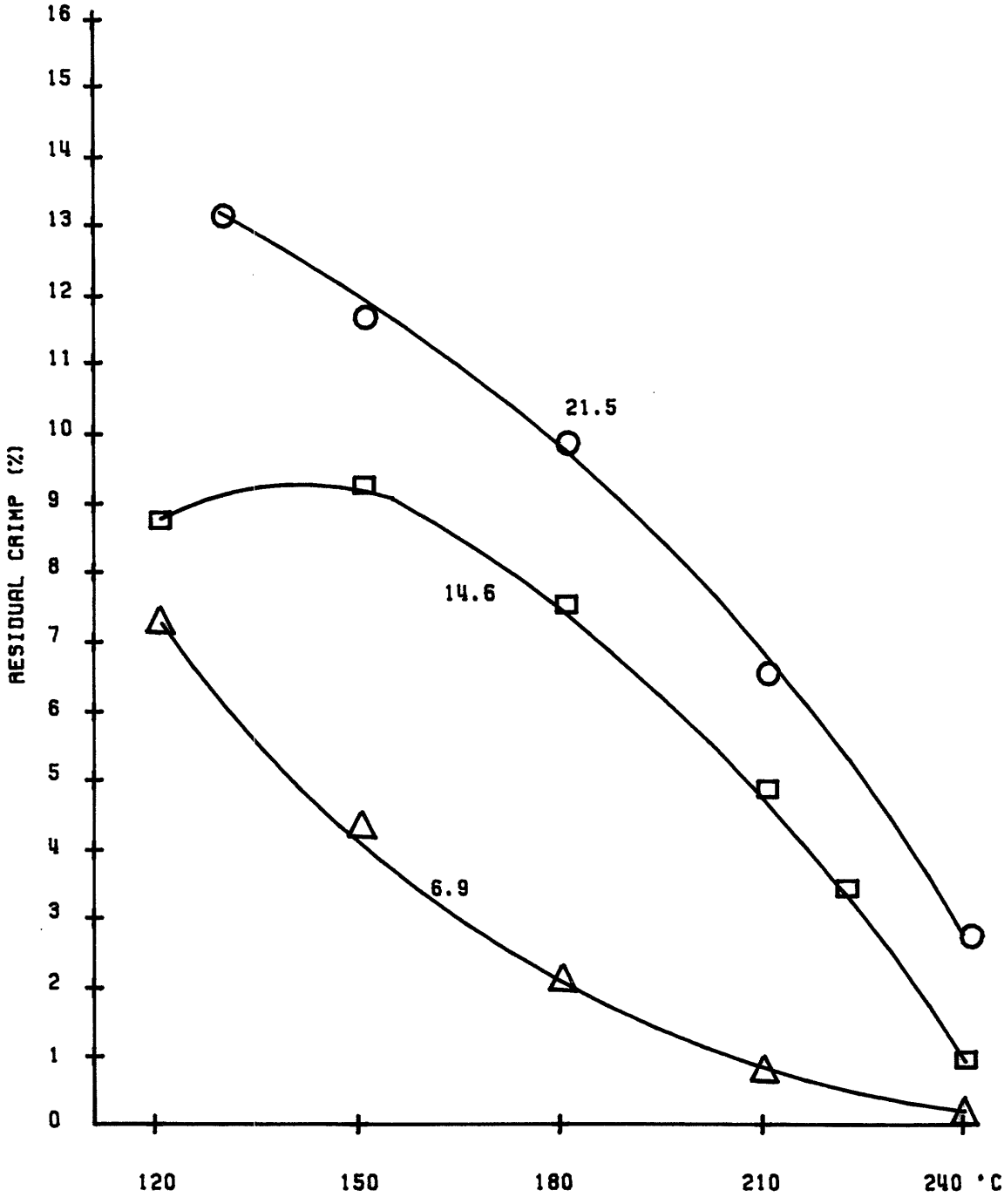

FIGURE 80: RESIDUAL CRIMP AS A FUNCTION OF SETTING TEMPERATURE AND OVERFEED. (LURAY STRETCH, 150/32, PET)

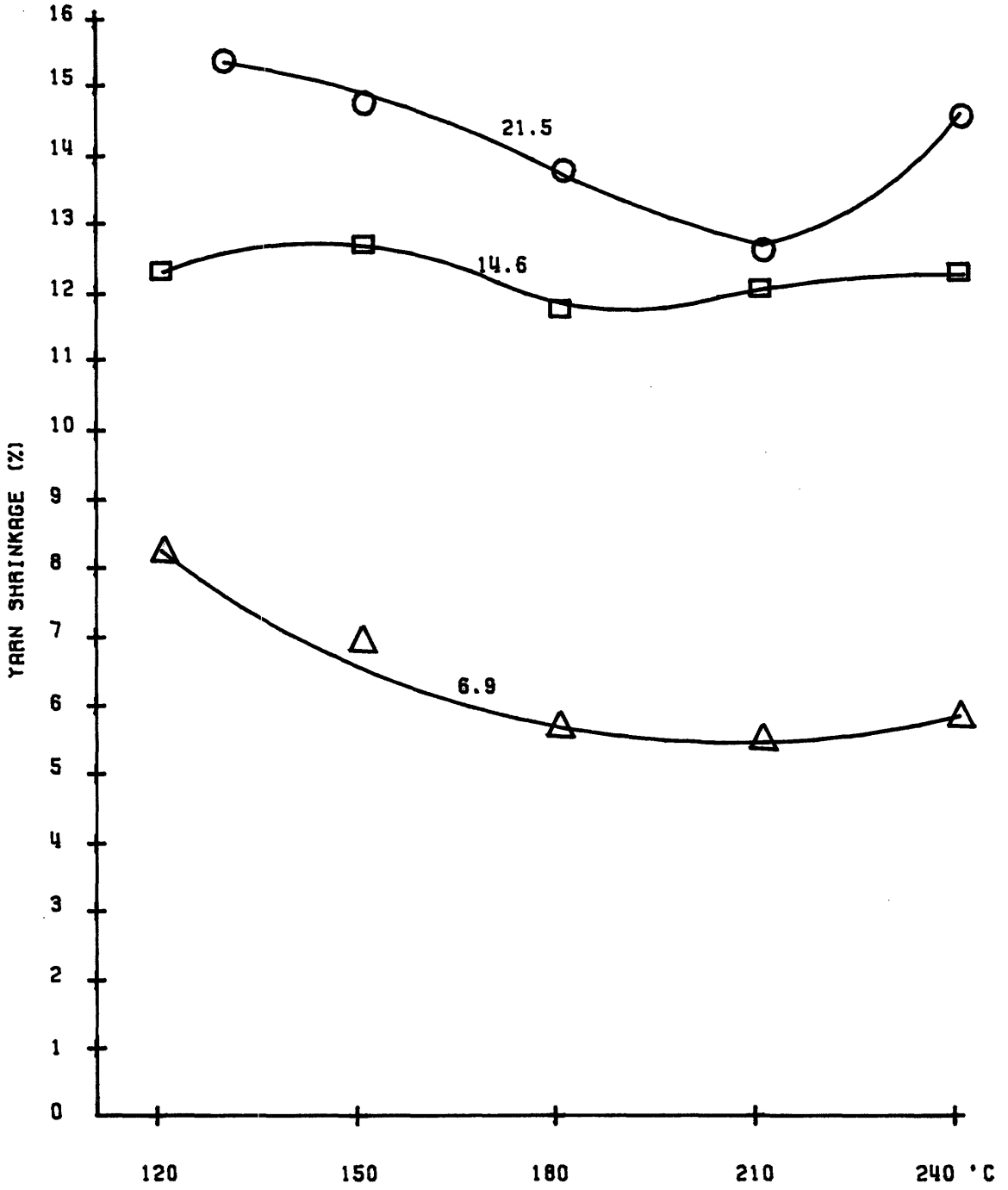

FIGURE 81: YARN SHRINKAGE AS A FUNCTION OF SETTING TEMPERATURE AND OVERFEED. (LURAY STRETCH, 150/32, PET)

The total yarn shrinkage increases with overfeed, but remains fairly constant with temperature, as shown in Fig. 81.

However, we did predict the occurrence of a maximum in crimp development for treatments around T_g that merely relax the temporary components of straight set without reducing the permanent set. This peak was observed in another series of tests by the author and also by Conkle [41]. In our tests, a two-ply stretch yarn (one textured S; one Z) of 300 total denier was subjected to a setting operation after an initial pre-tensioning to about 100 mgpd. The residual crimp was measured using about 2 mgpd (one paper clip) and 100 mgpd for the loads. The results are shown in Fig. 82. A maximum in residual crimp occurs for setting zone temperatures about 130°C. This is assumed to be just above T_g for the fibers. The location of the crimp peak is in keeping with Conkle's results on developed crimp.

B. Setting Zone Observations. Stretch Yarns with Primary Texturing Heater Differences. Two stretch yarns prepared by UNIFI, Inc. using the following texturing conditions on a Scragg Super Draw Set II: Speed-278 meters/min; Draw ratio-1.6 x 4; D/Y-1.71; S-Twist; no second heater; du Pont 12789 feed yarn; textured denier-150. The two yarns differed in primary heater temperature and are labelled accordingly as 190°C and 220°C in all figures.

Bow rotations and contraction for the two yarns are

shown in Figs. 83a,b and 84a,b. In Fig. 83, bow rotation in the warm yarn will go up as the torque is removed from the hot yarn. The 220°C and 190°C yarns reach the same level of bow rotations at 200°C and 180°C, respectively. This reflects the higher thermal stability of the yarn heat set at 220°C during texturing. The same trend applies to the other curves in this figure.

Yarn contraction during the setting operation is shown in Fig. 84. The peak contraction for the 220°C and 190°C yarns is at 200°C and 180°C as in Fig. 83. However, the lower temperature curve in Fig. 84b does not show the same type of behavior as the 180°C curve in Fig. 84a. The cold zone contraction in Fig. 84b at 160°C is much lower than that seen in any of the other tests. This could reflect higher zone tensions or yarn with low package crimp.

A clear understanding of the effect primary heater temperature has on the behavior of the yarn during setting can be obtained from Fig. 85 which combines yarn shrinkage, residual crimp, and filament shrinkage data for the two yarns. As expected, the yarn with higher PHT during texturing retains higher residual crimp and yarn shrinkage at all temperatures. The residual crimp and filament shrinkage curves for the two yarns are displaced horizontally by 20-30°C in accord with the PHT differences. Equal shrinkages occur at 20-30°C lower temperatures for the 190°C PHT yarn. Since these shrinkages will reduce the yarn's crimping tendency, the 190°C PHT yarn drops to a given residual crimp at

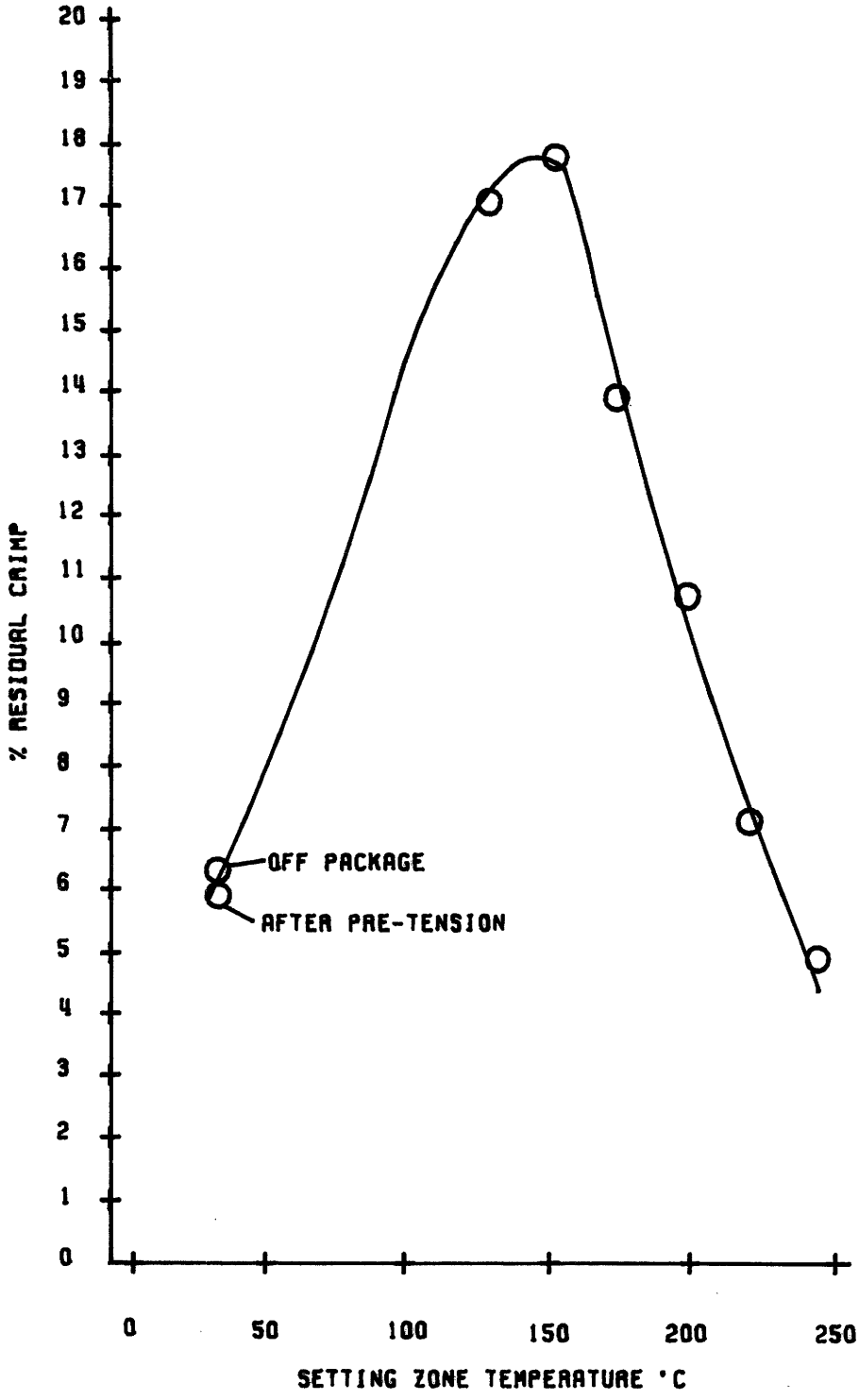

FIGURE 82: RESIDUAL CRIMP AS A FUNCTION OF SETTING ZONE TEMPERATURE. (2 PLY 150 DERNIER; TWIST SUBSITUTED; 14.6 ZONE OVERFEED; 1.5mgpd ⟶ 100mgpd)

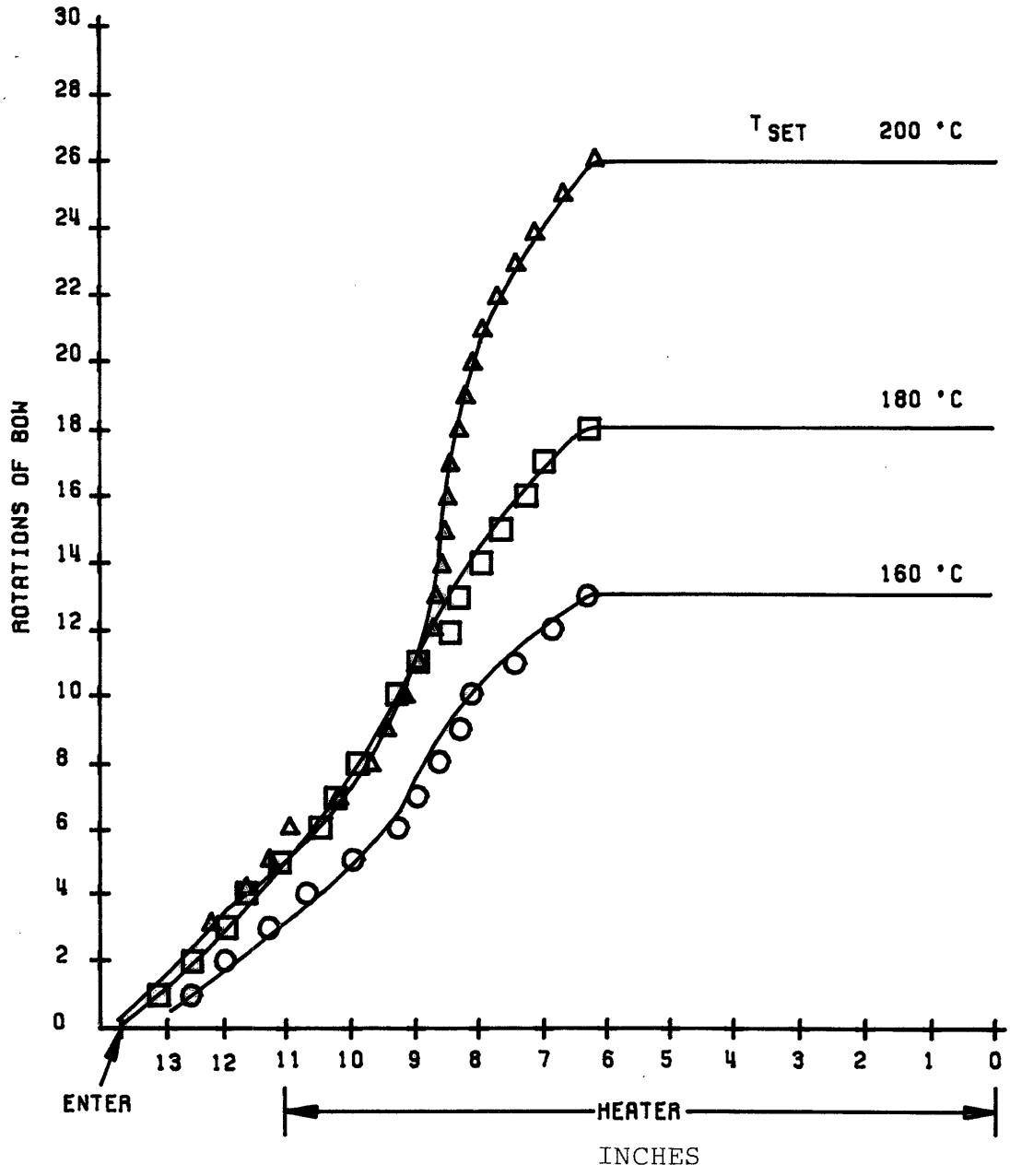

FIGURE 83A: BOW ROTATIONS DURING CONTINUOUS SETTING OPERATION. (STRETCH 150/34 PET PHT = 220 °C; 14.6% O.F.)

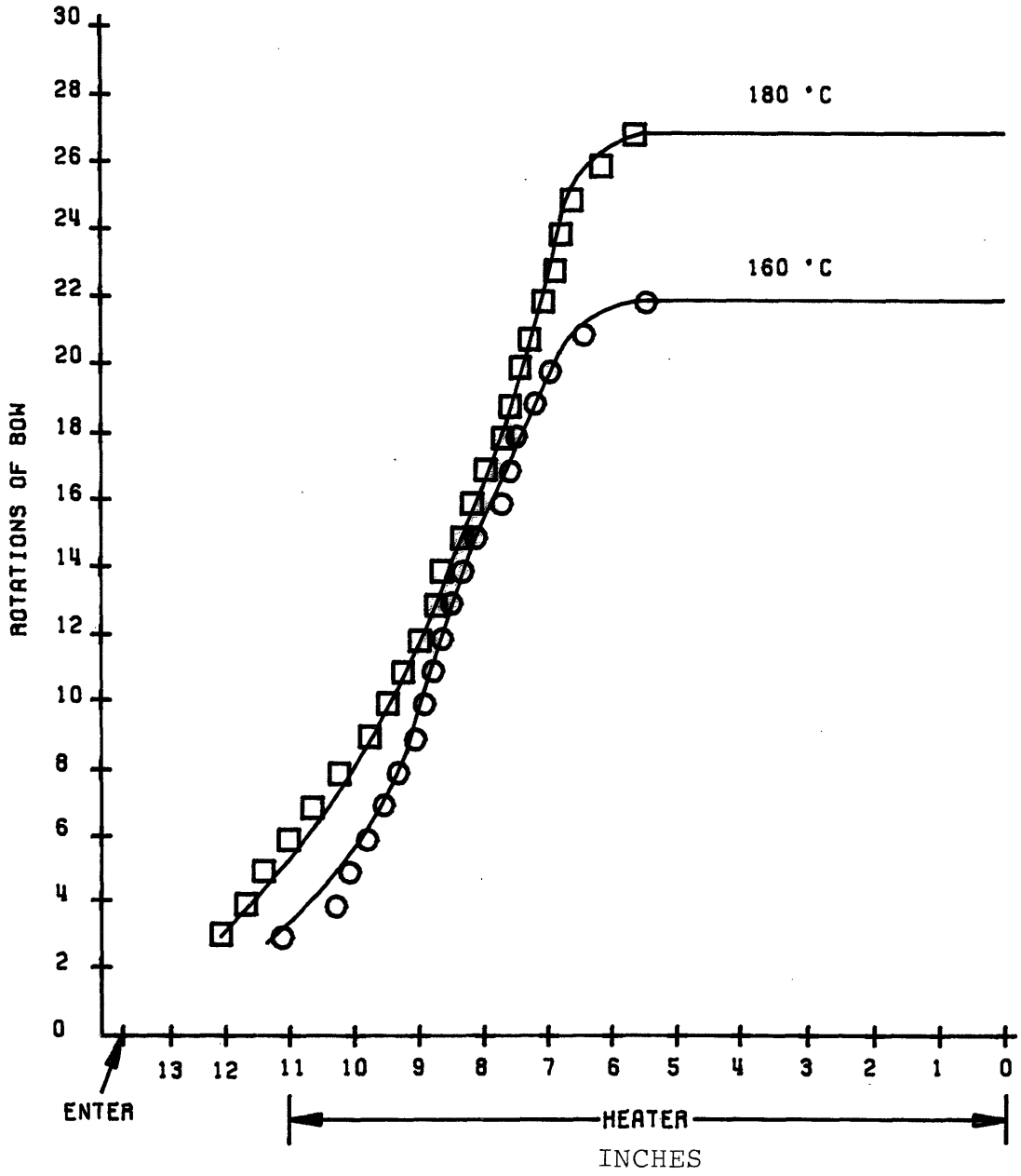

FIGURE 83B: BOW ROTATIONS DURING CONTINUOUS SETTING OPERATION. (STRETCH 150/34 PET PHT = 190 °C; 14.6% O.F.)

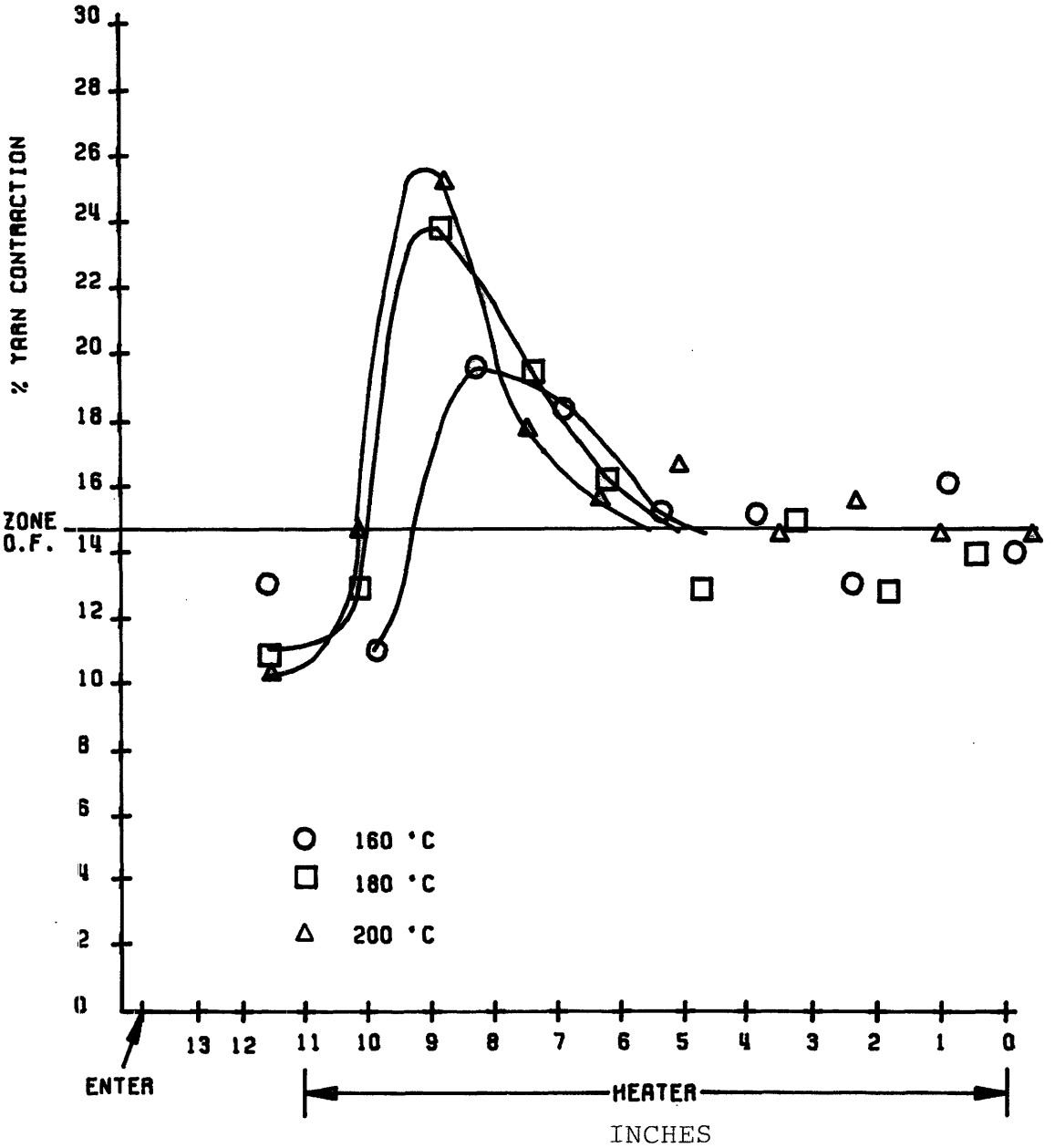

FIGURE 84A: YARN CONTRACTION DURING CONTINUOUS SETTING OPERATION. (STRETCH 150/34 PET, PHT = 220 °C; 14.6% O.F.)

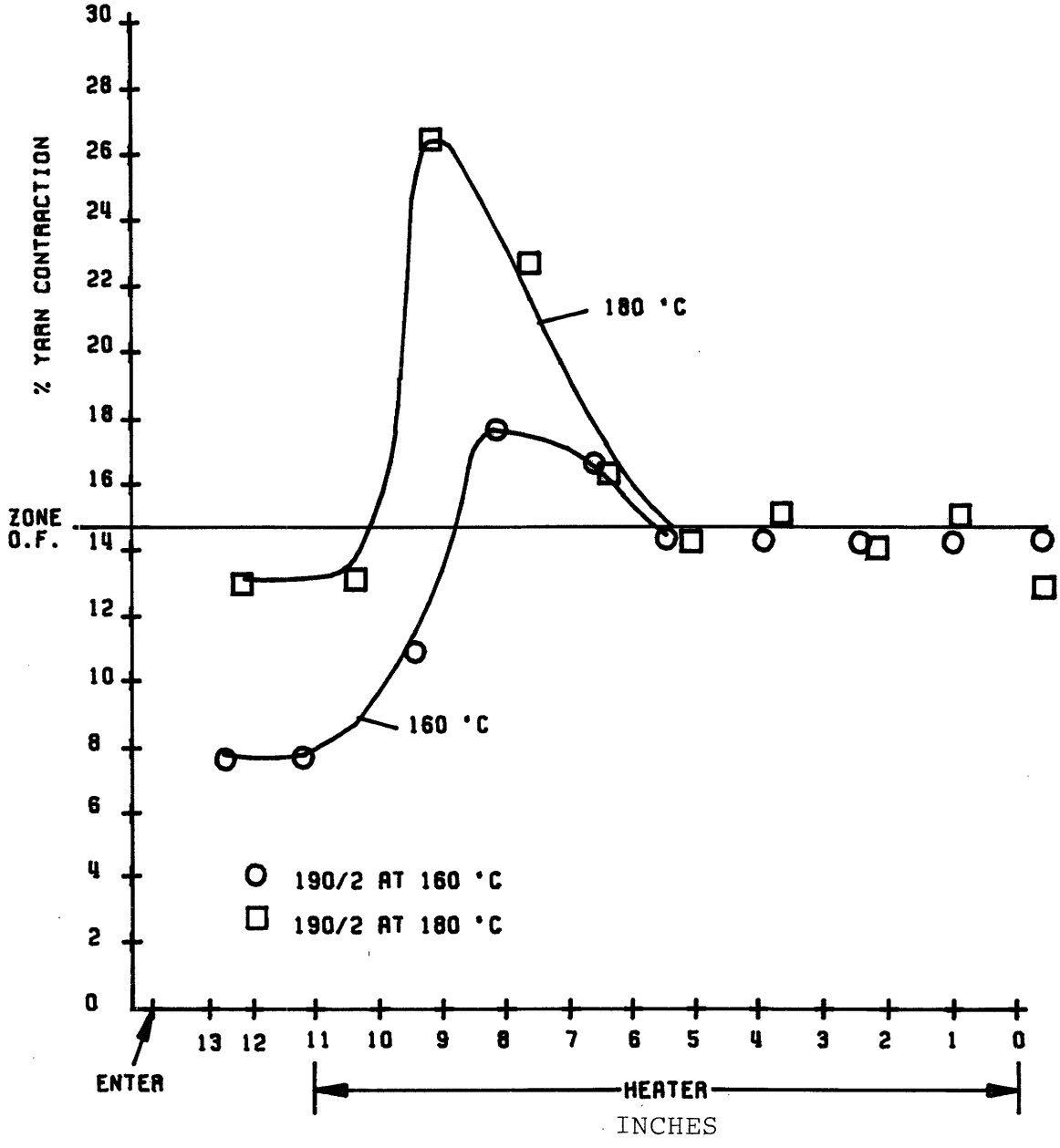

FIGURE 84B: YARN CONTRACTION DURING CONTINUOUS SETTING OPERATION. (STRETCH 150/34 PET, PHT = 190 °C; 14.6% O.F.)

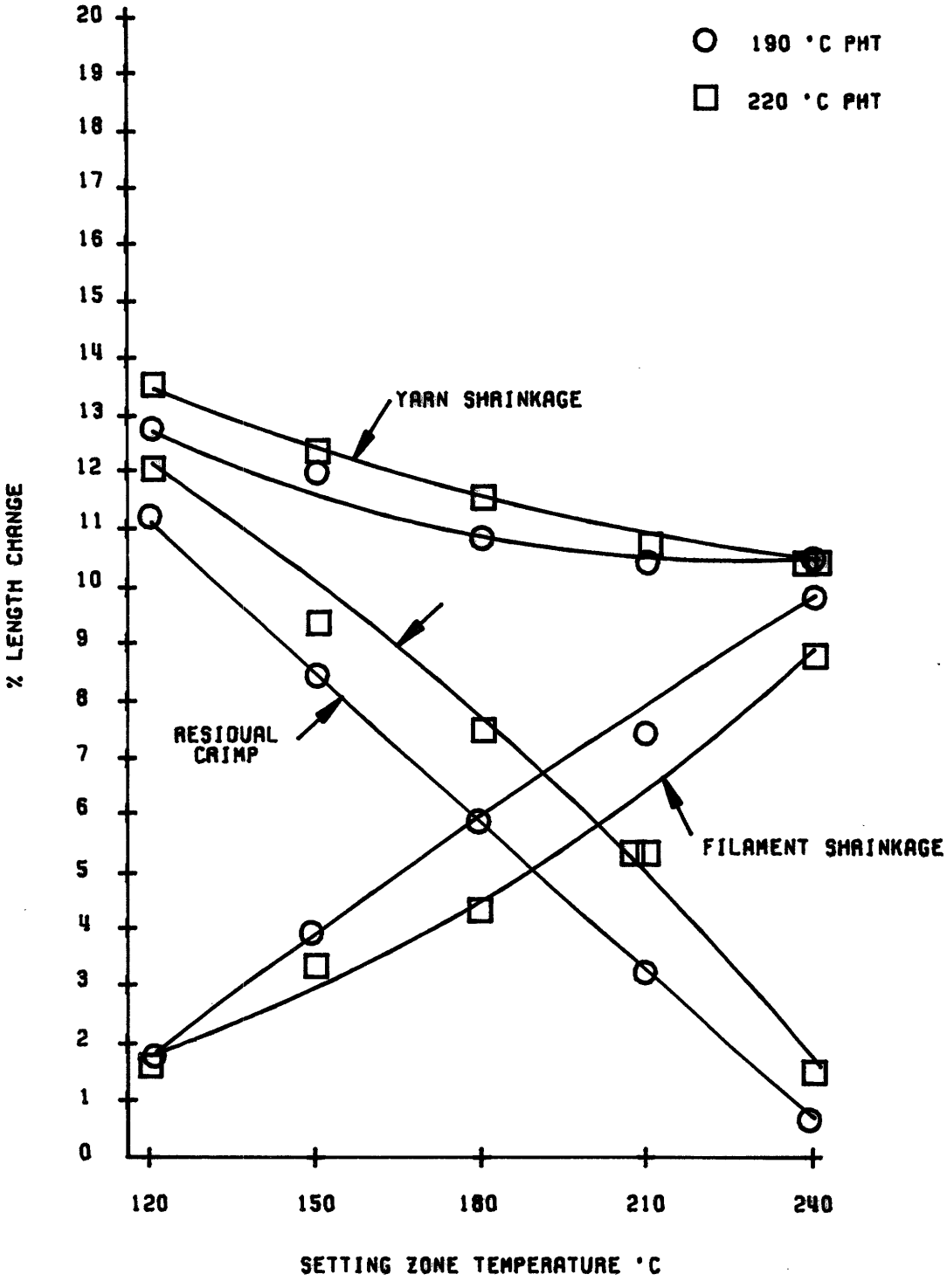

FIGURE 85: CHANGES IN YARN LENGTH AFTER SETTING AT 14.6 % OVERFEED. (UNIFI SAMPLES TEXTURED AT 190 °C AND 220 °C, 150/34 PET)

20-30°C lower temperatures.

More complete bow rotation information was obtained at 21.2% O.F. and 6.9% O.F. as shown in Figs. 86 and 87. In Figs. 86a,b the bow rotations for both yarns are seen to increase with setting zone temperature. The rotations at 150°C are about equal; at 180°C, the 190°C PHT yarn is torque relieved more completely and uptwists higher than the 220°C PHT yarn at the same temperature. At and above 210°C, the 220 and 190°C PHT yarns are torque relieved and develop about 11 and 8 TPI of retwist, respectively. The higher retwist is associated with better setting during texturing thereby giving a yarn with higher torque.

In contrast, at 6.9% overfeed (Fig. 87) the yarns show maximum bow rotations at intermediate setting temperature (180°C). At setting temperatures of 210°C and higher, filament shrinkage will be nearly equal to the total yarn contraction allowed by the zone overfeed, thus raising the zone tension. It is expected that this higher tension will reduce uptwisting by increasing the tension-induced untwisting torque shown in Fig. 66d. The bow rotations drop faster at 210°C and above for the 190°C PHT yarn, since it shrinks more than the 220°C PHT yarn at these temperatures.

Figures 88 and 89 show the associated length changes of the yarns during processing at these overfeeds. As the temperature is increased above T_g (120 → 150°C), the residual crimp falls rapidly at 6.9% overfeed, but not at 21.2%

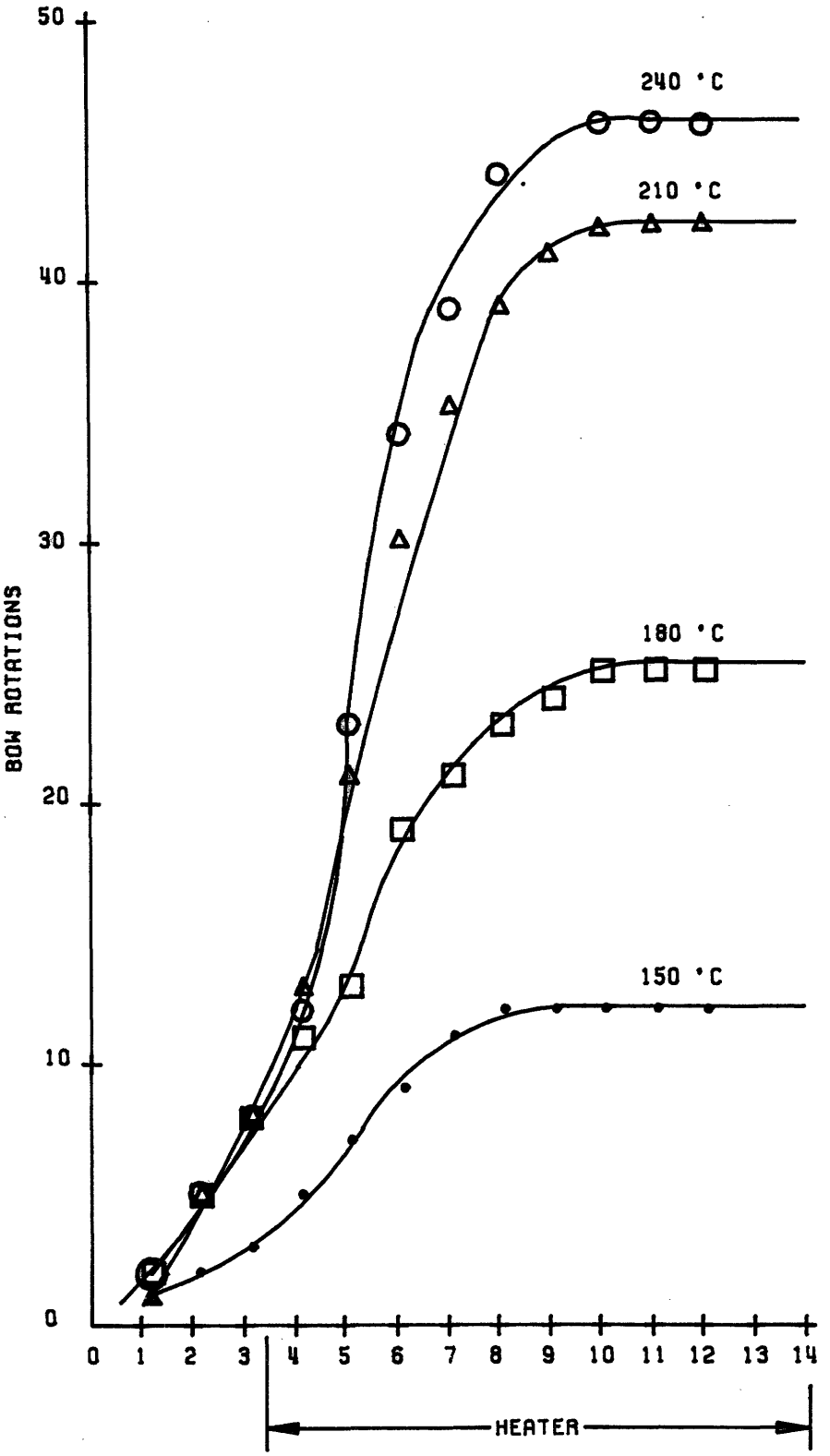

FIGURE 86A: BOW ROTATIONS DURING CONTINUOUS SETTING OPERATIONS. (UNIFI STRETCH, PHT=220 °C, 150/34 PET; 21.2% O.F.)

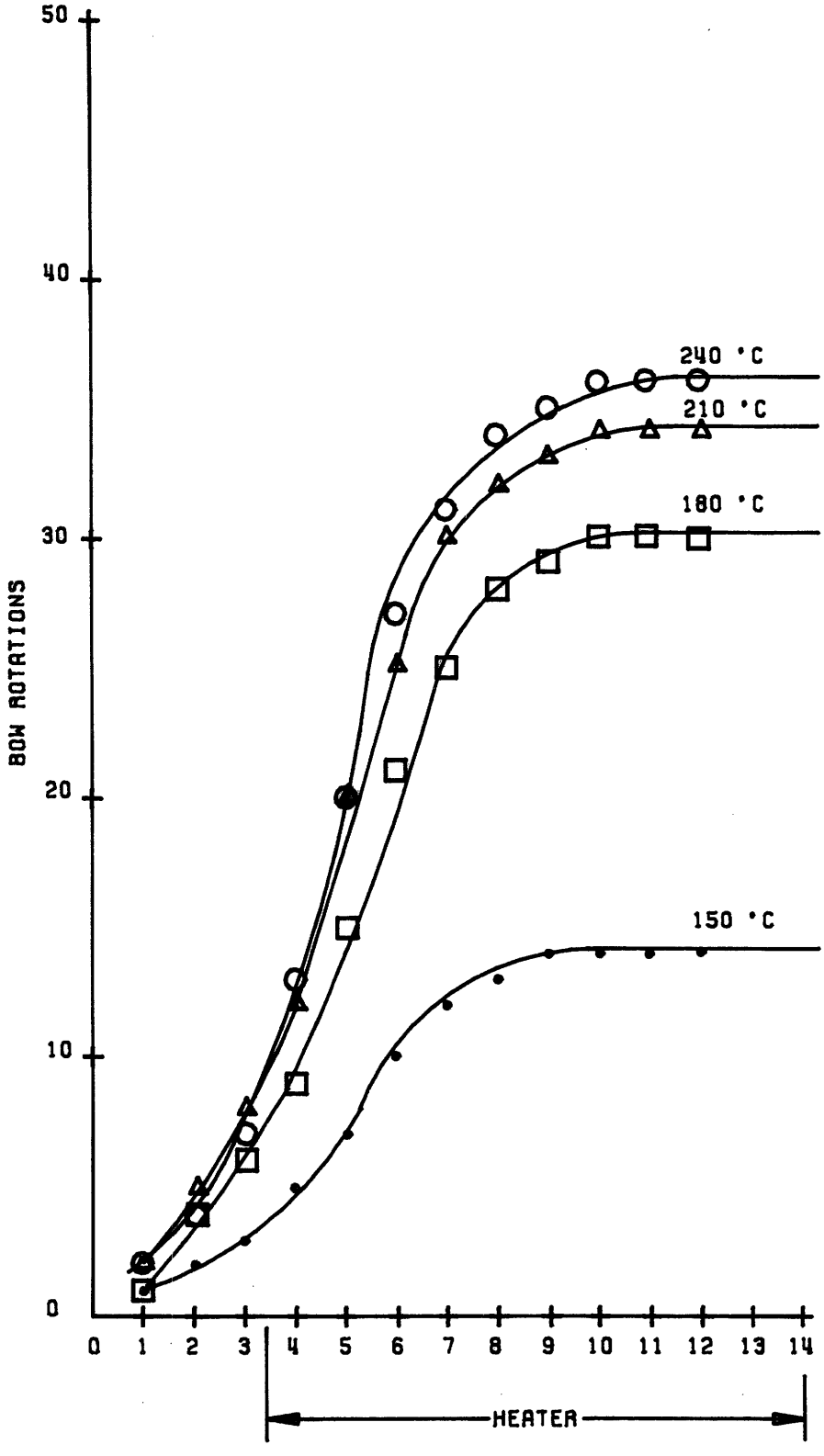

FIGURE 86B: BOW ROTATIONS DURING CONTINUOUS SETTING OPERATIONS. (UNIFI STRETCH, PHT=190 °C, 150/34 PET; 21.2% O.F.)

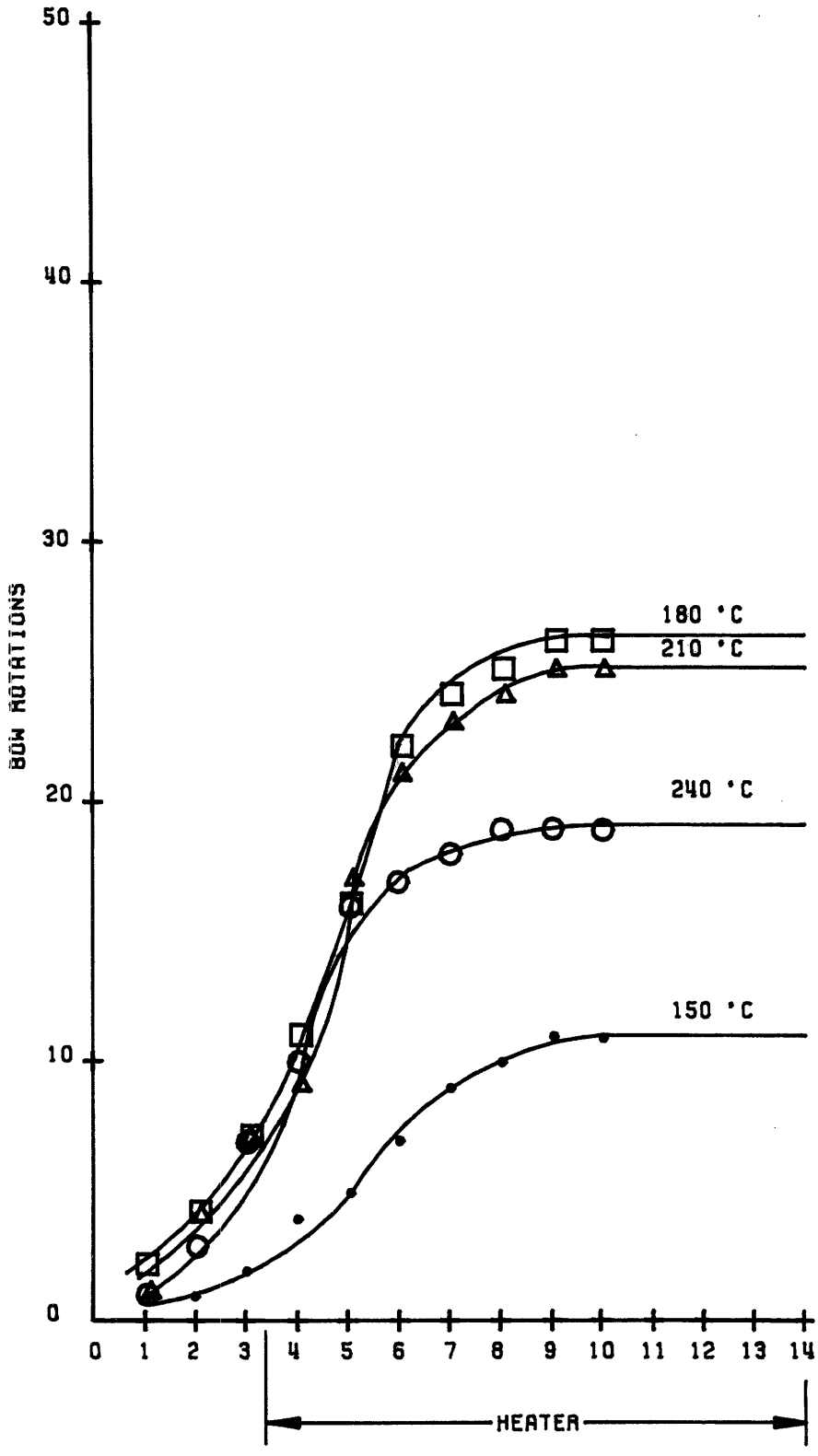

FIGURE 87A: BOW ROTATIONS DURING CONTINUOUS SETTING OPERATIONS. (UNIFI STRETCH, PHT=220 °C, 150/34 PET; 6.9 % O.F.)

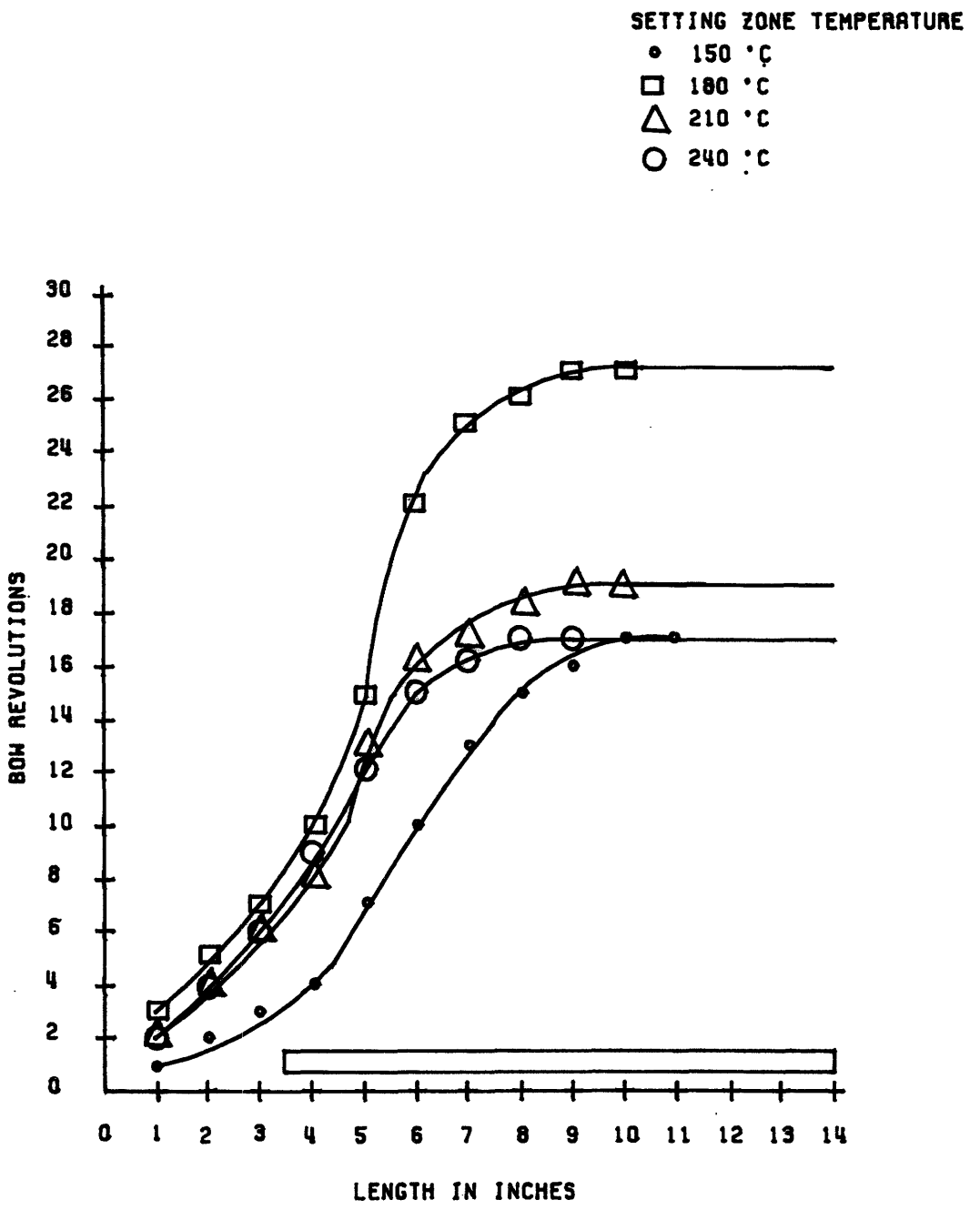

FIGURE 87B: BOW ROTATIONS DURING CONTINUOUS SETTING OPERATION. (UNIFI STRETCH, PHT = 190 °C, 150/34, PET; 6.9 % OVERFEED

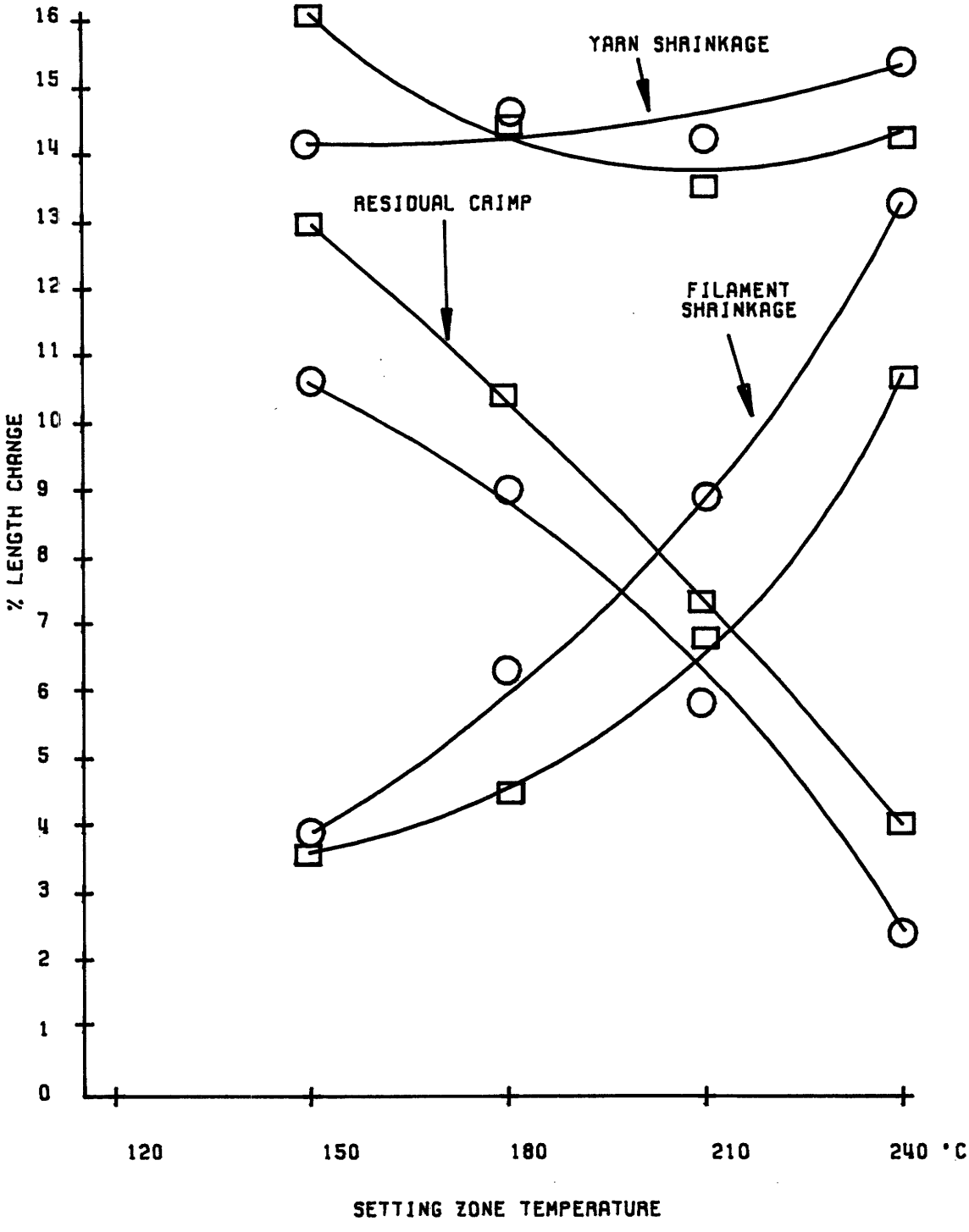

FIGURE 88: CHANGE IN YARN LENGTH AFTER SETTING AT 21.2% OVERFEED. (UNIFI SAMPLES, PHT=190 °C AND 220 °C, 150/34, PET)

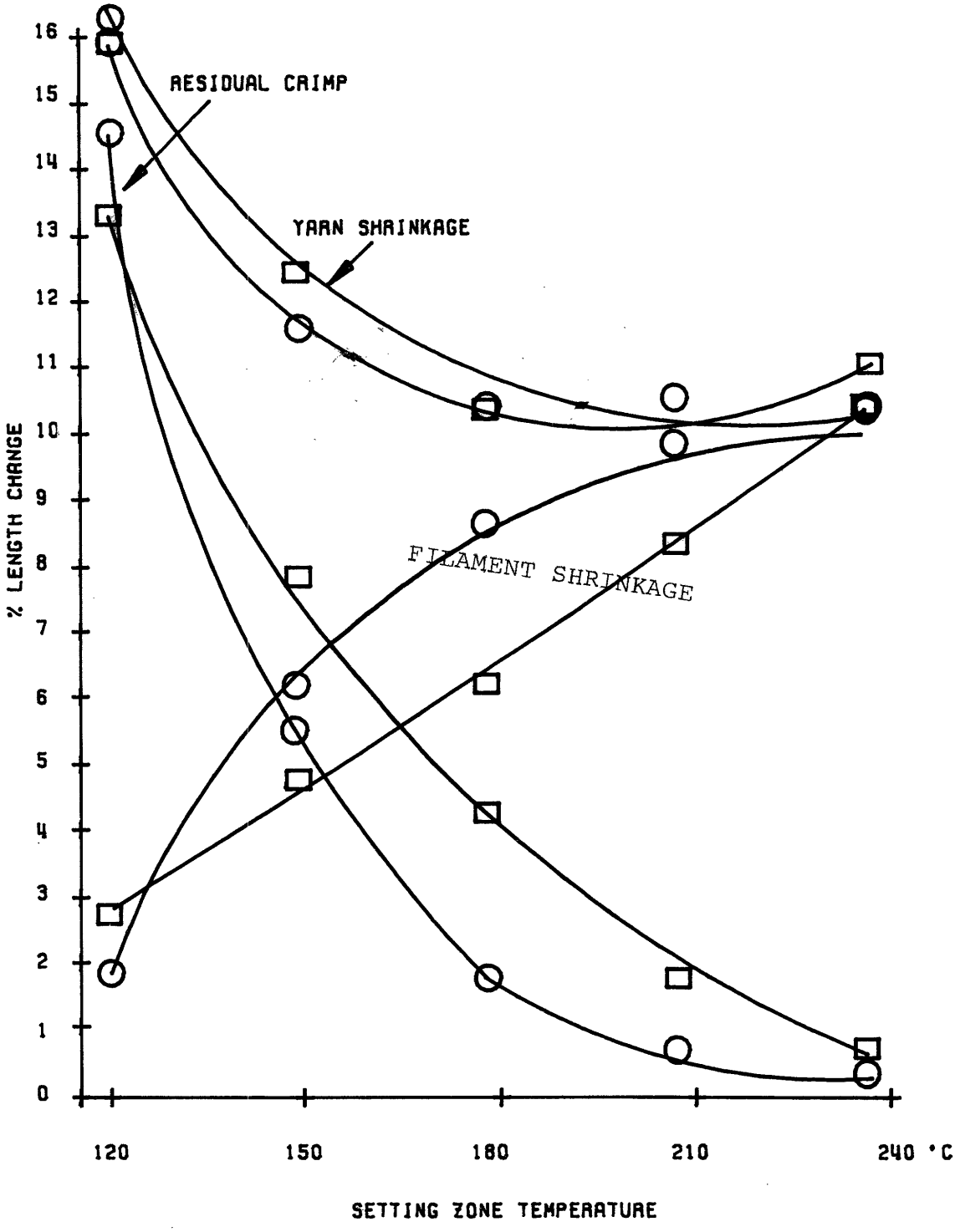

FIGURE 89: CHANGE IN YARN LENGTH AFTER SETTING AT 6.9 % OVERFEED. (UNIFI SAMPLES, PHT=190 °C AND 220 °C, 150/34, PET)

overfeed. The filament shrinkages are about 3% at both overfeeds at 150°C setting temperature, so the desetting is not related to additional shrinkage. The tension is much higher at 6.9% O.F. than at 21.2% O.F. This higher tension acting on the warm yarn will deset the yarn by mechanically pulling out the crimp.

The summary of residual crimp, filament shrinkage, and yarn contraction data for these two samples, with variations in PHT, are in Figs. 90, 91, and 92.

C. Observations of Yarn Behavior During Continuous Thermomechanical Treatments. Set Yarns with Texturing Variations. In the previous section, we saw that PHT differences in stretch yarns produced large differences in the yarn's behavior during a continuous setting operation. The following set of experiments was carried out on 9 of the 13 stretch textured yarns with controlled variations in texturing machine settings, as used in Chapter II. The 9 yarns selected were textured at the extreme values of machine settings (i.e. PHT, SHT, Draw Ratio, D/Y).

Figure 93 shows the average values of filament shrinkage and residual crimp for the 9 yarns. The yarn shrinkage is approximately 12%. This indicates that the setting zone tension was less than the 3.5 mgpd load used to measure the yarn shrinkage. The residual crimp and filament shrinkage show the now familiar interchange as the temperature is increased. The behavior of set yarns (Fig. 93) to a third

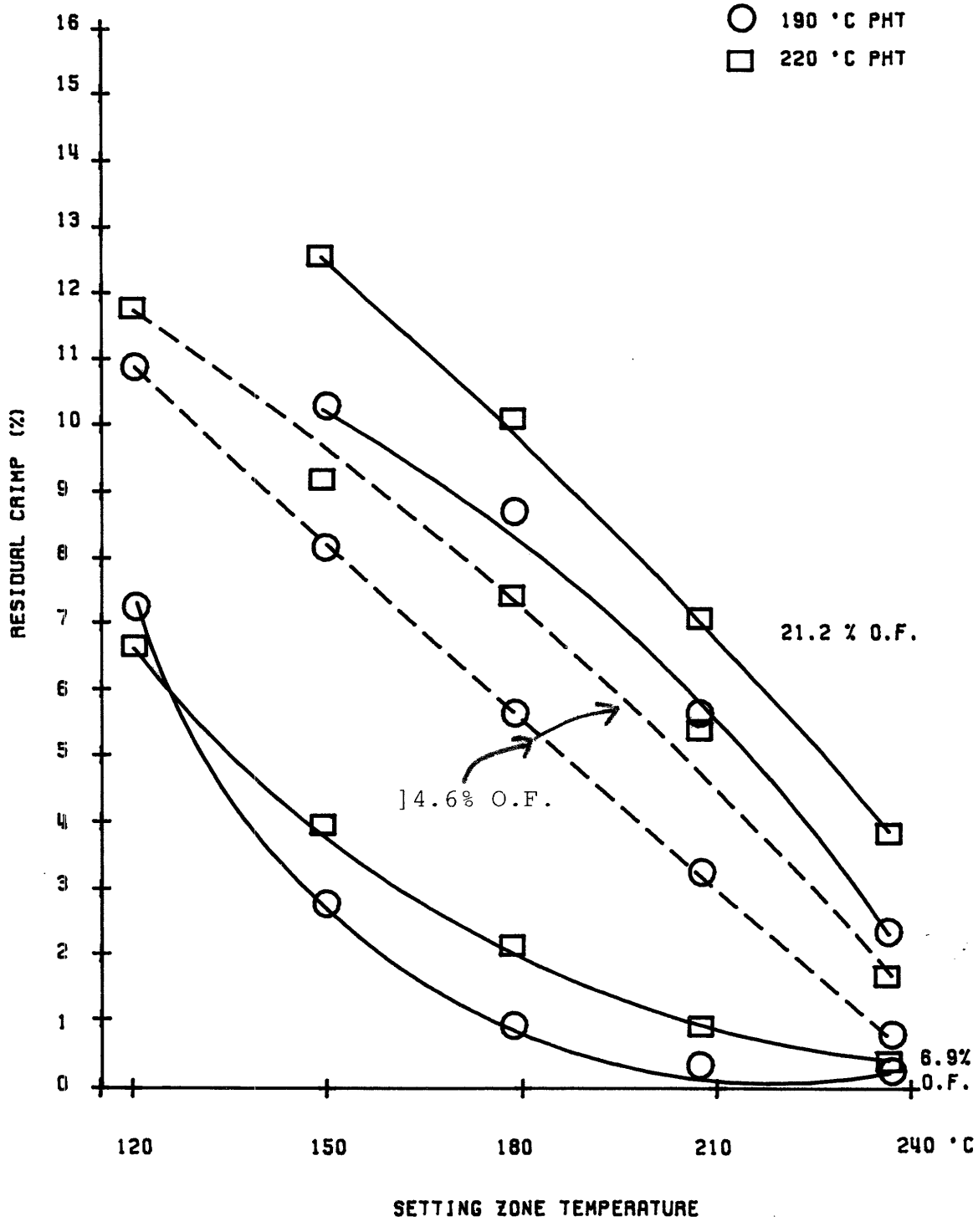

FIGURE 90: RESIDUAL CRIMP AS A FUNCTION OF SETTING ZONE OVERFEED AND TEMPERATURE. (UNIFI SAMPLES, PHT=190 °C AND 220 °C, 150/34, PET; 3 mgpd ⟶ 100 mgpd

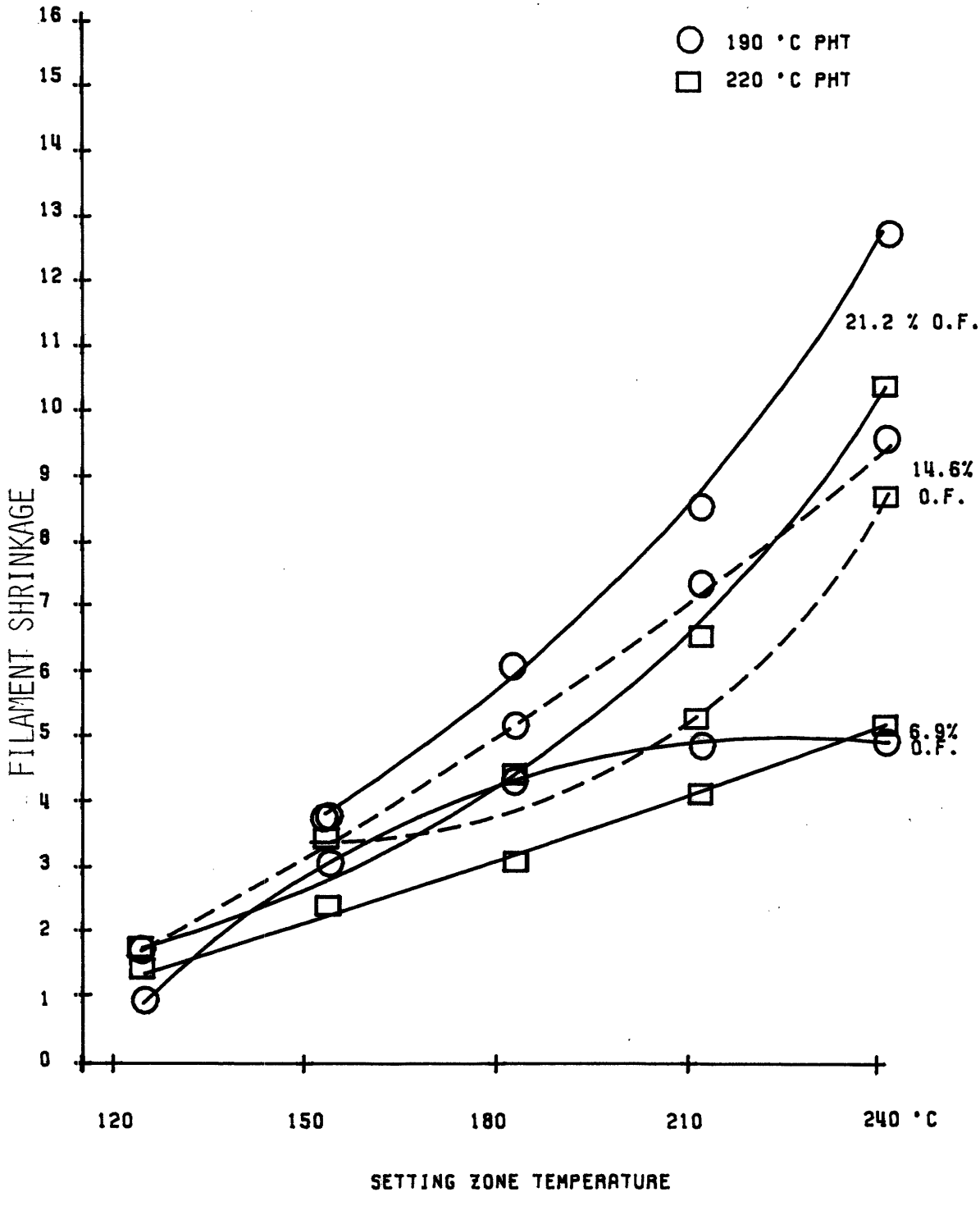

FIGURE 91: FILAMENT SHRINKAGE AS A FUNCTION OF SETTING ZONE OVERFEED AND TEMPERATURE. (UNIFI SAMPLES, PHT=190 °C AND 220 °C, 150/34, PET: 100 mgpd BEFORE ⟶ 100 mgpd AFTER)

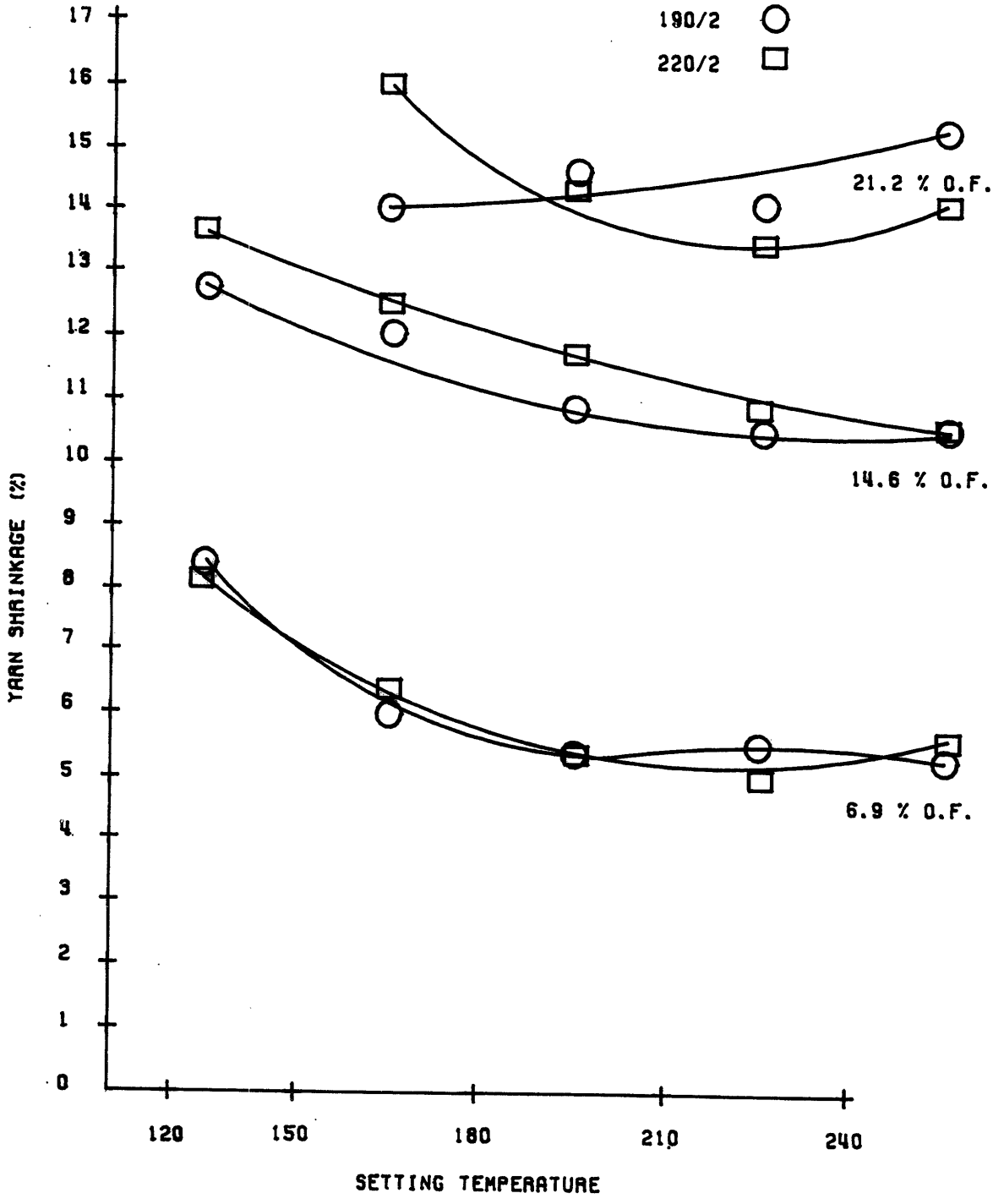

FIGURE 92: YARN SHRINKAGE AS A FUNCTION OF SETTING ZONE OVERFEED AND TEMPERATURE. (UNIFI SAMPLES, PHT = 190 °C AND 220 °C, 150/34, PET; 100 mgpd BEFORE ⟶ 3mgpd AFTER)

heat treatment can be compared with the behavior of stretch yarns (Fig. 85) to the same heat treatment. The set yarns (Fig. 93), as a result of their second heat treatment, retain more residual crimp and shrink less than the stretch yarns. For example, the crossover temperature (residual crimp = filament shrinkage) of set yarns (Fig. 93) is 215°C, compared to 195°C for the stretch yarns (Fig. 85). The second heat treatment that these yarns received at 185°C $\pm$ 10°C has stabilized the fiber fine structure by removing some of the shrinkage at low temperatures. Note that both sets of yarns shrink about 9.5% at 240°C when processed at 14.6% overfeed.

The behavior of the individual yarns with texturing variations is of interest, since we have seen that these yarns show differences in fabric appearance and large differences in measured yarn contraction at fixed load (1 mgpd) and temperature (150°C) using the testing instrument of Chapter II.

Figures 94 and 95 show the filament shrinkage and residual crimp after processing the yarns at 14.6% O.F. and 210 and 240°C, respectively. No significant differences in behavior were found at the lower treatment temperatures (i.e. 150°C, 180°C).

In Fig. 94, we see that primary texturing heater temperature, at which a yarn was previously processed, is the strongest factor in determining the yarn's residual crimp and filament shrinkage during subsequent thermo-

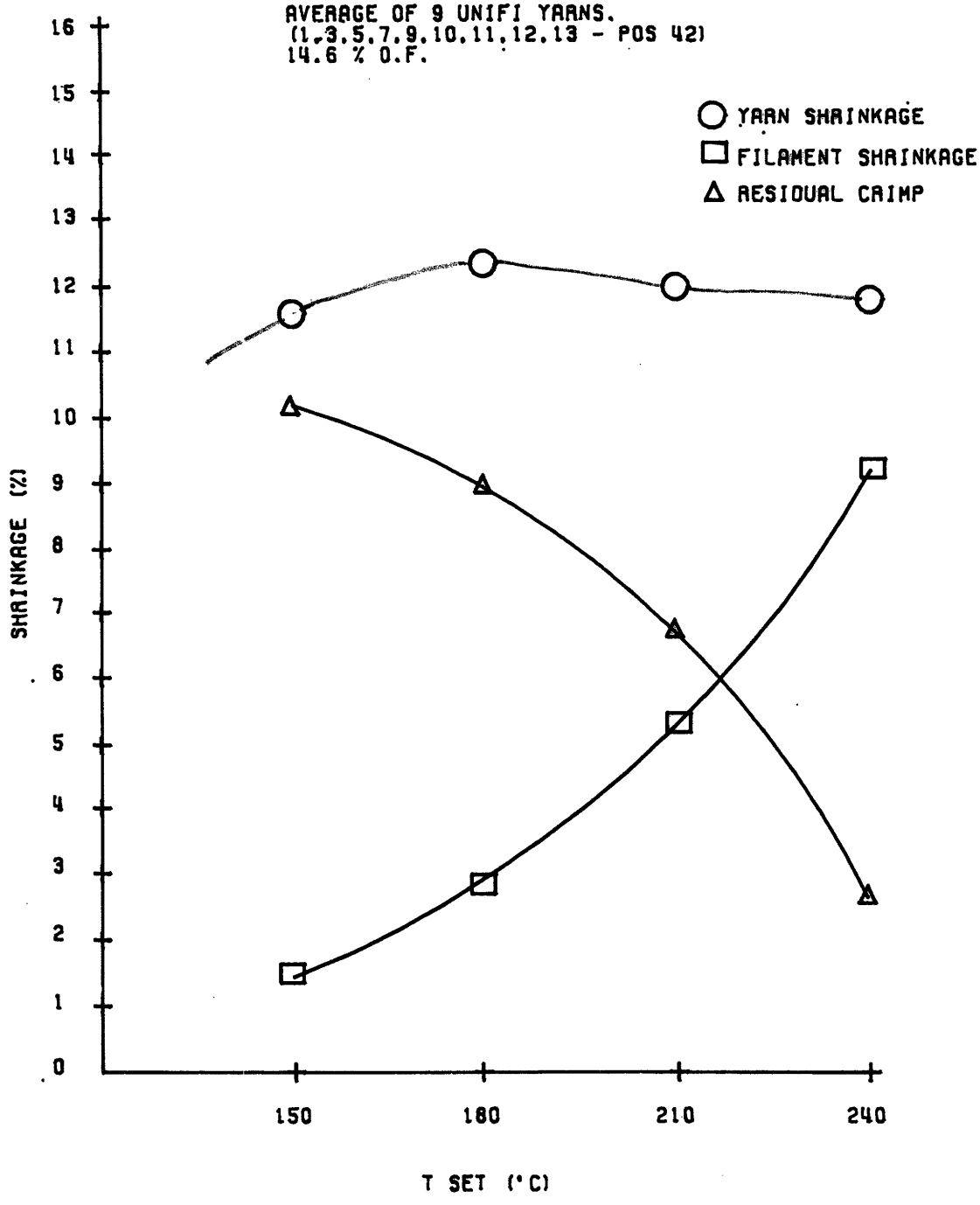

FIGURE 93: CHANGES IN YARN LENGTH OF SET YARNS AFTER A SECOND SETTING OPERATION. (AVERAGES FOR CONTROLLED VARIATION SAMPLES, 150/34, PET; 14.6 % O.F.)

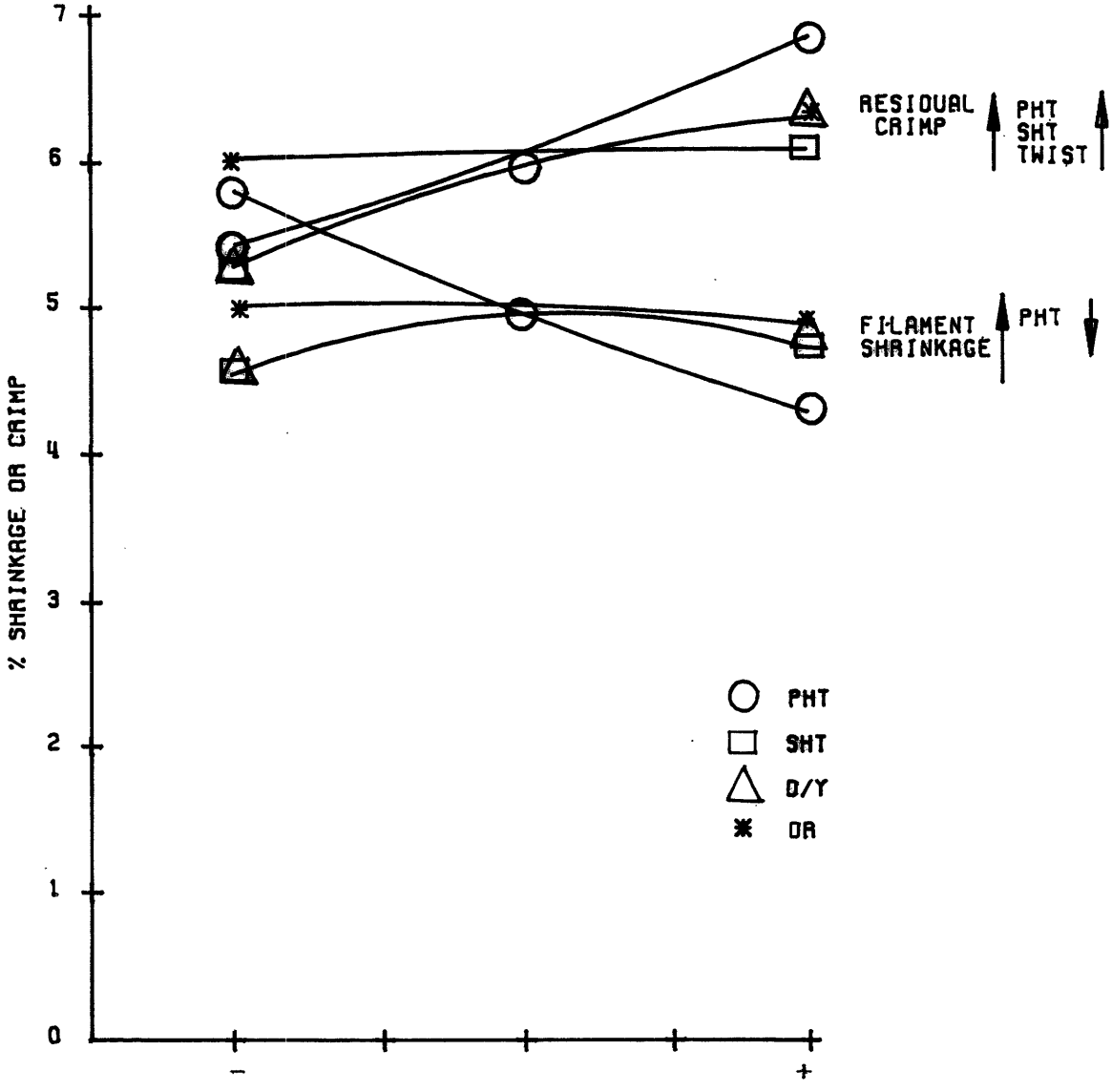

FIGURE 94: EFFECT OF TEXTURING VARIATIONS ON CHANGES IN YARN LENGTH AFTER A SECOND SETTING OPERATION. (UNIFI CONTROLLED VARIATION SAMPLES 150/34, PET; 14.6 % O.F., 210 °C)

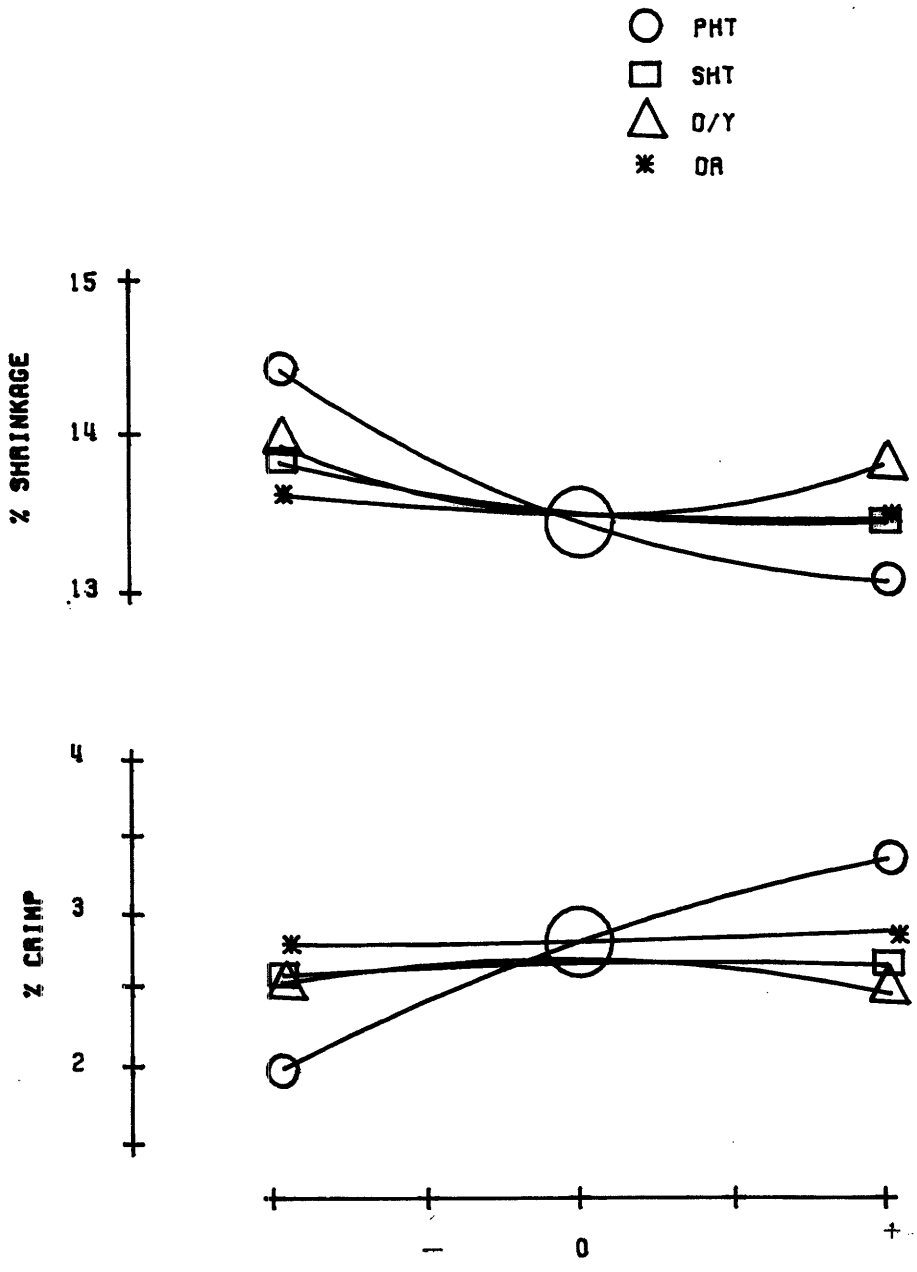

FIGURE 95: EFFECT OF TEXTURING VARIATIONS ON CHANGES IN YARN LENGTH AFTER A SECOND SETTING OPERATION. (UNIFI CONTROLLED VARIATION SAMPLES, 150/34, PET; 14.6 % O.F., 240 °C)

mechanical testing. Lowering the machine draw ratio and secondary heater temperature of a yarn during texturing also reduces the yarn's residual crimp. Figure 95 shows the dramatic reduction in residual crimp brought about by the increased filament shrinkage at 240°C. The primary heater temperature is the only texturing machine variation that produced significant differences in shrinkage or residual crimp.

4. Summary.

This chapter has reviewed the changes in properties of textured yarns produced by thermomechanical treatments of the yarns. Yarn temperature, yarn extension (or contraction), and time of treatment were found to be the factors governing the changes in properties of the textured yarns or the forces that develop during the treatments. The major changes in properties occurred during the first 0.6 - 2 seconds of heating.

As a complement to and as a means to understand the reported changes in yarn properties after thermomechanical treatments, the geometrical changes that occur during a thermomechanical treatment of a textured yarn were observed and measured. The yarn, during passage through a thermo-mechanical treatment, can be divided into four zones: the cold entry zone, the warming zone, the hot zone, and the cooled exit zone. Substantial differences in yarn twist and contraction were found to exist between the various zones. The yarn twist distribution was found to be consistent with the

existence of a "pseudo-spindle". Yarn contraction was highest in the warming zone. Twist non-uniformities that could lead to the tight spots reported by Lünenschloss et al. [140] were observed. Several results of note were obtained during simulations of the setting operation on a texturing machine.

The reduction in residual crimp of a textured yarn produced by such a thermomechanical treatment was found to be proportional to the amount of filament shrinkage during the treatment. The sum of residual crimp and filament shrinkage (as measured at the tension and torque of the threadline during the treatment) was found to equal the imposed overfeed of the treatment as required by length continuity.

Although no closed form solutions for the mechanics and geometry of a textured yarn during a thermomechanical treatment were obtained, the governing equations and boundary conditions for a four-zone model of such a treatment have been developed. The major obstacle in using these equations is the lack of constitutive relations for the textured yarn (i.e. the torque and tension as a function of the yarn's temperature, time, twist, and elongation). Qualitative explanations of the observed phenomena have been developed using preliminary data on the yarn torque and contraction as a function of temperature and time at constant load and twist [142].

REFERENCES

1. Pratt, H., Knit Barré--Causes and Cures, p. 3, Proc. AATCC Symposium, May 25-26, 1972, New York, N.Y.

2. Pratt, H., "Some Causes of Barré", Knitting Times, pp. 18-22 (June 13, 1977).

3. Klaeui, H., "Streaks in Warp Knitting", pp. 96-97, in Knit Barré--Causes and Cures, Proc. AATCC Symposium, May 25-26, 1972, New York, N.Y.

4. Hale, R.P., "A Simulation of Stripiness in Fabrics Made from Textured Yarns", JTI 66, p. 62 (1975).

5. Morizane, H., Suda, Y., Nakajima, F., "A Study on the Dyeing Behavior of a Model Fiber for a False Twisted Nylon Yarn with a Disperse Dye", Sen-i Gakkaishi 29, pp. T8-T13 (1973).

6. Vaidya, A.A., Nigam, J.K., "Minimizing Barriness in Textured Nylons", Textile Inst. and Ind. 15(3), pp. 96-101 (1977).

7. Holfeld, W.T., Pratt, H.T., "Moiré: Troublemaker in Knits", Amer. Dyestuff Reporter 61, 0. 58 (1972).

8. Grant, J., "Laboratory Analysis of Barré in Textured Polyester Doubleknit Fabric", pp. 12-14, in Knit Barré--Causes and Cures, Proc. AATCC Symposium, May 25-26, 1972, New York, N.Y.

9. Blore, James, "Knitting Machine Variables that Cause

Barré", pp. 87-89, in Knit Barré--Causes and Cures, Proc. AATCC Symposium, May 25-26, 1972, New York, N.Y.

10. Holfeld, W.T., Nash, J.L. Jr., "Knitting Machine Barré--A Multi-Fiber Problem", Can. Text. J. 93(1), pp. 67-73 (1976).

11. Coryell, J.W., Phillips, B.R., "Identification of Barré Sources in Circular Knits", TYAA Fall Technical Meeting, Greensboro, North Carolina (1977).

12. Clements, J.L., "The Relationship of Dye Uniformity of False Twist Textured Polyester Yarns to Fabric Streakiness", Knitting Times 42(15), pp. 72-78 (1972).

13. Goldin, M., "The Effect of Primary Heater Temperature and Dye Energy on Fabric Dye Uniformity", TYAA Fall Technical Meeting, Greensboro, North Carolina (1977).

14. Clarke, J.L., "Warping and Its Influences on Fabric Streakiness", pp. 92-95, in Knit Barré--Causes and Cures, Proc. AATCC Symposium, May 25-26, 1972, New York, N.Y.

15. Thwaites, J.J., "Linear Density Variations in Draw Textured Yarns", JTI 65, p. 353 (1974).

16. Lutz, O., "The Effect of Pattern Selection on Barré", pp. 90, 91, in Knit Barré--Causes and Cures, Proc. AATCC Symposium, May 25-26, 1972, New York, N.Y.

17. Hale, R.P., "The Prediction of Stripiness due to Rogues

in Knitted Fabrics", JTI 67(4), p. 129 (1976).

18. Dodson, V.R., Private Communication.

19. Brown, P., "Measurement of Barré in Fabric Form", pp. 7-11, in Knit Barré--Causes and Cures, Proc. AATCC Symposium, May 25-26, 1972, New York, N.Y.

20. Kok, C.T., Kruger, P.J., Lake, R., Turner, R., Van der Vlist, N., "A Photoelectric Instrument for the Assessment of Fabric Appearance and Structure", JTI 66 (5), p. 186 (1975).

21. Hallada, D.P., Holfeld, W.T., "Nylon Fabric Uniformity", pp. 33-38, in Knit Barré--Causes and Cures, Proc. AATCC Symposium, May 25-26, 1972, New York, N.Y.

22. Egbers, G., Weinsdörfer, H., "Problems and Future Trends in Texturing", Paper presented at M.I.T., Program on Texturing of Thermoplastic Yarns, July 1977.

23. Shealy, O.L., Kitson, R.E., "An Age-Stable Feed Yarn for Draw Texturing by the False-Twisting Process", TRJ 45, pp. 112-117 (1975).

24. Walters, J.P., Buchanan, D.R., "Glass-Transition Temperatures of Polyamide Textile Fibers. Part II: Relationships Between T_g and Dyeability", TRJ 47, p. 451 (1977).

25. Deopura, B.L., Sinha, T.B., Varma, D.S., "Dependence of Mechanical Properties on Crystalline, Intermediate and Amorphous Phases in Poly(Ethylene Terephthalate)

Fibers", TRJ 47, p. 267 (1977).

26. Beck, G.T., "Fiber Density as a Quality Control Method", TYAA Winter Technical Conference, Greensboro, North Carolina (1977).

27. Galil, F., "Studies in Polyester Fiber Morphology and Related Dyeing and Finishing Properties by the Critical Dissolution Time (CDT) Technique", TRJ 43, p. 615 (1973).

28. Dumbleton, J.H., Bell, J.P., Murayama, T., "The Effect of Structural Changes on Dye Diffusion in Poly(Ethylene Terephthalate)", J. Applied Poly. Sci. 12, pp. 2491-2508 (1968).

29. Klein, H., "Das Färben von Materialien aus Texturiertem Polyester unter Besonderer Berücksichtigung des Barré--Effektes", Chemiefasern 20(6), p. 473 (1970).

29A. Beckmann, W., Langheinrich, K., "Schwierigkeiten beim Färben von texturierten Polyesterfäden - Auswirkung auf Farbstoffauswahl und Anwendungstechnik", Melliand Textilberichte 51, pp. 316-321 (1970).

30. Prevorsek, D.C., Harget, P.J., Sharma, R.K., Reimschuessel, A.C., "Nylon 6 Fibers: Changes in Structure Between Moderate and High Draw Ratios", J. Macromolecular Sci. B8(1-2), p. 127 (1973).

31. Williams, J.L., Peterlin, A., "Transport Properties of

Methylene Chloride in Drawn Polyethylene as a Function of the Draw Ratio", J. Polymer Sci. A-2(9), p. 1483 (1971).

32. Sweet, G.E., Bell, J.P., "Relations Between Dye Diffusion and Fiber Structure in Nylon 6", TRJ 46, p. 447 (1976).

33. Hearle, J.W.S., Miles, L.W.C., Eds., The Setting of Fibres and Fabrics (1971), Merrow Publishing Company, Watford Herts, England.

34. Wilson, M.P.W., "Shrinkage and Chain Folding in Drawn Poly(Ethylene Terephthalate) Fibers", Polymer 15, p. 277 (1974).

35. Prevorsek, D.C., Butler, R.H., Lamb, G.E.R., "Influence of Fiber Properties on Wrinkling Behavior of Fabrics. Part V: Settability and Measurement of the Degree of Set in Yarns and Filaments", TRJ 45, p. 535 (1975).

36. Shishoo, R., Bergh, K., "Investigation of Degree of Set and Deset for PET and Nylon 66 Yarns", TRJ 47, p. 56, (1977).

37. Blankenstein, W.E., "Statistical Analysis of the Two-Stage (Autoclave) Process for Set-Textured Polyester", pp. 46-53, in Knit Barré--Causes and Cures, Proc. AATCC Symposium, May 25-26, 1972, New York, N.Y.

38. Vidhani, K., Nutting, T.S., "Bulked and Stretch Yarns

of Nylon 6.6 Produced by the False-Twist Process: A Comparison of Parent and Post-Treated Yarns, JTI 52(9), pp. 449-470 (1961).

39. Beck, G.T., "Fiber Density as a Quality Control Tool", pp. 68-70, in Knit Barré--Causes and Cures, Proc. AATCC Symposium, May 25-26, 1972, New York, N.Y.

40. Stein, W., Wallas, K., "Relationship Between the Properties of Textured Polyester Yarns and Knitwear Made Therefrom", Chemiefasern/Textil-industrie 23/75(8), p. 707 (1973).

41. Conkle, R., Private Communication.

42. Best, A., "Critical Dissolution Time as a Tool for Fabric Defect Analysis", Paper presented at the TYAA Spring Technical Conference, Greensboro, North Carolina (1977).

43. Greenwood, K., "The control of yarn quality in friction texturing", Chemiefasern/Textil-industrie 26/78, pp. 401-407 (1976). In German, English Translation E76-E83.

44. Backer, S., Yang, W-L., "Mechanics of Texturing Thermoplastic Yarns. Part I: Experimental Observations of Steady-State Texturing", TRJ 46, pp. 599-610 (1976).

45. Backer, S., Yang, W-L., "Mechanics of Texturing Thermoplastic Yarns. Part II: Experimental Observations of Transient Behavior", TRJ 46, pp. 724-733 (1976).

46. Backer, S., Brookstein, D., "Mechanics of Texturing Thermoplastic Yarns. Part III: Experimental Observations of Torsional Behavior of the Texturing Threadline", TRJ 46, pp. 802-809 (1976).

47. Thwaites, J.J., "Mechanics of Texturing Thermoplastic Yarns. Part IV: The Origin and Significance of the Torsional Behaviour of the False-Twist Threadline", Cambridge University Engineering Department, England, September 1974.

48. Backer, S., Brookstein, D., "Mechanics of Texturing Thermoplastic Yarns. Part V: Steady State Mechanics of Draw Texturing", TRJ 47, pp. 256-266 (1977).

49. Backer, S., Brookstein, D., "Mechanics of Texturing Thermoplastic Yarns. Part VI: Transient Mechanics of Draw Texturing", TRJ 47 (in press) (1977).

50. Bell, C.E., Backer, S., "Mechanics of Texturing Thermoplastic Yarns. Part VII: Cyclic Behavior During Pin-Spindle False Twist Texturing", submitted to TRJ for publication.

51. Naar, R.Z., "Steady-State Mechanics of the False-Twist Yarn Texturing Process", Sc.D. Thesis, M.I.T., Cambridge, Massachusetts (1975).

52. Brookstein, D., "On the Dynamics of Draw Texturing", Sc.D. Thesis, M.I.T., Cambridge, Massachusetts (1976).

53. Tayebi, A., "The Mechanics of False-Twist Textured Yarns", Sc.D. Thesis, M.I.T., Cambridge, Massachusetts (1973).

54. Bell, C.E., "Transient Phenomena in False Twist Texturing, M.S. Thesis, Department of Mechanical Engineering, M.I.T., Cambridge, Massachusetts (1976).

55. Thwaites, J.J., "Dynamic Behavior of the False-Twist Process", Paper presented at M.I.T. Summer Course on Mechanics of Texturing Thermoplastic Yarns (1977).

56. Thwaites, J.J., "The Mechanics of the False Twist Threadline", Paper presented at M.I.T. Summer Course on Mechanics of Texturing Thermoplastic Yarns (1977).

57. McGregor, R., Adeimy, J.A., "The Response of Textured Yarn Properties to Process Variables in Relation to Barré. Part I: Experimental Design and Dyeing Responses for Conventional False-Twist Pin-Textured Polyester Yarns", TRJ 47, pp. 477-484 (1977).

58. McGregor, R., Adeimy, J.A., "The Response of Textured Yarn Properties to Process Variables in Relation to Barré. Part II: Effects of Feed-Yarn Orientation and Correlations between Yarn Responses", TRJ 47, pp. 516-522 (1977).

59. McGregor, R., Grady, P.L., Montgomery, T., Adeimy, J.A., "The Response of Textured Yarn Properties to Process Variables in Relation to Barré. Part III: Thermo-

mechanical Measurements on Conventional False-Twist Pin-Textured Polyester Yarns", TRJ 47, pp. 598-603 (1977).

60. Hardegree, G.L., Buchanan, D.R., "Physical Properties of Textured Polyester Yarns: The Influence of Texturing Temperatures, TRJ 46, pp. 828-833 (1976).

61. Lünenschloss, J., Kirschbaum, E., "Die Temperaturmessung am laufenden Faden beim Falschdrahttexturieren mit hohen Geschwindigkeiten", Chemiefasern/Textilindustrie 25/77, pp. 937-940 (1975).

62. Morris, W.J., "Rates of Setting in Draw-Texturing", Publication of Shirley Institute, England.

63. Gupta, V.B., Natarajan, M., "Latent Crimp in False-Twist-Textured Polyethylene Terephthalate Yarn", TRJ 46, pp. 417-419 (1976).

63A. Gupta, V.B., "The Role of Winding Tension in Rendering Crimp Latent in False-Twist-Textured Yarn", TRJ 47, pp. 634-635 (1977).

63B. Familant, H.M., "Dependence of Latent Crimp on Wind-up Tension in the False-Twist Texturing Process", TRJ 47, pp. 448-449 (1977).

64. Lünenschloss, J., Fischer, K., "Torsion and Draw Texturing", International Textile Bulletin, World Edition Spinning 2/77, p. 129.

65. Egbers, G., Weinsdörfer, H., "High Speed Friction Texturing of Polyester Yarns", Chemiefasern/Textil-industrie 27/79(5), pp. 403-406 (1977).

66. Gupta, V.B., Amirtharaj, J., "The Effect of Tension and Twist on the Structure and Dyeability of Textured Polyethylene Terephthalate Yarn", TRJ 46(11), p. 785 (1976).

67. Rosenthal, F., "The Application of Greenhill's Formula to Cable Hockling", J. Applied Mechanics 98(12), p. 681 (1976).

68. Backer, S., Smith, S.C., Bell, C.E., Brogna, C., Kumar, V., "Progress Report on Development of Improved Quality Control Techniques in Draw-Texturing of POY-PET", M.I.T. Fibers and Polymers Report, 3/20/76.

69. Smith, S.C., Bell, C.E., Backer, S., "Progress Report on Development of Improved Quality Control Techniques in Draw-Texturing of POY-PET", M.I.T. Fibers and Polymers Report, 6/30/76.

70. Ward, I.M., "Mechanical Behavior of PET", J. Macromolecular Sci.-Physics B1(4),(12), p. 667 (1967).

71. Lünenschloss, J., Fischer, K., Osswald, W., "Investigation of the processes in the texturing zone during conventional and draw-texturing", Chemiefasern/Textil-industrie 27/79, pp. 119-125 (1977).

72. Moussa, N.A., "Heat Transfer to a Moving Threadline",

Paper presented at M.I.T. Course on Texturing of Thermoplastic Yarns, M.I.T., Cambridge, Massachusetts, 1977.

73. Bauer, K., "Grenzen des Maschinenbaues in der Falschzwirn-Texturierung", Chemiefasern/Textil-industrie 26/78, pp. 879-884 (1976) (in German).

74. Lünenschloss, J., Fischer, K., "Twist Control During the False Twist Process", Paper presented at M.I.T. Course on Texturing of Thermoplastic Yarns, M.I.T., Cambridge, Massachusetts, 1977.

75. Mutschler, G., "Decisive Parameters for obtaining a constant yarn quality in friction texturing", Chemie-fasern/Textil-industrie 26/78, pp. 884-891 (1976).

76. Carruthers, G.A., Yarn-twist sensing instrument and method, BP 1,266,450, (9/5/1969.

77. Lünenschloss, J., Coll-Tortosa, L., Fischer, K., "Messung der Fadendrehung und ihrer Schwankungen am laufenden Faden während des Texturiervorganges", Chemiefasern/Textil-industrie 23/75, pp. 297-301 (1973).

78. Wegener, W., Coll-Tortosa, L., "Die Wirkungsweise von Friktionsbüchsen auf die Drallerteilung bei ver-schiedenen Einstellungen der FD-Maschine", Textil Praxis 29, pp. 918-920, 1043-1046 (1974).

79. Toray Industries, Inc., Twist Monitor Product Literature, Catalog L-TM-501-B2 (1976).

80. Schierenbeck, D., Sholly, W., "Automatic twist control in friction texturing", Modern Textiles 56(7), pp. 30-33 (1975).

81. F.M.K. Ltd., "TENSCAN", Tension Monitor System, Product Literature, London, England.

82. Dupeuble, J-C., "Advantages of Solid Ceramics in Friction Texturing", Chemiefasern/Textil-industrie 27/79, pp. 126-130 (1977) (English Edition).

83. Daubeny, R. deP., Bunn, C.W., Brown, C.J., "The Crystal Structure of Poly(ethylene terephthalate)", Proc. Roy. Soc. (London) A226, pp. 531-542 (1954).

84. Knox, B.H., Weigmann, H.D., Scott, M.G., "Interactions of Nonaqueous Solvents with Textile Fibers. Part V: Application of the Solubility Parameter Concept to Polyester Fiber-Solvent Interactions", TRJ 45, pp. 203-217 (1975).

85. Rosborough, E.I., "Study of 'Frozen-in Strain' or Temperature Set in Textile Fibers", JTI 65(3), pp. 133-139 (1974).

86. Akzona, Inc., Vukoje, T., "Process and Apparatus for Producing a Variable-Diameter Alternate-Twist Yarn", USP 4,033,103, July 5, 1977.

87. Hedrix, J.E., Farmer, L.B., Kuhn, H.H., "Barré Control Through Simulated Dyeing with Fugitive Tints", Textile Industry 138, pp. 168-169 (1974).

88. Toray Industries, Inc., "FYL-500 Yarn Quality Analyzing System", Catalog FL-500-B2 (1976).

89. Lang, P., Haller, C., "The Measurement of Crimp Behavior of Textured Yarns", pp. 175-195, in New Ways to Produce Textiles, 1972 Annual Conference of Textile Institute. Textiles.

90. Valk, G., Berndt, H.-J., Heidemann, G., "Neue Ergebnisse zur Fixierung von Polyesterfasern", Chemiefasern und Textil-anwendungstechnik 21(5), pp. 1-8 (1971).

91. Denton, M.J., "The Structural Geometry and Mechanics of False-Twist-Textured Yarns", JTI 66, p. 80 (1975).

92. Thwaites, J.J., "Crimp Development in FT-Textured Yarns", Paper presented at M.I.T. Summer Course on Mechanics of Texturing Thermoplastic Yarns (1977).

93. Konopasek, M., "A Mechanical Model of Helical Elements in Textured Yarns", TRJ 46, 0. 278 (1976).

94. Sibilia, J.P. et al., "Structure/Property Relationships in Drawn PET Fibers", Polymer Paper 99, 167th ACS Meeting, Los Angeles (1974).

95. Schubert, G., "Die wichtigsten Eigenschaften der Falschdrahtgarne und ihre Bedeutung für die Wieterverarbeitung", Melliand Textilberichte 54(7), pp. 714-722 (1973).

96. Latzke, P.M., "Comparison of Different Test Methods for

the Determination of Crimp Potential of Textured Yarns", Melliand Textilberichte 56(5), pp. 355-360 (1975). (In German.) Shirley Institute Summary, May 1975.

97. Lünenschloss, J.W., "Prüfverfahren für texturierte synthetische Fäden", Melliand Textilberichte 7/52, pp. 760-772 (1971).

98. Dumbleton, J.H., "Spin orientation measurement in Polyethylene Terephthalate", TRJ 40, p. 1035 (1970).

99. Coppola, G., Frediani, P., "Differential Calorimetry Measurements on PET Polyester Fibers", Nuova Chim. 49 (10), pp. 37-39 (in Italian) (1973).

100. Gupta, V.B., Kumar, M., Gulrajani, M.L., "Dyeability Characteristics of Textured Polyethylene Terephthalate Yarns", TRJ 6, p. 463 (1975).

101. Thwaites, J.J., "The Mechanics of Friction Twisting", JTI 61, p. 116 (1970).

102. Klein, W., Trummer, A., "Draw-Texturizing Techniques with Special Reference to the Friction False-Twisting Process", Textile Manufacturer 1, p. 16 (1973).

103. Naik, A., Valencia, E., "Study of Different Parameters in Texturing by Means of the Deformation of Polyester Filaments", Melliand Textilberichte 58(11), p. 869 (1977).

104. Stein, W., Wallas, K., "Recent Results in Crimp Contraction-Force, Shrinkage-Force, and Extension-Force

Tests on Running Yarns", Melliand Textilberichte 58(8), p. 609 (1977).

105. Haile, W.A., Willingham, W.L., Caldwell, M.A., Forrester, R.C., "Preparation, Dyeing and Finishing of Woven Textured Polyester", American Dyestuff Reporter 66, Part I, pp. 48-52 (March 1977); Part II, pp. 32-44 (April 1977); Part III, pp. 59-62 (May 1977).

106. Willingham, W.L., "Dyeing Conditions--How They Contribute to Barré-free Fabrics", in Knit Barré--Causes and Cures, Proc. AATCC Symposium, May 25-26, 1972, New York, N.Y.

107. Batra, S.K., "Supplement to the Limit of Twist Analysis", Internal Report, Fibers and Polymers Laboratories, M.I.T., Cambridge, Massachusetts (1972).

108. Smith, S.C., "On the Feasibility of Using Dielectric Heating in False-Twist Texturing of Yarns", Internal Report, Fibers and Polymers Laboratories, M.I.T., Cambridge, Massachusetts (1977).

109. Egbers, G., "A Method of Continuous Crimp and Bulk Measurement", Paper presented at M.I.T., Cambridge, Mass., Summer 1974.

110. ENKA-Glanzstoff GmbH, "AKZO-Bauschigkeitsmessgerät", (Technical Information).

110 (A). Latzke, P.M., Hesse, R., Textilien Untersuchen - Prüfen - Auswerten, Schiele and Schön, Berlin (1974).

111. Lünenschloss, J., Helli, J.G., Hummel, E., "Der Einfluss der Garn- und Swirndrehungen und der Fasereigenschaften auf die Kringelneigung von Zwirnen", Melliand Textilberichte 41, pp. 933-941 (1960).

112. A.G. Heberlein and Company, "Method zur Bestimmung der Krangeltendenz von Kraüselgarnen", Informationsblett 1.13.

113. Dhingra, R.C., Postle, R., "The Measurement of Torque in Continuous-Filament Yarns", Part I, TRJ 65, p. 126, Part II, TRJ 65, p. 171 (1974).

114. Kawabata, S., Niwa, M., Mamiya, J., "Torsional Testing Apparatus and its Application to Experimental Investigation of the Relations between Torsional Properties of Yarns and Fibers", Journal of Textile Machinery Society of Japan 29(9), p. T119 (1976).

115. Okabayashi, N., Yamazaki, K., Terada, K., Negishi, T., "Measurement of Torsional Rigidity of Fibers", TRJ 67, pp. 429-433 (1976).

116. Krizik, J., Brookstein, D., Thwaites, J.J., Backer, S., Torque-Tension Meter, in preparation.

117. Lünenschloss, J., Fischer, K., "Effect of Twisting Head and Texturing Conditions on Twist Level Yarn Tensile Behavior During Conventional False-Twist Texturing and Simultaneous Draw-Texturing", Chemiefasern/Textilindustrie 24/76(7), pp. 547-549 (1974) (in German), Shirley Institute Summary, August 1974.

118. Stein, W., "Kräuselkontraktions-und Schrumpf-Kraftmessung am laufenden Faden", Chemiefasern 20, pp. 748-752 (1970).

118A. Stein, W., Wallas, K., "Kräuselkontraktions-und Schrumpfkraftprüfung texturierter Filamentgarne am laufenden Faden", Melliand Textilberichte 57, pp. 97-103 (1976).

118B. Gusack, J.A., Stephens, B.B., Stevens, J., "Continuous Evaluation of Yarn Crimp", USP 3,762,220, Filed 1/10/72.

119. Lünenschloss, J., Weinsdörfer, H., Teichmann, K.-H., "Eine Prüfmethode zur Kontinuierlichen Messung der Einkrauselung texturierter garne", Chemiefasern 21, pp. 41-49 (1971).

120. Chemstrand Stretch Woven Fabrics, Technical Information on Processing, Series N1, March 1962.

121. Stein, W., Van der Weyden, H., "Factors which Influence the Testing of Crimp Contraction According to DIN 53 840 on Textured Filament Yarns", Chemiefasern/Textil-industrie 25/77(12), pp. 1126, 1129-1132 (1975).

122. Heidemann, G., Berndt, H.J., "Moderne thermische Prüf-verfahren für Texturgarne", Chemiefasern/Textil-industrie 27/79(2), p. 134 (1977).

123. Berndt, H.-J., Bossmann, A., "Thermal analysis of heat set poly(ethylene terephthalate) fibres", Polymer 17, pp. 241-245 (1976).

124. Heidemann, G., Berndt, H.-J.,"Effektivtemperatur und Effektivspannung, zwei Messgrössen zur absoluten Bestimmung des Fixierzustandes von Synthesefasern", Melliand Textilberichte 57, pp. 485-488 (1976).

125. Stein, W.,"Neues universelles Prüfverfahren für Textilfäden", Melliand Textilberichte 55(2), pp. 123-126 (1974).

126. See [104].

127. Buchanan, D.R., Hardegree, G.L., "Thermal Stress Analysis of Textile Yarns", TRJ 47, pp. 732-739 (1977).

127A. Hardegree, G.L., "Kanebo Thermal-Stress Analysis for Polyester Yarns", Paper presented at TYAA Winter Technical Conference, Greensboro, North Carolina (1977).

128. Thermafil Product Literature, Herbert Stein, Private Communication.

129. Latzke, P.M., Hage, E., "Das Contractiometer, ein Gerät zur Bestimmung der Schrumpfkraft von synthetischen Garnen", Chemiefasern 21(4), p. 260 (1971).

130. Latzke, P.M., Hesse, R., Textilien: Prüfen, Untersuchen, Auswerten, Schiele & Schön, Berlin (1974).

131. Jarrell, Mark F., "Design and construction of a

laboratory texturing machine", B.S. Thesis, M.I.T., Department of Mechanical Engineering, Cambridge, Massachusetts (1974).

132. Dayvault, J.A., "Finishing Textured Polyester Double-knits for Menswear", Textile Chemist and Colorist 4(6), pp. 43-46 (1972).

133. Coryell, J.W., Phillips, B.R., Letter to UNIFI on Friction of Yarns and Its Effect on Barré.

134. Smith, S.C., Internal Report, M.I.T., Fibers and Polymers Laboratory, Cambridge, Massachusetts, 3/20/78.

135. Baudimont, E., "Effect of Texturing Conditions on Measurement of Crimp Contraction in FTF-textured Polyester Yarns", Industrie textile belge 16, pp. 51-59 (1974).

136. Denton, M.J., "Quality Control of Textured Yarns by Retractive Force Measurement", Shirley Institute Bulletin 45(5), pp. 149-152 (1972).

137. Denton, M.J., Morris, W.J., "Heat Setting and Yarn Texturing", Chapter 6, in The Setting of Fibres and Fabrics, J.W.S. Hearle and L.W.C. Miles, eds., Merrow Publishing Co., Ltd., Watford, Herts, England.

138. E. I. du Pont de Nemours & Co., Inc., "False-twist texturing of du Pont Nylon Yarns", Bulletin N-265, November 1973.

139. Shirley Institute, "Shirley Tube Test", Technical Instruction Manual, Shirley Developments Ltd., Manchester, England.

140. Lünenschloss, J., Fischer, K., Murata, T., "Effect of Heat-Setting Temperature and Overfeed in the Setting Zone and in Winding on the Properties of Textured Polyester Yarns", Chemiefasern/Textil-industrie 24/76 (10), pp. 825-826, 828-829 (1974).

141. Bruggisser, K.J., "Selected Applications of Large Deflection Analysis of Slender Bodies in Textile Mechanics", M.S. Thesis, Georgia Institute of Technology (1976).

142. Roger, J., Private Communication.

143. Wilson, M.P.W., "Shrinkage and Chain Folding in drawn poly(ethylene terephthalate) Fibers", Polymer 15, p. 277 (1974).

144. Dumbleton, J.H., "The Effect of Air and Oil Annealing on the Structure of Drawn Poly(ethylene terephthalate)", Polymer 10, p. 539 (1969).

145. Ribnick, A., "The Thermal Shrinkage of an Oriented Polyester Yarn as a Function of Time, Temperature, and Stress", TRJ 39, p. 742 (1969).

APPENDIX 1

Non-Uniform Yarn Geometry during Twisting and Untwisting

As shown by Fig. 14 in Chapter I, the threadline shape during false-twist texturing changes from a smooth single-twisted cylinder to a partially buckled or double-twisted shape as twist is increased still within the range of commercial interest. Nonetheless, there are few publications which treat this form of double twisting and the variables which motivate it. In this appendix we present the results of a short exploratory study of threadline buckling during dynamic twisting of monofilament yarns.

Figure A1-1 shows schematically the laboratory device constructed to twist the yarns dynamically at controlled tension and twist insertion.

The device is powered by a single motor (1) which drives a selsyn sender (2), receiver (3) pair and the input shaft of a (variable) speed reducer (5). The input feed (6) is coupled to the output shaft of the speed reducer (5); the receiver (3), or yarn twister, is mounted on a carriage (4) which moves on linear ball bushings along two parallel rods.

In operation, the parallel straight monofilaments are threaded through the input feed rolls and clamped to the shaft of the twister (3). When the drive motor (1) is energized, the filaments entering the device are twisted by the rotating receiver. Any desired level of twist can be achieved by

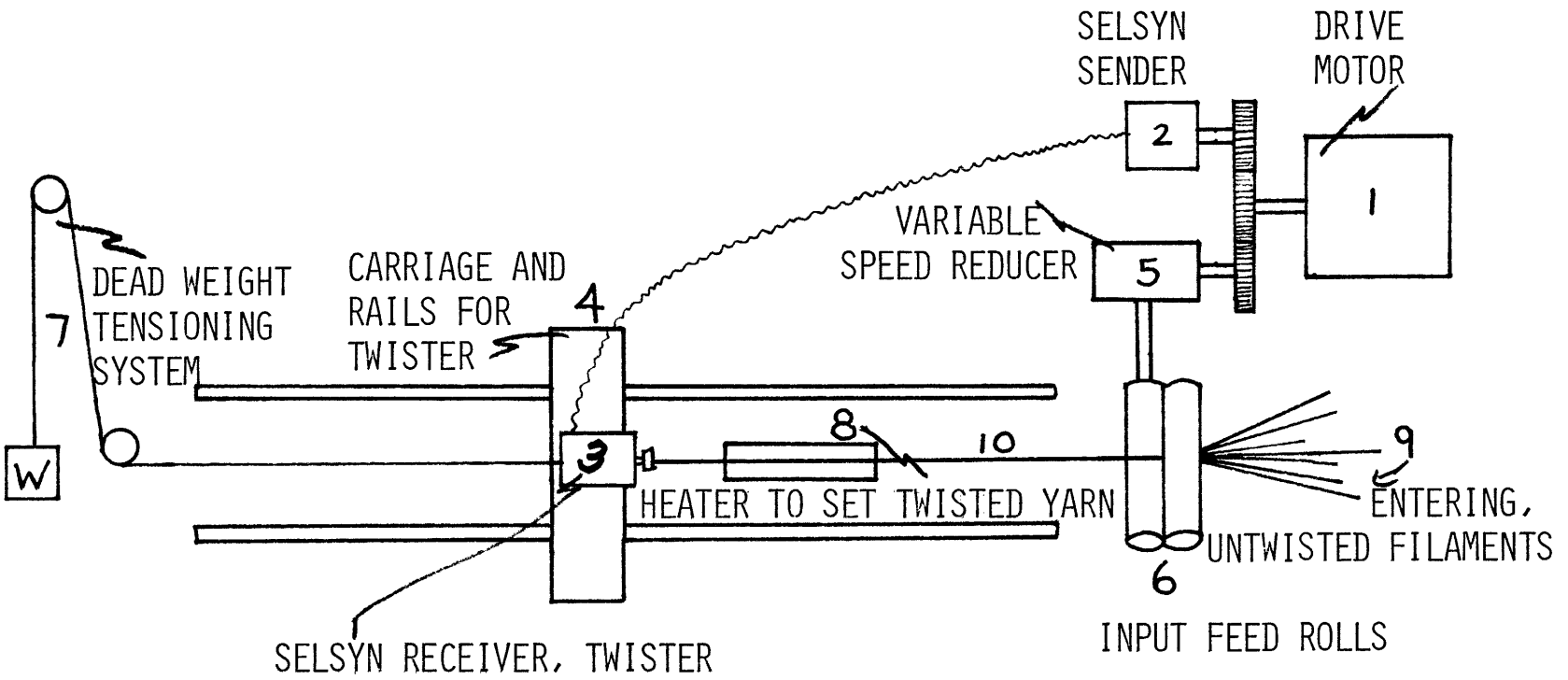

FIGURE A1-1. LABORATORY TWISTER FOR THREADLINE BUCKLING STUDIES

changing the input speed with respect to the constant twisting speed. A yarn heater (8) is included in the device to set permanently the twisted geometry in the yarn. Since the occurrence of torsional buckling depends on twist (torque) and tension, the tension in the threadline is controlled by a dead weight (7) acting on the twister carriage.

Two types of fully drawn monofilaments were used in the twisting experiments, i.e. a 20 mil polyester (2 GT), and a 380 denier nylon 66. During twisting, heater temperatures of 220°C and 210°C, respectively, were used for these two materials.

Although some twisting tests with 30 filament yarns were conducted during this brief study, all the test results reported here were obtained using 7 filament yarns. Figures A1-2, A1-3a, b show the typical yarn geometries after twisting a 7 x 20 mil PET yarn at 6.44, 5.75, and 6.12 turns per inch. Each of these figures is a composite of many photographs of short segments of the "set" twisted threadline. The yarns are under just enough tension to hold them in the parallel arrangement shown. To reconstruct the entire length of the twisted threadlines, the lettered strips should be arranged from left to right with the left side of strip B placed at the right side of strip A, etc., and with individual numbered yarns matching in each strip.

During twisting, the yarn tensions were increased as designated from top to bottom in each strip of yarns in both

FIGURE A1-2. GEOMETRY OF TWISTED, HEAT-SET YARNS AS A FUNCTION OF THREADLINE TENSION DURING TWISTING.

7 x 20 MIL PET; HEAT SET DURING TWISTING AT 220°C; 6.44 TURN/INCH. INSETS ARE ARRANGED A, B, C, D FROM TOP TO BOTTOM ON PAGE. WITHIN EACH INSET THE TENSION DURING TWISTING WAS 1.25, 1.85, 1.95, 2.25, 3.25 KG, FROM TOP TO BOTTOM.

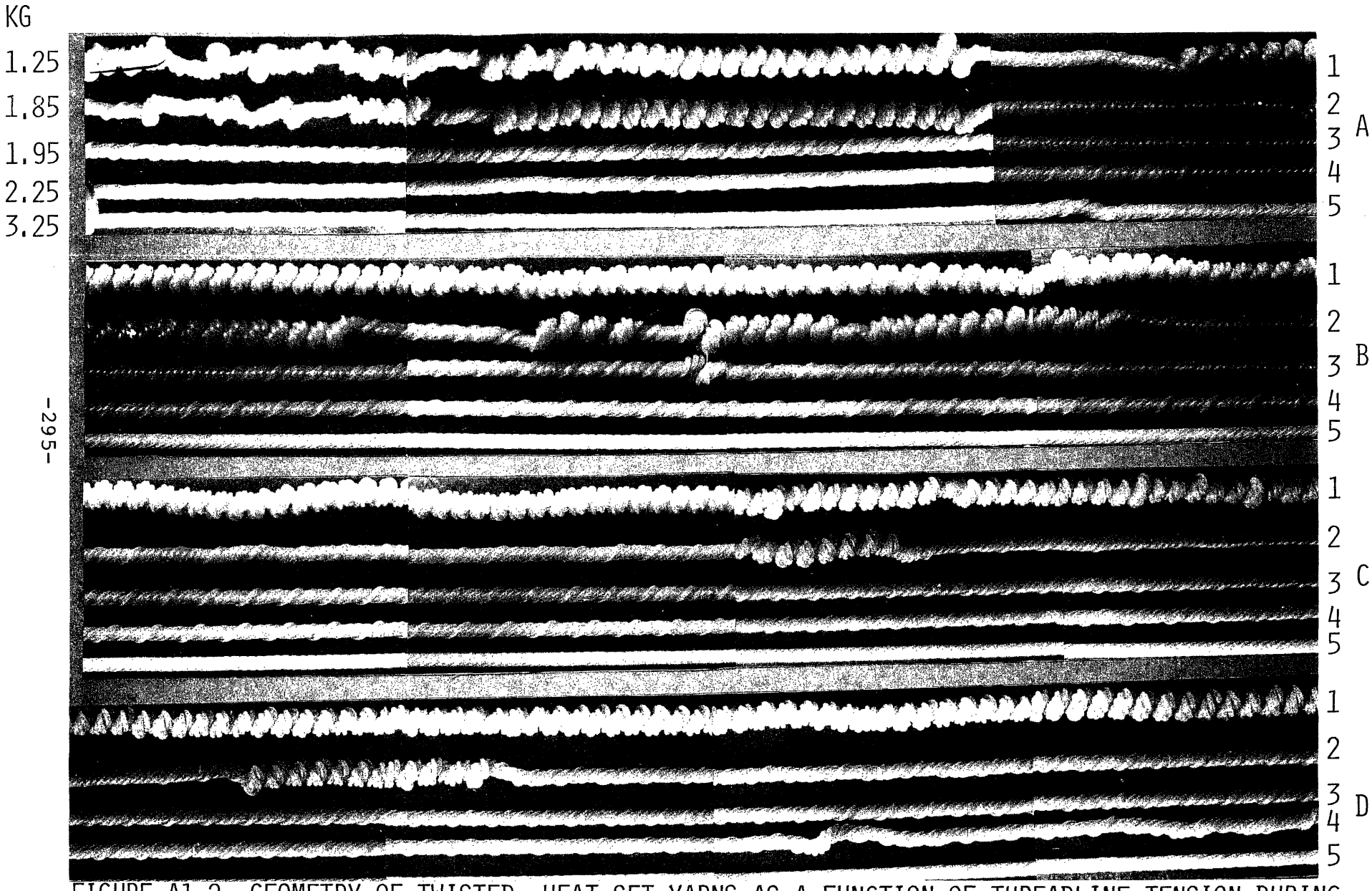

FIGURE A1-2. GEOMETRY OF TWISTED, HEAT-SET YARNS AS A FUNCTION OF THREADLINE TENSION DURING TWISTING. 220°C, 6.44 TPIB

FIGURE A1-3. GEOMETRY OF TWISTED, HEAT SET YARNS AS A FUNCTION OF THREADLINE TENSION DURING TWISTING.

A

7 x 20 MIL PET; 5.75 TURNS/INCH; INSERTS ARE ARRANGED A, B, C FROM TOP TO BOTTOM ON PAGE. WITHIN EACH INSERT THE TENSION DURING TWISTING WAS 0.8, 0.9, 1.0, 1.1, 1.3, 1.5, 1.7, 2, 2, 2 KG FROM TOP TO BOTTOM.

B

7 x 20 MIL PET; 6.12 TURNS/INCH. FOUR INSERTS. TENSION IN EACH INSERT DURING TWISTING WAS 1.0 - 1.3, 1.5, 1.7, 1.9, 2.1, 2.3 KG.

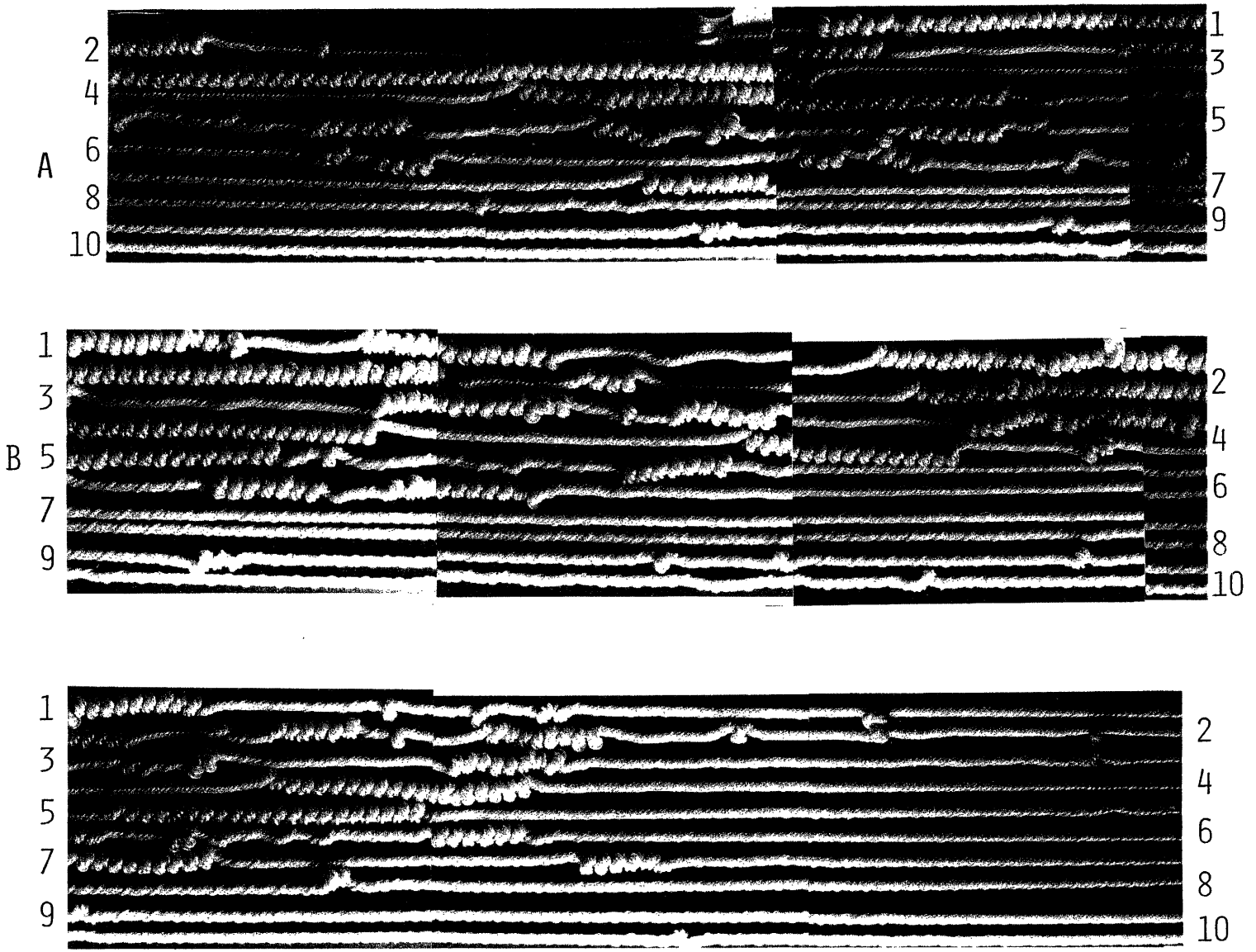

FIGURE A1-3A. 5.75 TPIB, 220°C

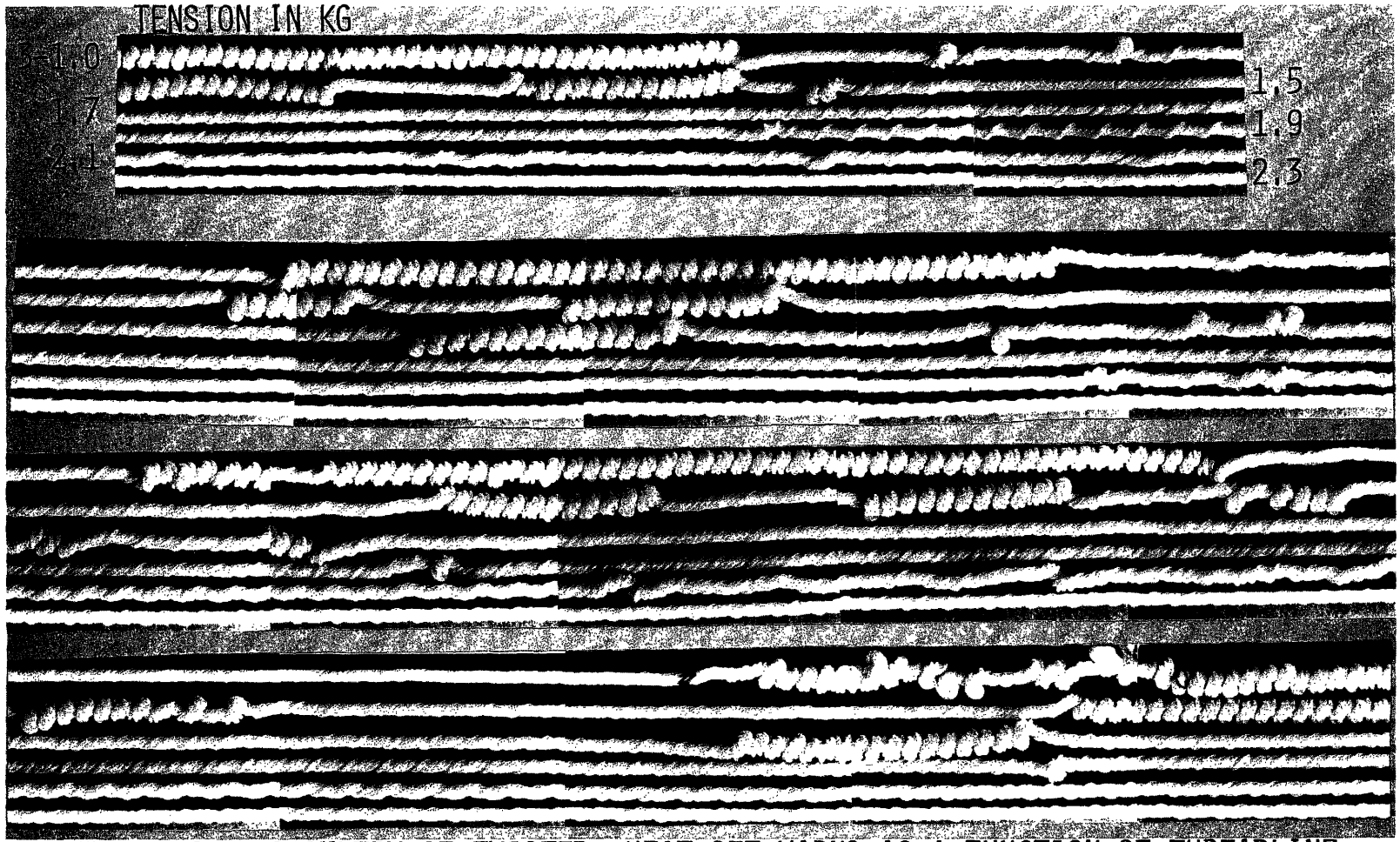

FIGURE A1-3B. GEOMETRY OF TWISTED, HEAT-SET YARNS AS A FUNCTION OF THREADLINE TENSION DURING TWISTING. 220°C. 6.12 TPIB

figures. As expected, for lower twists and/or for higher threadline tensions one observes less threadline buckling. Only at the lowest tensions were there indications of threadline snarling. For the most part, the double-twisted or torsionally buckled threadline manifested a fairly uniform structure. It appears that the yarn has been sharply bent and wrapped around the threadline axis to achieve the observed structure.

Figure A1-4 shows the amount of double-twisting or torsional buckling that occurs at different twist levels as a function of threadline tension. The amount of buckling decreases with higher tension and increases with higher twist. The surprising result is that only 110 mg/den of tension is sufficient to suppress buckling at all twist levels. This is of the order of magnitude of the fiber tension necessary to remove crimp in single filaments. Obviously, the experiments warrant repeating under other conditions before any significance can be given to the coincidence.

The occurrence of threadline buckling during texturing will directly affect its set geometry, but it will also affect filament setting by changing the heat transfer to the yarn. Figure A1-5 illustrates the filament geometry in 7 x 20 mil yarns twisted to the fixed level but at different tensile loads. In A1-5d we are shown the original twisted yarn samples. The top two samples (one buckled segment and one unbuckled segment) came from the same non-uniformly

FIGURE A1-4. BUCKLING AS A FUNCTION OF TWIST AND TENSION IN 7X20 MIL POLYESTER AT 220°C

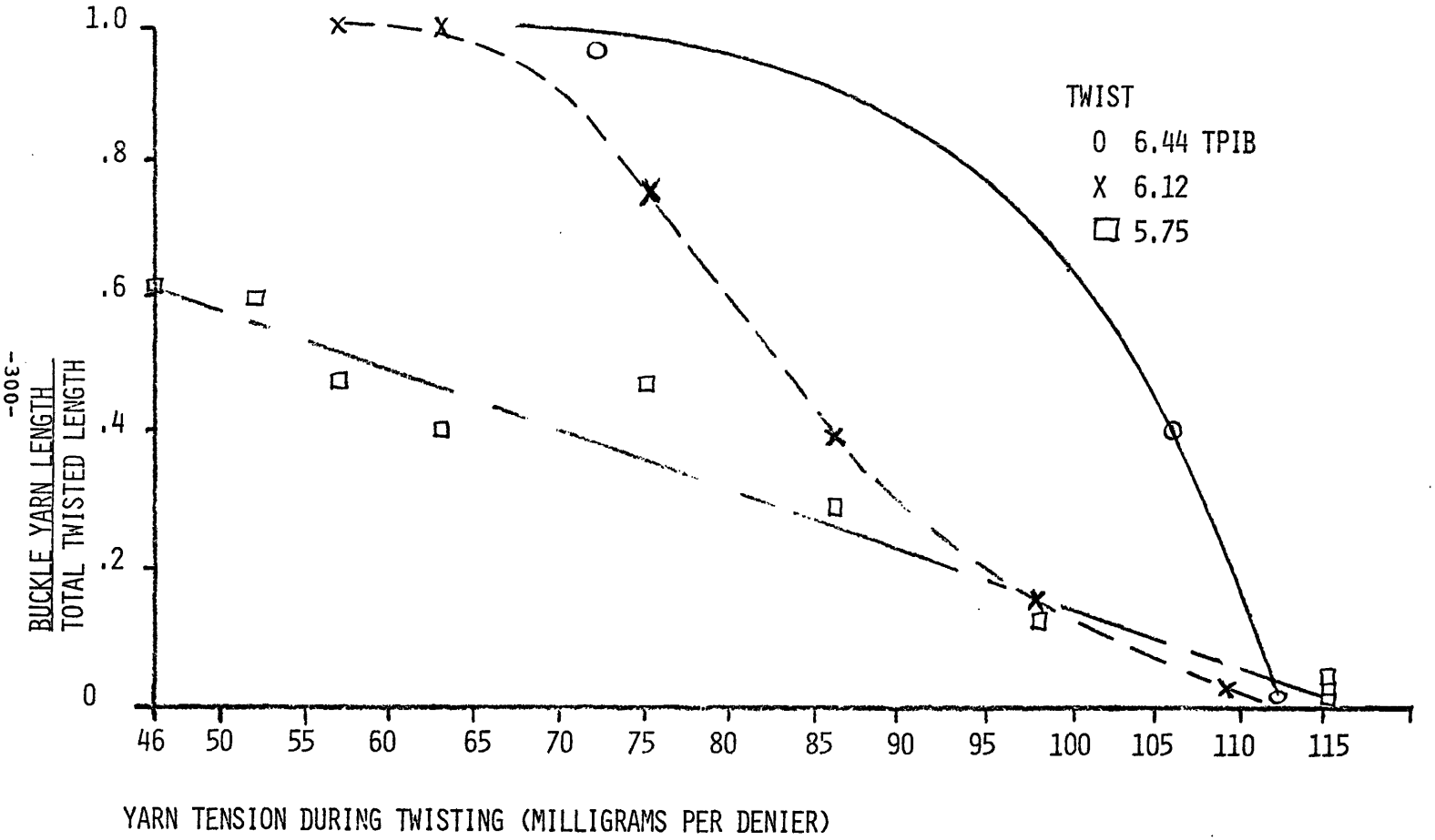

buckled threadline twisted to 6.5 TPIB under 1.75 KG tension. The lower yarn was twisted to 6.5 TPIB under 2.25 KG tension. Figures A1-5a and A1-5b show that two filaments appear to occupy the center of the yarn twisted at 1.75 KG tension, while there is a single central filament during the twisting at 2.25 KG. Both yarns have a single outermost filament. Structures of 2-4-1 versus 1-5-1 are reasonable models for the twisted yarns of A1-5a and b, respectively.

The buckled yarn sample of A1-5c was a very tight structure with filaments actually reversing direction (with respect to the yarn axis). The whole length of the sample could not be disassembled, but a single pitch length has been extracted and is shown in Fig. A1-5c.

One of the most interesting discoveries came when a partially buckled yarn was untwisted turn-by-turn, as shown in Fig. A1-6. The initial yarn sample under 1 KG of tension is shown in the upper left. The next 18 insets (which continue down the right hand column) were obtained after each successive turn of twist removal. The untwisting proceeded in three stages:

(1) removal of double twist (6 turns),

(2) untwisting of the initially double twisted segment (next 7 turns),

(3) untwisting of the initially single twisted segment and simultaneous reversed twisting of the filaments that were initially double

FIGURE A1-5. FILAMENT GEOMETRY AFTER DISASSEMBLING TWISTED, HEAT-SET YARNS. (7 x 20 MIL PET; HEAT SET AT 220°C; TWISTED TO 6.12 TURNS (IN).

A. FILAMENTS FROM YARN SINGLY TWISTED AT A THREADLINE TENSION OF 1.75 KG.

B. FILAMENTS FROM YARN SINGLY TWISTED AT THREADLINE TENSION OF 2.25 KG.

C. FILAMENTS FROM SINGLE "PITCH" OF YARN DOUBLY TWISTED AT 1.75 KG THREADLINE TENSION.

D. GEOMETRY OF YARNS BEFORE DISASSEMBLY.

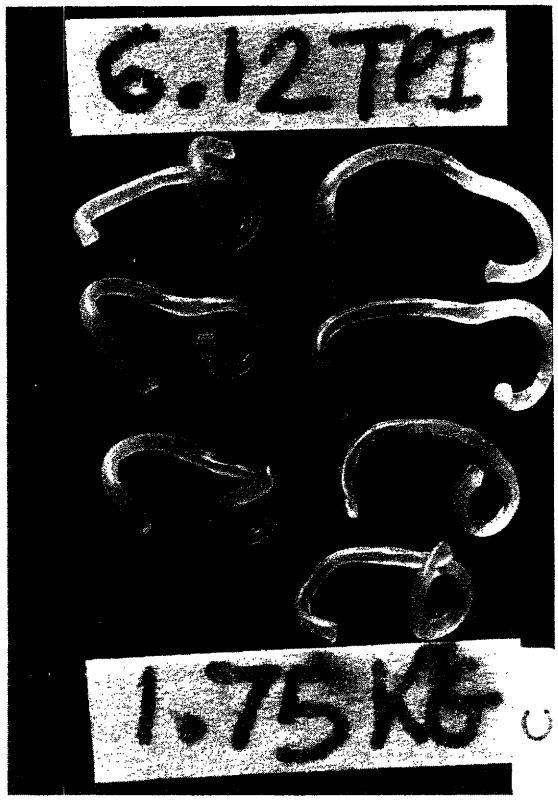

C

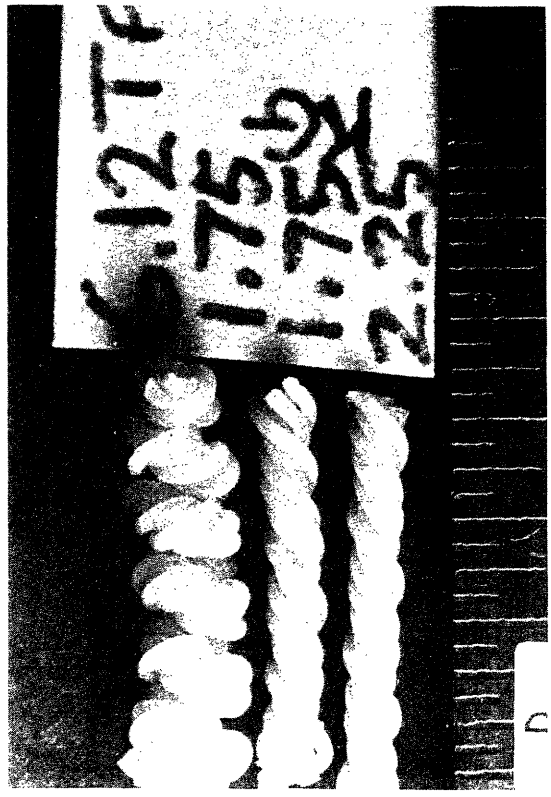

C

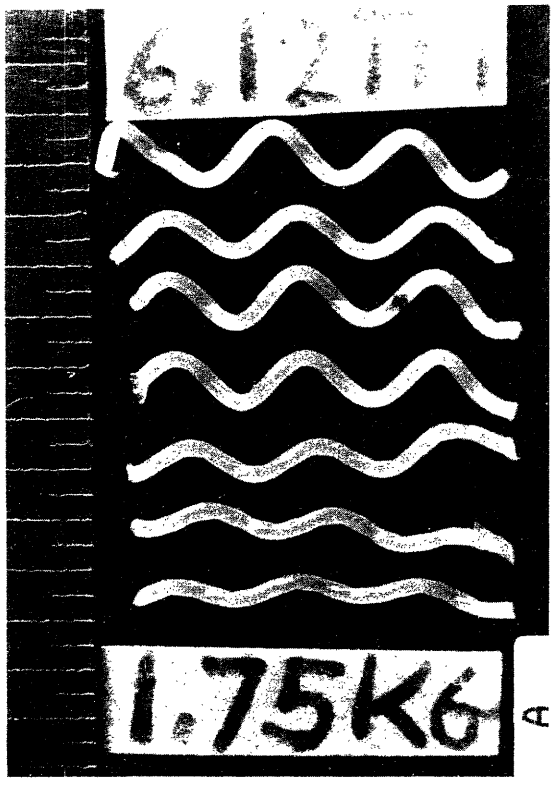

A

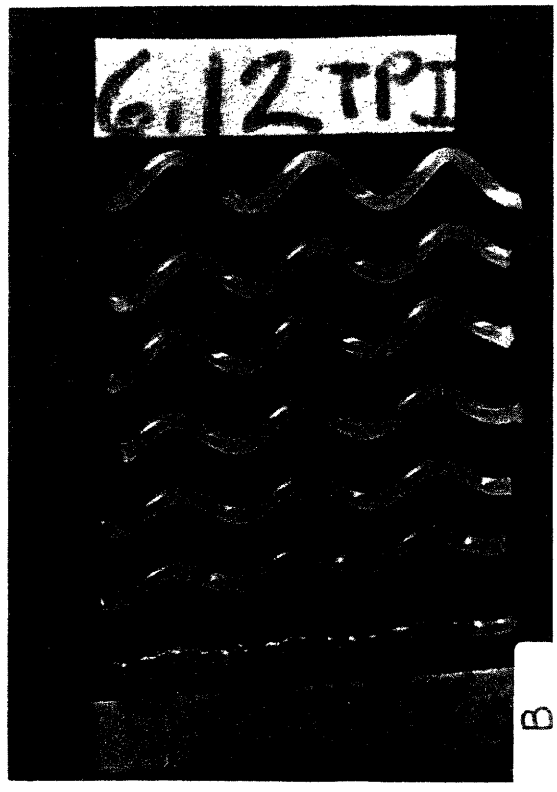

B

FIGURE A1-6. GEOMETRY OF A PARTIALLY BUCKLED YARN DURING UNTWISTING.

7 x 20 MIL PET, TWISTED AT 6.44 TURNS/INCH AT 1.75 KG TENSION; LEFT VERTICAL COLUMN OF INSETS SHOWS YARN GEOMETRY INITIALLY AND AFTER EACH OF THE FIRST 10 TURNS OF UNTWISTING. CENTER VERTICAL COLUMN OF INSETS SHOWS YARN GEOMETRY AFTER 11 TO 18 TURNS OF UNTWISTING (TOP 8 INSETS) AND AFTER 5, 10, 10% CONTRACTION FROM THE LENGTH AFTER 18 TURNS OF TWIST WERE REMOVED. RIGHT SIDE INSET SHOWS THE GEOMETRY OF THE FILAMENTS AFTER UNTWISTING.

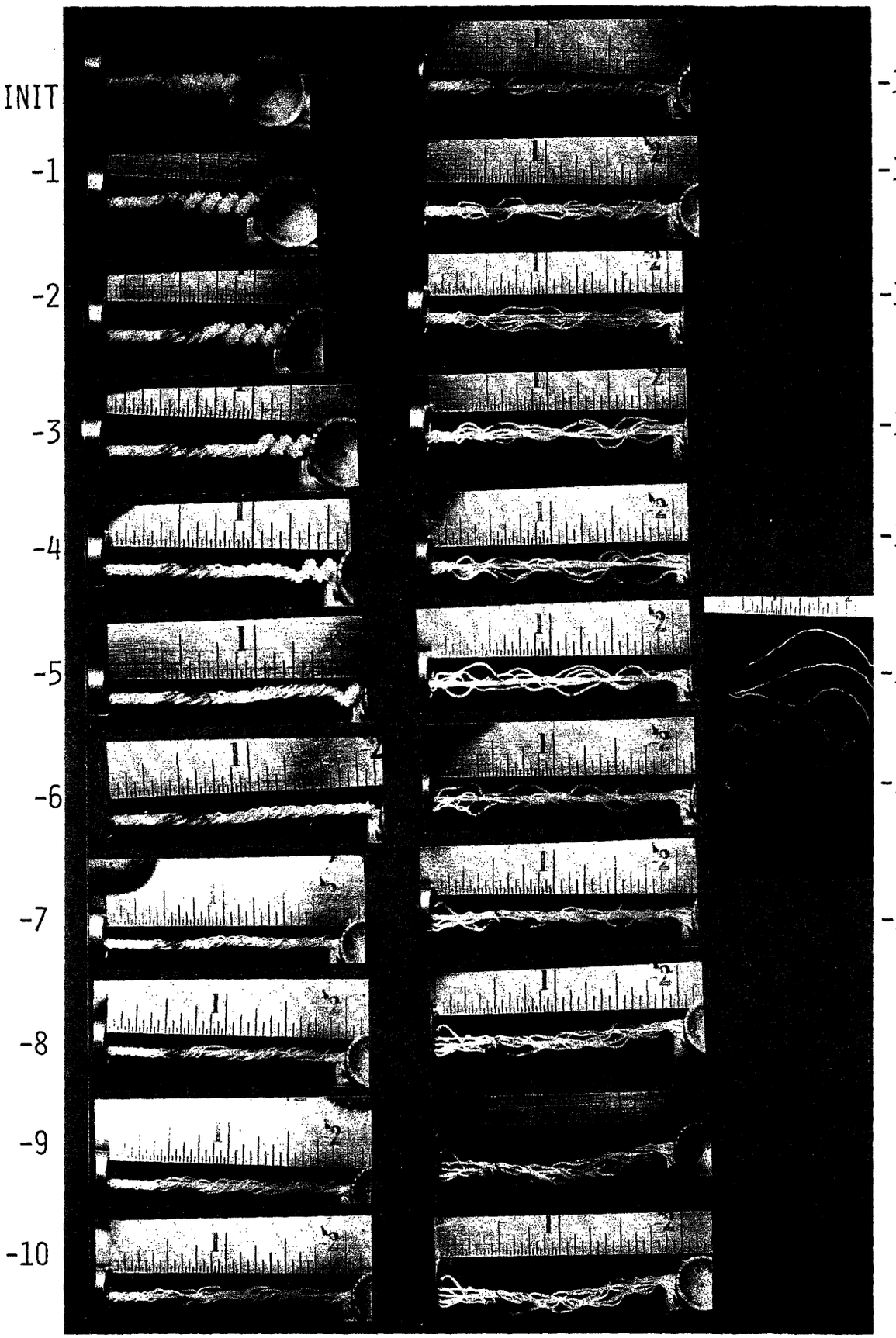

FIGURE A1-6. UNTWISTING OF 7 x 20 MIL PET @ 1 KG. TWISTED 6.44, TPIB @ 1.75 KG @ 220°C

twisted (next 5 turns).

The occurrence of non-uniform untwisting or even "over-untwisting" suggests that tight spots (untwisted regions) in twxtured yarns may be directly related to the mechanics of untwisting yarns which are partially buckled.

The same sequence of stages occurred during untwisting of a partially buckled 7 x 380 denier nylon yarn which had been heat set at 210°C during twisting at 18.7 turns per inch. under 700 grams tension. The sample appearance as set, and after the first 9 turns of untwisting, is shown in the top 10 inserts of Fig. A1-7. The next insert shows the sample after 20.5 turns of untwisting. The appearance of individual filaments after complete untwisting of the yarn is shown in the bottom insert. The filaments clearly show the different deformations associated with the buckled geometry.

The high level of crimp produced by double twisting a yarn may be very desirable and could lead to very high extensibility and bulk.

Figures A1-8 and A1-9 show the untwisting of a double twisted 7 x 380 nylon yarn. Figure A1-8 shows the original sample as twisted and after 1 to 17 turns of untwisting. Figure A1-9 shows the same sample after 20, 21, 22, 23, 24, 25, 30 and 35 5u4ns of untwisting. The lower three inserts show the untwisted sample at 25, 15, and 5% contraction from the untwisted length. The contracted filaments do not show the same tight coils shown in A1-7, since the filaments are

FIGURE A1-7. GEOMETRY OF A PARTIALLY BUCKLED YARN DURING UNTWISTING.

(7 x 380 DENIER NYLON 66, TWISTED AT 18.7 TPIB. AT 700 GRAMS TENSION; UNTWISTING AT 700 GRAMS TENSION; THE TOP 10 INSETS SHOW THE GEOMETRY OF THE YARN INITIALLY AND AFTER THE FIRST 9 TURNS OF UNTWISTING, THE NEXT INSET SHOWS THE YARN AFTER 20.5 TURNS OF UNTWISTING. THE BOTTOM INSET SHOWS THE GEOMETRY OF THE FILAMENTS AFTER THE YARN WAS FULLY UNTWISTED).

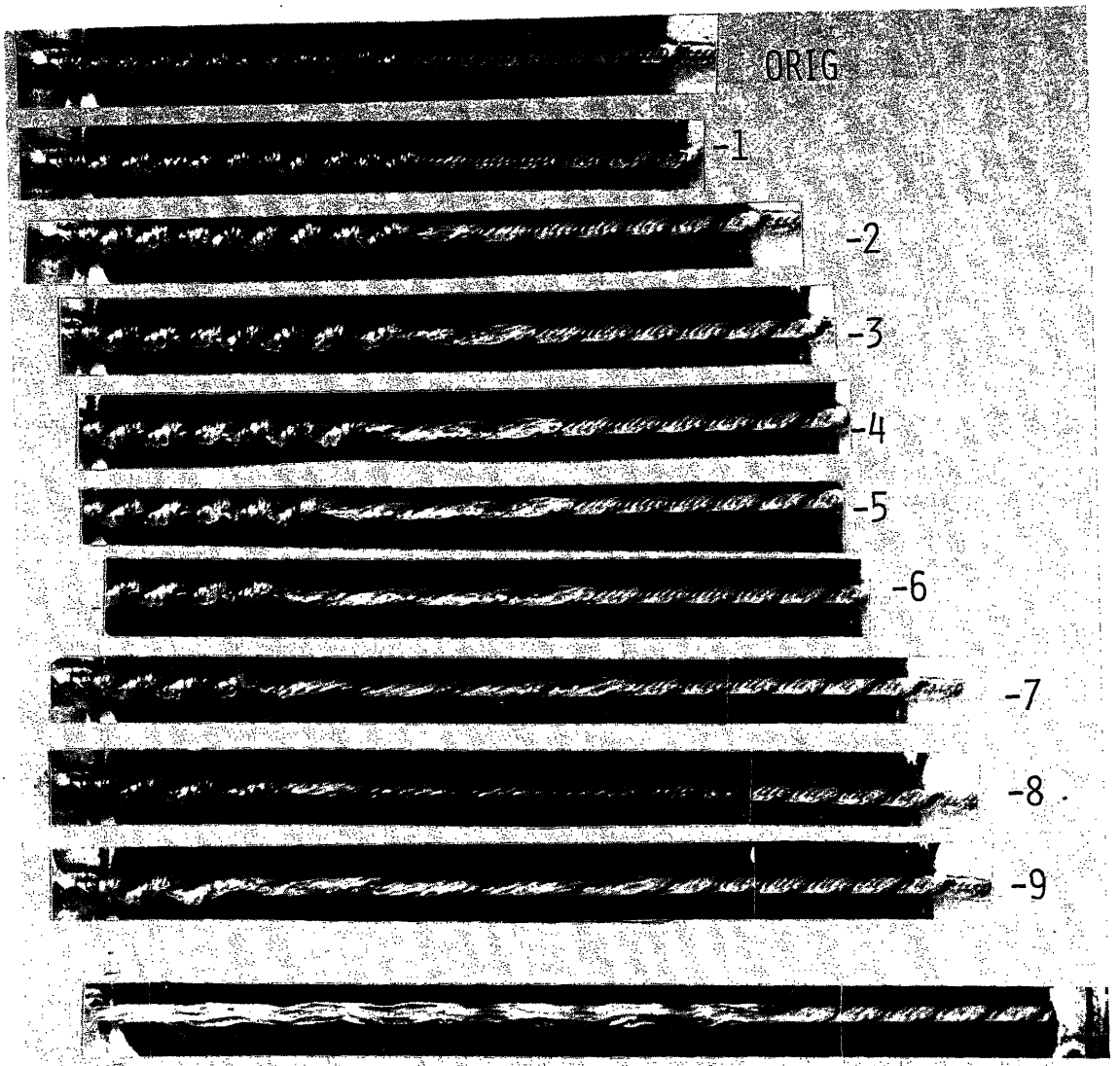

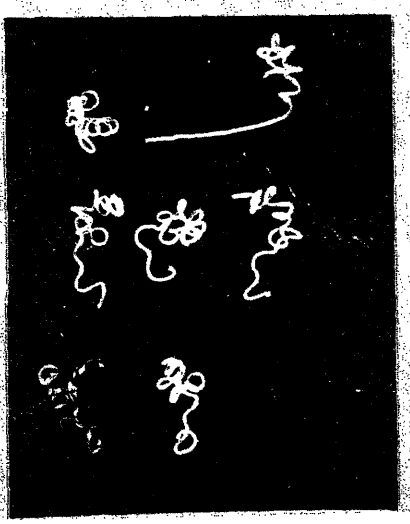

RESULTING UNTWISTED FILS

FIGURE A1-8. GEOMETRY OF A FULLY BUCKLED, OR DOUBLY TWISTED YARN DURING UNTWISTING. (7 x 380 DENIER NYLON 66; TWISTED AT 700 GRAMS TENSION AND 18.7 TPIB: HEAT SET AT 210°C. THE INSETS FROM TOP TO BOTTOM SHOW THE YARN INITIALLY AND AFTER THE FIRST 17 TURNS OF UNTWISTING .

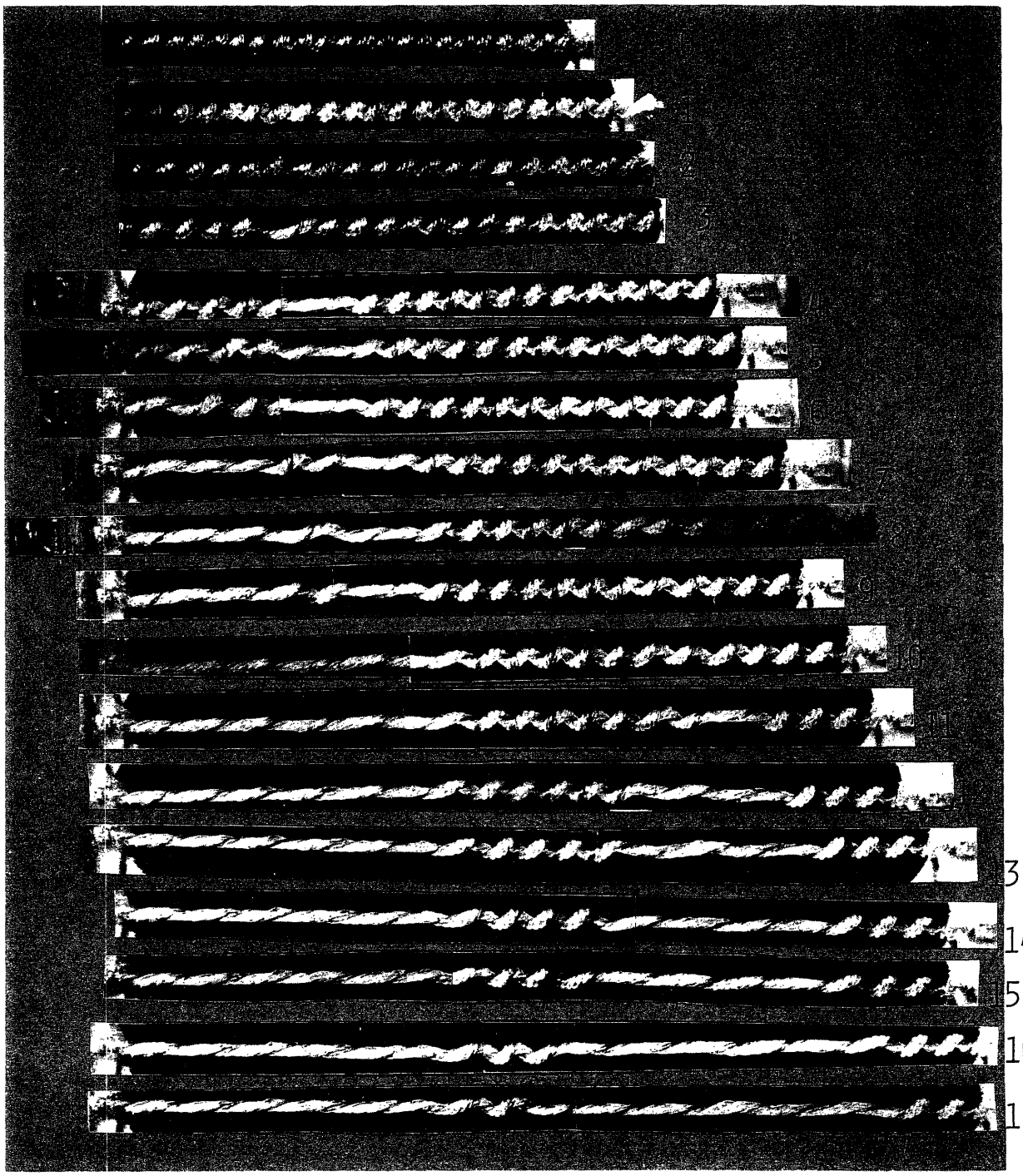
3
14
5
16
17

FIGURE A1-9. GEOMETRY OF A FULLY BUCKLED, OR DOUBLY TWISTED YARN DURING UNTWISTING.

CONTINUATION OF THE UNTWISTING PROCESS ON THE SAMPLE IN FIG. A1-8. THE TOP EIGHT INSETS SHOW THE YARNS' GEOMETRY AFTER 20, 21, 22, 23, 24, 25, 30, AND 35 TURNS OF UNTWISTING, RESPECTIVELY. THE BOTTOM THREE INSETS SHOW THE GEOMETRY OF THE FULLY UNTWISTED YARN AFTER 23, 15, 5% LENGTH CONTRACTION, RESPECTIVELY.

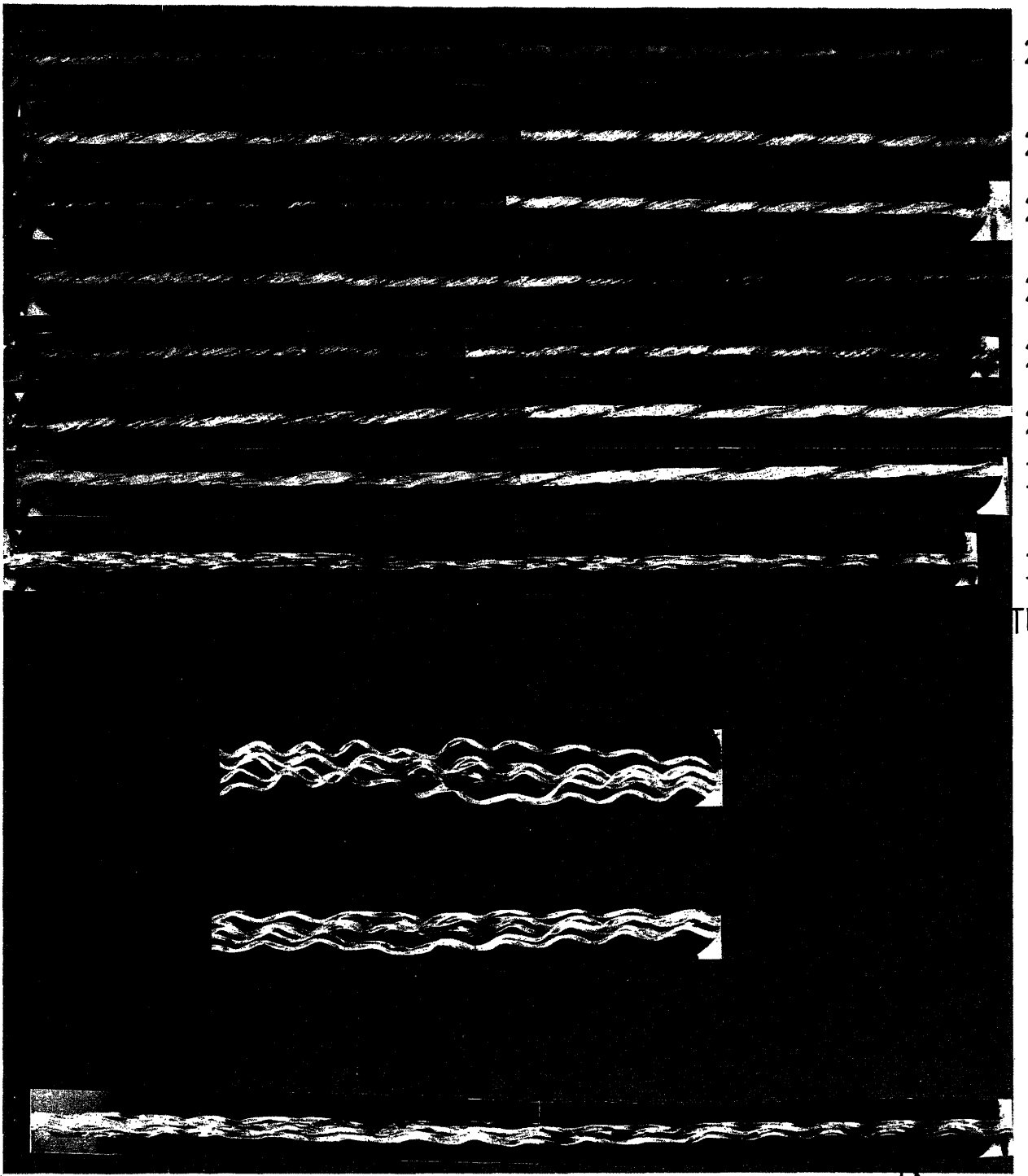
20
21
22
23
24
25
30
35
TURNS
44 + 5%

contracted less in Fig. A1-9 and are also subject to interactions with other filaments in the yarn.

The degree of filament interaction during untwisting of a single-twisted, 7 x 380 denier nylon yarn is shown in Fig. A1-10. The sample appearance as twisted and after 15 turns of untwisting is shown in the top 16 insets of this figure. The lower two insets are after the yarn has been contracted. The top inset shows that the sample has 10 turns of twist originally. The yarn uniformly opens up during the first 5 turns of untwisting. After 6 turns, a reversal of twist direction occurs at the right grip and propagates across the yarn during the next four insets to the point of no net twist in the yarn. Although the yarn is untwisted, (i.e. no net twist), it clearly does not have zero twist everywhere. In fact, half the yarn is still twisted in the original direction while the other half is reverse twisted. If one continues to untwist beyond the nominal "zero twist" point, the common reversal point migrates to the left, leaving the entire yarn reverse twisted, as shown in the 16th inset.

The simple process of twisting and untwisting a 7-filament yarn has been found to contain several interesting phenomena (hitherto unreported) that should be examined further, since this process is the very heart of the false-twist texturing process.

FIGURE A1-10. GEOMETRY OF AN UNBUCKLED YARN DURING UNTWISTING.

7 x 380 DENIER NYLON 66, TWISTED AT 18.7 TPIB, AND 700 GMS TENSION; HEAT SET AT 210°C; UNTWISTED AT 700 GMS TENSION. THE TOP 16 INSETS SHOW THE GEOMETRY OF THE YARN INITIALLY AND AFTER 15 TURNS OF UNTWISTING. THE LAST 2 INSETS SHOW THE GEOMETRY OF THE YARN AFTER 5 AND 10% CONTRACTION.

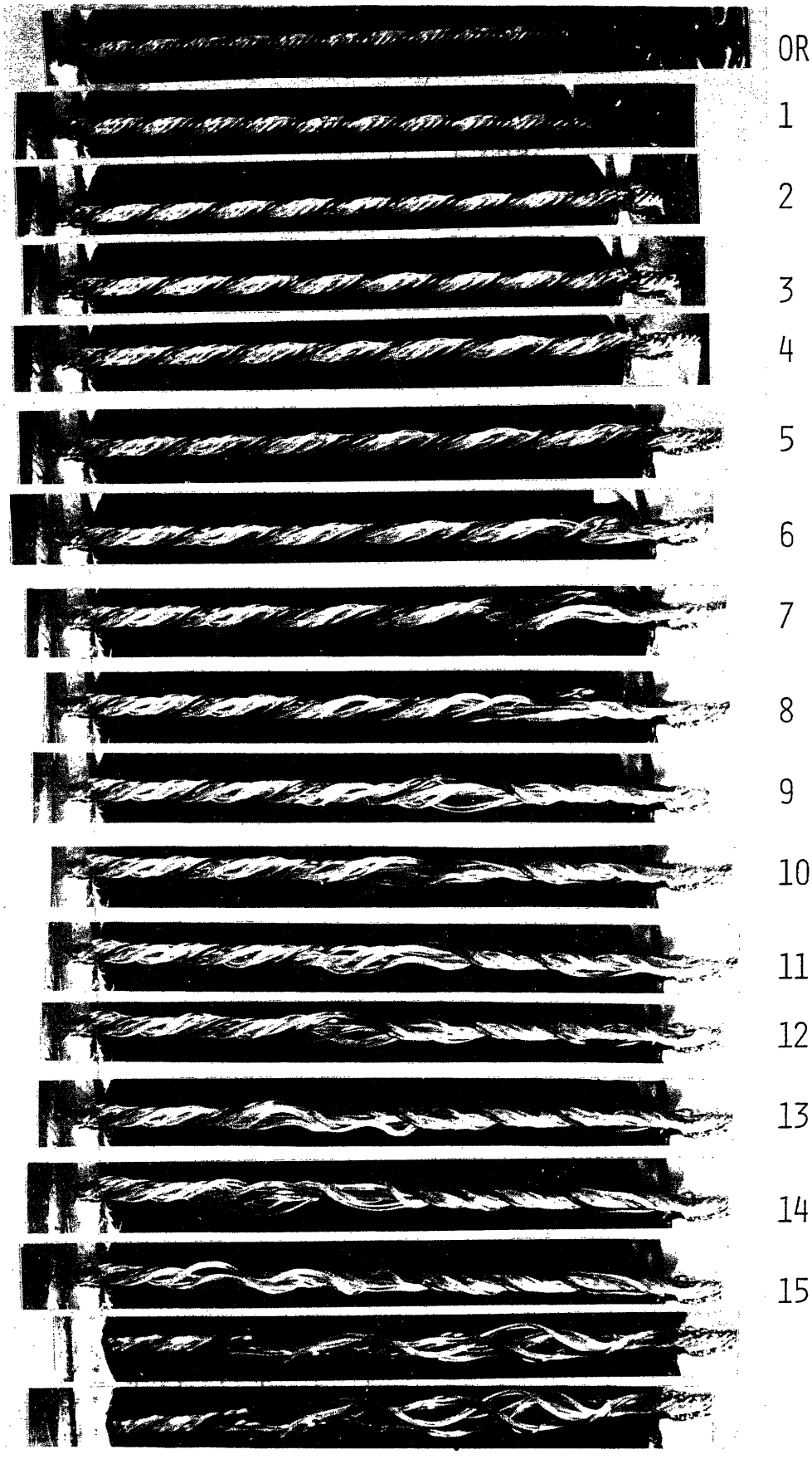
ORIG.
1
2
3
4
5
6
7
8
9
10
11
12
13
14
15

APPENDIX 2

Design of a Tight Spot Detector

Texturing imparts bulk and stretchiness to a continuous filament yarn. These properties depend on crimp formation in the yarn, which, in turn, is the result of heat setting the yarn in a twisted configuration and then untwisting the yarn. However, instabilities in the texturing process can produce yarn segments that have not been untwisted. Because of the much smaller diameter of the twisted filaments versus the collapsed, untwisted filaments, these twisted segments of yarn are called "tight spots".

It was felt that the occurrence of tight spots in a textured yarn might correlate with the subsequent performance of the yarn in fabric form, hence it was considered desirable to develop an instrument capable of on-line measurements of tight spots.

This Appendix describes the circuitry and operation of such an instrument. The instrument was conceived and constructed by the author. The detailed wiring diagrams generated by K. Yeager of the M.E.-C.E. Computer Center are not included here.

The instrument as shown in Fig. A2-1 used a linear array of 64 photodiodes to measure the width of a moving yarn (threadline). The length of the array was 0.128". The textured yarn was only .007" wide at a tight spot and therefore must be magnified. An optical microscope with a

FIGURE A2-1

IN THE FOREGROUND THE CONTROL CABINET IS SHOWN. IN THE BACKGROUND THE LINE SCANNER IS SHOWN MOUNTED ON A MICROSCOPE. THE MICROSCOPE IS FOCUSSED ON THE MOVING YARN WHICH IS ILLUMINATED BY THE LASER LIGHT SOURCE SHOWN AT THE RIGHT EDGE OF THE FIGURE.

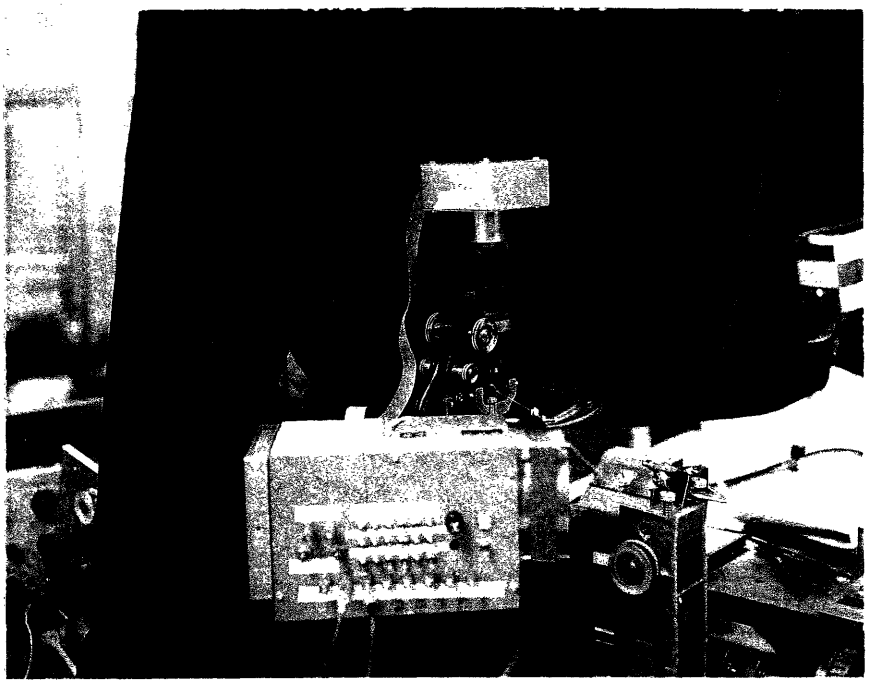

FIGURE A2-1

TIGHT SPOT DETECTOR FOR MOVING YARNS

special projection eyepiece was used to magnify and project the image of the moving threadline onto the array of photodiodes. A laser light source was required at most operating conditions.

The sequence of steps involved in measuring the number of tight spots per unit time (or length of moving yarn) was as follows:

(1) The voltage output of each of the 64 detectors was sampled at a rate determined by switch settings (Table A2-1). A higher scanning rate gives better resolution along the moving yarn. The voltage output from each detector is compared to a reference voltage. More light is reflected from the white filaments of the yarn than from the black idler roll over which the yarn is moving. The number of detectors with output voltage above reference voltage are counted for each scan of the array. This count is proportional to the local yarn width.

(2) The total number of detectors illuminated by the yarn is compared to a number (width threshold), determined by switch settings (Table A2-2). The threshold is close to the tight spot diameter.

TABLE A2-1

SCANNING RATE OF DETECTOR AS A

FUNCTION OF BIT SWITCHES

BITS*					TIME PER SCAN
1	2	4	8	SCANNING SPEED (KHz)	(MILLISECONDS)
0	0	X	X	200	0.3
1	1	0	0	100	0.6
1	0	0	0	50	1.2
0	1	0	0	20	3
1	1	0	1	10	6
1	0	0	1	5	12
0	1	0	1	2	30

---

*0 - off, 1 - on, X - do not care.

TABLE A2-2

WIDTH THRESHOLD AS A FUNCTION OF

SWITCH SETTINGS

BITS*						WIDTH THRESHOLD
1	2	4	8	16	32	
X	1	0	0	0	0	2
X	0	1	0	0	0	4
X	1	1	0	0	0	6
X			.			.
			.			.
X			.			.
X	1	1	1	1	1	62

---

*0 - off, 1 - on, X - don't care

TABLE A2-3

LENGTH OF VARIABLE TIME PERIOD

USED TO TOTALIZE TIGHT SPOTS

BITS* 1 2 4 8	VARIABLE TIME PERIOD (SECONDS)
1 1 0 0	0.1
1 1 0 1	1.0
1 1 1 0	10.0
1 0 0 0	0.2
1 0 0 1	2.0
1 0 1 0	20
0 1 0 0	0.5
0 1 0 1	5.0
0 1 1 0	50
0 0 0 0	1
0 0 0 1	10
0 0 1 0	100

*0 - off, 1 - on.

(3) Each time the number of detectors illuminated crosses the width threshold (2 elements hysteresis), a pulse signifying the occurrence of a tight spot is generated.

(4) The tight spots are counted for 100 seconds and for a shorter, variable time period.

Figure A2-2 shows the block diagram of the instrument. The various counted quantities are converted (D-A) to provide for continuous analog observation of the variation in yarn width along the length of the yarn. The voltage levels from each of the photodiodes during a given scan and a scope triggering signal were available on the control panel.

FIGURE A2-2

1. MOVING YARN WITH TIGHT SPOTS.
2. MICROSCOPE OBJECTIVE LENS.
3. MICROSCOPE (PROJECTION) EYEPIECE.
4. 64-ELEMENT LINEAR ARRAY OF PHOTODIODES.
5. VOLTAGE COMPARATOR AND COUNTER.
6. COUNT COMPARATOR WITH 2-COUNT HYSTERESIS.
7. FIXED TIME TIGHT SPOT TOTALIZER.
8. VARIABLE TIME TIGHT SPOT TOTALIZER.
9. DISPLAY OF TOTAL TIGHT SPOTS.
10. CIRCUITS FOR TIMING SIGNALS AND CONTROL.
11. LASER LIGHT SOURCE.

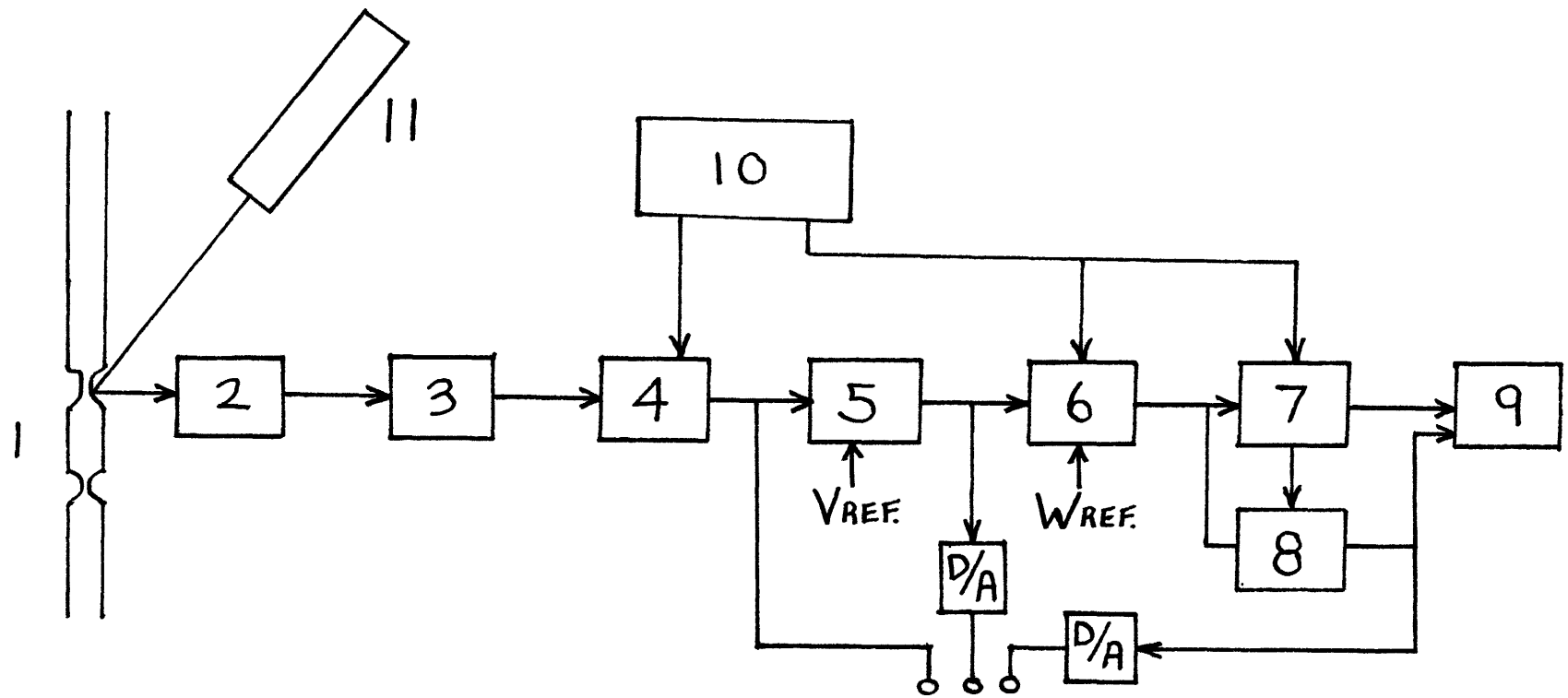

FIGURE A2-2: BLOCK DIAGRAM OF TIGHT SPOT DETECTOR

APPENDIX 3

Details of Batch Thermomechanical Tests

This section is concerned with the exploratory study of various modes of interpretation of thermomechanical tests on textured yarns.

Table A3-1 shows cold tension of the yarn after 2.2% contraction. For the case of 0.1 gpd coldworking stress, the cold tension in the select yarn is clearly different (95% confidence) from that in light and dark yarns. The difference in cold tension between yarn grades is less significant after an 0.5 gpd coldworking stress. After coldworking at 1.0 gpd, the differences between yarn grades are high, but the variation in the yarns or the test procedure is too great to permit a claim of statistically significant differences. Coldworking at 1.0 gpd reduces the yarn's cold tension much more than 0.5 gpd or 0.1 gpd coldworking.

The yarn tension increases rapidly when the 130°C heater is brought into contact with the yarn. The "peak" tension is reached after a short time (<1 minute). The final tension is measured after 10 minutes of heating. The tension rises rapidly as the mobility of the extended chains bridging crytallites is increased above their T_g. When these "tie" molecules become unentangled after longer periods of heating, a general creep, or flow, of the structure can begin. These competing processes account for the occurrence of the tensile peak or overshoot. An additional small reduction in tension

TABLE A3-1. PRIMARY ASPECTS OF THERMALLY-INDUCED TENSION-TIME CURVES

Grade	Coldworking Stress	Cold Tension after 2.2% Contraction	Peak Hot Tension	Time to Reach Peak	Hot Tension After 10 min.
Dark		5.7 to .33	25.2 ± .47	0.14 ± .06	17.3 ± .32
Select	0.1	8.9 to 0.72	24.5 ± .01	0.32 ± .04	17.8 ± .02
Light		6.2 ± .41	24.4 ± .30	0.19 ± .01	18.0 ± .54
Significant Differences		S>D,L @ 95%	D>S,L @ 66%	S>D,L @ 95%	
Dark		6.0 ± .48	27.6 ± .06	0.34 ± .30	22.2 ± 1.65
Select	0.5	7.3 ± .47	28.3 ± 1.05	0.15 ± .07	21.5 ± .13
Light		4.9 ± .47	25.9 ± .10	0.22 ± .11	21.3 ± .23
Significant Differences		S>D>L @ 66%	D,S>L @ 95%		
Dark		3.1 ± .96	36.6 ± 1.10	0.6 ± .01	42.9 ± 2.6
Select	0.1	2.2 ± .21	38.2	0.29 ± .014	40.6 ± 2.7
Light		1.2 ± .12	34.7 ± .76	0.55 ± .021	37.6 ± .01
Significant Differences		D>L @ 66%		S<D,L @ 95%	D L @ 95% D,S L @ 66%
	(g.p.d.)	(gf)	(gf)	(min.)	(gf)

may be expected to result from continuing flow under the combined action of temperature and force at longer times (5-10 minutes).

The hot tension peak, final tension, and time to reach the peak tension are also shown in Table A3-1. They all increase dramatically as a result of the 1.0 gpd coldworking. These results are in keeping with the results of other workers, and suggest that additional chain orientation and crystallite destruction have occurred at this high load. The more highly oriented and less permanently restrained material will tend to shrink more or develop higher shrinkage forces if prevented from doing so. The longer time to reach the peak tension is consistent with the higher T_g of the more oriented chains [28].

In looking at the data in Table A3-1, we see specifically that light yarn is different (95%) from the dark and/or select yarn in peak tension after a 0.5 gpd coldworking. At 0.1 gpd, the peak tension of the dark yarn is different (66%) from that of select and light yarns. At both the 0.1 and 1.0 gpd levels of coldworking, the time to reach the peak for select yarn is significantly different (95%) than for dark and/or light yarn. The select yarn is slower in reaching peak tension at low coldworking and vice versa. The final hot tension does not discriminate between yarns except after 1.0 gpd coldworking, where hot tension of the light yarn was less than that for the dark yarn (at 95% confidence level and

less than that for both dark and/or select yarns at the 66% confidence level. None of these primary aspects of the thermally induced tension give a clear ranking (e.g. D>S>L) of the yarn grades that is highly significant (95% or better).

Table A3-2 shows additional derived quantities from the hot force-time curves. The thermally-induced tension is here defined as the increase in tension from the cold tension to the hot final tension at the given contraction. After an 0.1 gpd coldworking treatment, the select yarn was significantly different (95%) from the dark and light yarns on this basis. No significant differences in thermally-induced tension exist between yarn grades after 0.5 and 1.0 gpd pretreatments. The effect of increasing the coldworking tension on the thermally-induced tension increase is very clear, however. The yarns treated at 1.0 gpd had 4X the tension buildup associated with the 0.1 gpd pretreatments and 2.5X that associated with the 0.5 gpd treatment. The increased cold working results in a more straightened cold geometry leading to lower contracted load, but the additional orientation resulting from this coldworking produces a higher tensile force during the heating experiment.

The changes in yarn tension from 5 to 10 minutes after exposure to 130°C are also shown in Table A3-2. After coldworking at 0.1 gpd, these subsequent hot yarn tension changes ranked the yarns select<dark<light at a confidence level of

TABLE A3-2. DERIVED ASPECTS OF THERMALLY INDUCED TENSION-TIME CURVES

	Thermally Induced Tension Change	Tension Change From 5 10 min	Rate of Hot Tension Build-up	Tension at 10 min / Peak Tension
Dark	11.6 ± .02	-.15 ± .21	200 ± 75.6	69 ± .01
Select .1	8.9 ± .74	-.47 ± .09	76 ± 8.2	74 ± 1.6
Light	11.8 ± .13	+.05 ± .05	130 ± 7.8	74 ± 1.3
Significant Differences	S<D,L @ 95%	S<D<L @ 66% S<L @ 95%		D<S,L @ 95%
Dark	16.2 ± 2.14	-.07 ± .06	140 ± 127	80 ± 6.15
Select .5	14.1 ± .34	-.40 ± .32	210 ± 107	74 ± 1.63
Light	16.5 ± .24	-.005 ± .007	140 ± 70	74 ± 1.34
Significant Differences				
Dark	39.8 ± 3.61	+2.5 ± .66	61 ± 1.4	117 ± 4.2
Select 1.0	38.4 ± 2.89	+2.4 ± .21	120 ± 18.4	114 ± 3.5
Light	36.4 ± .12	+1.3 ± .18	70 ± 24.7	109 ± 2.1
Significant Differences				D>L @ 66%
	(gpd)	(gf)	(gf)	(gf/min)	(%)

(66%) and select<light at a confidence level of (95%). After heavy (1.0 gpd) coldworking, the yarn tension is still increasing after 10 minutes at 130°C. This slow recovery could be associated with motions of crystallites recovering from their (stress) deformed configuration.

The rate of tension buildup is here defined as the peak tension divided by the time to reach it. The results of such a calculation are shown in Table A3-2. The rate of tension buildup is not dramatically effected by the coldworking stress level. The rate of tension buildup probably corresponds to the rate dictated by the polymer and the rate of temperature rise generated in the yarn by the heater. Therefore, it should be constant for all the samples in these experiments.

The variability of tension buildup in the yarns was greatest at 0.5 gpd pretreatment stress. This suggests the conversion of the existing fiber structure which is preserved at 0.1 gpd to another form. At stresses of 1.0 gpd, the conversion is almost complete; at stresses of 0.5 gpd, the conversion is only partially completed and this results in higher scatter in the data. As seen in Fig. 19, 0.5 gpd corresponds to the "yield" point of textured polyester yarns.

The ratio of final hot tension to peak hot tension is also shown in Table A3-2. At low levels of coldworking (0.1 and 0.5 gpd) the final tension is less than the peak tension. At 1.0 gpd, there is a local peak followed by a gradual rise in tension to a higher level than the peak tension. At

0.1 gpd of pretreatment, the dark yarn had a lower hot tension ratio than either the select or light yarn (95%). At 1.0 gpd, the dark yarn had a higher hot tension ratio (66%) than the light. The significance of these findings in terms of fiber structure is not clear at this time.

None of the previously mentioned characteristics of the tension-time curves for the heated yarns provides a statistically significant basis for grading the yarns in a manner consistent with their appearance in a dyed hoseleg.